Nanocatalysis in Ionic Liquids
Syntheses, Characterisation and Application of Nanoscale Catalysts

Acknowledgement

I would like to thank Dr. Martin Prechtl for giving me the opportunity to work on and to write my thesis in his group.

Furthermore, I want to thank Prof. Dr. Annette Schmidt for the preparation of the second report of this dissertation.

Dr. Sebastian Sahler and Dr. Lisa Czympiel are acknowledged for proofreading and linguistic revision of this work as well as all the help within the last years.

I want to thank all my colleagues, Jong-Hoo Choi, Christian Gedig, Maria Hentschel, Leo Heim, Silas Robke and Hannelore Konnerth for preparative support and helpful discussion as well as for a great time in the lab.

Prof. Dr. Ning Yan and his whole group at the National University of Singapore are acknowledged for giving me the opportunity to work abroad, all the help during my stay in Singapore and the memorable and pleasant time.

Dr. Lasse Greiner and Dr. Sakthivel Mariappan are acknowledged for their support at the Dechema Instititute (Frankfurt a.M.) for TEM analysis.

Ralf Müller is acknowledged for XPS investigations, Dr. Christina Heinrichs and Ireneus Grzesiak are kindly acknowledged for support with XRD analyses. Furthermore, I want to thank Dr. Stefan Roitsch for TEM analyses and helpful discussion.

Special thanks are directed to the Evonik Foundation for financial and personal support during my PhD time. In particular, I would like to thank Susanne Peitzmann, Prof. Dr. Wolfgang Leuchtenberger and my mentor Dr. Matthias Rochnia, who have always supported my scientific work.

I am grateful for the enduring support of my family and the personal back-up within the last nine years. Falco Fox and Christopher Klinkenberg are acknowledged for always giving a good advice or simply for listening.

Finally, I want to thank Norah for the support during my studies. I am deeply thankful for the time we have spent together and her patience during that time.

Abstract

In this work, immobilized metal- and metaloxide nanoparticles were used as nanoscale catalysts in chemical reactions. Palladium nanoparticles, which catalyze classical C-C cross-coupling reactions (*Heck-*, *Suzuki-* or *Sonogashira* reactions), were grafted in the pores of carbonized wood. Several recycling reactions with remarkable performance could be realized. Furthermore, Cu_2O nanoparticles were synthesized in tetra-*n*-butylphosphonium acetate, an ionic liquid with high stabilizing potential and low melting point. These nanoparticles could be used as a recyclable decarboxylation catalyst for 2-nitrobenzoic acids and as a catalyst for *Buchwald-Hartwig* reactions. Depending on the reaction parameters or functional groups of the substrates, the catalyst showed moderate to excellent activity and recyclability. Inspired by the straight forward synthesis of palladium and copper oxide nanoparticles from simple metal salts with acetate ions as reductive species, a more general method for the synthesis of nanoscale materials has been developed in this work. Copper, silver, nickel oxide and zinc oxide nanoparticles have been synthesized via microwave irradiation in two different ionic liquids, as well as from two different precursors, respectively. Apparently, a wide range of nanostructures can be realized in ionic liquid systems with the assistance of acetate anions and without the necessity of ligands, surfactants, inert conditions or any further additives.

Besides some reviewing paragraphs, the ongoing experimental but unpublished work, which is in continuation of the above stated topics, is also presented, including deuteration experiments, deoxygenation reactions and decarboxylative cross-coupling reactions. In sum, the syntheses, characterization and evaluation of nanoscale catalytic systems is presented. Examples for new nanoparticle/ionic liquid systems, new and already established catalyses, which have not been realized with nanoparticle catalysts in ionic liquids so far as well as their performance concerning activity, stability and recyclability have been investigated.

Kurzzusammenfassung

Immobilisierte Metall- und Metalloxidnanopartikel finden in dieser Arbeit Verwendung als nanoskalige Katalysatoren für chemische Reaktionen. So wurden z.B. Palladiumnanopartikel, als Katalysatoren für C-C-Kreuzkupplungsreaktionen, wie die *Heck-*, *Suzuki-* oder *Sonogashira*reaktion eingesetzt. Als Substrat für die Immobilisierung diente carbonisiertes Holz, in dessen Poren die Partikel eingelagert wurden. Der geträgerte Katalysator konnte in allen drei Reaktionen mehrfach recycelt werden und lieferte dabei gute Ausbeuten der jeweiligen Kupplungsprodukte.

Darüberhinaus wurden Cu_2O Nanopartikel in Tetra-*n*-butyl-phosphonium Acetat, einer ionischen Flüssigkeit mit stabilisierenden Eigenschaften und niedrigem Schmelzpunkt, dargestellt. Die Partikel dienten sowohl als Katalysator für Decarboxylierungsreaktionen von 2-Nitrobenzoesäurederivaten als auch für *Buchwald-Hartwig*-Reaktionen. In Abhängigkeit von Reaktionsparametern oder funktionellen Gruppen an den Edukten, zeigten die Katalysatoren eine durchschnittliche bis exzellente Aktivität und eine ebenso gute Recyklierbarkeit.

Inspiriert durch diese einfache und geradlinige Synthese von Palladium- und Kupferoxidnanopartikeln wurde eine allgemeine Synthesemethode zur Darstellung von Nanomaterialien in dieser Arbeit entwickelt. Dabei beruht die Partikelsynthese hauptsächlich auf der Reduktion einfacher Metallsalze durch Acetationen. Kupfer-, Silber-, Nickeloxid- und Zinkoxidnanopartikel wurden durch Mikrowellensynthese in zwei verschiedenen ionischen Flüssigkeiten und aus zwei verschiedenen Vorstufen (Präkursoren) dargestellt. Offenbar kann eine Vielzahl verschiedener Nanomaterialien in ionischen Flüssigkeiten unter Zuhilfenahme von Acetationen dargestellt werden. Dabei kann auf die Verwendung von zusätzlichen Liganden, oberflächenaktiver Substanzen, inerter Reaktionsbedingungen oder anderer Additive verzichtet werden.

Neben zwei zusammenfassenden Arbeiten geben weiterführende und auf den oben genannten Themengebieten basierende experimentelle Abschnitte einen Überblick über zusätzliche Anwendungsgebiete der hier vorgestellten Cu_2O Nanopartikeln, sowie von Pd/Cu bimetallischen Nanopartikeln, wie z.B. Deuterierungsexperimente, Deoxygenierungsreaktionen und decarboxylierende Kreuzkupplungen.

Zusammenfassend werden in dieser Arbeit die Synthese, Charakterisierung und Bewertung nanoskaliger Katalysatorsyteme vorgestellt. Es werden Beispiele für neuartige Nanopartikel/ionische Flüssigkeitssysteme vorgestellt, sowie bisher noch nicht mit Nanopartikeln realisierte Katalysen in ionischen Flüssigkeiten sowie deren Leistungsfähigkeit hinsichtlich Aktivität, Stabilität und Wiederverwendbarkeit untersucht.
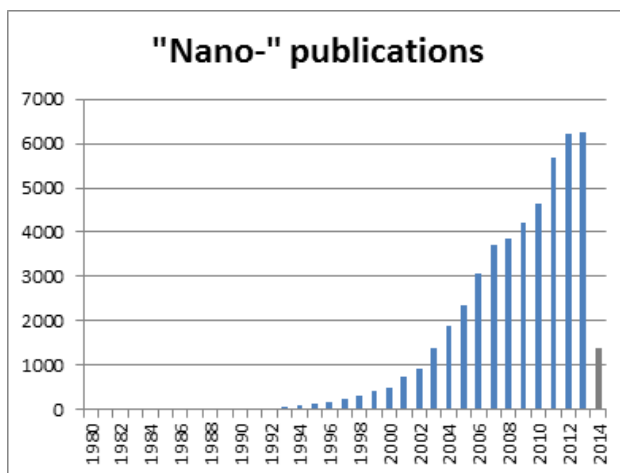
Contents

1 | Introduction

Nano science plays an important and even further emerging role equally in academia and industrial research. Our everyday life is by now highly influenced and related to achievements arisen from technologies of the tiniest.[1–3] On the one hand, people who are not familiar with these, often fear certain (or uncertain) threats and hazards accompanied with the term "nano".[4–6] On the other hand, industrial companies distinguish technological (and of course economical) opportunities in this area in order to develop new and efficient products.[1, 4, 5, 7, 8]

Apparently, academic scientists are supposed to take the role of an arbiter between both antagonists, to avert serious harm from our society and to ensure technological development and wealth.

What we today call "nano science" has its origins already back in the 17th century.[9–11] Nano material based compounds and colloids, e.g. of gold, have already been synthesized in 1676 by *A. Cassius* and *J. Kunckel*, though lacking structural and chemical understanding.[12, 13] According to what we know today, is, that even the Romans have synthesized nanosized gold particles to colour glasware.[14] *M. Faraday* was the first who really recognized the synthesis of very small particles.[15] Within the last 35 years, the science of metal and metal oxide nano structures has developed with increasing velocity (Figure 1.1). Not only the synthesis of nano struc-

Figure 1.1: The amount of publications concerning nano technology has emerged within the last 30 years.

tures by *Bönnemann et al.*[16, 17] or the first fundamental studies of so-called "ultra-fine" particles conducted by *C. Granqvist* and *R. Buhrmann*[18] made these materials interesting for different applications in physics and chemistry as well as for medical purposes. The high expectations of earlier years are now critically reconsidered with respect to actual progresses in method development and technological advantages realized. In fact, there has to be a certain and considerable scientific benefit by using nanoscale materials.

1.1   Introducing Remarks

Nowadays, nano-sized materials are well characterized since electron microscopy, X-ray and light scattering methods have evolved and have become standard techniques in today's laboratories.[19–21] Although widely used in biological, physical or chemical science there is an ongoing discussion about a satisfying definition of what nano materials really are. In principle, the word "nano" refers to a simple mathematical prefix or factor 10^{-9}. By this, nano materials should be sized between 1 and 1000 nm.

However, there are several inherent optical, electrical or chemical properties and characteristics, which are only attributed to a far smaller subset. These properties and characteristics are provided by nano structured compounds with new functionalities, which differ eminently from the respective counterparts in bulk state.[22, 23] As a matter of fact, this defines a chemical compound as a (functional) material. Although there is no clear size-delimitation for "nano-characteristics", nano materials are defined by the European Commission to be in the range of 1-100 nm.[24] Unless there is no clear and international accepted definition of the term "nano material", this dissertation and the terminology used herein is strictly guided by this proposal of the European Commission.

1.2   Ionic Liquids

Molten salts usually require high temperatures so as not to congeal. However, these compounds have aroused academic interest for the first time in the early 1940s and were tentatively investigated. *E. Heymann* and *H. Bloom* belong to the first in natural sciences, who took a deeper look at the physical and chemical properties of inorganic salts and their mixtures, e.g. melting point, electric conductivity and activation energy of ionic migration.[25] In many respects, the use of molten salts as solvents (initially for electrochemical reactions) was of major interest. As the melting points of classical inorganic compounds were too high for their convenient use in the lab and to extent the amount of investigable substances, usually alkali or earth-alkali fluorides and alkali nitrates with melting points between 360-450 °C and 250-300 °C were used, respectively.

As the melting points of molten salts were still too high in order to investigate sensitive organic molecules, salt-like compounds with high ionic character exhibiting an even lower melting point, were re-discovered. These consisted of a (rather) organic cation and an inorganic anion. In fact, *J. Weiner* and *S. Gabriel* synthesised ethanol/ammonium nitrate already in 1888,[26] whereas ethyl ammonium nitrate (EtNH$_3$ NO$_3$) was synthesized by *P. Walden* in 1914.[27] The terminus "molten salt" was regularly used till the 1970s.[28] Thereafter, this class of organic/inorganic salts was renamed into "ionic liquids" (IL) and further developed. Molten salts should therefore only include melts of inorganic salts.[29] Today ionic liquids are defined as chemical compounds merely consisting of poorly coordinated ion pairs, that melt below 100 °C. ILs which melt below 25 °C are called room temperature ionic liquids (RTIL) and are of certain preparative interest.[30]

1.2.1   Varieties of Ionic Liquids

A wide range of cations and anions in numerous combinations and variations are known today. The most common cation motifs are of pyridinium-, imidazolium-, pyrrolidinium-, ammonium- or phosphonium-type (Figure 1.2). The amount of normally applied anions outnumbers the corresponding cations by far. Usually weakly coordinating anions are used, but in principle all kinds of inorganic anions like halides, nitrate, tetrafluoroborate, hex-

afluorophosphate and sulfates as well as organic anions like triflates (OTf, trifluoromethyl-sulfonate), alkylsulphates, N-triflates (NTf$_2$, *N,N*-bis(trifluoromethylsulfonyl)imide) or di-cyanamides are common.[31,32]
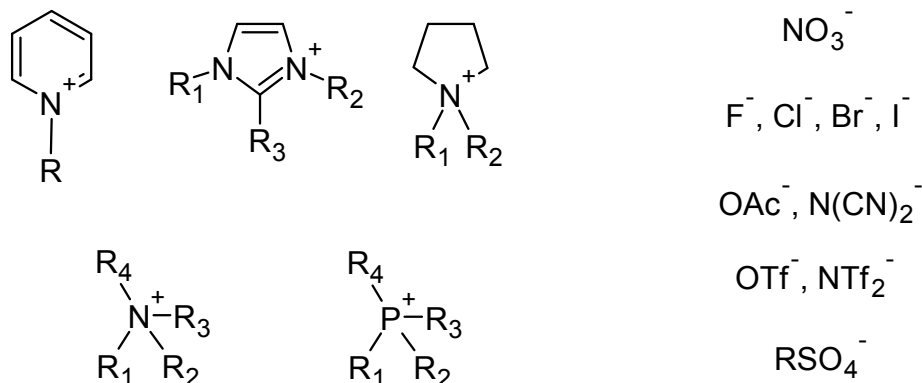
Figure 1.2: Selection of cations and anions commonly used in ionic liquids.

Alkyl side chains of the cations can be substituted with various functional groups, which influence the physico-chemical properties of the ionic liquid. For this reason, ILs are considered as "designer solvents".[33] Common functionalisations are hydroxyl-,[34] nitrile-[35] or carboxylate groups.[36] Even though ionic liquids are comparatively expensive, they bear numerous advantages in comparison to classical solvents. In contrast to commonly used solvents, ILs usually fulfill more than one function within a chemical reaction which makes them interesting for "green" chemical applications. ILs can be used as (co-)solvents,[37] promoters/catalysts,[38] surfactants and ligands[39] or reductive agents.[40] The use of ionic liquids reduces or even avoids the extensive application of additives in many ways, leading to a significantly lower degree of contamination of the reaction medium and final products.

1.2.2   Properties of Ionic Liquids

The modern definition of ionic liquids separates them from classical molten salts. Despite the fact, that molten salts and ionic liquids build up ion clusters in their liquid state[41] and that both types of compound classes melt at relatively low temperatures, there are distinct differences. Molten salts consist of inorganic anions and cations both bearing a definite and clearly localized charge. As classical solid state salts they build up a crystal lattice with a definite and highly symmetrical long range order. The arrangement of a three-dimensional network, bound together by strong inter ionic bonds, leads to high melting points of the majority of inorganic salts like sodium chloride (Table 1.1). These can be reduced by increasing the entropy within the crystal lattice, e.g. by combination of small anions and big cations (e.g. LiCl) or the use of salt mixtures, which directly leads to molten salts.[42] On the contrary, an ionic liquid usually consists of an organic cation and an inorganic anion, like 1,3-dimethylimidazolium chloride (mmim Cl) or 1-butyl-3-methylimidazolium chloride (bmim Cl). The cation's charge is partly delocalized within the carbon structure or sometimes even delocalized over an aromatic ring-system.[43] The ionic organic species do not have a spherical shape and are generally not symmetrical at all.[44] Moreover, alkyl groups with a high degree of freedom lead to an inhomogeneous ionic structure of the ionic liquid and therefore the lattice energies can easily be overcome, so that the melting points of these compounds are low.[45] A low tendency for hydrogen bond interactions[46,47] and a

big and unsymmetrical counter ion leads to a further decrease of the melting point.[31,48] However, like many other liquids, ILs show structural motifs even in the molten state. At first glance, it is impossible to bring this in line with the inhomogeneous ionic structure. It is, in fact, more a matter of sub-structure of lower order, which should not be mixed up with ionic long-range order, as *J. Dupont* and co-workers could show.[39] Today, we know that the differences between molten salts and ionic liquids do not lead to the replacement of one or the other, but refine their distinct application in physical or chemical investigations.

Table 1.1: Melting points of salts, molten salts and ionic liquids.[29]

	melting point [°C]		melting point [°C]
NaCl	801	emim Cl	87
LiCl	615	emim NO_3	38
mmim Cl	125	emim BF_4	6
bmim Cl	65	emim CF_3CO_2	−14

Besides the above stated structural and electrical properties, ionic liquids show extremely low vapour pressures. The negligible tendency for vaporisation is even true for higher temperatures. Their decomposition temperature is also very high but depends on side chains and functional groups.[29] Some ionic liquids can be heated up to 350 °C and still show long-term thermal stability (12 h and more). The boiling points of many ionic liquids are not explicitly mentioned, because they are often coincidental with their decomposition points. Nonetheless, some ionic liquids, i.e. emim NTf_2 or dmim NTf_2, have been successfully distilled at 300 °C and 6 mbar within 4-6 h by *K. Seddon, J. Widegren* and co-workers in a Kugelrohr apparatus.[49] Mainly imidazolium based ionic liquids show high thermal stability. The fractions of decomposed IL in the distillate were usually below 1% and could not be distinguished from initial contamination. In sum, many ILs show a wide liquid region ($\Delta T = T_{boil} - T_{melt} = 150\text{-}310$ °C) which is far beyond that of for instance water ($\Delta T = 100$ °C) or dichloromethane ($\Delta T = 136$ °C).

Although ionic liquids are made up of ion clusters,[41] they cannot be treated as polar solvents in general. Many ILs are hardly miscible with water and show phase separation. Polarity, but also acidity and basicity differ tremendously according to substituents and functional groups. These properties have been summarized for conventional solvents and are named *Kamlet-Taft parameters* α, β and π^*.[50] *P. Jessop* and *D. Jessop* have determined the Kamlet-Taft parameters for several ionic liquids:[51] α, β and π^*-values vary strongly depending on the combination of cation and anion. Hence, ionic liquids show very favourable solvating properties for a broad range of polar and non-polar substances.

Other remarkable properties of many ionic liquids are relatively low electrical and thermal conductivities, which is surprising, due to their ionic nature. They also exhibit high specific heat capacities, high viscosity and frequently show chemical and physical inertness. Since ionic liquids differ significantly in their physico-chemical properties (see Kamlet-Taft parameters) a prediction of the latter is, if not impossible, at the very least not reliable.

1.2.3   Applications of Ionic Liquids

Even though ionic liquids show remarkable properties, up to now there is limited industrial use for them, especially in the synthesis of bulk chemicals. The most cited industrial

process in which ILs play a role, is "ionikylation".[52] This represents the synthesis of gasoline additives with high research octane numbers (RONs) based upon *iso*-butane to yield trimethylpentanes. The used ionic liquid (bmim $AlCl_4$) replaces hazardous hydrofluoric acid and sulfuric acid, which is highly beneficial due to the low toxicity of the ionic liquid. $AlCl_3$, HCl and CuCl are added to the ionic liquid as catalyst precursors and to provide sufficient acidity. Another process including ionic liquids was presented by BASF and called BASIL process.[53] To be precisely, alkylimidazoles were added as a base and after protonation they form the ionic liquid which can easily be separated. That means, the imidazolium IL itself is not active in the whole reaction at all. A more convincing application for ILs could be their use in batch reactions for the synthesis of fine chemicals. *R. Giernoth et al.* showed that ionic liquids can act as pharmaceuticals simply by functionalization of imidazolium-based ionic liquids in combination with various anions.[54] They show remarkable antibiotic and analgesic activity. Due to their large liquid region, ionic liquids are used as transportation fluids for thermal energy (heat carrier) in solar thermal energy plants.[55] bmim BF_4 for example shows liquid behaviour between -71 °C and 450 °C (thermal degradation is not monitored over a long period). Due to their high heat capacity, ionic liquids are also superior as (thermal) energy storage media. The assembly and performance of lithium ion batteries could be significantly improved by using ionic liquids as electrolyte. In 2005 *N. Takami et al.* presented a lithium/air-cell working for 56 days with a discharge capacity of 5,360 mAh/g by using emim NTf_2 – commercially available batteries show capacities of 1,700-2,500 mAh.[56]

Although the usage of ionic liquids to dissolve biomass seems to be a new and upcoming trend for the usage of ionic liquids, *C. Graenacher* already stated in 1934, that cellulose could be dissolved in "halide salts of nitrogen containing bases", such as 1-benzylpyridinium chloride or 1-ethylpyridinium chloride, at temperatures above 100 °C.[57] However, in those days the utilization of biomass as feedstock material has not been of economical interest as it is today. In fact, the dissolution of biomass and the separation of its components to make the latter suitable as feedstock for the synthesis of future base- and fine chemicals is a major goal in ionic liquid science.[58] Lignin and (hemi-)cellulose belong to the largest and naturally most abundant resources. Common ionic liquid motifs for solubilisation of cellulose are pyrrolidinium and imidazolium chlorides.[59] While the synthesis of furfural and its derivatives is already advanced concerning the lab-scale,[60] all processes for industrial applications still show economical disadvantages and are technically demanding. It would be desirable to exploit this source of raw material because the recent key source for chemicals of great value - crude fossil oil - will run short in a few decades. A comprehensive overview about current techniques and technologies is given elsewhere.[61]

1.2.4   Nanoparticles in Ionic Liquids

In chemical catalyses the interaction between catalyst, substrates/educts, products and surfactants plays a critical role concerning the outcome of the reaction. Dealing with nanoparticles in ionic liquids, the IL is simultaneously the solvent and surfactant. During nanoparticle syntheses, the ionic liquid provides a reaction matrix for the synthesis of the crystal seeds and the particle ripening, but also prevents intensive particle growth and aggregation by so-called electrosteric shielding (Figure 1.3 C, D).[30] This is a combination of coulombic repulsive (electrostatic) interaction, which is known from ionic additives (Figure 1.3 B) and steric shielding, arising from bulky surfactants (ligands or polymers, Figure 1.3 A). In contrast to surfactants which are anchored to the particle surface, coordinated and unbound IL molecules are in a dynamic equilibrium. Functional groups of the ionic liquid's side-chains, like CN, OH, NH_2 etc. can intensify the interaction with the

nanoparticle surface[62,63] and improve the shielding of the nanoparticle (Figure 1.3).[64,65] During a catalytic reaction, catalyst and educt form an activated complex. On the one hand, this is supposed to happen directly on the surface of a nanoparticle, which is commonly true in hydrogenation reactions in ionic liquids. On the other hand, the nanoparticle can also serve as a reservoir for molecular catalyst species. The latter can be leached from the particle surface either by oxidative addition/insertion or stepwise by dissolution of small metal clusters and further leaching. Cross-coupling reactions for example are supposed to be catalyzed by molecular species and do not form educt/catalyst complexes on the surface of nanoparticles. The true mechanism for the generation of molecular catalyst species out of a nanoparticle reservoir is hardly investigated and only little understood as *Beletskaya et al.* recently showed.[66]
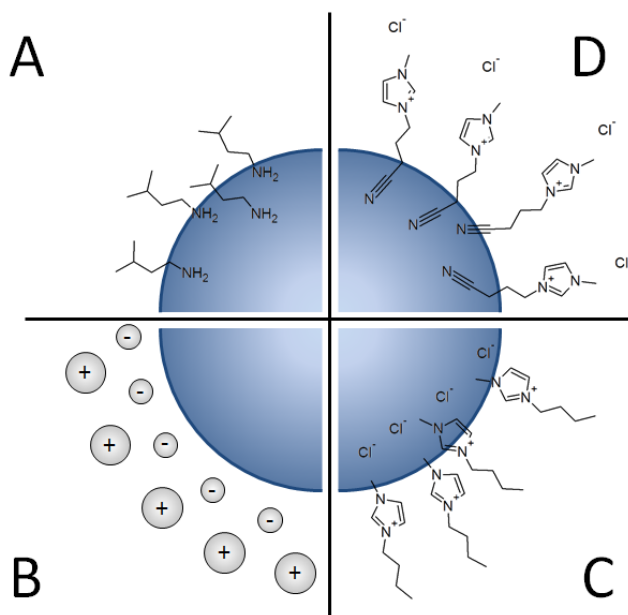
Figure 1.3: Surfactants of particles: **A** amines as surfactants (steric shielding), **B** ionic salts as surfactants (electrostatic shielding), **C** ionic liquids as surfactant (electrosteric shielding), **D** functionalized ionic liquids as surfactants (electrosteric shielding).

1.3 Nanoparticles and Nanoscale Structures

Nanoparticles and other nano structures of higher dimensionality are known in manifold geometries and symmetries.[67,68] Triangular, hollow, octahedral, tetrahedral and of course spherical shapes are well known for nanoparticles. Rods, wires, belts and ribbons can be realized for one-dimensional nano structures, whereas platelets and flakes are considered to be two-dimensional structures. Nanoscale lattices and frameworks rather belong to three-dimensional nano structures. However, a distinct subdivision into these four dimensionalities cannot be made: A clear differentiation between these objects is difficult, because they always show a three-dimensional extension. The prefixes 0D, 1D, 2D and 3D rather indicate the major growth directions (Figure 1.4). Nanoparticles are known for the majority of metals, e.g. in their elemental form, as transition metal chalcogenides and halides or as composition of main group elements. Already in the early 20th century, nanoparticles, especially of the late transition metals and their oxides, have aroused interest

concerning their use as catalysts in chemical reactions, although they were often called colloids or colloidal particles, due to their behavior to be incorporated in stable dispersions.[69] In literature phrases like nano cluster, nano powder or nano crystals are sometimes utilized. The latter refers to mainly inorganic and highly crystalline nano particles, whereas nano clusters should be sized below 10 nm. Nano powders, however, are supposed to represent agglomerates and aggregates of nanoparticles with sizes below 1000 nm. Nevertheless, those phrases are not common nor internationally accepted.[70]
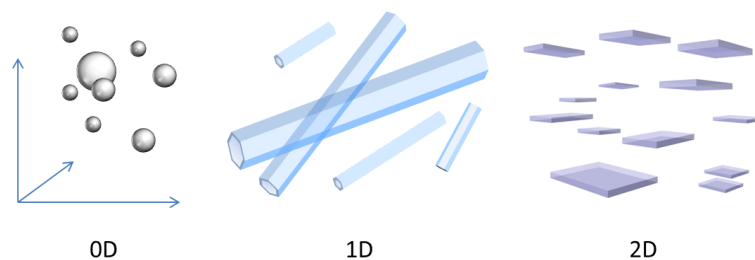
Figure 1.4: Zero-, one- and two-dimensional nano structures.

1.3.1 Syntheses of Nanoscopic Materials

Nanometer sized structures have not been invented or firstly realized by mankind, but are naturally abundant in fine powders like ashes or dusts, in minerals like opals, in the biosphere (e.g. on surfaces of leaves or animal feet) or are formed by viruses.[71] Though, most of the anthropogenic nano materials are synthesized accidentally in industrial combustion or during the production of construction materials. For the specific synthesis of nanoparticles there are two main principles: The *top-down* method, including grinding and milling of powders, ablation techniques from targets or etching. On the contrary, the *bottom-up* methods involve precipitation, sol-gel processes, vapour depositions, lithography or epitaxy.[72,73] For chemical applications, solvothermal syntheses of nano materials are very popular and well investigated.[74,75] They bear the advantage to control size and shape by adjusting the reaction parameters without the necessity of technically sophisticated set-ups. Moreover, doping and surface functionalisation can be easily performed by adding the corresponding additives to the reaction medium.

The principle of the nanoparticle formation is often referred to the *LaMer-mechanism* introduced by *V. K. LaMer* and co-workers in the early 1950s.[76,77] In short, the *LaMer-mechanism* proposes, that nucleation can only occur in supersaturated (precursor-) solutions. Initially the concentration of the pecursor should rapidly increase (phase I Figure 1.5). In accordance with statistical mechanics, the energy barrier of nucleation can only be surmounted in supersaturated solutions, where the probability of bimolecular stepwise additions is sufficiently high (phase II Figure 1.5). The formation of nuclei leads to a decrease of the concentration in the solution which ceases the nucleation. Further growth of each nucleus by diffusion controlled agglomeration (e.g. *Ostwald* ripening) leads to consumption of the particle precursor (phase III Figure 1.5). This temporal separation of nucleation and growth is the key idea of the *LaMer-mechanism*.

In contrast, *M. A. Watzky* and *R. G. Finke* proposed a different course of events.[78] They introduced a mechanism in which again, nucleation and growth are separated in time, but the nucleation is of slow and of continuous manner without the dependency on supersaturated solutions. Furthermore, the particle growth is fast and the rate determining

step is the auto-catalytic and surface-controlled incorporation of monomers to the particle. This means, particle growth is not controlled by diffusion. The proposed mechanism is confirmed by their experimental data showing the precipitation of Ir nanoparticles with $[Bu_4N]_9P_2W_{15}Nb_3O_{62}$ as surface stabiliser. It is also in good agreement with the theory and findings of *J. Turkevich* and co-workers from 1951 who showed that nanoparticles can also be synthesized from a bittern not showing supersaturation.[79]
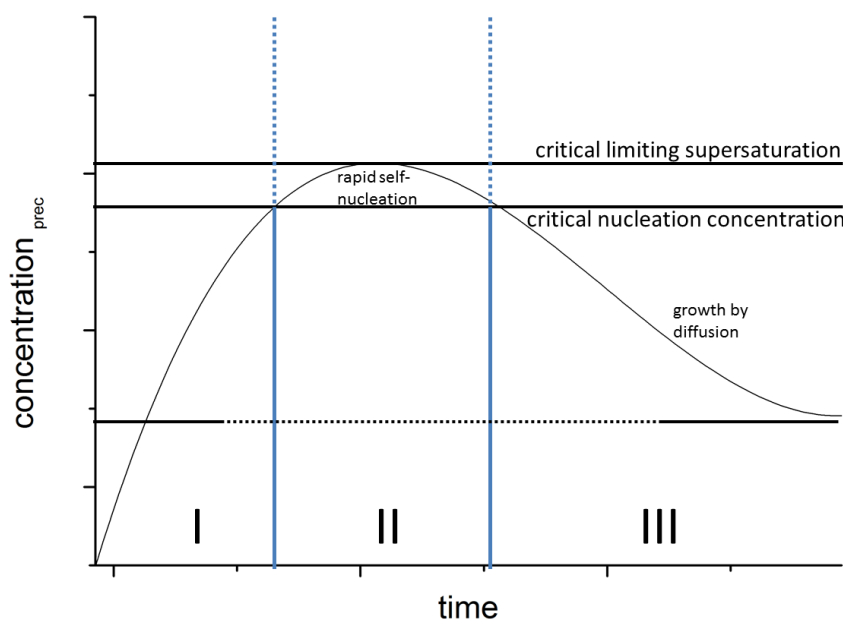
Figure 1.5: Graphical sketch of the *LaMer*-mechanism. I) Increasing precursor concentration, II) self nucleation and III) diffusion controlled growth of nano structures. Adapted from ref.[76]

Of course, there are plenty of different types of precursors for the solvothermal synthesis of nanoparticles. The most convenient way to synthesise particles is to use an affordable, non-toxic and insensitive precursor, like simple metal salts. In some cases it is highly recommended to use rather sophisticated as-prepared single source precursors (especially in the case of mixed-metal particles) to prevent or minimize the contamination with undesired by-products such as halides or sulfides.[80,81] Designed mixed metal precursors also bear the advantage to simplify the build-up of hybrid structures. Hybrid structures of nanoparticles represent a distinct group of nano structures - in fact, hybrid structures also exist for 1D, 2D or 3D structures and are built up analogously.[82–84]
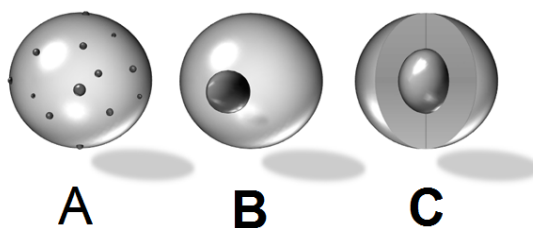
Figure 1.6: Three types of hybrid materials: **A** Surface decorated particle, **B** core-shell particle and **C** solid core-shell particle.

The most common hybrid nanoparticle type is the so-called core-shell particle (Figure 1.6), which is a particle core made of compound A surrounded by a shell made of compound B.[85] In terms of definition it does not matter if the particles' surface is only enriched by one component or is solely composed of the latter. Furthermore, the core and the shell are not necessarily solidly linked.[86] Nanoparticles with a surface functionalisation (sometimes also called: decoration) represent another group of hybrid materials. Hereby, smaller nanoparticles or nanoscale structures are anchored on the particles' surface but do not cover it completely.[87, 88] If nanoparticles are surrounded by an organic surfactant one speaks of organic-inorganic (O-I) hybrid nano materials.

In solvothermal syntheses the build-up of nanoparticles can either occur by reduction or by oxidation of the precursor, by thermal decomposition or base-/acid-catalyzed polymerization. Reduction of the particle precursor mainly leads to metal nanoparticles (M-NP) but can also yield, i.e. chalcogenides of lower oxidation state. Basically all kinds of reducing agents can be used for the synthesis of nanoparticles, like $NaBH_4$,[89] citric acid,[90] (poly)-alcohols,[91, 92] silanes[93] and amines.[94, 95] Gaseous reducing agents like molecular hydrogen are very popular because of their clean and residue-free use.[96]

Oxidation of nanoparticles usually occurs during their synthesis under non-inert conditions and leads to metal oxide nanoparticles (MO-NP) of different structures and morphologies.[97, 98] In a way, atmospheric oxygen is the most common oxidant. Noble metals like Pd tend to withstand oxidation under ambient conditions. Higher oxygen pressures[99] or high calcination temperatures in an inorganic matrix[100] lead to finely divided PdO nanoparticles, though. Thermal decomposition of metal(0) complexes (mainly) leads to M-NP. Typical complexes can be for instance M(COD)- or $M(CO)_x$-type. Mild reaction conditions are characteristic for this kind of nanoparticle synthesis.[96] Base- or acid-catalyzed solvothermal syntheses are similar to sol-gel syntheses but do not lead to (hydro-)gels; instead rather colloidal dispersions are built up.

For solvothermal processes two methodologies are mainly used to generate temperatures which are required to induce particle formation – thermal and microwave assisted heating. Especially for nanoparticle syntheses the way of heating is crucial for the outcome of the reaction, since size, shape and morphology can be influenced by the heating ramp, the duration and the shape of the heating source (surface vs. spot heating).[101, 102] Besides thermal heating, microwave assisted irradiation or heating via IR-radiation have been intensively investigated.[103]

1.3.2 Physical and Chemical Properties of Nanoscopic Materials

Nanoscale particles or structures of higher dimensionality can be seen as the link between bulk materials and materials of molecular and atomic size. On the one hand, nanoparticles show versatile and unique physical and chemical surface effects (adsorption, surface reactions etc.). On the other hand, small particles form stable dispersions and seem to be dissolved in liquids. In contrast to bulk materials, the amount of surface atoms is significantly higher (Figure 1.7), the smaller the considered nanoparticles are, which is especially true for particles sized below 10 nm.[104]

In fact, the underlying factor for these astonishing abilities is the Gibbs energy G_{total} of the considered structure.[105] For particles the Gibbs energy is composed of the Gibbs energy of the bulk material G_{bulk} and the Gibbs surface energy $G_{Surface}$:[106]

$$G_{total} = G_{bulk} + \gamma A_{Surface} \tag{1.1}$$
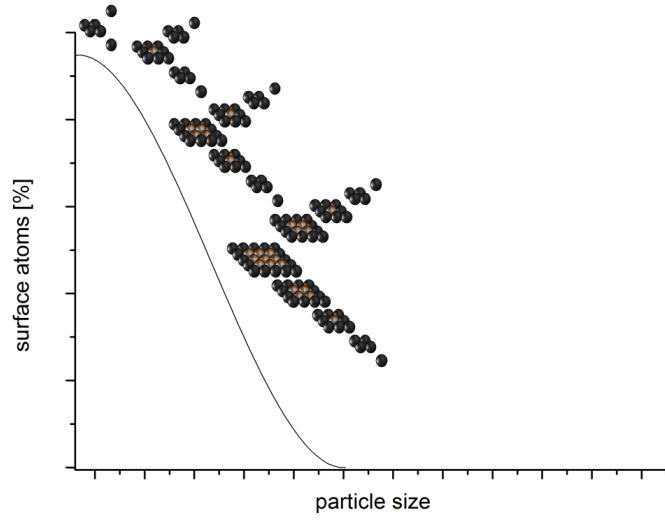
Figure 1.7: This schematic drawing demonstrates qualitatively how the relative amount of surface atoms is decreasing with growing particle size.

$$G_{Surface} = \gamma A_{Surface} \tag{1.2}$$

γ - surface tension, $A_{Surface}$ - nanoparticle surface

One can clearly see that the nanoparticle's surface $A_{Surface}$ contributes tremendously to the Gibbs energy, whilst it is negligible for macroscopic particles or bulk material.[107,108] This is also true for the solubility of particles, which is described by the *Ostwald-Freundlich* equation.[109]

$$\frac{S}{S_0} = exp(\frac{2\gamma V_m}{RTr}) \tag{1.3}$$

S - Solubility, S_0 - Solubility of bulk material, R - gas constant, T - temperature, V_m - molar Volume, r - particle radius.

The solubility of the particle increases drastically considering the above stated equation as the particle size decreases. According to this relationship the surface energy and particle size strongly determine the solubility of the nano material, which is obvious from what is experimentally well known: Small particles are better soluble than bigger ones. Besides the dissolution of small particles, the precipitation of nanoparticles from a dispersion leading to bulk or aggregated material is another challenging point. In the simplified case of spherical metallic nanoparticles the total free interaction energy between two particles $E_{interaction}$ is given by the sum of all applied *van-der-Waals* forces (mainly attractive) E_{vdw} and electrostatic forces (mainly repulsive) E_{est}:[110]

$$E_{interaction} = E_{vdw} + E_{est} \tag{1.4}$$

In this case, the pH-value and the ionic strength influence the net force (attractive or repulsive) significantly, leading to aggregation or to a stable dispersion.[111] At a certain pH-value (or a concentration value for other ions in non-aqueous media), the so-called

point of zero charge (pHZPC), the surface charge of the nanoparticle is compensated which consequently leads to aggregation. In order to prevent nanoparticle aggregation the sum of repulsive forces must overcome the sum of attractive forces, which is already stated in the *Derjaguin-Landau-Verwey-Overbeek* (DLVO) theory and its extensions (for further details it is kindly referred to ongoing literature).[111,112] Besides electrostatic forces the extended DLVO theory includes also non-electrostatic forces mainly attributed to surface functionalisations and cavities which are responsible for interaction with solvent molecules (Figure 1.8).[113] These interactions are mainly of steric nature, but also osmotic forces arising from solvent molecules within the surfactant layer and an elastic energy contribution (due to entropy loss upon coating layer compression) are considered.
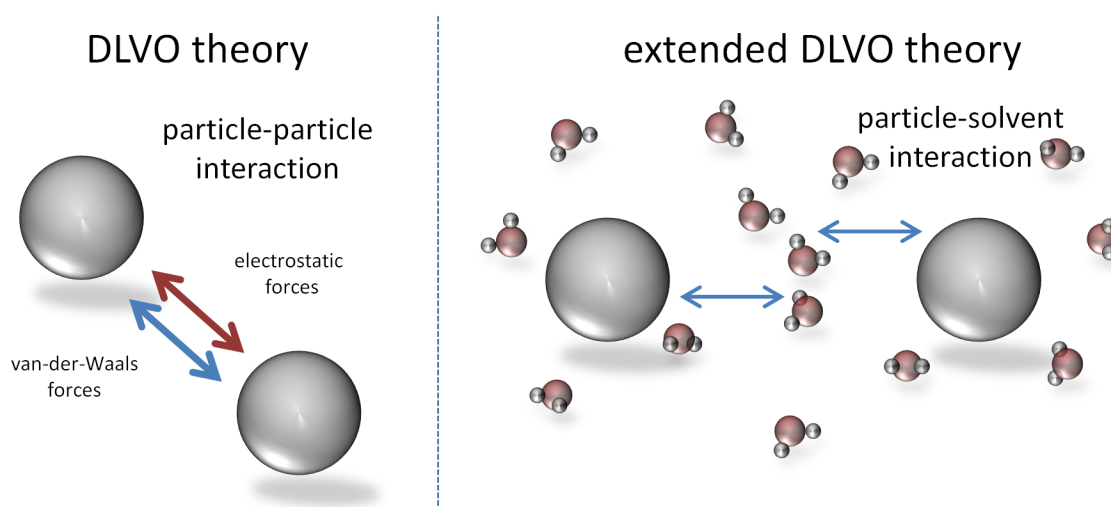
Figure 1.8: Schematic view of the DLVO and extended DLVO theory.

As the diameter of nanoscale materials becomes smaller, optical and electrical effects which are rather unexpected can be observed. This is especially true if the size of the considered nano material decreases to the range of the length of an electromagnetic wave (e.g. photon). As the materials are now confined in one or more dimensions, the energy levels start to differ from those in bulk state and become discrete.[114] The resulting effects are e.g. quantum confinement and surface plasmon resonance. The macroscopic phenomena resulting from these effects are colored nanoparticle dispersions,[115] decreased melting points,[116] superparamagnetism[117] or semiconductive behavior of nano materials, which show dielectric behavior in the bulk state.[118]

1.3.3 Application of Nanoparticles

The unique properties of nano materials and especially of nanoparticles have been intensively investigated within the last three decades. Numerous new inventions have emerged out of these innovative materials and led to industrial applications and products.[119,120] Nanoparticles are today commonly incorporated into textiles, coatings and cosmetics. Typical for these low-cost applications are compounds like TiO_2, SiO_2 and Al_2O_3.[121–124] Nanoparticles seem to have big potential as semi conductive materials for hydrogen generation (water-splitting), as (gas-)sensors, for light-harvesting applications or in integrated circuits. Cheap materials as ZnO are very promising for semi conductor applications due to its mechanical and chemical robustness as well as its abundance.[125,126] Nanoparticles

are already used for medical applications, for targeted medication and drug delivery, prosthesis cementation and anti-cancer therapy.[127] Due to their ability to be easily absorbed by human cells, small nanoparticles can also be used for treatments in very sensitive parts of the human body. Current investigation focuses on the development of anti-fungal, antibacterial and antiphlogistic particles.[128] As the nanoparticles surface-to-volume ratio is extremely high, it can be used as a surface template. Surfactants can be applied to the surface and go for filtering of drinking water,[129, 130] detoxification of air or absorption of gases.[131]

Reinforcement of common materials like plastics or fabric composites is another big target for the application of nano materials.[132] Usually the use of small amounts of nanoparticles or nano fibres is sufficient to increase the mechanical strength of structural elements.[133] In these cases, the nanoparticles transfer their own properties to the surrounding medium, leading to an overall stabilization. The aim is to produce components of lower weight to save energy in transportation, heating and production applications. In terms of construction materials, nanoparticles have also become additives of high demand.[134] Nanoscale structures are incorporated in technical glues,[135] insulating materials, concrete[136] or cement blends[137] or used to change hydrophilic to hydrophobic behavior of outdoor coatings.[138, 139]

1.4 Catalyses

This chapter describes nanoparticles as catalysts and gives mechanistic insights into the reaction pathways of catalyses, which will be discussed in the following section. It is subdivided into nanocatalysis in classical solvents and nanocatalysis in ionic liquids.

1.4.1 Nanocatalysis

The application of nanoparticles as catalysts for chemical reactions is one of the most developing research areas in chemical science. In 1927 *W. Hückel* already presented Pt, Pd, Ir and Os colloids as catalysts for hydrogenation and oxidation reactions.[69] The colloid syntheses were already mentioned by *C. Paal* and *C. Amberger* between 1904 and 1907.[140–143] Further work on colloidal catalysts was performed by *A. Skita* and *W. A. Meyer* between 1912 and 1923 mainly for hydrogenation reactions.[144] The scientific success of homogeneous catalysis more and more displaced colloidal catalysis in the following years. In 1996 *Bönnemann's* group contributed essentially to the rediscovery of the catalytic abilities of nanoparticles of Pt and Rh.[16, 17, 145] These have also been employed for hydrogenation and oxidation reactions of organic substrates. In the same year *M. Reetz* presented the first Pd nanoparticle catalyzed C-C coupling reactions.[146, 147] In the following years, the catalyst loading of the *Heck* reaction could even be improved in co-operation with *J. G. deVries*.[148] Catalysts for other types of reactions have been discovered at the end of the 1990s. *J. H. Ding* and *D. L. Gin* showed a tandem hydrogenation/*Heck* olefination in 2000 with Pd nanoparticles as catalysts.[149] *M. A. El-Sayed* presented Pd nanoparticles as effective catalysts for *Suzuki* reactions.[150] Today, all kinds of (late) transition metal elements heve been realized on the nanoscale and used as catalysts. The most popular ones are metals of the platinum group (Ru,[151] Rh,[152] Pd,[153] Os,[154] Ir,[155] Pt[156]), usually showing the highest activities and selectivity for hydrogenations, cross-coupling reactions, (de-)functionalisation and metathesis reactions. Lately, nanoparticles consisting of Fe,[35, 157] Co[158] and Ni[159] were shown to be active in several reactions, too. The coinage metals Cu, Ag and Au represent a further potent group of nanoscale catalysts, e.g. for "click" chemistry, steam reforming,

oxidation or hydrosilylation reactions.[160–163] Especially gold, usually known as an element resisting numerous reactions in bulk state, changes its reactivity and catalytic potential in the nanoscale. The chemistry of gold nano catalysts prospered within the last 10 years and the noble metal has become a quite popular catalyst material.

As the price of many nano catalysts and their precursors (mainly those of the platinum group as well as gold) is disproportionally high, the demand for cheaper and more resistive catalysts, which are also applicable in industrial processes, rises.[35,157,159,164] Due to their low price, unique redox resistivity and feasible synthesis, most oxide materials of common transition metals are considered as alternative for established noble metals. Some typical representatives of transition metal oxide catalysts are iron oxides,[165,166] copper oxides,[167,168] nickel oxide[169] and zinc oxide.[125,126] These catalysts show good results in certain catalyses, like steam reforming or coupling reactions, but their reactivity is usually not comparable to sophisticated noble metal catalysts. Nevertheless, intensive work and optimization is done on the performance of nanoscale transition metal oxide catalysts.

1.4.2 Carbon-Carbon Cross-Coupling Reactions

Classical cross-coupling reactions of *Suzuki-*,[170] *Heck-* or *Sonogashira*-type[171] are well known in literature and the reaction mechanisms have already been elucidated for homogeneous systems.[172] Of course, these C-C coupling reactions differ in the applied catalyst metals or coupling reagents and there are also differences in their exact reaction mechanism, which is especially true for the Heck olefination. But in sum, there is a very general catalytic cycle shown in Figure 1.9 which describes all C-C cross-coupling reactions sufficiently and emphasizes the similarities between them.
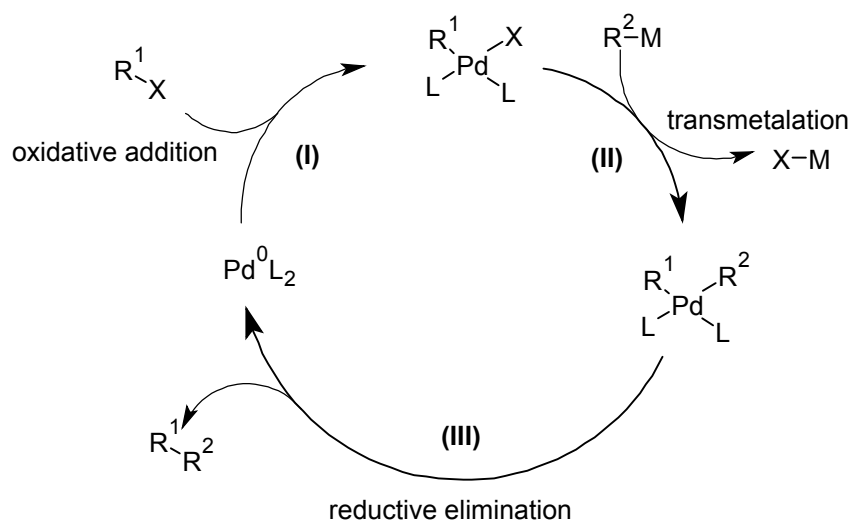
Figure 1.9: Palladium catalysed carbon-carbon cross-coupling mechanism.

Usually, the oxidative addition (**I**) is the starting point in the catalytic cycle, because it is the rate determining step. A M(0) species, commonly used is Pd, undergoes a insertion into a C-X bond (where X is usually a halide or pseudohalide). During this step, the catalyst is oxidized from oxidation state 0 to oxidation state II. After that, the preformed M(II) complex undergoes transmetalation (**II**) with another organometallic compound. For *Suzuki* reactions, organoboron compounds are used, in *Sonogashira* reactions organocopper

species are preformed. In *Heck* reactions the transmetalation does not occur, due to a missing organometallic compound. The reaction pathway continues via a base induced β-hydride-shift. The organometalate complex $M(II)R^1R^2$ can now undergo a reductive elimination (**III**) to yield the coupled product R^1R^2 and the regenerated M(0) catalyst. R^1 and R^2 can be aryl-, vinyl- or alkynyl-groups (which are nowadays readily available). By this, cross-coupling reactions lead to a plethora of different coupling products which makes them versatile synthetic tools. Usually, an additional base is required for all cross-coupling reactions.

1.4.3 Carbon-Heteroatom Cross-Coupling Reactions

C-Y (Y = N, O, S) cross coupling reactions are of special interest, due to the wide spread prevalence of carbon heteroatom bonds in natural compounds. One of the most popular C-N cross coupling reactions is the *Buchwald-Hartwig* reaction. During the catalytic process usually an aryl halide is coupled with an amine to give an aryl amine derivative (e.g. aniline). The reaction steps (**I**) and (**III**) are supposed to be analogue to the C-C cross coupling reactions (see Figure 1.9), but the transmetalation step is missing and replaced by a base promoted amination of the organo-metalate (**II**) followed by the reductive elimination (**III**).[172]

1.4.4 Deoxygenation and Decarboxylation Reactions
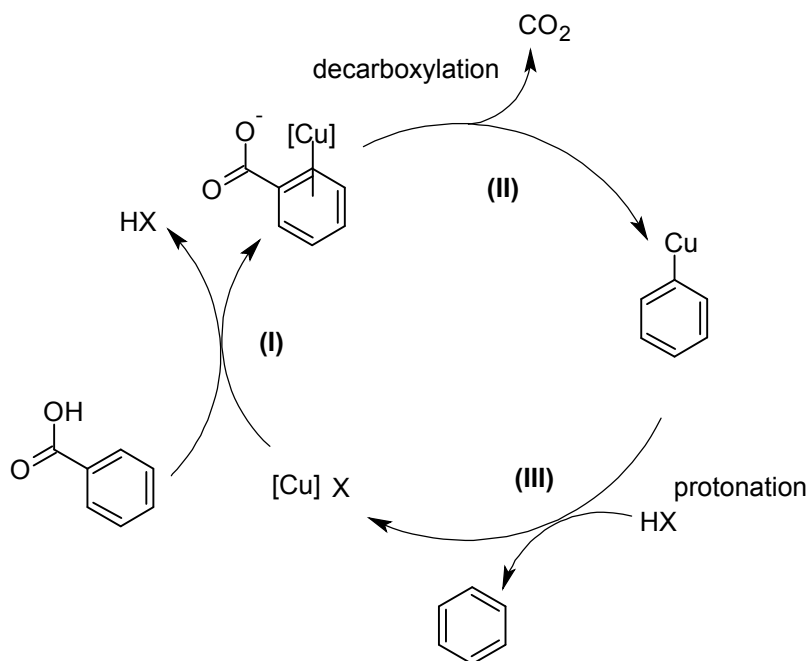
Figure 1.10: Mechanistic overview of a decarboxylative defunctionalisation.

Besides (cross-) coupling reactions, defunctionalisation reactions of organic molecules are of great benefit. However, this kind of catalysis is far less investigated and sparsely understood. Breaking a C-C bond (345 kJ/mol) is nearly impossible at mild conditions without the use of a catalyst.[173] Since carboxylate groups are a very common motif in natural abundant chemical compounds like lignin or fatty acids,[174] it is highly desirable to decarboxylate them. In fact, this is one of the main concerns of biomass conversion into

bulk chemicals.[61] Fatty acids can undergo different kinds of deoxygenation reactions including decarbonylation and decarboxylation.[175] Usually a Cu(I) or Pd(II) catalyst serves as decarboxylation catalyst in the first and rate determining reaction step (Figure 1.10). Thereby, the transition metal is coordinatively added to the carboxylate (**I**) and then inserts into the C-C bond via extrusion of CO_2 ((**II**), Figure 1.10). After aqueous (protic) work-up, the aryl-metalate is protonated to yield the defunctionalized product (**III**).

1.4.5 Decarboxylative Cross-Coupling Reactions
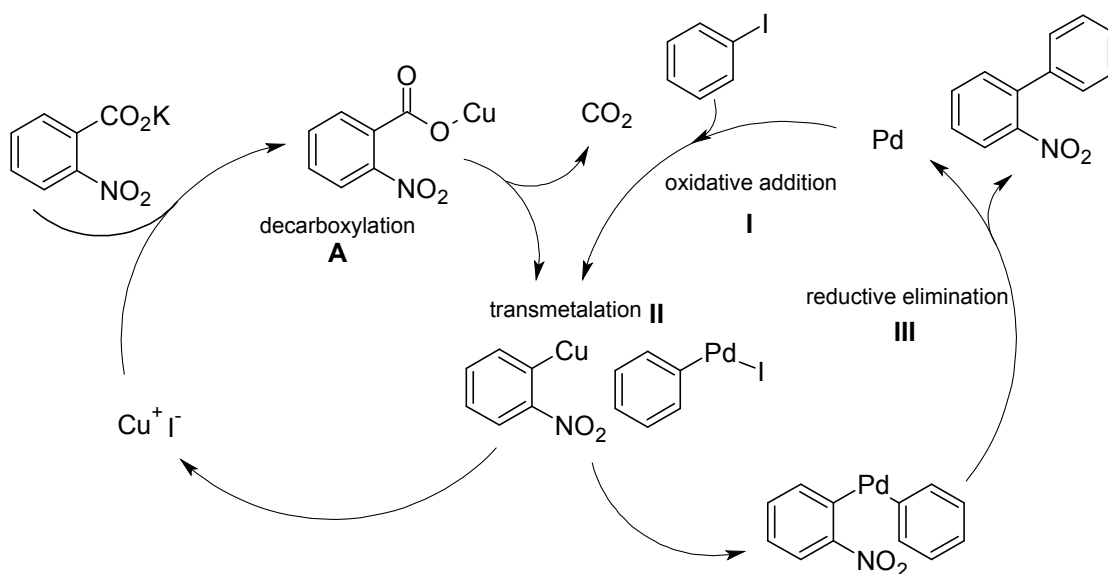
Figure 1.11: Proposed mechanism for the decarboxylative cross-coupling reaction with Cu(I) and Pd(0) as catalysts.

Alternatively, benzoic acids can not only be decarboxylated, but also serve as coupling partners in C-C cross-coupling reactions. *Myers et al.*[176] and later *Gooßen et al.*[177] presented a versatile decarboxylative cross-coupling reaction of various benzoic acids. In an aprotic milieu a stable aryl-Cu compound can be formed via decarboxylation (**A** in Figure 1.11). Subsequently the aryl cuprate can undergo a transmetalation (**II**) with another organometalate (aryl-Pd) which is generated by an oxidative addition (**I**) to an aryl halide. After the transmetalation, the copper catalyst is released to the reaction medium and the bis-organometalate undergoes reductive elimination (**III**), yielding the final coupling product. The use of stoichiometric amounts of organometallic compounds (like organoboron, organotin etc.) is not necessary in this cross-coupling reaction. As decarboxylation catalyst also Pd[176] or Ag[177] can be used. The decarboxylative cross-coupling has not been realized with nanocatalysts yet.

1.4.6 Catalysis in Ionic Liquids

The main scientific topics in ionic liquid investigation are chemical reactions, catalyses and catalyst preparations as well as the interaction between ionic liquids and nanoparticles. Since these sub-chapters closely correlate with each other they are treated together in this work. Chemical reactions realized and promoted by ionic liquids (which were intended

and did not happen by accident) were firstly described in the late 1980s. *J. S. Wilkes* in 1986 showed that *Friedel-Crafts* reactions could be conducted in acidic chloroaluminate ionic liquids in which the ionic liquid acted as the catalyst itself.[178] One year earlier, in 1985, *S. E. Fry* and *N. J. Pienta* presented a nucleophilic aromatic substitution reaction in phosphonium halide melts.[179] Later on, in 1990, *Y. Chauvin et al.* presented a propene dimerization in ionic liquids like bmim Cl, bmpyrr Cl and *n*-Bu$_4$PCl with chloroaluminate salts as additives.[180] In the same year, *J. S. Wilkes* and *R. T. Carlin* demonstrated successfully the *Ziegler-Natta* polymerization of ethylene in bmim Cl with a titanium/aluminate catalyst dissolved.[181] The development of ionic liquids led to the usage of tetrafluoroborate anions, which show a much lower sensitivity towards functional groups as the chloroaluminates do. *Y. Chauvin et al.* presented a hydroformylation of olefins with a rhodium catalyst in bmim BF$_4$.[182,183]

All the above introduced reactions and catalyses were supposed to be homogeneous; the catalyst itself is dissolved as metal ion or as a complex in the ionic liquid. In 1996, *D. E. Kaufmann* and co-workers published a *Heck* olefination in tetraalkyl ammonium and tetraalkyl phosphonium "molten salts" with remarkable yields.[184] Interestingly, they made a slight remark concerning the precipitation of Pd(0) clusters and the stabilizing effect of the molten salt. This is supposed to be the first (maybe accidentally) proven catalysis driven by nanoparticles stabilized in an ionic liquid. *M. T. Reetz et al.*[146,147] as well as *M. Beller et al.*[185] also showed the activity of Pd nanoparticles, but not the stabilizing effects of ionic liquids. In the same year, *T. Jeffery* found out that tetraalkyl ammonium salts (bromides, hydrogen sulfates and chlorides) had a beneficial effect on *Heck*-type reactions with a utilized Pd(0) catalyst.[186] They were added and supposed to act as a base, but showed their remarkable effect only when added in excess. Two years later, in 1998, *T. Jeffery* and *M. David* introduced a more generalized method also utilizing *n*-Bu$_4$NOAc, which became widely known as "*Jeffery*-system" for the synthesis of Pd(0) catalysts.[187] *M. T. Reetz* and *E. Westermann* could proof in 2000 that the high amount of tetraalkyl ammonium salt had a stabilizing effect on the formed nanoparticles and was therefore the catalyst(-reservoir).[188] In 2003 *V. Caló* and his group presented a *Heck* olefination catalyzed by Pd nanoparticles in *n*-Bu$_4$NBr (TBAB) as pure reaction medium - and not as a base, as intended in previous reports.[189] *M. T. Reetz* and *J. G. de Vries* further developed the Jeffery-system and minimized the amount of used Pd nanoparticle catalyst in a *Heck* reaction to the range of 0.1-0.00125 mol%.[148,157] This was the initial spark for an upcoming and extensive investigation on the use of ionic liquids as reaction media for nano catalyses.

Today many catalytic applications with nanoparticles in ionic liquids are equal to homogeneous catalysis or show superior yields. Very prominent are Pd nanoparticles in C-C cross-coupling reactions. *Deshmukh et al.* introduced a *Heck* olefination of aryl iodides with alkenes and alkynes in bmim Br and bmim BF$_4$ with Pd nanoparticles already in 2001 at temperatures as low as 30 °C with ultrasonic enhancement.[190] In 2009 *V. Caló* and co-workers showed, that deactivated alkenes and aryl chlorides can be coupled smoothly with Pd nanoparticles in *n*-Bu$_4$NBr with n-Bu$_4$NOAc as base.[37] There are also examples for nanoparticle catalyzed cross-couplings in ionic liquids for the *Suzuki-Miyaura* or the *Sonogashira* coupling. One interesting approach towards biphenyl derivatives was presented in 2009 by *J. Durand*.[191] Pd nanoparticles in bmim PF$_6$ showed remarkable activity for the coupling of bromobenzenes with phenylboronic acid. Within one hour, complete conversion was achieved. 1-Methyl-3-(2-mercaptoacetoxyethyl) imidazolium chloride as a

functionalized imidazolium based ionic liquid was used by *H. J. Zhang et al.* to perform a *Sonogashira* cross coupling reaction. Iodobenzene and phenyl acetylene can be coupled smoothly.[192] Furthermore, *Ullmann* and *Stille* reactions are known with nanoscale nanoparticles.[193] Since the examples for nanoparticle catalyzed cross-coupling reactions are numerous in literature, a comprehensive review about Pd nanoparticle catalyzed cross-coupling reactions in ionic liquids can be found in Chapter 3 (3.6 Coupling Reactions in Ionic Liquids: Metal Nanoparticles).[193]

Besides cross-coupling reactions, also nanoscale hydrogenative catalysis is commonly conducted in IL media. *J. Dupont et al.* introduced a rhodium and iridium nanoparticle catalyzed hydrogenation of alkenes in bmim BF_4 and bmim PF_6, respectively.[194, 195] Later on, the Pd nanoparticle catalyzed hydrogenation of alkynes could be established in C_3CNmim NTf_2, too.[196] Important to note are also hydrogenation reactions of arenes (toluene, cyclohexene...) with Ir,[197] Rh,[198] Pt[199] or Ru[200] nanoparticles in various imidazolium based ionic liquids. These are capable to hydrogenate aromatic bonds and employ a completely different reaction mechanism on the nanoparticles' surface. Besides this, typical functionalisation reactions like borylations,[201] hydrosilylations[202] or *Fischer-Tropsch* reactions[203] are known with nanoscale catalysts in ionic liquids. And also catalytic defunctionalisation reactions like decarboxylations[40] or hydrodehalogenations[204] with Cu_2O and Pd nanoparticles are known, respectively.

2 | Scientific Aim

Establishing new synthetic methods for nano materials as catalysts for chemical reactions and their implementation into chemical reactions, with a focus on decarboxylative reactions, is the aim of this dissertation. The here presented topic is threefold: Nanoparticle synthesis and coincident incorporation into ionic liquids as well as the use of the nanoparticle/IL system in catalysis. Additionally, two overviewing articles concerning homogeneous and nanoscale catalyses shall highlight state of the art developments and background.
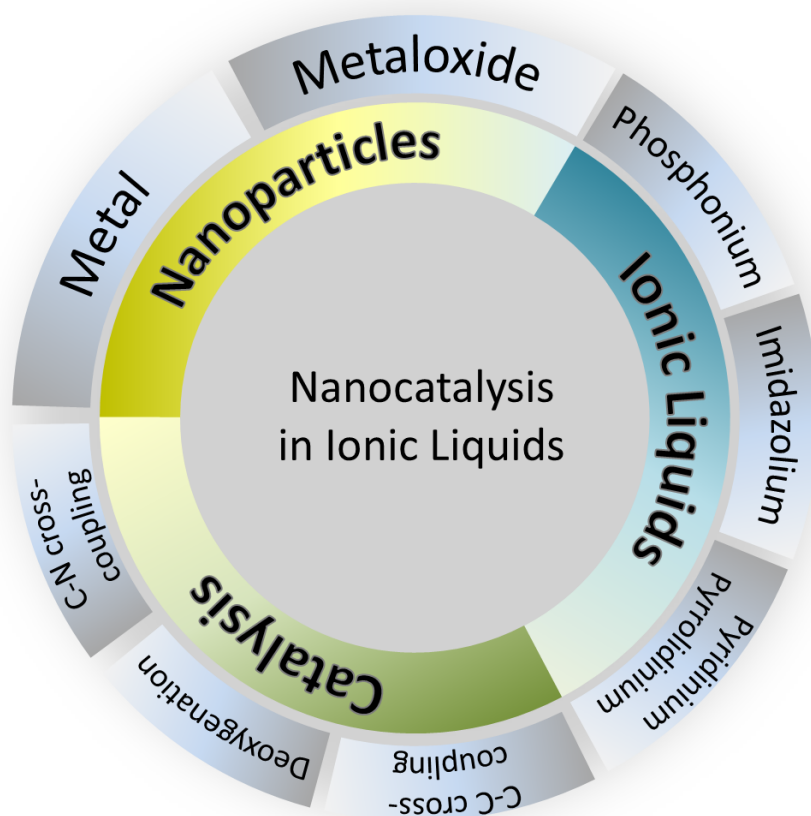
Figure 2.1: Subdivision of topics in this dissertation.

A versatile set of ionic liquids as reaction media for the nanoparticle syntheses is crucial. At first, this set should contain new as well as well-known ILs, in order to compare shape, size and morphology of the synthesized nano structures. Besides very popular imidazolium-based ionic liquids, which have been used for several other homogeneous, heterogeneous and

also nanoscale catalyses, phosphonium-based ionic liquids should be used as well. Their application in nano catalysis is rather scarce, even though they show remarkable stabilizing properties for nanoparticles.[184] The aspiration towards the ionic liquids is demanding: Low toxicity, low melting points and outstanding stabilizing effects towards the nanoparticles. With regard to the principles of "Green Chemistry", the synthesis of the ILs should be simple, few-stepped and straight forward, since their purification is challenging and would involve undesirable and toxic additives or produce extensive amounts of waste.

Secondly, nanoparticle precursors which are readily available and easy to handle, are supposed to be used and no purification should be necessary. The synthesis of sophisticated precursors often seems to be beneficial to yield pure and homogeneously divided nanoparticles, but involves large amounts of resources (energy, time, feedstock). To overcome these limitations with simple precursors, the reaction parameters and the work-up should preferably be sophisticated and optimized. Usually metal halides ($CuCl_2$, $PdCl_2$) are used as cheap precursors. However, halide ions are known to be fairly strong coordinating ligands (blocking the particle surface) and they further contaminate the catalytic phase.[38] In this context, acetate- and carbonate-based precursors might be more convenient, as they simply decarboxylate at elevated temperatures. The extrusion of non-toxic and gaseous CO_2 does not soil the catalytic phase at all. Furthermore, it is a central aim in this project to avoid reductive additives for the nanoparticle synthesis. Although molecular hydrogen is often utilized in thermal reductions of nanoparticle precursors and is thereby called environmentally friendly, it is mainly produced during syn-gas reactions. This involves not only a high energy consumption and an extensive CO_2 emission, but also the use of fossil resources which is environmentally unfavourable. The here presented approach renounces the use of additives and tries to establish a reductive milieu provided by the ionic liquid or the catalyst precursor itself.

In the third place, it is further designated to show the catalytic properties of a variety of selected nano materials and herein it should be demonstrated that well-known and homogeneously catalyzed reactions can also be conducted with nanoscale catalysts. Today the number of publications about nanoscale catalysis is emerging. But surprisingly, there is only little literature about new nanoscale reactions, e.g. *Stephens-Castro-*, *Buchwald-Hartwig-* or *Negishi*-reactions have not been realized for nanocatalyses although other classical cross-coupling reactions are well known with nanocatalysts. Up to now, the decarboxylation of benzoic acids are likewise unknown on the nano scale.

3 | Results and Discussion

In this dissertation the following chapter "Results and discussion" comprises five already published manuscripts and one published book-chapter. All text-content, pictures, schemes and tables are under copyright of Wiley-VCH (Weinheim) or the Royal Society of Chemistry (London) and reproduced with the corresponding permission (see Appendix). All publications are formatted to DIN A4 as claimed by attachment 4.b.3 of the PhD regulations 10/05/2012 (Anhang 4.b.3 der "Ordnung zur Änderung der Promotionsordnung der Mathematisch-Naturwissenschaftlichen Fakultät der Universität zu Köln vom 10. Mai 2012"). The following articles, listed in the order in which they appear in this thesis, are included:

Original research papers:

- M. T. Keßler, C. Gedig, S. Sahler, P. Wand, S. Robke, M. H. G. Prechtl*, "Recyclable Nanoscale Copper(I) Catalyst in Ionic Liquid Media for Selective Decarboxylative C-C Bond Cleavage" *Catal. Sci. Technol.* **2013**, 3, 992-1001 (full paper).

- M. T. Keßler, S. Robke, S. Sahler, M. H. G. Prechtl*, "Ligand-free copper(I) oxide nanoparticle-catalysed amination of aryl halides in ionic liquids" *Catal. Sci. Technol.* **2014**, 4, 102-108 (full paper).

- M. T. Keßler, M. K. Hentschel, C. Heinrichs, S. Roitsch, M. H. G. Prechtl*, "Fast track to nanomaterials: Microwave assisted ionothermal synthesis in ionic liquid media" *RSC Adv.* **2014**, 4, 14149-14156 (full paper).

- F. Heinrich, M. T. Keßler, S. Dohmen, M. Singh, M. H. G. Prechtl*, S. Mathur*, "Molecular Palladium Precursors for Pd^0 Nanoparticle Preparation by Microwave Irradiation: Synthesis, Structural Characterization and Catalytic Activity" *Eur. J. Inorg. Chem.* **2012**, 36, 6027-6033 (full paper).

Review articles/ secondary sources:

- M. T. Keßler, J. D. Scholten, F. Galbrecht, M. H. G. Prechtl*, "*Coupling Reactions in Ionic Liquids*" in "*Palladium-Catalyzed Cross-Coupling Reactions - Practical Aspects and Future Developments*" **2013**, ch. 6, p. 201-231, Wiley-VCH, Weinheim (book-chapter). DOI: 10.1002/9783527648283.ch6

- M. T. Keßler, M. H. G. Prechtl*, "Palladium Catalysed Aerobic Dehydrogenation of C-H Bonds in Cyclohexanones", *ChemCatChem* **2012**, 4, 326-327 (highlight-paper). DOI: 10.1002/cctc.201100361

Additional and unpublished work is given at the end of this chapter including Pd/Cu bimetallic catalyst preparation, deoxygenation reactions, a regioselective deuteration of 2-nitrobenzoic acid and the decarboxylative cross-coupling of 2-nitrobenzoic acid and iodobenzene.

3.1 Recyclable Nanoscale Copper(I) Catalyst in Ionic Liquid Media for Selective Decarboxylative C-C Bond Cleavage
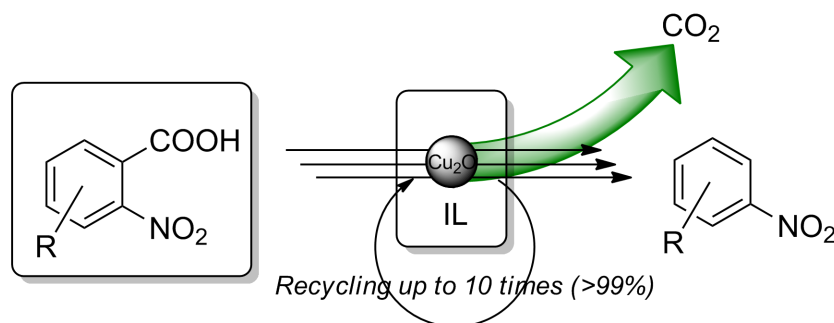
Michael T. Keßler,[a] Christian Gedig,[a] Sebastian Sahler,[a] Patricia Wand,[a] Silas Robke,[a] and Martin H.G. Prechtl[a*]

Here we report the synthesis and application of finely divided Cu_2O nanoparticles (Cu_2O-NPs) in the range from 5.5 nm to 8.0 nm in phosphonium ionic liquids as the first recyclable and effective catalytic system for smooth, ligand- and additive-free protodecarboxylation of 2-nitrobenzoic acid as model substrate and further derivatives. The reactions run with low catalyst loadings and result in quantitative yield in ten consecutive recycling experiments. In addition, this system is highly selective towards electron-poor 2-nitrobenzoic acids.

Catalysts are crucial mediators for most reactions in synthesis. They are used for bond-breaking and bond-making reactions in the sustainable production of bulk- and fine-chemicals.[1−3] In recent years modern nanocatalysis has emerged much interest in this field of scientific research as a useful and efficient tool for functionalisation and defunctionalisation reactions.[4,5] Carboxyl groups belong to the most common functionalities in organic molecules and catalytic decarboxylation reactions are therefore extremely useful and environmentally benign tools to eliminate surplus carboxylate groups in organic compounds. Furthermore, decarboxylative carbon-carbon cross coupling reactions are initiated by a decarboxylative step of a carboxylate salt, which represents a cheap substitute for expensive organometallic (e.g. organo-boron, organo-tin, organo-zinc) reagents.[6]
Nowadays metal nanoparticles, such as ruthenium,[7−15] platinum,[16] iridium,[17−19] palladium,[5,20−31] cobalt,[32] and iron[33] revealed their high potential of for their application[34] in homogeneous and heterogeneous catalysis, including hydrogenation,[7] hydrogenolysis,[35] Fischer-Tropsch reactions[32,36] and cross-coupling reactions.[4,5,21,23] Copper[37] and especially copper(I)oxide[38] nanoparticles combine the high catalytic activity of precious metals with easy providing and low costs. One drawback of neat metal and metal oxide nanoparticles is their poor recyclability and leaching effects leading to decreasing yields.[39] To overcome this problem, usually expensive nitrogen or phosphor containing ligands, surfactants or polymers are used to protect the nanoparticle surface from agglomeration, aggregation

and from leaching.[7,21] Ionic liquids (ILs) are promising reagents for surface protection, stabilising agent as well as green, non-hazardous solvents.[40] Ionic liquids exhibit a negligible vapour pressure, tunable solubilisation properties for several organic and inorganic compounds and are (electro-) chemically inert.

Additionally an ionic liquid phase containing the metal or metal oxide catalyst can be recycled several times without significant drop of yield.[23,40−42] Nitrogen containing ionic liquids, such as imidazolium, pyridinium or pyrrolidinium ILs with various counter anions are commonly used in nanocatalysis recycling experiments.[38,40,43] There are some reports about application of copper and copper oxide nanoparticles in ionic liquids, however most are related to electrochemistry and microelectronics and only very few report about application as catalysts in the wide field of organic synthesis.[37,38,40,44−54] The first report about colloidal copper catalyst for the coupling of aryl halides and activated olefins was reported by Heck in 1972.[54] More recently, it has been shown that nanoscale copper catalysts are released from copper bronze in ionic liquid media and these particles were active for the Heck reaction.[45] Further copper nanoparticle IL-systems were active for well-known reactions like the Stille,[46] Sonogashira,[44] and Buchwald-Hartwig coupling.[47] Moreover, copper nanocatalysts in IL support the coupling of aryl halides with ammonia yielding anilines,[55] diaryl ethers (or thioethers) are obtained by coupling phenols with aryl halides,[40,50,53] and unexpected coupling of olefines with THF was observed.[49] Unsurprisingly, copper nanocatalysts are also active for the homocoupling of alkynes, known as Ullmann coupling.[48,52]

A challenging reaction for the evaluation of nanoscale catalysts is the protodecarboxylation.[56,57] Notably, this reaction has not been evaluated yet for nanoscale catalysts in ionic liquids. Usually the model system for copper catalysts is the Ullmann reaction.[5,48,52] The protodecarboxylation reaction is a very smart method to defunctionalise an electron deficient aromatic ring carrying a carboxylic acid as potential leaving group in the presence of a Cu(I) catalyst. While highly activated carboxylic acids (e.g. perfluorinated benzoic acids) readily decarboxylate without any catalyst,[58] the removal of carboxylate groups from simple aromatic acids is much more complicated and often requires harsh reaction conditions, an inadequate use of copper or even more expensive silver salts as well as large amounts of additives.[59] In the present work we show that nanoscale copper(I)oxide (Cu_2O-NPs) embedded in ionic liquids is an active and recyclable catalyst for this reaction.

3.1.1 Synthesis of Cu_2O nanoparticles

The copper(I)oxide nanoparticles presented here were synthesised via thermal decomposition of basic $CuCO_3$ in different ionic liquid media. In this system no additional reducing agent, such as hydrazine or hydrogen, is necessary for the reduction of Cu(II) to Cu(I). We assume the structural nature and polarity of the ionic liquid plays a beneficial role in the reductive formation of Cu_2O nanoparticles. In previous works it has been shown that Pd nanoparticles are obtained by thermal decomposition of $Pd(OAc)_2$ in IL.[60] Furthermore, studies about the formation of ruthenium and nickel nanoparticles by decomposition of organometallic precursors in ionic liquids showed that (I) the anion plays an important role and (II) the IL itself is capable of inducing the decomposition by reaction with a complex.[9] In these cases minor amounts of IL suffered from decomposition and only traces of volatile compounds were detected in the gaseous phase, indicating decomposition of the IL. The nanoparticle synthesis in 3-butyl-1,2-dimethylimidazolium bis(trifluoromethyl-sulfonyl)imide (bmmim NTf_2) led to bulk material of Cu_2O (Table 3.1, Entry 1). Other imidazolium based ionic liquids (3-butyl-1-methylimidazolium bis(trifluoromethyl-sulfonyl)-imide (bmim NTf_2)) or pyridinium based ionic liquids (butylpyridinium bis

Table 3.1: Various ionic liquids for Cu_2O nanoparticle synthesis.

No.	prec.	IL	T [°C]	type	d [nm]
1	$CuCO_3$	bmmim NTf_2	120	n.d.	n.d.
2	$CuCO_3$	bmim NTf_2	120	n.d.	n.d.
3	$CuCO_3$	bpy NTf_2	120	n.d.	n.d.
4	$CuCO_3$	C_3CNmim NTf_2	120	n.d.	n.d.
5	$CuCO_3$	n-Bu_4POAc	120	Cu_2O	5.5 ($\pm$1.2)
6	$CuCO_3$	(n-$Bu_4P)_2SO_4$	120	n.d.	n.d.
7	$CuCO_3$	(n-$Bu_4P)_2SO_4$	160	Cu_2O	8.0 ($\pm$2.7)
8	$Cu(NO_3)_2$	n-Bu_4POAc	160	n.d.	n.d.
9	$Cu(OAc)_2$	n-Bu_4POAc	160	n.d.	bulk
10	CuI	n-Bu_4POAc	160	n.d.	n.d.
11	CuF_2	n-Bu_4POAc	160	n.d.	n.d.

Reaction conditions: Cu = 1 mmol Cu salt, 1 g IL, 3 h; n. d. = no decomposition; [a] particle size was determined by TEM.

(trifluoromethyl-sulfonyl)imide (bpy NTf_2)) were not able to decompose the copper salt even at elevated temperatures (Table 3.1, Entry 2+3). The use of copper(II)acetate did not improve the quality of particles either - no stable dispersion was observable, but bulk material was formed which indicates too fast decomposition. We tried a large variety of other simple copper salts, as copper nitrate, but there was no decomposition into Cu_2O detectable. We switched to alkyl-phosphonium-ILs as a low melting and more polar reaction medium.

$$CuCO_3 \xrightarrow[\text{n-Bu}_4\text{POAc}]{\text{3 h, 120 °C}} Cu_2O\text{-NP}$$
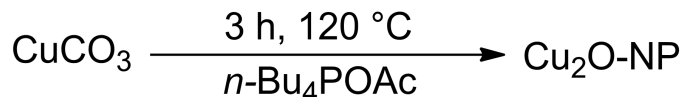
Scheme 3.1: Cu_2O nanoparticle synthesis in n-Bu_4POAc.

Tetrabutylphosphonium acetate (n-Bu_4POAc) and tetrabutylphosphonium sulphate ((n-$Bu_4P)_2SO_4$) seemed adequate because of their lower melting point and polarity in contrast to nitrogen containing ILs (Scheme 3.1).
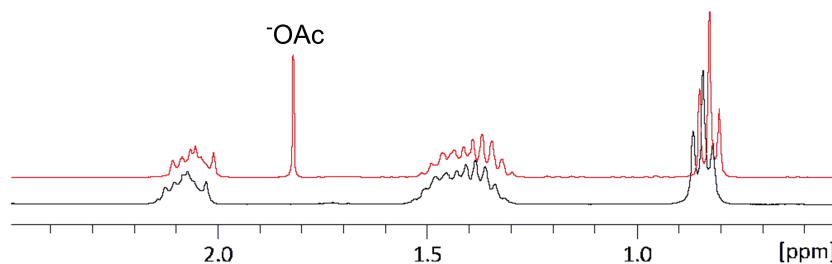
Figure 3.1: ^{1}H-NMR spectra of n-Bu_4POAc before (upper spectrum) and after (lower spectrum) the decomposition of $CuCO_3$. The acetate signal (δ=1.88 ppm) disappeared completely.

We were able to synthesise Cu_2O nanoparticles with small size and narrow size-distribution by simple thermal decomposition at 120 °C for 3 h as undoubtly confirmed by TEM and XRD. To explain the exact reaction pathway of the formation of Cu(I), we analysed the dispersion of the Cu_2O-NPs in (n-Bu$_4$POAc) IL by ^{1}H-NMR and ^{31}P-NMR, as well as by means of gaseous phase analysis with online-mass spectrometry.

After the completed nanoparticle synthesis, the ^{31}P- as well as the ^{1}H-NMR spectra showed no decomposition of the phosphonium cation at 120 °C, but the signals of the acetate protons completely vanished (Figure 3.1, $\delta = 1.83$ ppm). This indicates that Hofmann elimination does not play a relevant role in the reduction of Cu(II) to Cu(I), during the thermal treatment in n-Bu$_4$POAc at 120 °C, and it confirms that the acetate is capable to act as a reducing agent of the copper salt. Similar observations are known for other metal acetates.[60] During Hofmann elimination one would obtain trialkyl phosphine which could then subsequently result in trialkylphosphine oxide and Cu(I). However, the phosphonium cation remains mainly intact, whereas large amounts of CO_2 are formed due to decomposition of the acetate ions which can be detected by mass spectrometry.

The analysis of the gaseous phase by mass spectrometry showed only minor decomposition products (butene fragments; m/z = 56 and 55) of the degradation of the phosphonium cation in contrast to the extrusion of CO_2 (Figure 3.2). This means, the IL itself acts as a reducing and surface-protecting agent as well as the solvent. We detected large amounts of carbon dioxide (m/z = 44) in the gaseous phase (Figure 3.2) indicating that acetate ions are decomposed and act as reducing agent for the metal(II) species, where the IL cation plays a minor role for the reduction of the metal(II) species, but influences the stabilisation of NPs.[60] Further detected components were dinitrogen (m/z = 28/14), water (m/z = 18) and other components of air. For
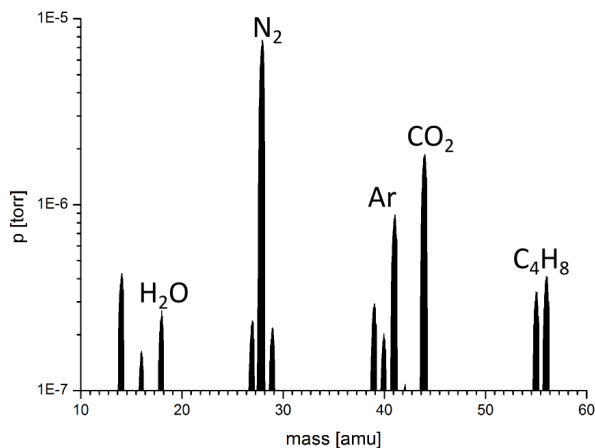
Figure 3.2: Online gas-phase mass-spectrogram recorded after the decomposition of $CuCO_3$ in n-Bu$_4$POAc at 120 °C.
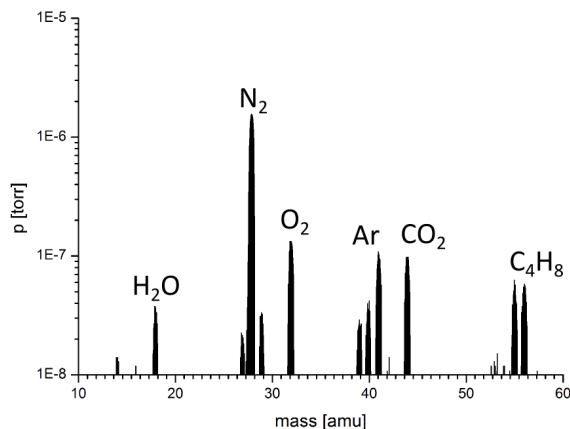
Figure 3.3: Online gas-phase mass-spectrogram recorded after the decomposition of $CuCO_3$ in (n-Bu$_4$P)$_2$SO$_4$ at 160 °C.

the decomposition in $(n\text{-Bu}_4P)_2SO_4$, where no acetate ions are present, the reduction only takes place at elevated temperatures (160 °C) and Hofmann elimination products are detectable in a further gas-phase mass-spectrogram (Figure 3.3) and in the ^{31}P-NMR spectrum a new peak appears (Figure 3.4, $\delta = 57.5$ ppm). A significant amount of butene fragments (m/z = 56 and 55) is detectable in the gas-phase mass-spectrogram during the decomposition of $CuCO_3$ in $(n\text{-Bu}_4P)_2SO_4$ at 160 °C.

Other signals correspond to air compounds like oxygen, nitrogen and water. Furthermore, a new phosphorus species (tributyl phosphine oxide) is detectable in the ^{31}P-NMR spectrum (57.5 ppm),[61] taken from the reaction mixture right after completion of the nanoparticle synthesis. Due to the extremely low vapour pressure of the ionic liquids, the Cu_2O nanoparticles could be characterised directly in the IL medium using TEM techniques and additionally by XRD. TEM pictures of Cu_2O nanoparticles both in $n\text{-Bu}_4POAc$ and in $(n\text{-Bu}_4P)_2SO_4$ are shown in Figure 3.6 and Figure 3.7. The average diameter of the monodispersed and uniformly shaped Cu_2O nanoparticles is about 5.5 nm (±1.2 nm) in $n\text{-Bu}_4POAc$ and 8.0 nm (±2.7 nm) in $(n\text{-Bu}_4P)_2SO_4$, respectively. The different sizes of the NPs arouse from two different reaction mechanisms and reaction temperatures in the decompositions.

Figure 3.4: ^{31}P-NMR spectra of $(n\text{-Bu}_4P)_2SO_4$ before (upper sprectrum) and after (lower spectrum) the decomposition of $CuCO_3$ at 160 °C. The signal at 57.5 ppm corresponds to tributylphosphine oxide.[61]

In $n\text{-Bu}_4POAc$ at 120 °C the acetate ion is the reductant whereas in $(n\text{-Bu}_4P)_2SO_4$ a higher temperature is necessary (160 °C) and Hofmann elimination of the tetrabutylphosphonium cations leads to tributylphosphine which readily reduces Cu(II) to give Cu(I) and tributylphosphine oxide. The particles are finely separated and show a homogeneous spherical shape. The XRD pattern clearly shows pure Cu_2O without any impurities of other copper species (Figure 3.5). The signals at small angles originate from the preparation foil for the XRD-samples. According to the Scherrer equation the nanocrystalite size corresponds to 24 nm, which is larger than the particle size determined by TEM analysis, which might be due to aggregation during preparation of the XRD-powder sample (see experimental section), however it confirms the formation of Cu_2O-nanoparticles. Moreover, the size of nanoparticles in powder XRD patterns is often overestimated in case of a broader particle size distribution; vice versa for a very narrow size distribution determined by TEM the nanocrystallite size determined by XRD fits well.[62,63] In the present case of the larger particles the vast majority of copper(I)oxide is in the inner shells of the nanoparticles.

This results in large reflexes in the XRD patterns which overlay reflexes of smaller particles. The estimated diameter by the Scherrer equation can therefore be considered as an upper size limit of the nanoparticles in the NP/IL dispersion. Regarding the evaluation of the nanoscale Cu_2O for their application in catalysis, the surface to volume ratio of the
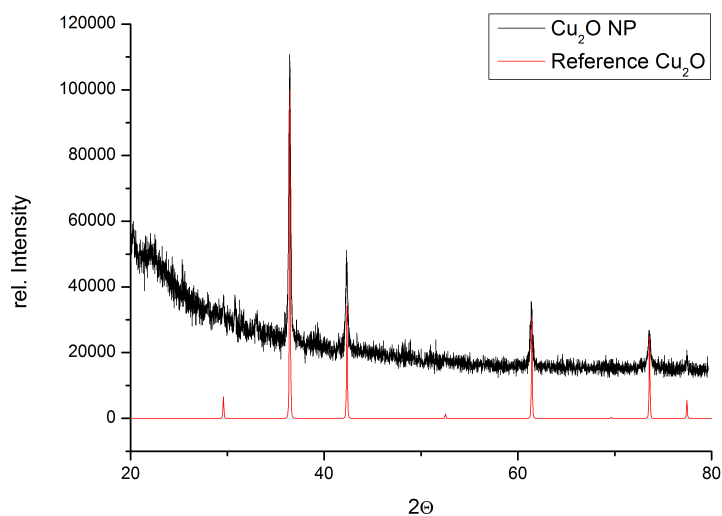
Figure 3.5: XRD-pattern of Cu_2O (cubic Cu_2O) nanoparticles synthesised in tetrabutylphosphonium ionic liquid n-Bu_4POAc.
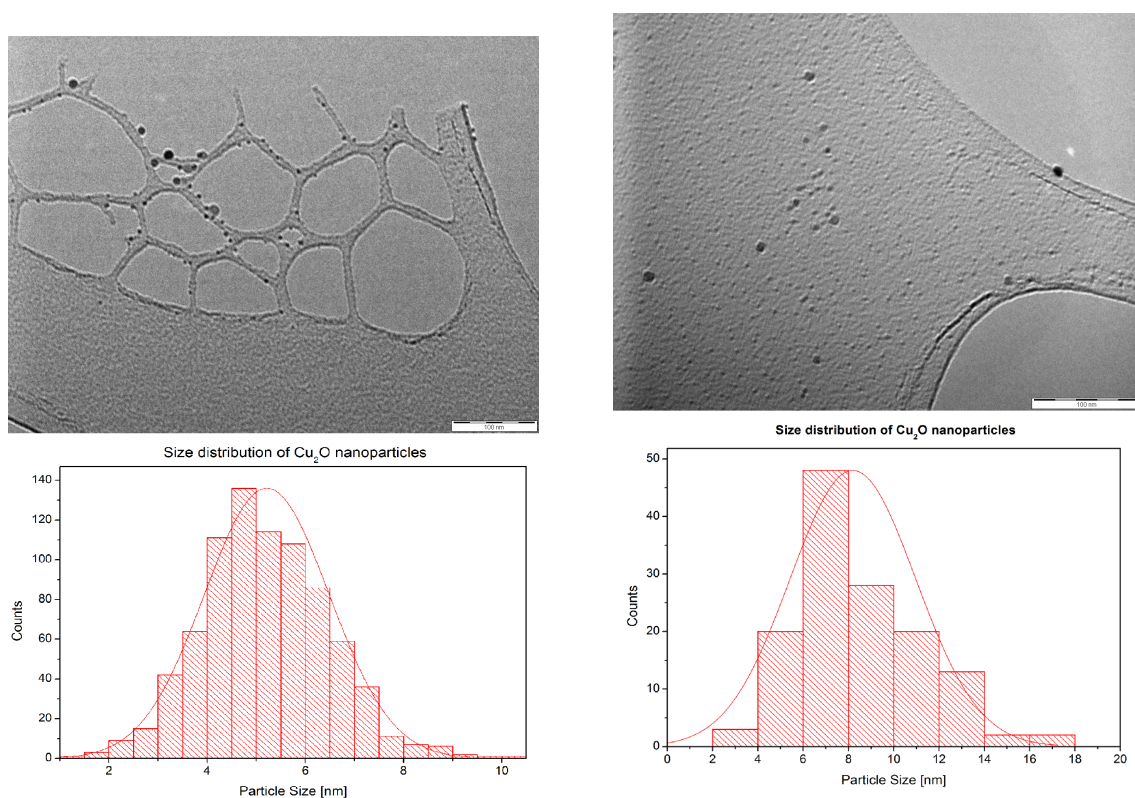
Figure 3.6: TEM picture (top) of Cu_2O nanoparticles synthesised in n-Bu_4POAc and size distribution (bottom) – the average diameter is 5.5 nm (± 1.2 nm). The scale bar of the TEM image is 100 nm.

Figure 3.7: TEM picture (top) of Cu_2O nanoparticles synthesised in (n-$Bu_4P)_2SO_4$ and size distribution (bottom) – the average diameter is 8.0 nm (± 2.7 nm). The scale bar of the TEM image is 100 nm.

particles must be considered. Although we cannot exclude that some partial aggregations and topology changes might occur,[64] merely copper ions on the surface are capable to act as catalyst. For the determination of the percentage of copper ions in Cu_2O exposed to the surface, we calculated the volume of a spherical particle of Cu_2O in n-Bu_4POAc with a diameter of 5.5 nm. The volume is about $87.1 \, nm^3$ containing approx. 4477 Cu(I) ions. Applying the magic number methodology,[65−67] as the established tool for the general evaluation of cluster formation and surface to volume ratio, the particle contains approximately 1563 Cu(I) ions exposed to the surface (taking into account the stoichiometry and composition of the elemental cell of Cu_2O). This means that 35% of the Cu(I) are surface ions and potentially active in a heterogeneous catalysed reaction. For the Cu_2O-NPs in $(n$-$Bu_4P)_2SO_4$ with a mean diameter of 8.0 nm about 26% of the Cu(I) are surface ions. Interestingly, the obtained nanoparticles form dispersions in other solvents such as acetone, isopropanol or even water, which make them highly interesting for synthetic application in nanocatalytic reactions and multiphase reactions.

3.1.2 Protodecarboxylation reactions
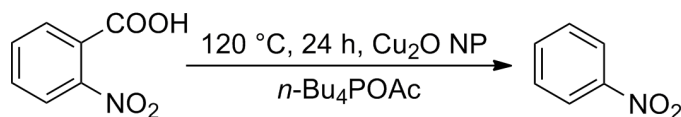
Scheme 3.2: Protodecarboxylation of 2-nitrobenzoic acid **1** with Cu_2O nanoparticles in n-Bu_4POAc.

For the evaluation of the catalytic properties of the Cu_2O nanoparticles, we chose the protodecarboxylation reaction. This reaction has been tested previously only with molecular copper complexes and copper salts, but not with nanoscale catalysts and none of the previous catalyst systems was suitable for recycling.[56,57]

The nanoscale copper catalysts have been prepared as described above using $CuCO_3$. Additionally, $Cu(OAc)_2$ and $Cu(NO_3)_2$ have been tested in ionic liquid media for the protodecarboxylation under different reaction conditions for the decarboxylation of 2-nitrobenzoic acid **1** (Table 3.2). Then the benzoic acid derivative and optional additives as well as water were added to the reaction medium. Quantitative yield could be obtained with Cu_2O nanoparticles derived from copper carbonate (3 mmol) in n-Bu_4POAc (Table 3.2; Entry 6). Considering that 35% of the Cu(I) are surface ions, roughly 1.05 mmol $(105 \, mol\%_{surface})$ of the Cu(I) in the particle is potentially active for promoting the C-C bond cleavage reaction in benzoic acid **1**. Lowering the copper concentration to 1 mmol, hence $35 \, mol\%_{surface}$ of the Cu(I) are exposed to the surface, remarkably still 61% of the benzoic acid *1* is catalytically decarboxylated at 120 °C (Entry 2). A catalyst loading of $17.5 \, mol\%_{surface}$ Cu_2O nanoparticles in $(n$-$Bu_4P)_2SO_4$ IL showed a conversion in the same range (51%) at 160 °C (Entry 7). Taking into account the larger particle size of the Cu_2O-NPs in $(n$-$Bu_4P)_2SO_4$ (8.0 nm) the activity is comparable to those in n-Bu_4POAc.

Interestingly the initially used additives like KF and K_2CO_3 were not necessary for the reaction nor did they improve yields. The reaction shows remarkable temperature sensitivity. At temperatures below 100 °C no product could be obtained (Entry 1). The optimal temperature is between 120 °C and 160 °C depending on the IL and the used copper salt. The best conversions using Cu_2O-NPs $(35 \, mol\%_{surface})$ could be obtained after 24 h as shown in Figure 3.8. After an initiation period of about two hours, the yield increases almost linearly reaching a top value of 65% after 24 h and stagnates. Even a reaction

Table 3.2: Variation of the reaction conditions and ionic liquid media for the protodecarboxylation of 2-nitrobenzoic acid **1**.

Entry	cat.	IL	additives	T [°C]	yield * %
1	Cu_2O-NP^a	n-Bu$_4$POAc		80	1
2	Cu_2O-NP^a	n-Bu$_4$POAc		120	61
3	Cu_2O-NP^a	n-Bu$_4$POAc	KF, K_2CO_3	120	59
4	Cu_2O-NP^a	n-Bu$_4$POAc	KF	120	58
5	Cu_2O-NP^a	n-Bu$_4$POAc	K_2CO_3	120	55
6	Cu_2O-NP^b	n-Bu$_4$POAc		120	100
7	Cu_2O-NP^c	(n-Bu$_4$P)$_2$SO$_4$		160	51
8	$CuCO_3$^{d}	bmim OMs		120	39
9	$Cu(OAc)_2$^{d}	bmim OMs		120	24
10	$Cu(NO_3)_2$^{d}	bmim OMs		160	39
11	$CuCO_3$^{d}	C_3CNmim OAc		120	23
12	Cu_2O^{e}	n-Bu$_4$POAc		120	20

Reaction conditions: ^{a} 1 mmol 2-nitrobenzoic acid **1**, Cu_2O-NPs (35 mol%$_{surface}$) in 1 g IL, ^{b} with Cu_2O-NPs (105 mol%$_{surface}$), ^{c} Cu_2O-NPs (17.5 mol%$_{surface}$) in 1 g IL, ^{d} 1 mmol 2-nitrobenzoic acid **1**, 1 mmol Cu-source in 1 g IL, ^{e} commercial copper(I)oxide. Reaction time: 24 h. * Conversions were determined by ^{1}H NMR and hexamethyldisilane as internal standard.
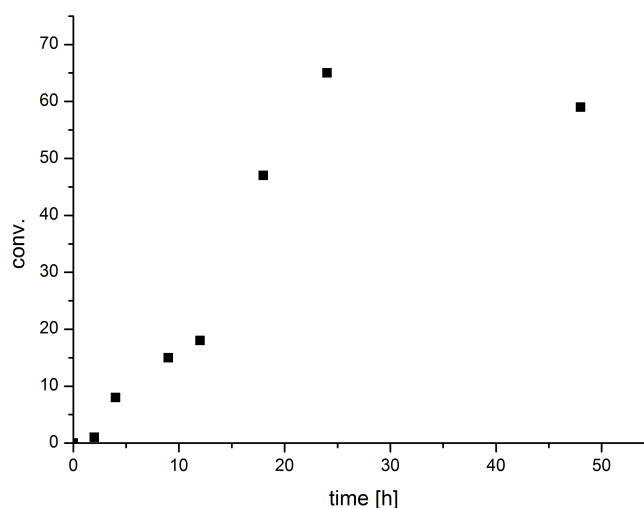
Figure 3.8: Conversion of 2-nitrobenzoic acid **1** into nitrobenzene **2** in n-Bu$_4$POAc at 120 °C depending on the reaction time.

time of about 48 h does not lead to an enhanced conversion. 3-Butyl-1-methylimidazolium bis(trifluoromethyl-sulfonyl)imide (bmim NTf$_2$) is a relatively nonpolar ionic liquid, which does not dissolve inorganic salts sufficiently and is not miscible with water, has been proven to be unsuitable for the decarboxylation reaction. A simple and halide-free polar ionic liquid is 3-butyl-1-methyl imidazolium methylsulfonate (bmim Ms; Entry 8-10). Although bmim Ms is a nitrogen containing IL with a high melting point, it is readily soluble in water and forms a viscous liquid. The conversions of the protodecarboxylation in bmim Ms were (<40%), but significantly lower than in n-Bu$_4$POAc (Entry 2). Interestingly, in bmim Ms it is even possible to use copper salts like Cu(OAc)$_2$ or Cu(NO$_3$)$_2$ to promote the decarboxylation of 2-nitrobenzoic acid **1**. The activation energy of the decarboxylation is depending on the copper-source (Cu$_2$O-NP, Cu(NO$_3$)$_2$, Cu(OAc)$_2$...) and on the polarity of the solvating medium (n-Bu$_4$POAc, ((n-Bu)$_4$P)$_2$SO$_4$, bmim Ms...). The formation and stabilisation of two transition states during the decarboxylation step are crucial for the reaction temperature, which has already been calculated with DFT-methods by *Su and co-workers*.[68] All polar ionic liquids used here form homogeneous suspensions, and the organic products can be easily separated by extraction with nonpolar organic solvents. The relatively high viscosity of the catalytic phase simplifies the extraction and separation step with e.g. Et$_2$O or n-pentane, therefore the organic product can be easily isolated and the catalytically active IL-phase is recyclable for further batch experiments.
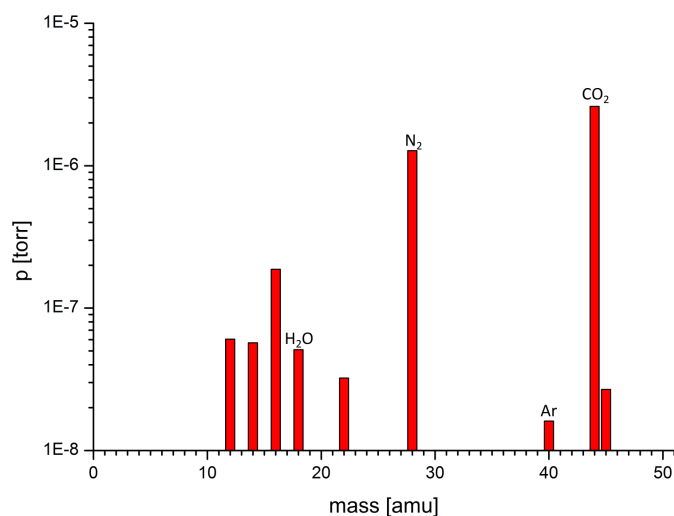
Figure 3.9: Mass spectrum of the gas phase in a typical protodecarboxylation reaction measured at 1.75 bar.

The gaseous products have been analysed by mass-spectrometry. The mass spectrum (Figure 3.9) shows clearly, that no further side reaction took place and that CO$_2$ is extruded in high amounts. About 61% of the analysed gas probe corresponds to carbon dioxide (m/z= 44), 30% dinitrogen and 4% oxygen as well as minor amounts of nitrogen and water. The probe was taken directly out of the autoclave system via a mass flow controller.

3.1.3 Recycling experiments

As previously described, the phosphonium ionic liquids used here are superior concerning nanoparticle protection, due to long term stabilisation of the nanoparticle dispersions. Additionally, the ILs exhibit a polarity, which makes them interesting for recycling experiments. The product nitrobenzene **2** can be separated by extraction with a nonpolar organic solvent without leaching of the nanoparticles or of the ionic liquid itself. Interestingly the residual phase containing the Cu_2O nanoparticles can be recycled several times (up to ten times, see below), by simple reloading with carboxylic acid as substrate. In the following diagram the recycling experiments with the corresponding yields are shown (Figure 3.10).
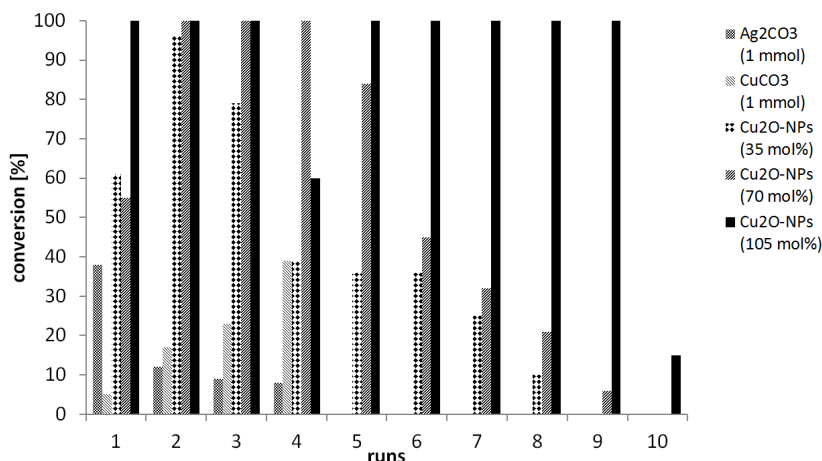
Figure 3.10: Recycling experiments of the decarboxylation of 2-nitrobenzoic acid **1** in IL media.

The best results concerning long-term stability of the catalyst, recyclability and conversion have been obtained in n-Bu_4POAc with an amount of 105 mol%$_{surface}$ of Cu_2O-NPs, quantitative conversion has been obtained in almost all runs giving a total TON of 88 accumulated over the ten runs (Figure 3.10; black scales). After ten runs the catalyst loading can be considered as 10.5 mol%$_{surface}$. Catalyst loadings of 70 mol%$_{surface}$ Cu_2O-NPs (7.0 mol%$_{surface}$ after ten runs) showed after the initial first run quantitative conversion in the next three runs, then the conversions decreased significantly after each run (Figure 3.10; dark grey scale). Lowering the catalyst loading to 35 mol%$_{surface}$ (3.5 mol%$_{surface}$ in ten runs) the yields increased after the first run drastically and reached a remarkable top yield of about 96% (Figure 3.10; dashed grey scale). Even after five cycles there was a considerable amount of nitrobenzene **2** detectable and up to eight reactions in one batch could be carried out. The recycling experiments with $CuCO_3$ in bmim Ms, showed low conversions (<40%) over four runs and then no further activity has been observed (light grey scales). Although silver salts are known to be superior decarboxylation catalysts,[59,69] Ag_2CO_3 in bmim Ms only resulted in conversions <40% in four runs (Figure 3.10; grey scale bars; left). Obviously the ionic liquid itself plays a crucial role in both the nanoscale decarboxylation reaction and in the nanoparticle synthesis.
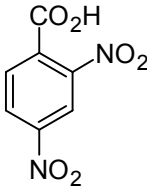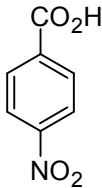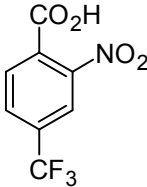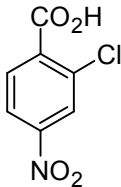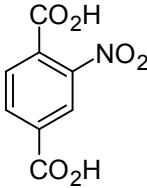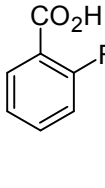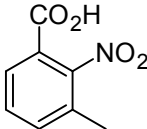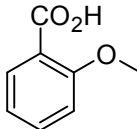
3.1.4 Substrate scope of benzoic acid derivatives

To prove the versatility of the nanocatalyst system we performed the decarboxylation reaction on different benzoic acid derivatives. The reaction could be performed with moderate to good conversions with 2-nitrobenzoic acid derivatives (Table 3.3, Entry 1-10). Conver-

sions of about 65% to 40% could be reached with halide substituents of a 2-nitrobenzoic acid derivative in para-position (Entry 5 and 6). Other electron-withdrawing groups in para-position, like a nitro- or a trifluoromethyl-group, seem to be beneficial, too (Entry 1 and 2). Only low conversions could be reached with substituents in meta-position (Entry 7-9) except methyl-groups (Entry 4 and 10). Interestingly no conversion of other benzoic acid derivatives could be observed (Entry 11-22) – even with highly electron-deficient benzoic acids, like 2-chloro-4-nitrobenzoic acid (Entry 13) and 2-chloro-4-fluorobenzoic acid (Entry 17). In fact, the nitro group in ortho-position seems to be crucial for the nanoparticle catalysed decarboxylation of the benzoic acid derivatives – maybe due to a coordination of the nitro-group to the surface of a nanoparticle. In contrast, a single nitro group in para-position did not lead to an increasing conversion (Entry 12).
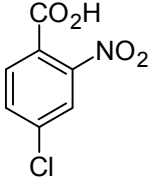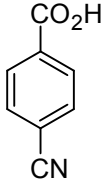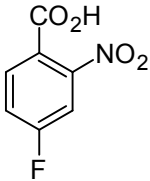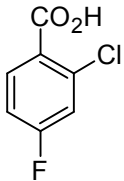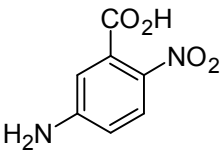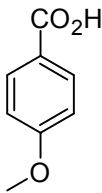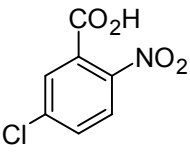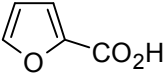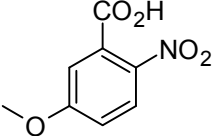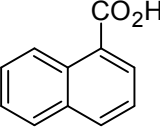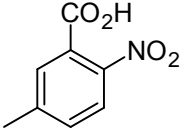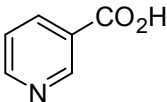
Table 3.3: Substrate screening for protodecarboxylation reactions of different benzoic acids in n-Bu$_4$POAc with Cu$_2$O nanoparticles.
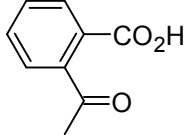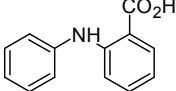
Entry	Acid	Conv.^{a} [%]	Entry	Acid	Conv.^{a} [%]
1		24	12		0
2		32	13		0
3		10	14		0
4		30	15		0

Table 3.3: Substrate screening for protodecarboxylation reactions. *(Continuation)*

Entry	Acid	Conv.[a] [%]	Entry	Acid	Conv.[a] [%]
5		65	16		0
6		40	17		0
7		10	18		0
8		21	19		0
9		15	20		0
10		26	21		0

Table 3.3: Substrate screening for protodecarboxylation reactions. *(Continuation)*

Entry	Acid	Conv.[a] [%]	Entry	Acid	Conv.[a] [%]
11		0	22		0

Reaction conditions: 1 mmol benzoic acid **1–22**, 1 mmol Cu_2O in 1 g n-Bu$_4$POAc, 24 h, 120 °C.[a] Conversions were determined by ^{1}H-NMR and hexamethyldisilane as the internal standard.

3.1.5 Chemo-selectivity in mixtures of benzoic acids

Table 3.4: Chemo-Selectivity of the nanoscale protodecarboxylation in presence of a selection of different benzoic acid derivatives.

Entry	Acid A	Acid B	yield [%] A:B	sel. [%] A:B
1	**1**	**12**	57:0	100:0
2	**1**	**13**	39:0	100:0
3	**1**	**15**	50:0	100:0
4	**1**	**16**	48:0	100:0
5	**1**	**17**	23:0	100:0
6	**1**	**18**	47:0	100:0
7	**1**	**23**	78:0	100:0
8	**1**	**24**	62:0	100:0

Reaction conditions: [a] Acid A: 1 mmol 2-nitrobenzoic acid **1**, Acid B: 1 mmol benzoic acid (4-nitrobenzoic acid **12**, 4-nitro-2-chloro benzoic acid **13**, 2-methoxybenzoic acid **15**, 4-cyanobenzoic acid **16**, 2-chloro-4-fluoro benzoic acid **17**, 4-methoxybenzoic acid **18**, 2-sulfonic benzoic acid **23**, 4-aminobenzoic acid **24**,), Cu_2O-NPs (35 mol%$_{surface}$) in 1 g IL, Reaction time: 24 h. *Yields were determined by ^{1}H-NMR and hexamethyldisilane as internal standard.

One very important issue is the selectivity of decarboxylation reactions towards different benzoic acid derivatives. Usually copper catalysed protodecarboxylation reactions can be easily conducted with benzoic acids containing an electron deficient aromatic ring-system – no matter which kind of substituents they bear.[56] Therefore, we tried to decarboxylate selectively the model substrate in a reaction mixture with different benzoic acids. This nanocatalytic approach is the first that can selectively decarboxylate 2-nitrobenzoic acid **1** in the presence of other benzoic acids with comparable electron poor aromatic rings with considerable yields. Even 4-nitro-2-chloro benzoic acid **4** is not affected under the reaction parameters given here (Table 3.4, Entry 2). In all cases the selectivity for decarboxylation was 100% towards **1** (Table 3.4). Interestingly, the yield of the decarboxylation product, nitrobenzene **2**, varied between 23-78% depending on the presence of the second benzoic

acid. The lowest conversion of 2-nitrobenzoic acid **1** into nitrobenzene **2** was obtained in presence of 4-chloro-2-fluoro benzoic acid **3** (23%; Table 3.4, Entry 1), and the highest conversion (78%) was possible in presence of 2-sulfonic benzoic acid **5**. The influence of the second benzoic acid regarding the different conversions during the decarboxylation of 2-nitrobenzoic acid **1** is still unclear.

3.1.6 Experimental

General

n-Bu$_4$POH in 40 wt% aqueous solution, basic CuCO$_3$, CuF$_2$ and all benzoic acids (**1**, **2-10**) were obtained from ABCR® Chemicals, CuI and methylimidazole were purchased from Sigma Aldrich®, methane sulfonyl chloride was purchased from Fluka®. Cu(NO$_3$)$_2$ and Cu(OAc)$_2$ were used from chemicals stock of the institute. All chemicals were used without further purification and all reactions were conducted without inert conditions.
^{1}H-NMR and ^{31}P-NMR spectra were recorded on a Bruker® AVANCE II 300 spectrometer at 298 K (300.1 MHz, external standard tetramethylsilane (TMS)). The obtained Cu$_2$O nanoparticles were analysed by powder X-ray diffractometry (STOE®-STADI MP, Cu-K$_\alpha$ irradiation, $\lambda = 1.540598$ Å) and by TEM Phillips® EM 420, 120 kV. Mass spectra were recorded on HIDEN® HPR-20QIC equipped with Bronkhorst® EL-FLOW Select mass flow meter/controller. Experiments for gas phase analysis at elevated pressure were performed in a stainless steel autoclave purchased from Carl-Roth® with a direct connection to the MS-spectrometer via the mass flow controller.

n-Bu$_4$POAc

The synthesis of n-Bu$_4$POAc is adapted from ref. 47 and modified to our preparative demands. In a 100ml round bottom flask 50 ml 40 wt% tetrabutylphosphonium hydroxide solution (72.4 mmol; n-Bu$_4$POH) is mixed with 4.12 ml (72.4 mmol) of 99% acetic acid under vigorous stirring. After further stirring for 25 min the residual water is removed under reduced pressure at 60 °C. The resulting ionic liquid is further dried under reduced pressure for 72 h leaving a hygroscopic waxy solid behind. Yield 20.8 g (95%). ^{1}H-NMR (300 MHz, rt, CDCl$_3$): δ (ppm) = 2.07-2.18 m (8H), 1.48-1.58 q (8H), 1.36-1.48 q (8H), 0.86-0.93 t (12H). ^{31}P-NMR (60 MHz, rt, CDCl$_3$): δ (ppm) = 33.25.

(n-Bu$_4$P)$_2$SO$_4$

Tetrabutylphosphonium sulphate was synthesized analogously with a 10% sulphuric acid solution (72.4 mmol). The resulting ionic liquid was a hygroscopic waxy solid. Yield: 27.8 g (99%) ^{1}H-NMR (300 MHz, rt, CDCl$_3$): δ (ppm) = 2.06-2.18 q (8H), 1.47-1.59 q (8H), 1.36-1.48 q (8H), 0.86-0.93 t (12 H). ^{31}P-NMR (60 MHz, rt, CDCl$_3$): δ (ppm) = 33.25.

All other ILs were synthesized according to literature known methods.[7,9,42,70,71]

Nanoparticles synthesis

The Cu$_2$O nanoparticles were synthesized in an oven-dried 25ml crimp top vial equipped with a butyl-rubber septum and a glass stirring bar. 1 mmol (221 mg) basic CuCO$_3$ was suspended in 1 g IL and heated to 120 °C for 3 h while stirring at 500 rpm in a vial holder. The resulting precipitate was a brownish red dispersion of Cu$_2$O nanoparticles in IL. The particles in IL could be easily dispersed in acetone, ethanol or isopropanol.

Sample preparation for TEM analysis

A droplet of Cu_2O-NPs embedded in IL was dispersed in acetone and a slight amount of this dispersion was placed in a holey carbon-coated copper grid. Particle size distributions were determined from the digital images obtained with a CCD camera. The NPs diameter was estimated from ensembles of 400 particles (800 counts) chosen in arbitrary areas of the enlarged micrographs. The diameters of the particles in the micrographs were measured using the software Sigma Scan Pro 5 and Lince Linear Intercept 2.4.2.

Sample preparation for XRD analysis

The nanoparticle dispersion was dispersed in 10 ml acetone and centrifuged to yield a dark brown precipitate, which was filtered of and washed three times with acetone. The powder was dried under vacuum and prepared between two plastic disks before measurement.

Procedure for protodecarboxylation reactions

The resulting nanoparticle dispersion was cooled to room-temperature (see nanoparticle synthesis). 1 mmol 2-nitrobenzoic acid **1** (167 mg) was then added to the dispersion and heated to 120 °C for 24 h. After cooling to room temperature the reaction mixture was extracted with 3x10 ml Et_2O. The organic phase was separated and the solvent removed under reduced pressure. The residue was analysed by ^{1}H-NMR (internal standard: hexamethyldisilane, 0.1 mmol, 20 μl) and compared with literature data. In the chemo-selectivity experiments 1 mmol of benzoic acids **3-10** has been added to the mixture.

3.1.7 Conclusion

We showed a versatile and simple method to synthesize Cu_2O nanoparticles in tetrabutylphosphonium acetate and sulphate resulting in small and uniformly sized nanocatalysts with an average diameter of 5.5 nm ($\pm$1.2 nm) and 8.0 nm ($\pm$2.7 nm), respectively. These incorporated nanoparticles are very potent in catalysing protodecarboxylation reactions of 2-nitrobenzoic acid **1** and derivatives with low catalyst loadings especially in recycling reactions. The IL/nanocat. system was compared to other IL/nanocat. systems with different polar and nonpolar ionic liquids as well as different copper-precursors, showing predominance concerning yield and recyclability. This catalytic phase, consisting of nanocatalysts in the ionic liquid, is superior for recycling experiments and can be recycled up to ten times. Pointing out that this is the first nanoscale and the first recyclable catalyst proven to be active for decarboxylation reactions.

3.1.8 Acknowledgement

3.1.9 Notes and references

[a] University of Cologne, Department of Chemistry,
Institute of Inorganic Chemistry, Greinstraße 6, 50939 Cologne, Germany.

E-Mail: martin.prechtl@uni-koeln.de;
http://catalysis.uni-koeln.de; Fax: 0049 221 4701788

1. A. Fukuoka and P. L. Dhepe, *Chem. Rec.*, **2009**, 9, 224-235.

2. J. Julis, M. Holscher and W. Leitner, *Green Chem.*, **2010**, 12, 1634-1639.

3. A. Behr, J. Eilting, K. Irawadi, J. Leschinski and F. Lindner, *Green Chem.*, **2008**, 10, 13-30.

4. D. Astruc, *Inorg. Chem.*, **2007**, 46, 1884-1894.

5. M. H. G. Prechtl, J. D. Scholten and J. Dupont, *Molecules*, **2010**, 15, 3441-3461.

6. A. G. Myers, D. Tanaka and M. R. Mannion, *J. Am. Chem. Soc.*, **2002**, 124, 11250-11251.

7. M. H. G. Prechtl, M. Scariot, J. D. Scholten, G. Machado, S. R. Teixeira and J. Dupont, *Inorg. Chem.*, **2008**, 47, 8995-9001.

8. M. H. G. Prechtl, J. D. Scholten and J. Dupont, *J. Mol. Catal. A*, **2009**, 313, 74-78.

9. M. H. G. Prechtl, P. S. Campbell, J. D. Scholten, G. B. Fraser, G. Machado, C. C. Santini, J. Dupont and Y. Chauvin, *Nanoscale*, **2010**, 2, 2601-2606.

10. T. Gutel, J. Garcia-Anton, K. Pelzer, K. Philippot, C. C. Santini, Y. Chauvin, B. Chaudret and J. M. Basset, *J. Mater. Chem.*, **2007**, 17, 3290-3292.

11. T. Gutel, C. C. Santini, K. Philippot, A. Padua, K. Pelzer, B. Chaudret, Y. Chauvin and J. M. Basset, *J. Mater. Chem.*, **2009**, 19, 3624-3631.

12. P. S. Campbell, C. C. Santini, F. Bayard, Y. Chauvin, V. Colliere, A. Podgorsek, M. F. C. Gomes and J. Sa, *J. Catal.*, **2010**, 275, 99-107.

13. P. S. Campbell, C. C. Santini, D. Bouchu, B. Fenet, K. Philippot, B. Chaudret, A. A. H. Padua and Y. Chauvin, *Phys Chem Chem Phys*, **2010**, 12, 4217-4223.

14. G. Salas, A. Podgorsek, P. S. Campbell, C. C. Santini, A. A. H. Padua, M. F. C. Gomes, K. Philippot, B. Chaudret and M. Turmine, *Phys Chem Chem Phys*, **2011**, 13, 13527-13536.

15. G. Salas, C. C. Santini, K. Philippot, V. Colliere, B. Chaudret, B. Fenet and P. F. Fazzini, *Dalton T*, **2011**, 40, 4660-4668.

16. C. W. Scheeren, G. Machado, S. R. Teixeira, J. Morais, J. B. Domingos and J. Dupont, *J. Phys. Chem. B*, **2006**, 110, 13011-13020.

17. G. S. Fonseca, A. P. Umpierre, P. F. P. Fichtner, S. R. Teixeira and J. Dupont, *Chem. Eur. J.*, **2003**, 9, 3263-3269.

18. G. S. Fonseca, J. D. Scholten and J. Dupont, *Synlett*, **2004**, 1525-1528.

19. J. Dupont, G. S. Fonseca, A. P. Umpierre, P. F. P. Fichtner and S. R. Teixeira, *J. Am. Chem. Soc.*, **2002**, 124, 4228-4229.

20. M. H. G. Prechtl, J. D. Scholten and J. Dupont, in *Ionic Liquids: Applications and Perspectives*, ed. A. Kokorin, InTech, Vienna, **2011**, pp. 393-414.

21. C. C. Cassol, A. P. Umpierre, G. Machado, S. I. Wolke and J. Dupont, *J. Am. Chem. Soc.*, **2005**, 127, 3298-3299.

22. C. S. Consorti, R. F. de Souza, J. Dupont and P. A. Z. Suarez, *Quim Nova*, **2001**, 24, 830-837.

23. A. Balanta, C. Godard and C. Claver, *Chem. Soc. Rev.*, **2011**, 40, 4973-4985.

24. S. Jansat, M. Gomez, K. Philippot, G. Muller, E. Guiu, C. Claver, S. Castillon and B. Chaudret, *J. Am. Chem. Soc.*, **2004**, 126.

25. F. Fernandez, B. Cordero, J. Durand, G. Muller, F. Malbosc, Y. Kihn, E. Teuma and M. Gomez, *Dalton T*, **2007**.

26. S. Jansat, J. Durand, I. Favier, F. Malbosc, C. Pradel, E. Teuma and M. Gomez, *Chemcatchem*, **2009**, 1.

27. D. Sanhes, E. Raluy, S. Retory, N. Saffon, E. Teuma and M. Gomez, *Dalton T*, **2010**, 39.

28. I. Favier, A. B. Castillo, C. Godard, S. Castillon, C. Claver, M. Gomez and E. Teuma, *Chem Commun*, **2011**, 47.

29. I. Favier, D. Madec, E. Teuma and M. Gomez, *Curr. Org. Chem.*, **2011**, 15.

30. E. Raluy, I. Favier, A. M. Lopez-Vinasco, C. Pradel, E. Martin, D. Madec, E. Teuma and M. Gomez, *Phys Chem Chem Phys*, **2011**, 13.

31. L. Rodriguez-Perez, C. Pradel, P. Serp, M. Gomez and E. Teuma, *Chemcatchem*, **2011**, 3.

32. M. Scariot, D. O. Silva, J. D. Scholten, G. Machado, S. R. Teixeira, M. A. Novak, G. Ebeling and J. Dupont, *Angew. Chem. Int. Ed.*, **2008**, 47, 9075-9078.

33. M. Mayer, A. Welther and A. Jacobi von Wangelin, *Chemcatchem*, **2011**, 3, 1567-1571.

34. J. D. Scholten, M. H. G. Prechtl and J. Dupont, in *Handbook of Green Chemistry*, ed. P. T. Anastas, Wiley Interscience, Weinheim, **2011**, vol. 8.

35. N. Yan, Y. A. Yuan, R. Dykeman, Y. A. Kou and P. J. Dyson, *Angew. Chem. Int. Ed.*, **2010**, 49, 5549-5553.

36. C. X. Xiao, Z. P. Cai, T. Wang, Y. Kou and N. Yan, *Angew. Chem. Int. Ed.*, **2008**, 47, 746-749.

37. D. Raut, K. Wankhede, V. Vaidya, S. Bhilare, N. Darwatkar, A. Deorukhkar, G. Trivedi and M. Salunkhe, *Catal. Commun.*, **2009**, 10, 1240-1243.

38. M. Swadzba-Kwasny, L. Chancelier, S. Ng, H. G. Manyar, C. Hardacre and P. Nockemann, *Dalton T*, **2012**, 41, 219-227.

39. L. D. Pachon and G. Rothenberg, *Appl. Organomet. Chem.*, **2008**, 22, 288-299.

40. R. S. Schwab, D. Singh, E. E. Alberto, P. Piquini, O. E. D. Rodrigues and A. L. Braga, *Catal. Sci. Technol.*, **2011**, 1, 569-573.

41. V. Calo, A. Nacci, A. Monopoli and F. Montingelli, *J. Org. Chem.*, **2005**, 70, 6040-6044.

42. D. B. Zhao, Z. F. Fei, T. J. Geldbach, R. Scopelliti and P. J. Dyson, *J. Am. Chem. Soc.*, **2004**, 126, 15876-15882.

43. S. R. Dubbaka, D. B. Zhao, Z. F. Fei, C. M. R. Volla, P. J. Dyson and P. Vogel, *Synlett*, **2006**, 3155-3157.

44. M. B. Thathagar, J. Beckers and G. Rothenberg, *Green Chem.*, **2004**, 6, 215-218.

45. V. Calo, A. Nacci, A. Monopoli, E. Ieva and N. Cioffi, *Org. Lett.*, **2005**, 7, 617-620.

46. J. H. Li, B. X. Tang, L. M. Tao, Y. X. Xie, Y. Liang and M. B. Zhang, *J. Org. Chem.*, **2006**, 71, 7488-7490.

47. C. T. Yang, Y. Fu, Y. B. Huang, J. Yi, Q. X. Guo and L. Liu, *Angew. Chem. Int. Ed.*, **2009**, 48, 7398-7401.

48. F. Nador, L. Fortunato, Y. Moglie, C. Vitale and G. Radivoy, *Synthesis-Stuttgart*, **2009**, 4027-4031.

49. J. Y. Kim, J. C. Park, H. Song and K. H. Park, *Bull. Korean Chem. Soc.*, **2010**, 31, 3509-3510.

50. T. J. Hu, X. R. Chen, J. Wang and J. Huang, *Chemcatchem*, **2011**, 3, 661-665.

51. P. P. Arquilliere, C. C. Santini, P. H. Haumesser and M. Aouine, *Ecs Transactions*, **2011**, 35, 11-16.

52. F. Alonso and M. Yus, *ACS Catal.*, **2012**, 2, 1441-1451.

53. B. C. Ranu, R. Dey, T. Chatterjee and S. Ahammed, *ChemSusChem*, **2012**, 5, 22-44.

54. R. F. Heck and J. P. Nolley, *J. Org. Chem.*, **1972**, 37, 2320-2322.

55. H. J. Xu, Y. F. Liang, Z. Y. Cai, H. X. Qi, C. Y. Yang and Y. S. Feng, *J. Org. Chem.*, **2011**, 76, 2296-2300.

56. L. J. Goossen, R. T. Werner, N. Rodriguez, C. Linder and B. Melzer, *Adv. Synth. Catal.*, **2007**, 349, 2241-2246.

57. L. J. Goossen, F. Manjolinho, B. A. Khan and N. Rodriguez, *J. Org. Chem.*, **2009**, 74, 2620-2623.

58. R. A. Snow, C. R. Degenhardt and L. A. Paquette, *Tetrahedron Lett.*, **1976**, 4447-4450.

59. J. Cornella, C. Sanchez, D. Banawa and I. Larrosa, *Chem Commun*, **2009**, 7176-7178.

60. R. Venkatesan, M. H. G. Prechtl, J. D. Scholten, R. P. Pezzi, G. Machado and J. Dupont, *J. Mater. Chem.*, **2011**, 21, 3030-3036.

61. H. T. Liu, J. S. Owen and A. P. Alivisatos, *J. Am. Chem. Soc.*, **2007**, 129, 305-312.

62. H. Borchert, E. V. Shevehenko, A. Robert, I. Mekis, A. Kornowski, G. Grubel and H. Weller, *Langmuir*, **2005**, 21, 1931-1936.

63. Y. Zhong, D. H. Ping, X. Y. Song and F. X. Yin, *J. Alloys Comp.*, **2009**, 476, 113-117.

64. J. Dupont and J. D. Scholten, *Chem. Soc. Rev.*, **2010**, 39, 1780-1804.

65. B. K. Teo and N. J. A. Sloane, *Inorg. Chem.*, **1985**, 24, 4545-4558.

66. K. S. Weddle, J. D. Aiken and R. G. Finke, *J. Am. Chem. Soc.*, **1998**, 120.

67. A. P. Umpierre, E. de Jesus and J. Dupont, *Chemcatchem*, **2011**, 3, 1413-1418.

68. L. Q. Xue, W. P. Su and Z. Y. Lin, *Dalton T*, **2011**, 40, 11926-11936.

69. S. Seo, J. B. Taylor and M. F. Greaney, *Chem Commun*, **2012**, 48.

70. C. C. Cassol, G. Ebeling, B. Ferrera and J. Dupont, *Adv. Synth. Catal.*, **2006**, 348, 243-248.

71. Y. G. Cui, I. Biondi, M. Chaubey, X. Yang, Z. F. Fei, R. Scopelliti, C. G. Hartinger, Y. D. Li, C. Chiappe and P. J. Dyson, *Phys Chem Chem Phys*, **2010**, 12, 1834-1841.

3.2 Ligand-free copper(I) oxide nanoparticle-catalysed amination of aryl halides in ionic liquids

Michael T. Keßler, Silas Robke, Sebastian Sahler and Martin H. G. Prechtl*
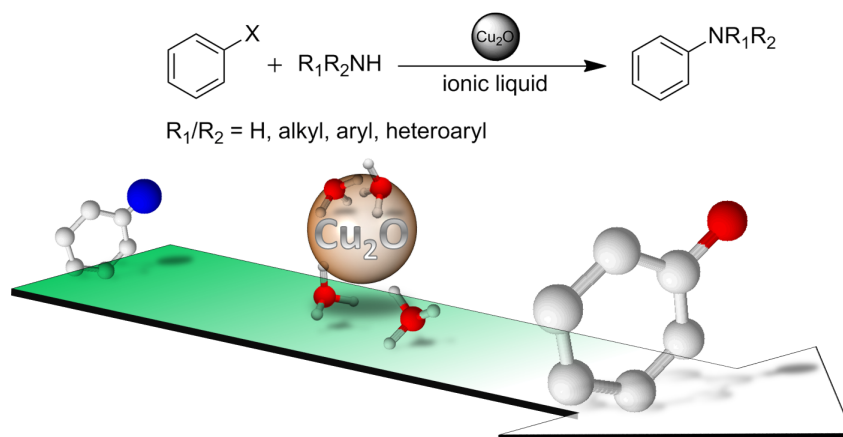
In the following, we present a simple and feasible methodology for a C–N coupling reaction using nanoscale Cu_2O catalysts incorporated in n-Bu_4POAc ionic liquid media. It is shown that a wide range of amines and aryl halides can be coupled selectively in high yields, without the use of ligands or additives (bases) and without precautions against water or air. All catalyses can be carried out with a nanoparticle catalyst loading as low as 5 mol%, based on the used precursor.

3.2.1 Introduction

Cross coupling reactions belong to the most important and synthetically versatile reactions in chemical synthesis. C–N coupling reactions have been known for years and can easily be conducted with (noble) metal catalysts, e.g. palladium or nickel.[1,2] Unfortunately, these catalysts are, though used in low loadings, extremely expensive or suffer from the disadvantage of toxicity.[3,4] In the last decade, scientific research has focussed on the development of inexpensive and less toxic metals such as iron[5−8] and copper.[9−11] One promising catalyst turns out to be copper(I) oxide which showed remarkable activity in homogeneous as well as heterogeneous C–N bond formation reactions.[12−14] Homogeneously driven copper(I) catalysed C–N bond formation sometimes requires only homeopathic catalyst loadings, but the use of ligands, base or other additives as well as inert conditions are usually necessary.[15−17] Heterogeneous C–N cross coupling catalysed by copper(I) requires rather harsh reaction conditions but does not need ligands and shows a good reaction workup.[18,19] However, up to now nanoscale copper(I) catalysed cross coupling reactions, especially C–N bond formation, have rarely been reported in scientific literature[13,20−22] or show drawbacks in

versatility and catalyst loadings.[20,22−25] Furthermore, it would be more convenient to conduct catalysis at temperatures right below the boiling point of water without the necessity for ligands, additives and inert reaction conditions.[26] Nonetheless, we want to establish a Cu_2O nanocatalyst which combines the advantages of classical homogeneous and heterogeneous catalyses. On the one hand, Cu(I) nanocatalysts show good yields and high TONs under moderate reaction conditions; on the other hand, excellent reaction workup and low product contamination are secured. Apart from a few publications,[20,23] Cu_2O nanoparticles (Cu_2O-NPs) were considered as rather unreactive and nonversatile catalysts, which was why they seemed to be useless in C–N coupling reactions. As a rather toxic alternative with adequate activity and versatility, CuI is widely employed.[21,27] Usually solvents can alter the chemo-physical properties of catalysts.[28] Ionic liquids (ILs) are widely known as so-called "designer solvents". They can act as promoters and activators, [29,30] as protecting agents and stabilisers,[28,30−35] as reducing agents[11,30,35] and certainly as (co-)solvents themselves for molecular and nanoscale species.[36−39] Only limited reports about the use and influence of ionic liquids as solvents for nanocatalytic C–N cross coupling reactions are known.[40,41] To the best of our knowledge, publications about the incorporation and stabilisation of Cu_2O nanoparticles in ionic liquid media and their use for catalytic amination reaction have not been reported yet. Herein we established a new approach to catalytic C–N couplings with Cu_2O-NP in ionic liquid media. With regard to future applications for a recyclable catalytic system, we tried in particular to simplify the reaction process. The influence of the reaction parameters such as reaction time, temperature and catalyst loading as well as the influence of additives, solvents or inert atmosphere were investigated. Finally, we could establish a versatile methodology for the coupling of iodo- and bromobenzenes with a broad scope of amines and ammonia with a remarkable selectivity. It has to be pointed out that the synthesis of the Cu_2O nanoparticles proceeds directly in the used ionic liquid from cheap precursors like basic $CuCO_3$ with subsequent C–N coupling reactions. The as-synthesised nanoparticles are not separated or purified in an additional step but can be directly used as catalysts for amination reactions. In contrast to many other homogeneous and heterogeneous catalyses, the presented coupling reaction in ionic liquid medium turns out to have no necessity for ligands, additional base, additives or an inert atmosphere and can even proceed in the presence of water at temperatures below 80 °C.

3.2.2   Synthesis of the catalytic nanoparticle phase

In addition to thermal decomposition,[35] laser ablation or sputtering methods,[42] reduction with hydrogen or hydrazine solution[43,44] using ionic liquid as a reducing agent for the synthesis of Cu_2O nanoparticles in terms of reduction of the precursor is a potential alternative. We have recently published a low-temperature synthesis of Cu_2O nanoparticles in n-Bu_4POAc elsewhere.[11] The obtained nanoparticles had an average diameter of 5.5 nm (± 1.2 nm), pointing out that basic $CuCO_3$ usually decomposes to CuO at 295 °C.[45] In our low temperature synthesis, $CuCO_3$ is converted to Cu_2O-NPs via an "ionic liquid-induced" reduction at 120 °C (Scheme 3.3).[11]

3.2.3   Amination reactions with ammonia

Amination reactions of iodobenzene and its derivatives with aqueous ammonia solution belong to the most common and most desired reactions in chemical synthesis. Both reactants are inexpensive, easy to handle and readily available. It is well known that Cu(I) in homogeneous[46,47] as well as in heterogeneous[48,49] catalysis promotes cross coupling reactions. In our case, we were pleased to see that iodobenzene couples smoothly even with
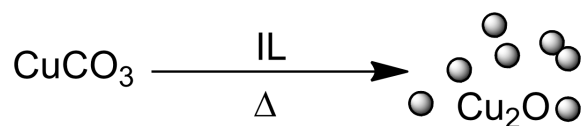
Scheme 3.3: Synthesis of Cu(I) oxide nanoparticles by thermal reduction of copper(II) carbonate in ionic liquid medium.
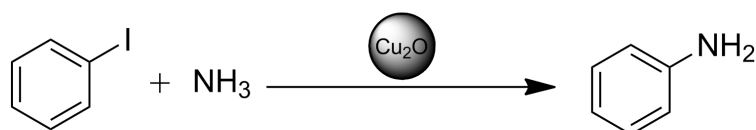
Scheme 3.4: Amination of iodobenzene with aqueous ammonia solution as a test reaction for the activity of the Cu_2O NPs in IL.

ammonia in aqueous solution, in the presence of a ligand-free Cu_2O nanocatalyst in n-Bu_4POAc (Scheme 3.4). It is quite uncommon that the yields were satisfactory or high at temperatures of about $75–85\,°C$ within $24\,h$ even in the absence of an additional base (see Table 3.5, entries 7, 10–13). Different ionic liquids as reaction media were investigated by varying the anion as well as the cation to change the polarity of the ionic liquid. Polarity, basicity and acidity, which are crucial attributes for application in catalysis, are summarized in the so-called Kamlet–Taft parameters.

We tried other polar ionic liquids with different Kamlet–Taft parameters[50] for the synthesis of Cu_2O from $CuCO_3$, pointing out that the particles obtained in n-Bu_4POAc were the most active. Rather apolar ionic liquids such as 1-butyl-3-methylimidazolium N,N-bistrifluoromethylsulfonylimide (bmim NTf_2) and 1-butyl-2,3-dimethylimidazolium N,N-bistrifluoromethylsulfonylimide (bmmim NTf_2) are not capable of reducing the Cu(II) species.[11] Therefore, we were not surprised that we could not detect any nanoparticles in the ionic liquids. Furthermore, Cu(II) salts do not support the amination of aryl halides very well (Table 3.5, entries 1 and 2). However, highly polar ionic liquids often suffer from high melting points ((n-$Bu_4P)_2SO_4$) and seem to be impractical as reaction media (Table 3.5, entry 6). The obtained reaction mixtures show high viscosities, leading to a rather inhomogeneous intermixture of educts and the catalytic IL-phase.

Nevertheless, acetate-based ionic liquids combine both low melting points and the ability to form Cu_2O. The catalytic activities of the formed copper(I) species, 1-butyl-3-methylimidazolium acetate (bmim OAc) and butylmethylpyrrolidinium acetate (bmpyrr OAc), are rather low (Table 3.5, entries 3 and 4); only the high polarity of the reaction medium seems to support the amination reaction (Table 3.5, entry 5). Interestingly, only the nanoparticles generated in n-Bu_4POAc show good results in the amination of iodobenzene with a yield of about 61% (Table 3.5, entries 7 and 10-13).

With n-Bu_4POAc as our reaction medium of choice, we investigated the influence on the reaction time towards the yield. We observed that the conversion of iodobenzene to

Table 3.5: Variation of the reaction parameters and a selection of ionic liquids as reaction media for the arylation of ammonia.

Entry	IL	T [°C]	t [h]	Cat.-load.[b] [mol%]	add.	conv.[c] [%]
1	bmim NTf_2	85	24	100[a]		0
2	bmmim NTf_2	85	24	100[a]		0
3	bmim OAc	85	24	100		38
4	bmpyrr OAc	85	24	100		< 1
5	bmim Cl	85	24	100[a]		34
6	$(n\text{-}Bu_4P)_2SO_4$	85	24	100		0
7	$n\text{-}Bu_4POAc$	85	24	100		61
8	$n\text{-}Bu_4POAc$	85	24	100	K_2CO_3	63
9	$n\text{-}Bu_4POAc$	85	24	100	KI	59
10	$n\text{-}Bu_4POAc$	85	16	100		64
11	$n\text{-}Bu_4POAc$	85	16	10		83
12	$n\text{-}Bu_4POAc$	100	24	100		40
13	$n\text{-}Bu_4POAc$	75	16	10		92

Reaction conditions: 1 mmol iodobenzene, 1 ml NH_3 (aq., 20%, 12 mmol), Cu-cat in 1 g IL.[a] No Cu_2O-NPs detectable. [b] Based on used precursor amount ($CuCO_3$). [c] Conversions were determined using ^{1}H NMR with hexamethyldisilane as the internal standard.
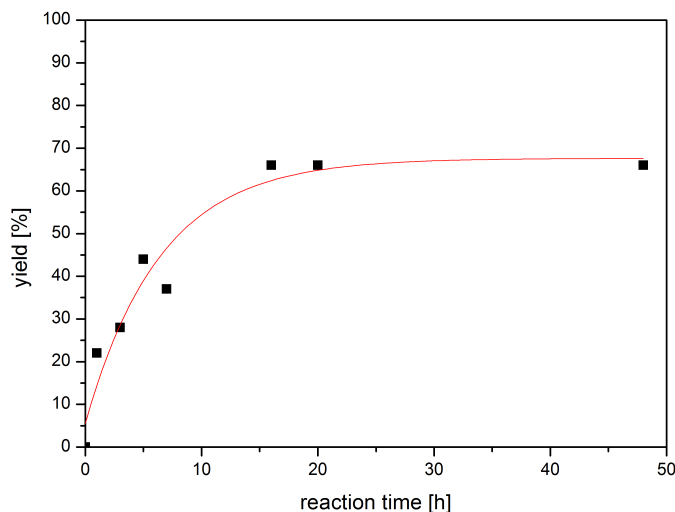
Figure 3.11: Plot of reaction time and corresponding yield of aniline. The maximum yield is reached within 16 h at 85 °C.

aniline increases drastically with time and a maximum conversion could be reached after 16 h (64%) (Figure 3.11, Table 3.5, entry 10). Investigation of the catalyst loading showed that a decrease in the amount of Cu_2O raised the yield drastically. The maximum value of about 83% was achieved using only 10 mol% of the catalyst (Table 3.5, entry 11). The
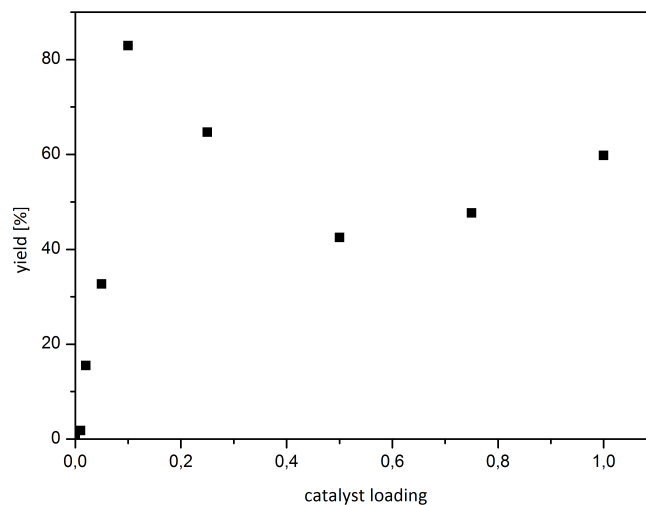
Figure 3.12: Correlation between reaction temperature and corresponding yield of aniline. The best results could be achieved at 75 °C within 16 h and a catalyst loading of 10 mol%.

catalyst loading is referred to as the amount of catalyst precursor applied. In fact, due to the high surface/volume ratio of the particles, the amount of real active catalyst is even lower.[11,41] Loadings of the catalyst below 10 mol% as well as loadings higher than 10 mol% lowered the yield of aniline. Moreover, with high catalyst loadings, the system's miscibility probably suffers due to the higher viscosity of the liquid phase. Analogous to several other publications dealing with Pd- or Ni-NPs, it is possible that the Cu_2O-NPs act as a catalyst reservoir for Cu(I), and a molecular species might act as the active species.[32,51] There are different ways of how a molecular species can theoretically be leached from the particle surface as Beletskaya and co-workers have revealed.

Usually there is an equilibrium between leaching and the Ostwald-ripening of the particles. In this context, the synonym "nanosalt" is introduced for metal–chalcogen nanoparticles.[51] Up to now, the mechanism for the leaching effect has not been intensively investigated, but usually the Ar–X species is believed to generate molecular metal species by oxidative addition.[26] During the extraction of the reaction mixture using *n*-pentane, copper species can be leached out of the catalytic phase and contaminate the final product. In order to investigate the amount of copper in the organic phase, ICP-OES measurements revealed that the extract contains only a maximum of 0.041 μmol (lowest value found: 0.00029 μmol) copper. Based on the utilised amount of catalyst precursor ($CuCO_3$ 0.05 mmol), the leached copper amount is equivalent to a maximum of 0.082%, which is remarkably low. Moreover, the outcome of the amination reaction catalysed by Cu(I) oxide nanoparticles could be improved further by adjusting the reaction temperature. The yields can effectively be increased to an excellent yield of 92% at temperatures as low as 75 °C (Table 3.5, entry 13). The higher conversions at lower temperatures are most likely related to the low boiling point of ammonia; thus, the concentration in the liquid phase is higher at lower temperature. It is a remarkable fact that a ligand- and additive-free approach shows best results far below the boiling point of water, which makes the reaction also possible in water. Most other ligand free approaches need temperatures between 100 °C and 135 °C.[16] A further increase in the reaction temperature affects the yield of
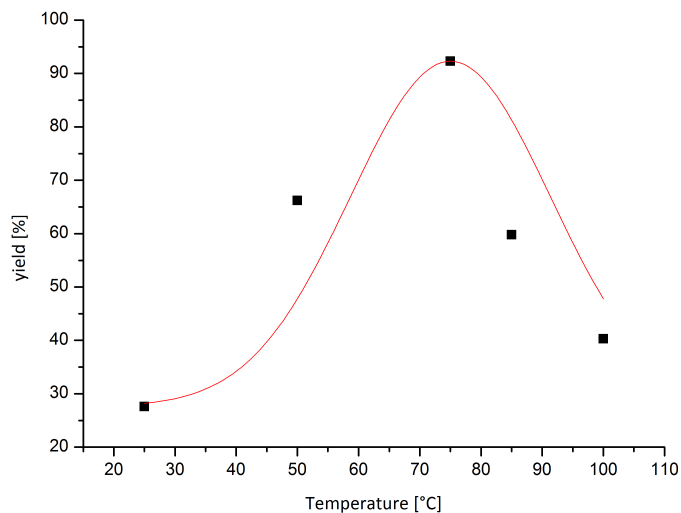
Figure 3.13: Correlation between yield and copper catalyst for the amination of iodobenzene.

aniline negatively (Figure 3.12). The addition of additives like a base (K_2CO_3) or KI (Table 3.5, entries 8 and 9) to change the pH-value or to simulate a different copper(I)-species did not improve the yield of aniline measurably. Obviously it is not necessary to neutralise the HX species,[16,19] which is produced during the reaction process, by an additional base.
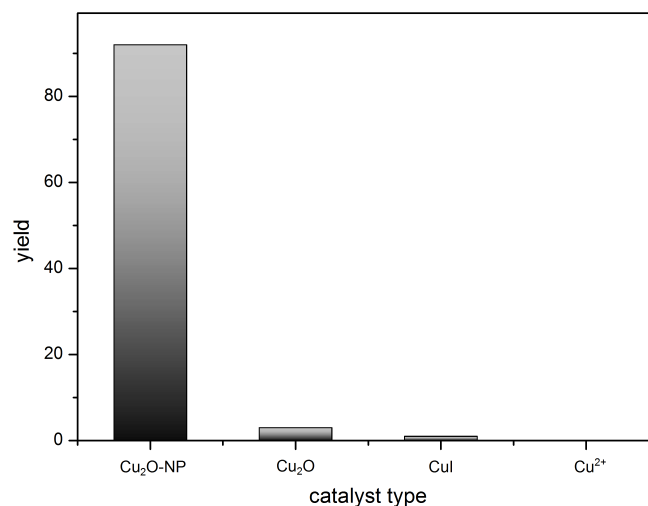
Figure 3.14: Correlation between yield and copper catalyst for the amination of iodobenzene.

On the one hand, the acetate ionic liquid may act as a buffer reagent and keep the pH-value constant, and on the other hand, ammonia can act as a proton scavenger as well. In comparison to the used copper(I) oxide nanoparticles, we investigated different (bulk) copper salts in oxidation states (I) and (II) (Figure 3.14). In contrast to ref. 17,

we could not show activity for Cu^{2+} species in our reaction sequence. All used Cu(II) salts ($Cu(NO_3)_2$, $CuSO_4$, $CuCl_2$, $Cu(OAc)_2$ and CuF_2) failed completely in catalysing the amination of iodobenzene with ammonia under the same conditions. A competing reaction might be the formation of a stable $Cu(NH_3)_4{}^{2+}$ complex which colours the reaction mixture immediately. CuI (as used in other manuscripts)[22] and bulk Cu_2O applied in ionic liquid media showed very poor activity of 1% and 3% yields, respectively.

3.2.4 Reactions with primary and secondary amines

R_1/R_2 = H, alkyl, aryl, heteroaryl
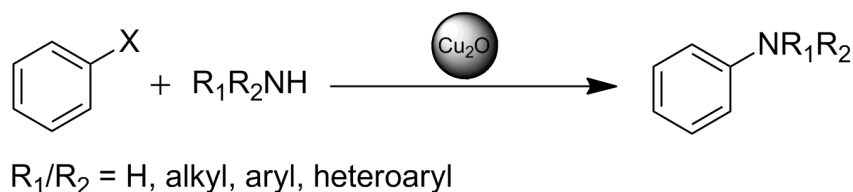
Scheme 3.5: Amination of aryl halides with primary and secondary amines.

Table 3.6: Variation of primary amines for the coupling with iodobenzene under optimised reaction conditions.

Entry	amine	cat.-load. [mol%][b]	yield[a] [%]
1	CH_3-NH_2	10	65
2	CH_3-NH_2	5	65
3	n-Bu-NH_2	5	71
4	iso-Bu-NH_2	5	95
5	cHex-NH_2	5	77
6	n-Oct-NH_2	5	90
7	iso-Pr-NH_2	5	99
8	$tert$-Bu-NH_2	5	57
9	$C_6H_5NH_2$	5	65

Reaction conditions: 1 mmol iodobenzene, 1 ml prim. amine (CH_3-NH_2 (40 wt%) 12.9 mmol, n-Bu-NH_2 10.1 mmol, iso-Bu-NH_2 10.6 mmol, cHex-NH_2 8.7 mmol, n-Oct-NH_2 6.0 mmol, iso-Pr-NH_2 11.6 mmol, $tert$-Bu-NH_2 9.5 mmol, C_6H_5-NH_2 10.7 mmol), Cu-cat in 1 g (3.1 mmol) IL, reaction temperature: 75 °C, reaction time: 16 h.[a] Conversions were determined using ^{1}H NMR with hexamethyldisilane as the internal standard. [b] Based on used precursor amount ($CuCO_3$). No by-products could be detected.

In order to show the versatility of our catalytic system, aryl halides were coupled with primary and secondary amines as well. Due to the increasing electron density at the nitrogen atom, there is a distinct tendency for per-N-substitution reactions to give mono-, di- and tri-substituted amines, as well as quaternary ammonium salts in an undesirable product mixture.[52]

Hence the reaction sequence, the reaction conditions as well as the workup must prevent per-arylation and guarantee the selective synthesis of only one product (Scheme 3.5). As a starting point, N-arylation reactions of iodobenzene with primary amines were chosen

Table 3.7: Variation of secondary amines for the coupling with iodobenzene at optimised reaction conditions.

Entry	amine	cat.-load. [mol%]^b	yield^a [%]
1	Et$_2$NH	5	65
2	n-Bu$_2$NH	5	16
3	piperidine	5	99
4	Ph$_2$NH	5	0
5	morpholine	5	99
6	L-proline	5	33

Reaction conditions: 1 mmol iodobenzene, 1 ml sec. amine (Et$_2$NH 9.6 mmol, n-Bu$_2$NH 5.9 mmol, piperidine 10.1 mmol, Ph$_2$NH 6.9 mmol, morpholine 11.5 mmol, L-Prolin 11.7 mmol), Cu-cat in 1 g (3.1 mmol) IL, reaction temperature: 75 °C, reaction time: 16 h.^{a} Conversions were determined using ^{1}H NMR with hexamethyldisilane as the internal standard. ^{b} Based on used precursor amount (CuCO$_3$). No by-products could be detected.

with a catalyst loading of 10 mol%. The results of the arylation experiments are listed in Table 3.6, showing remarkable results concerning yields and catalyst loadings. We were pleased to find out that we could reduce the loading of the copper-catalyst to 5 mol% without a significant loss in activity (Table 3.6, entry 2). The best results could be obtained with linear and branched alkyl amines (65%–99%, Table 3.6, entries 2–4 and 6–8), followed by cyclic (77%, Table 3.6, entry 5) and aryl amines (65%, Table 3.6, entry 9). The low yields of the coupling between iodobenzene and methyl amine can be explained by the rather low electron density (e.g. compared to n-butyl amine). No further arylation of the desired secondary amine was detectable, which might be in correlation with the high excess of primary amine in the reaction mixture. A similar screening with secondary amines is shown in Table 3.7. In summary, the conversions of the coupling between secondary amines and aryl halides are slightly lower in comparison to the conversions of the coupling between primary amines and aryl halides. This might be due to emerging steric effects. The starting materials (secondary amines) and products (tertiary amines) are much bulkier and thus slightly disfavoured in the transmetallation steps. Diethylamine gave a satisfactory yield of 65% (Table 3.7, entry 1). There was on the contrary no conversion detectable when diphenylamine was used as the amination reagent (Table 3.7, entry 4). Nevertheless, there are also some examples which verify the versatility of this method with good to excellent results (e.g. morpholine and piperidine, both 99%, Table 3.7, entries 3 and 5). These heterocyclic compounds are less bulky than common secondary alkyl amines due to their fixed ring structure. No by-products, such as perarylated ammonium derivatives, could be detected in the reaction mixture.

3.2.5 Screening of different aryl halides

We were also able to show that our catalytic system was capable of coupling different substituted bromo- and iodoaryl derivatives with both ammonia and amines. The reaction tolerates functionalities like OH-, alkyl or methoxy groups on the aromatic ring. Although the yields are rather low in some cases, the reaction tolerates some common functional groups. Again, steric effects caused by substituents in the vicinity of the halide (Table 3.8,

entries 6, 7, and 9) seem to hamper the amination completely. Aryl chlorides do not undergo amination reaction at temperatures as low as 75 °C (Table 3.8, entry 4).

Table 3.8: Variation of aryl halides for the coupling with ammonia, diethylamine and piperidine at optimized reaction parameters.

Entry	aryl-X	amine	cat.-load. [mol%][b]	yield[a] [%]
1	C_6H_5Br	NH_3	10	12
2	3-iodoanisole	NH_3	5	92
3	4-iodotoluene	NH_3	10	79
4	1,2-dichlorobenzene	Et_2NH	5	0
5	C_6H_5Br	Et_2NH	5	10
6	2-iodophenol	Et_2NH	5	0
7	2-iodoanisole	Et_2NH	5	0
8	3-iodoanisole	Et_2NH	5	24
9	2-iodotoluene	Et_2NH	5	0
10	4-iodotoluene	Et_2NH	5	33
11	3-iodoanisole	piperidine	5	93
12	4-iodotoluene	piperidine	5	85

Reaction conditions: 1 mmol aryl halide, 1 ml piperidine (10.1 mmol), Et_2NH (9.6 mmol) or ammonia solution (20%, 12 mmol), Cu-cat in 1 g (3.1 mmol) IL, reaction temperature: 75 °C, reaction time: 16 h.[a] Conversions were determined using ^{1}H NMR with hexamethyldisilane as the internal standard. [b] Based on used precursor amount ($CuCO_3$). No by-products could be detected.

3.2.6 Conclusion

In conclusion, we established an efficient C–N coupling reaction catalysed by Cu_2O nanoparticles. Therefore we consciously avoided rather toxic catalyst materials, for example, CuI. We could show the versatility of this method in about 30 examples. The coupling of aryl halides with ammonia or primary or secondary amines gave exclusively the corresponding primary, secondary or tertiary amines in satisfactory to excellent yields and selectivity. The nanoparticle catalyst was synthesised in *n*-Bu_4POAc – a polar ionic liquid with low melting point – which acted as a reaction medium, reductant and stabilising agent. Additionally the as-prepared catalyst did not require any workup and could subsequently be used for the amination reaction. The catalyst loading was as low as 5 mol%, and the whole reaction as well as the workup requires neither inert conditions nor any additional ligands, base or further additives. In sum, this protocol shows benefits in versatility, selectivity, efficiency and preparative demand which clearly distinguishes it from previous publications. Our future work will focus on a recyclable catalytic system.

3.2.7 Experimental

General

An aqueous solution of *n*-Bu_4POH (40 wt%) and basic $CuCO_3$, as well as all other copper salts and $LiNTf_2$, was obtained from ABCR Chemicals®. 1-chlorobutane, 1,2-

dimethylimidazole and 1-methylimidazole, and all primary and secondary amines, as well as all aryl halides, were purchased from Sigma Aldrich®. Sulphuric acid, acetic acid, aqueous NH_3 solution (20%), K_2CO_3 and KI were obtained from the chemical stock of the institute. All chemicals were used without further purification, and all reactions were conducted under non-inert conditions. ^{1}H-NMR and ^{31}P-NMR spectra were recorded using a Bruker® AVANCE II 300 spectrometer at 298 K (300.1 MHz, external standard tetramethylsilane (TMS)). The obtained Cu_2O nanoparticles were analysed using a powder X-ray diffractometer (STOE®-STADI MP, Cu-K_α irradiation, $\lambda = 1.540598$ Å) and a TEM Phillips® EM 420, 120 kV as described in ref. 11. The ionic liquid n-Bu_4POAc and the Cu_2O nanoparticles were prepared according to our previous report.[11] All other ILs were synthesized according to literature-known methods.[30,33,34,53,54] All ICP-OES measurements (Cu leaching) were performed on an AMETEK® Spectro Arcos equipped with an ESI SC4-DX autosampler and run using the Spectro Smart Analyser Vision software. Two identical reaction samples were prepared for the amination of iodobenzene with ammonia. The reaction mixtures were extracted with n-pentane according to the procedure for amination reactions (see above). n-pentane was completely removed under reduced pressure, and the residue was digested in 2 ml of 65% HNO_3 at 90 °C for 3 h to give a clear yellow solution. The crude solution was allowed to cool to room-temperature and diluted to 1 : 50 and 1 : 100 (sample 1), as well as to 1 : 50 and 1 : 500 (sample 2). Every probe was measured three times and correlated with a reference material and a blank probe. The characteristic spectral lines at 224.7 nm and 324.7 nm were used to determine the amount of leached copper-catalyst.

Ionic liquid synthesis

The synthesis of n-Bu_4POAc is adapted from ref. 11 and modified to our preparative demands. In a 100ml round bottom flask, 50 ml of 40 wt% tetrabutylphosphonium hydroxide solution (72.4 mmol; n-Bu_4POH) is mixed with 4.12 ml (72.4 mmol) of 99% acetic acid under vigorous stirring. After further stirring for 25 min, the residual water is removed under reduced pressure at 60 °C. The resulting ionic liquid is subsequently dried under reduced pressure for at least 72 h leaving a colourless hygroscopic and waxy solid behind. Yield: 20.8 g (95%). ^{1}H-NMR (300 MHz, rt, $CDCl_3$): δ (ppm) = 2.07–2.18 m (8H), 1.48–1.58 q (8H), 1.36–1.48 q (8H), 0.86–0.93 t (12H). ^{31}P-NMR (60 MHz, rt, $CDCl_3$): δ (ppm) = 33.25.

Nanoparticle synthesis

The Cu_2O nanoparticles were synthesised in an oven-dried 25ml crimp top vial equipped with a butyl-rubber septum and a glass stirring bar. 0.05 mmol (11 mg) of basic $CuCO_3$ was suspended in 1 g (3.1 mmol) IL and heated to 120 °C for 12 h while stirring at 500 rpm in a vial holder. The resulting catalytic phase was a brownish red dispersion of Cu_2O nanoparticles in IL. The particles in IL could be easily dispersed in acetone, ethanol or isopropanol.

Procedure for amination reactions

The as-prepared nanoparticle dispersion was allowed to cool down to room temperature in the 25ml crimp-top vial. Then 1 mmol aryl halide and 1 ml of amine or ammonia solution (NH_3 (20 wt%) 12 mmol, CH_3-NH_2 (40 wt%) 12.9 mmol, n-Bu-NH_2 10.1 mmol, iso-Bu-NH_2 10.6 mmol, cHex-NH_2 8.7 mmol, n-Oct-NH_2 6.0 mmol, iso-Pr-NH_2 11.6 mmol, $tert$-Bu-NH_2 9.5 mmol, C_6H_5-NH_2 10.7 mmol, Et_2NH 9.6 mmol, n-Bu_2NH 5.9 mmol, piperidine

10.1 mmol, Ph$_2$NH 6.9 mmol, morpholine 11.5 mmol and L-Prolin 11.7 mmol) were added with vigorous stirring. The vial was closed again and heated up to 75 °C for 16 h. The reaction mixture was cooled and extracted with *n*-pentane (3x5 ml). The organic phases were combined, and the solvent was evaporated under reduced pressure. The residue was analysed using ^{1}H-NMR techniques (internal standard: hexamethyldisilane, 0.1 mmol, 20 μl) and compared with literature data.

3.2.8 Acknowledgement

3.2.9 Notes and References

1. M. H. Ali and S. L. Buchwald, *J. Org. Chem.*, **2001**, 66, 2560–2565.

2. S. Nagao, T. Matsumoto, Y. Koga and K. Matsubara, *Chem. Lett.*, **2011**, 40, 1036–1038.

3. G. K. Bielmyer, C. Decarlo, C. Morris and T. Carrigan, *Environ. Toxicol. Chem.*, **2013**, 32, 1354–1359.

4. E. Patel, C. Lynch, V. Ruff and M. Reynolds, *Toxicol. Appl. Pharmacol.*, **2012**, 258, 367–375.

5. S. Gulak and A. Jacobi von Wangelin, *Angew. Chem. Int. Ed.*, **2012**, 51, 1357–1361.

6. M. Mayer, A. Welther and A. Jacobi von Wangelin, *ChemCatChem*, **2011**, 3, 1567–1571.

7. A. Welther, M. Bauer, M. Mayer and A. Jacobi von Wangelin, *ChemCatChem*, **2012**, 4, 1088–1093.

8. A. Welther and A. Jacobi von Wangelin, *Curr. Org. Chem.*, **2013**, 17, 326–335.

9. P. P. Arquilliere, C. C. Santini, P. H. Haumesser and M. Aouine, *ECS Trans.*, **2011**, 35, 11–16.

10. P. Arquilliere, P. H. Haumesser and C. C. Santini, *Microelectron. Eng.*, **2012**, 92, 149–151.

11. M. T. Kessler, C. Gedig, S. Sahler, P. Wand, S. Robke and M. H. G. Prechtl, *Catal. Sci. Technol.*, **2013**, 3, 992–1001.

12. R. T. Gephart, D. L. Huang, M. J. B. Aguila, G. Schmidt, A. Shahu and T. H. Warren, *Angew. Chem. Int. Ed.*, **2012**, 51, 6488–6492.

13. S. J. Ahmadi, S. Sadjadi, M. Hosseinpour and M. Abdollahi, *Monatsh. Chem.*, **2011**, 142, 801–806.

14. P. J. Ji, J. H. Atherton and M. I. Page, *J. Org. Chem.*, **2012**, 77, 7471–7478.

15. S. L. Buchwald and C. Bolm, *Angew. Chem. Int. Ed.*, **2009**, 48, 5586–5587.

16. Z.-J. Liu, J.-P. Vors, E. R. F. Gesing and C. Bolm, *Green Chem.*, **2011**, 13, 42–45.

17. P.-F. Larsson, A. Correa, M. Carril, P.-O. Norrby and C. Bolm, *Angew. Chem. Int. Ed.*, **2009**, 48, 5691–5693.

18. J. W. Tye, Z. Weng, A. M. Johns, C. D. Incarvito and J. F. Hartwig, *J. Am. Chem. Soc.*, **2008**, 130, 9971–9983.

19. A. Correa and C. Bolm, *Adv. Synth. Catal.*, **2007**, 349, 2673–2676.

20. S. Uk Son, I. Kyu Park, J. Park and T. Hyeon, *Chem. Commun.*, **2004**, 778–779.

21. H. J. Xu, Y. F. Liang, Z. Y. Cai, H. X. Qi, C. Y. Yang and Y. S. Feng, *J. Org. Chem.*, **2011**, 76, 2296–2300.

22. B. C. Ranu, R. Dey, T. Chatterjee and S. Ahammed, *ChemSusChem*, **2012**, 5, 22–44.

23. S. Jammi, S. Krishnamoorthy, P. Saha, D. S. Kundu, S. Sakthivel, M. A. Ali, R. Paul and T. Punniyamurthy, *Synlett*, **2009**, 3323–3327.

24. B. X. Tang, S. M. Guo, M. B. Zhang and J. H. Li, *Synthesis-Stuttgart*, **2008**, 1707–1716.

25. M. Kidwai, S. Bhardwaj and S. Poddar, *Beilstein J. Org. Chem.*, **2010**, 6, 35.

26. I. P. Beletskaya and A. V. Cheprakov, *Organometallics*, **2012**, 31, 7753–7808.

27. G. Lefevre, G. Franc, C. Adamo, A. Jutand and I. Ciofini, *Organometallics*, **2012**, 31, 914–920.

28. M. H. G. Prechtl, J. D. Scholten and J. Dupont, *J. Mol. Catal. A: Chem.*, **2009**, 313, 74–78.

29. C. C. Cassol, A. P. Umpierre, G. Machado, S. I. Wolke and J. Dupont, *J. Am. Chem. Soc.*, **2005**, 127, 3298–3299.

30. M. H. G. Prechtl, P. S. Campbell, J. D. Scholten, G. B. Fraser, G. Machado, C. C. Santini, J. Dupont and Y. Chauvin, *Nanoscale*, **2010**, 2, 2601–2606.

31. J. Dupont and J. D. Scholten, *Chem. Soc. Rev.*, **2010**, 39, 1780–1804.

32. C. S. Consorti, F. R. Flores and J. Dupont, *J. Am. Chem. Soc.*, **2005**, 127, 12054–12065.

33. C. C. Cassol, G. Ebeling, B. Ferrera and J. Dupont, *Adv. Synth. Catal.*, **2006**, 348, 243–248.

34. M. H. G. Prechtl, M. Scariot, J. D. Scholten, G. Machado, S. R. Teixeira and J. Dupont, *Inorg. Chem.*, **2008**, 47, 8995–9001.

35. R. Venkatesan, M. H. G. Prechtl, J. D. Scholten, R. P. Pezzi, G. Machado and J. Dupont, *J. Mater. Chem.*, **2011**, 21, 3030–3036.

36. V. Calo, A. Nacci, A. Monopoli and P. Cotugno, *Angew. Chem. Int. Ed.*, **2009**, 48, 6101–6103.

37. V. Calo, A. Nacci, A. Monopoli and P. Cotugno, *Chem.–Eur. J.*, **2009**, 15, 1272–1279.

38. C. Amiens, B. Chaudret, M. Respaud and P. Lecante, *Actual. Chim.*, **2005**, 19–27.

39. L. M. Lacroix, S. Lachaize, F. Hue, C. Gatel, T. Blon, R. P. Tan, J. Carrey, B. Warot-Fonrose and B. Chaudret, *Nano Lett.*, **2012**, 12, 3245–3250.

40. C. T. Yang, Y. Fu, Y. B. Huang, J. Yi, Q. X. Guo and L. Liu, *Angew. Chem. Int. Ed.*, **2009**, 48, 7398–7401.

41. I. Geukens, J. Fransaer and D. E. De Vos, *ChemCatChem*, **2011**, 3, 1431–1434.

42. H. Wender, L. F. de Oliveira, P. Migowski, A. F. Feil, E. Lissner, M. H. G. Prechtl, S. R. Teixeira and J. Dupont, *J. Phys. Chem. C*, **2010**, 114, 11764–11768.

43. M. Ranjbar, S. Fardindoost, S. M. Mahdavi, A. I. Zad and N. Tahmasebi G, *Sol. Energy Mater. Sol. Cells*, **2011**, 95, 2335–2340.

44. M. H. G. Prechtl, J. D. Scholten and J. Dupont, *Molecules*, **2010**, 15, 3441–3461.

45. H. Henmi, T. Hirayama, N. Mizutani and M. Kato, *Thermochim. Acta*, **1985**, 96, 145–153.

46. S. M. Islam, S. Mondal, P. Mondal, A. S. Roy, K. Tuhina and M. Mobarok, *Inorg. Chem. Commun.*, **2011**, 14, 1352–1357.

47. Y. Zou, H. Lin, P. A. Maggard and A. Deiters, *Eur. J. Inorg. Chem.*, **2011**, 4154–4159.

48. P. Liu, P. H. Li and L. Wang, *Synth. Commun.*, **2012**, 42, 2595–2605.

49. X. Qi, L. Zhou, X. Jiang, H. Fan, H. Fu and H. Chen, *Chin. J. Catal.*, **2012**, 33, 1877–1882.

50. P. G. Jessop, D. A. Jessop, D. B. Fu and L. Phan, *Green Chem.*, **2012**, 14, 1245–1259.

51. V. P. Ananikov and I. P. Beletskaya, *Organometallics*, **2012**, 31, 1595–1604.

52. G. Verardo, A. G. Giumanini and P. Strazzolini, *Synth. Commun.*, **1994**, 24, 609–627.

53. D. B. Zhao, Z. F. Fei, T. J. Geldbach, R. Scopelliti and P. J. Dyson, *J. Am. Chem. Soc.*, **2004**, 126, 15876–15882.

54. Y. G. Cui, I. Biondi, M. Chaubey, X. Yang, Z. F. Fei, R. Scopelliti, C. G. Hartinger, Y. D. Li, C. Chiappe and P. J. Dyson, *Phys. Chem. Chem. Phys.*, **2010**, 12, 1834–1841.

3.3 Fast track to nanomaterials: microwave assisted synthesis in ionic liquid media

Michael T. Kessler,[a] Maria K. Hentschel,[a] Christina Heinrichs,[a] Stefan Roitsch[b] and Martin H. G. Prechtl*[a]

Herein we present a general approach to metal and metal oxide nanoparticles using simple metal salts as starting materials. The reducing agent can be delivered in the form of the anion incorporated into the metal precursor respectively ionic liquid. Exemplary we demonstrate the synthesis of Cu and Ag as well as ZnO and NiO nanoparticles generated either from acetate or carbonate salts. All particles are synthesised by microwave heating without the necessity of inert conditions. Two different types of ionic liquids have been used as reaction media – tetra-*n*-butylphosphonium acetate (*n*-Bu$_4$POAc) and 1-butyl-2,3-dimethylimidazolium N,N-bis(trifluoromethylsulfonyl)imid (bmmim NTf$_2$). In this case, the choice of the ionic liquid seems to have significant influence on the size, shape and dispersity of the synthesised particles. It is clearly shown that the acetate anion present in all reaction mixtures can act as an inexpensive and nontoxic reducing agent. The final products in solid, liquid and gaseous phase have been characterised by XRD, TEM, NMR, FT-IR and online gas-phase MS.

3.3.1 Introduction

Ionic liquids (ILs) emerge more and more as highly desirable multipurpose solvents. They show extraordinary chemical and physical properties with low melting points, negligible vapour pressure,[1] high chemical inertness and tuneable polarity, acidity and basicity.[2] Due to these properties ionic liquids represent solvents which can be designed for each and every reaction by variation of anion and cation as well as by incorporation of functional and/or coordinating groups.[3] It is the spirit and purpose of ionic liquids to cover

as many objectives as possible. In these terms they can make numbers of classical additives dispensable. Accordingly, ionic liquids are very popular concerning the synthesis of zero- and one-dimensional nanostructures.[4−7] Ionic liquids can act as solvents, cosolvents, [8−11] promoters,[12,13] reducing agents,[12−15] capping or protective agents and surfactants.[3,16] Despite their low melting points, ionic liquid phases show structural properties of lower order: they consist of polar and nonpolar nanoscale regimes which make them ideal templates for nanoscale synthesis.[16−18] In recent years, metal and metal oxide nanoparticles (NPs) have attracted much attention in academic and industrial research. Their unique properties revealed a completely new field for applications; even for compounds which have been sufficiently investigated in bulk state.[19−21] Their high surface to volume ratio makes them attractive for catalytic and medical applications; the quantum size effect of small particles[22] shows remarkable results in photochemistry and nonlinear optics.[23,24] However, nanoparticles – as all nanoscale structures – are thermodynamically disfavoured and show high tendency for agglomeration and aggregation. Surfactants, such as polymers/ dendrimers,[25−28] ligands and especially ionic liquids sufficiently shield the nanoparticles' surface and effectively prevent agglomeration.[12−15,19,29,30]
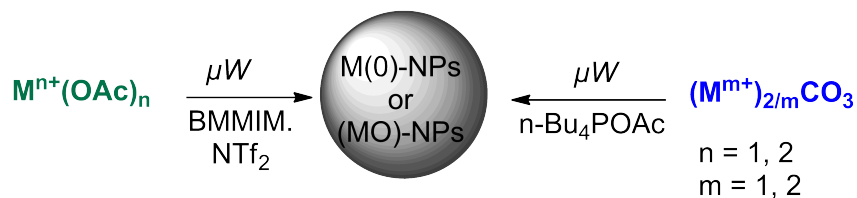
Scheme 3.6: General synthesis of metal and metal oxide nanoparticles by microwave synthesis. M = Cu, Ni, Ag, Zn.

Nanoparticles can be synthesised in various ways. There are several top-down and bottom-up methods with their inherent advantages and disadvantages.[15,31−33] Solvothermal syntheses are very well investigated and represent a versatile tool for the preparation of nanomaterials.[34−36] They bear the advantage to control size and shape by adjusting the reaction parameters. For convincing results solvents or even solvent mixtures must be varied. Additives, surfactants and precursor-loadings have to be adapted.[37−39] One versatile synthesis of late transition metal-(oxide) particles in pure ionic liquid would be favourable because of their high demand in scientifc research, which is especially applicable for Cu, Ag, NiO and ZnO.[5,7,40−43] Reactions should be carried out without any additives, without precautions against moisture or oxygen and at best with an environmentally benign reducing agent. Herein, we present a general nanoparticle synthesis using tetra-n-butylphosphonium acetate (n-Bu$_4$POAc) or 1-butyl-2,3-dimethylimidazolium N,N-bis(trifluoromethylsulfonyl)imid (bmmim NTf$_2$) as reducing agent respectively stabiliser. Exemplary we synthesised nanoparticles of NiO-NP, ZnO-NP, Ag-NP and Cu-NP (Scheme 3.6). The particles – generated from metal carbonates (in n-Bu$_4$POAc) or metal acetates (in bmmim NTf$_2$) – are synthesised by microwave heating. Further investigation of the solid phase (particles), the liquid phase (IL) and the gaseous phase (by-products) is implemented.

3.3.2 Results and discussion

Microwave synthesis of Cu(0)- and Ag(0)-nanoparticles

Silver and copper nanoparticles were obtained both in n-Bu$_4$POAc from silver carbonate (Ag$_2$CO$_3$) and copper carbonate (CuCO$_3$), respectively, and in bmmim NTf$_2$ from silver acetate (AgOAc) and copper acetate monohydrate (Cu(OAc)$_2$·H$_2$O). The syntheses were conducted under microwave heating. TEM pictures were taken from the as-synthesised nanoparticles. In Figure 3.15 the copper nanoparticles obtained in n-Bu$_4$POAc are presented as well as a size distribution of the particles. The copper particles obtained in the phosphonium based IL were synthesised at temperatures of 160 °C within 10 min and show an average diameter of 4.8 nm ($\pm$1.7 nm). The monodisperse particles are homogeneously distributed in the ionic liquid film. Previously, we have shown that the thermal decomposition of copper carbonate in n-Bu$_4$POAc at temperatures as high as 120 °C leads to the growth of Cu$_2$O nanoparticles.[14] Interestingly, adjusting the reaction parameters (temperature, time and heating method) is suitable as a sensitive tool for the predetermination of the particles final oxidation state, yielding in the present case Cu(0) nanoparticles. The copper nanoparticles obtained in bmmim NTf$_2$ (see Figure 3.16) have been synthesised at temperatures as high as 235 °C within 3 min. The majority of the particles have an average diameter of about 4.9 nm ($\pm$1.1 nm) and the incorporation into the ionic liquid effectively prevents further crystal growth or agglomeration but not the aggregation of the small nanoparticles.
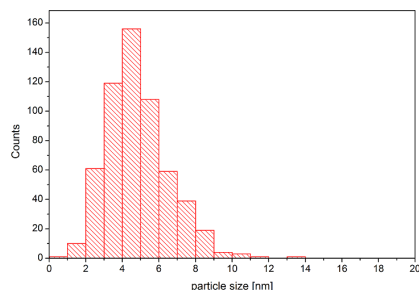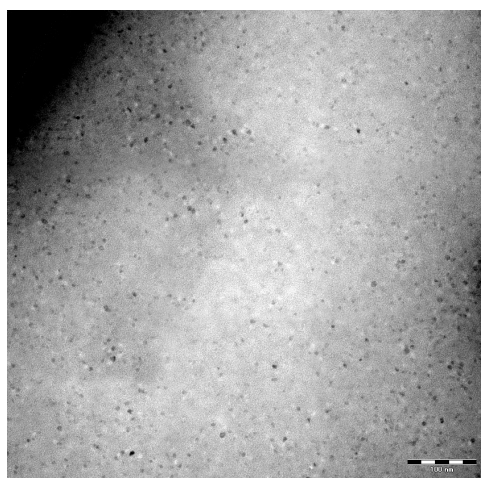
Figure 3.15: Cu-NPs synthesised in n-Bu$_4$POAc (scale bar 100 nm). The mean particle diameter is 4.8 nm.
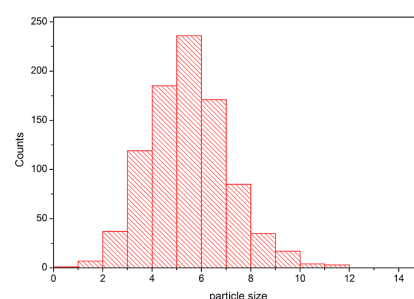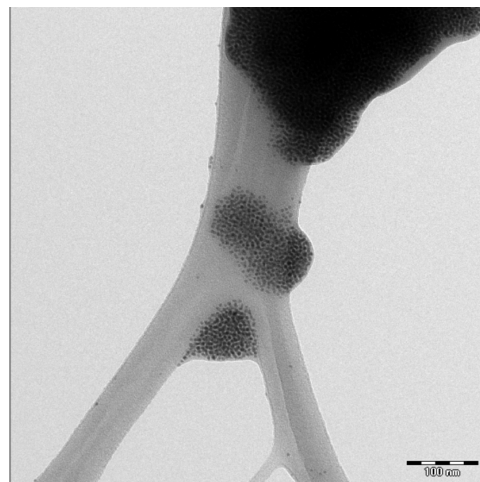
Figure 3.16: Cu-NPs synthesised in bmmim NTf$_2$ (scale bar 100 nm). The mean diameter is 4.9 nm.

For both samples the XRD-pattern confirms pure Cu(0) (ESI, Figure 3.24). Due to the smaller particle size obtained in n-Bu$_4$POAc, the XRD reflexes are less intensive compared to those synthesised in bmmim NTf$_2$. In an analogous way silver nanoparticles were synthesised in both ionic liquids via microwave irradiation. Figure 3.17 shows the TEM image depicting the as-synthesised Ag nanoparticles in n-Bu$_4$POAc and in Figure 3.18 the Ag nanoparticles obtained in bmmim NTf$_2$. The size distribution of the particles is shown in the histogram. The synthesis of silver nanoparticles in n-Bu$_4$POAc yields small and uniformly shaped particles which show a bimodal diameter distribution with a major maximum at 6.7 nm ($\pm$0.1 nm) and a minor maximum at 15.6 nm ($\pm$0.8 nm) (Figure 3.17).
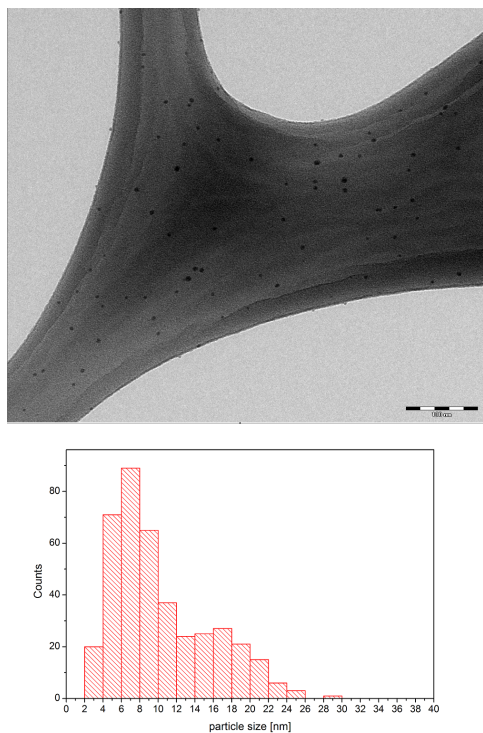
Figure 3.17: Ag-NPs synthesised in n-Bu$_4$POAc (scale bar 100 nm). The major maximum is at 6.7 nm and the minor maximum at 15.6 nm.
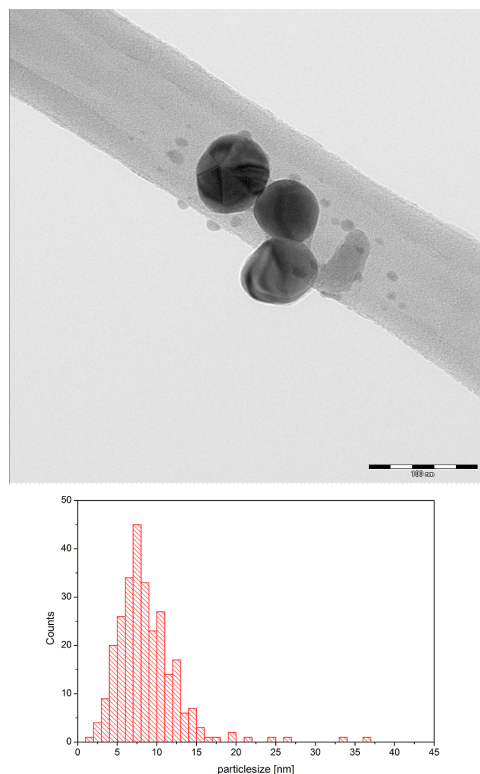
Figure 3.18: Ag-NPs synthesised in bmmim NTf$_2$ (scale bar 100 nm). The mean diameter is 12.2 nm.

These nanoparticles are very homogeneously distributed and show no agglomerated sites. The silver nanoparticles obtained in n-Bu$_4$POAc have been synthesised at 100 °C in 90 s. Contrary silver particles synthesised in bmmim NTf$_2$ show a higher degree of polydispersity. The particles have an average diameter of 12.2 nm ($\pm$15.4 nm) (Figure 3.18). Nevertheless, few particles in the range of 20–60 nm are obtained as well. No residual AgOAc was detected in the reaction mixture after 5 min at a synthesis temperature of about 200 °C. An XRD-pattern of the particles can be found in ESI Figure 3.25 confirming phase purity. Obviously, the use of different ionic liquids strongly influences the growth of the nanoparticles. n-Bu$_4$POAc is a very polar ionic liquid with low melting point (mp = 55 °C); contrary bmmim NTf$_2$ is a room temperature ionic liquid (mp = -4 °C) with a relatively low polarity. Apparently, the shielding of the more polar phosphonium ionic liquid seems to be more effective and inhibits the agglomeration of the metal nanoparticles.[43,44] In contrast, the synthesis of pure metal nanoparticles in the imidazolium-based ionic liquid leads to a higher polydispersity. Additionally, the phosphonium based ionic liquid shows an excellent

covering and incorporation of the metal nanoparticles (even on the TEM grid).[45,46] This can be attributed to the partial charge of the metal particles surface which is beneficial for coulomb interactions between the particle and the polar IL (electrosteric shielding).[47,48]

Microwave synthesis of NiO and ZnO nanoparticles

NiO- and ZnO-nanoparticles could be obtained both in n-Bu$_4$POAc from nickel carbonate hexahydrate (NiCO$_3$·6H$_2$O) and zinc carbonate (ZnCO$_3$), and in bmmim NTf$_2$ from zinc acetate dihydrate (Zn(OAc)$_2$·2H$_2$O). Due to a better dispersibility of nickel acetate in 1-butyl-3-methylimidazolium N,N-bis(trifluoromethylsulfonyl)imid (bmim NTf$_2$), the NiO particles are synthesised in the latter. In Figure 3.19 and Figure 3.20 NiO nanoparticles synthesised in either n-Bu$_4$POAc or bmim NTf$_2$ are shown. Particles synthesised in n-Bu$_4$POAc have an average diameter of only 5.8 nm ($\pm$1.7 nm), but show a high degree of aggregation. The particles were synthesised at temperatures as high as 200 °C within 10 min. Furthermore, the size distribution is rather broad and even nanoparticles sized between 15 nm and 30 nm are present.
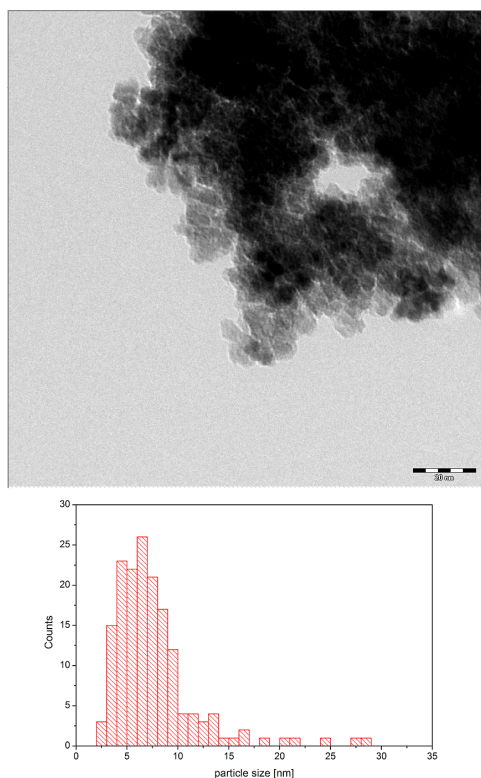
Figure 3.19: TEM-picture of nickel-(II)oxide nanoparticles (5.8 nm) synthesised in n-Bu$_4$POAc (scale bar 20 nm) with size distribution.
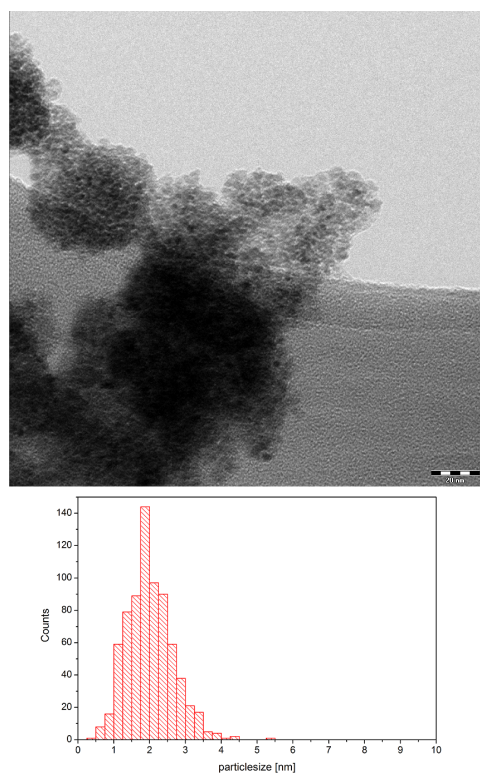
Figure 3.20: TEM-picture of nickel-(II)oxide nanoparticles (2.0 nm) synthesised in bmim NTf$_2$ (scale bar 20 nm) with size distribution.

The NiO nanoparticles obtained from 1-butyl-3-methylimidazolium N,N-bis(trifluoromethylsulfonyl)imid (bmim NTf$_2$) at temperatures of about 250 °C are even smaller – their average diameter is only 2.0 nm ($\pm$0.6 nm). They are all uniformly shaped and show a high tendency for aggregation (due to the small size). Within 30 min only the reflexes of NiO can be detected as shown in the XRD in ESI Figure 3.26 indicating no substantial precursor residue or further impurities, moreover no precursor residual could be detected

by FT-IR (see ESI, Figure 3.30). In both cases the XRD reflexes show only a low intensity, due to the small particle size. ZnO nanoparticles were also synthesised in both ionic liquids via microwave irradiation. The particle precursor $ZnCO_3$ for the nanoparticles in n-Bu$_4$POAc was converted into zinc oxide within 10 min at 220 °C. The precursor for the zinc oxide nanoparticles in bmmim NTf$_2$ was zinc(II)acetate dihydrate (Zn(OAc)$_2$·2H$_2$O). Nanoparticles could be obtained within 15 min at temperatures of about 225 °C. The TEM pictures of the as-synthesised nanoparticles in n-Bu$_4$POAc are shown in Figure 3.21. Those synthesised in bmmim NTf$_2$ are shown in Figure 3.22. The nanoparticles obtained in n-Bu$_4$POAc show an average size of 22.2 nm (±10.2 nm), whereas the nanorods synthesised in bmmim NTf$_2$ have an average length of 189.3 nm (±61.5 nm) and an average diameter of 50.9 nm (±18.2 nm). All nano-sized materials show only a low degree of aggregation and nearly no agglomeration. Both materials were investigated by XRD techniques as can be seen in ESI Figure 3.27. Both XRD pattern are in agreement with the reference pattern (given in red). They show no residual zinc precursor (zinc carbonate or zinc acetate). In case of the nickel oxide nanoparticles, those synthesised in bmmim NTf$_2$ are smaller than those synthesised in n-Bu$_4$POAc. Although the zinc oxide structures synthesised in bmmim NTf$_2$ are larger than the particles obtained in n-Bu$_4$POAc, they show a high tendency for one-dimensional elongation. From this point of view and in contrast to metal nanoparticles, a rather apolar ionic liquid seems to stabilise metal oxide nanostructures much better and can also lead to a directed growth of 1D nanostructures.

This can be attributed to a low ordered pre-structure of imidazolium based ionic liquids originating from an intrinsic self-organisation caused by a hydrogen-bond network.[16,18] Hence, the reaction medium (the ionic liquid) is divided into nanometer-sized polar and nonpolar regions, which are supposed to be beneficial for the growth of metal oxide nanostructures.[49−51] This can also lead to directed growth of nanostructures which has been already shown by Antonietti *et al.* and summarised by Taubert *et al.*[52,53]

Investigation of the liquid phase (ionic liquid)

In order to determine the reductive species which are responsible for the reduction of the Cu^{2+} and Ag^+ ions in the reaction mixture, the ionic liquid was investigated by NMR and ATR-IR methods. The Ni^{2+} and Zn^{2+} species are not reduced by the ionic liquid. The reaction media has been investigated by ^{1}H-, ^{19}F- and ^{31}P-NMR techniques. As can be seen in ESI Figure 3.28 the phosphonium based ionic liquid n-Bu$_4$POAc can act as reducing agent in two ways: on the one hand the acetate ion can act as the reducing medium (forming (n-Bu$_4$P)$_2$CO$_3$ and carbon dioxide) as previously reported.[14] Consequently the CH_3 signal for the acetate methyl group at 2.05 ppm vanishes or shows a loss of intensity. This is the case for all four reactions. In the synthesis of Ag particles the acetate signal only slightly decreases. On the other hand the phosphonium ion can be converted into tributylphosphine (via Hofmann elimination) and oxidised to tributylphosphinoxide. Accordingly, tributylphosphine can act as reducing agent, too. In ESI Figure 3.29 the ^{31}P-NMR spectra of all reaction mixtures after the nanoparticle synthesis are shown (including a reference spectrum for pure n-Bu$_4$POAc). In all ^{31}P-NMR spectra one can clearly see the large signal at 33.3 ppm corresponding to the phosphonium species. Another signal at 44.2 ppm appears in the spectra – corresponding to a tributylphosphinoxide – of the high-temperature syntheses of Cu-, Ni(II)O- and Zn(II)O nanoparticles. Due to the high temperature during the synthesis (160–220 °C) the phosphonium cations partially undergo Hofmann elimination. The pure ionic liquid and the reaction mixture for the synthesis of Ag nanoparticles (reaction temperature 100 °C) obviously do not show these signals. In
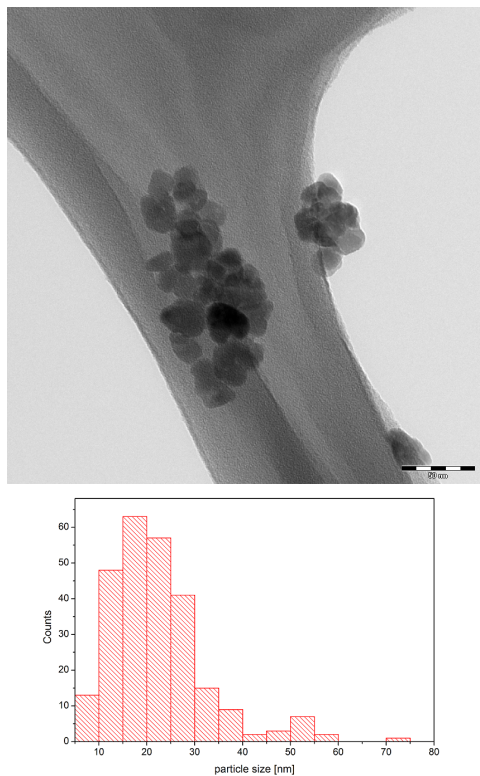
Figure 3.21: TEM-picture of zinc oxide nanoparticles (22.2 nm) synthesised in n-Bu$_4$POAc (scale bar 50 nm) with size distribution.
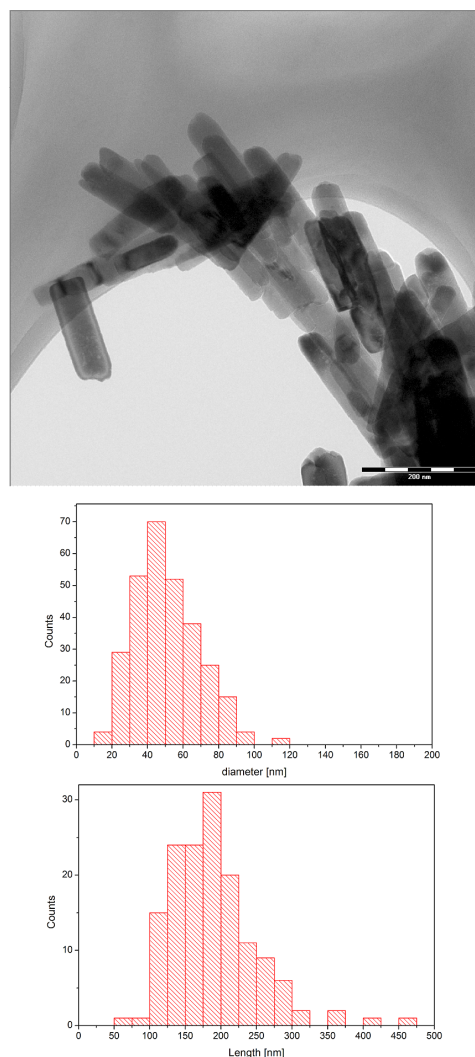
Figure 3.22: TEM-picture of zinc oxide nanorods (diameter: 50.9 nm, length: 189.3 nm) synthesised in bmmim NTf$_2$ (scale bar 200 nm) with size distribution.

comparison to the IR-spectrum of the pure n-Bu$_4$POAc ionic liquid (see ESI, Figure 3.30) the IR-spectrum of the reaction mixture of Ag(0) nanoparticles in n-Bu$_4$POAc still shows a strong signal at 1580 cm^{-1} which is in good agreement with the literature known data for acetate-carbonyl and which is already confirmed by ^{1}H-NMR analysis. In contrast, there is no significant but still a smaller peak (slightly shifted to 1460 cm^{-1}) in the IR-spectrum of the reaction mixture of NiO nanoparticles in n-Bu$_4$POAc indicating the presence of another but different carbonyl species. This confirms the hypothesis that a considerable amount of the acetate is oxidised to carbonate at higher temperatures. This is in good agreement with the already published data which can be found in ref. 14. 1-Butyl-2,3-dimethylimidazolium N,N-bis(trifluoromethylsul- fonyl)imide (bmmim NTf$_2$) is a more temperature stable ionic liquid. Temperatures of up to 250 °C do not lead to decomposition. In the following the ^{1}H-NMR spectra of pure bmmim NTf$_2$ and two examples of the reaction mixtures (Cu and

Ag nanoparticle syntheses) are shown (ESI, Figure 3.31). Similar to the ^{1}H- the ^{19}F-NMR spectra show only one species – corresponding to the trifluoromethyl-groups – confirming that the NTf$_2$ anions do not decompose or react either (see ESI, Figure 3.32). The IR spectra of bmmim NTf$_2$ and two corresponding reaction mixtures after the nanoparticle synthesis confirm the above made conclusions that the ionic liquid does not undergo any substantial decomposition (see ESI, Figure 3.33).

Investigation of the gaseous phase

During the particle synthesis the gas-phase was investigated by online gas-phase mass spectrometry (gas-phase MS). We investigated the gas-phase of the reductive decomposition of copper carbonate in n-Bu$_4$POAc and compared it to the reductive decomposition of copper acetate in bmmim NTf$_2$. One can clearly see in ESI Figure 3.34 three main signals. The signal at 44 m/z corresponds to significant amounts of CO$_2$, generated during the decomposition of the acetate anions of the ionic liquid.[14] This means that the acetate is not only oxidised to carbonate, but mainly decarboxylated to carbon dioxide, which correlates with the investigation of synthesis of copper(I)oxide nanoparticles (Cu$_2$O-NP) in n-Bu$_4$POAc.[14,54] Signals at 28 m/z and 16 m/z are correlated to dinitrogen and O$_2$$^{2+}$, respectively. Due to the lower concentration of acetate ions in the reaction mixture using bmmim NTf$_2$ as solvent, the amount of extruded carbon dioxide is significantly lower.

Figure 3.23: Gas-phase mass spectrogram of volatile compounds of the reductive decomposition of copper(II)acetate in bmmim NTf$_2$. Argon (m/z = 40, m/z = 20) is used as carrier gas.
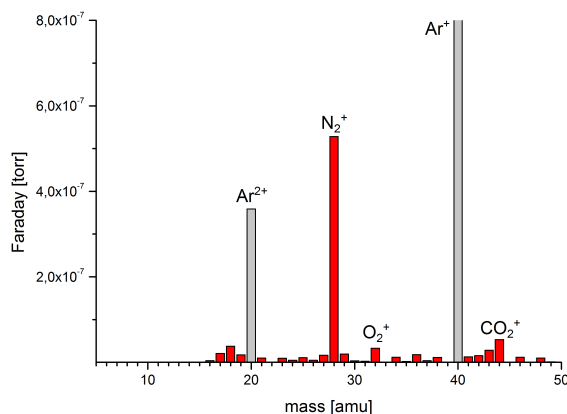
A constant stream of argon was used to transport the gas probe into the MS (see Figure 3.23). Hence, the amount of CO$_2$ (m/z = 44) in the mass spectrum is rather small, but 1.6-times higher than the oxygen amount, though indicating that the acetate ion acts as reducing agent, regardless whether it originates from the ionic liquid or the nanoparticle precursor.

3.3.3 Experimental

General

All reactions were carried out in a Monowave 300 microwave (Anton Paar®) with a maximum power of 850 W at 2.45 MHz. The microwave was equipped with a ruby-thermometer and an IR-reference thermometer as well as a stirring unit. Reactions can be carried out up to a maximum pressure of 30 bar and a maximum temperature of 300 °C. Reaction-mixtures were handled without precautions against water/moisture or air/oxygen in 4 ml microwave-borosilicate vials equipped with a Teflon/silicon septum and a quartz inlet for

the thermometer. Aqueous solution of n-Bu$_4$POH (40 wt%), CuCO$_3$·Cu(OH)$_2$, Ag$_2$CO$_3$, NiCO$_3$·6H$_2$O and ZnCO$_3$ were purchased from ABCR Chemicals®. Acetic acid (99%), Cu(OAc)$_2$·H$_2$O and Ni(OAc)$_2$·4H$_2$O were used from the chemicals stock of the institute. AgOAc and Zn(OAc)$_2$·2H$_2$O were obtained from Alfa Aesar®. 1,2-Dimethylimidazol, 1-butanol and methane sulfonyl chloride were purchased from Sigma Aldrich®. All chemicals were used without further purification prior to use. Tetra-n-butylphosphonium acetate (n-Bu$_4$POAc) and 1-butyl-2,3-dimethylimidazolium N,N-bis(trifluoromethyl)sulfonylimid (bmmim NTf$_2$) were synthesised according to literature known methods.[3,13,54−57] ^{1}H-, ^{19}F- and ^{31}P-NMR spectra were recorded on a Bruker® AVANCE II 300 spectrometer at 298 K (300.1 MHz, 272 MHz, 121 MHz, external standard tetramethylsilane (TMS)). IR spectra were taken on Bruker® alpha Platinum ATR with a diamond-ATR-module. The obtained nanoparticles were analysed by powder X-ray diffractometry (STOE®-STADI MP, Cu-K$_\alpha$ irradiation, $\lambda = 1.540598$ Å) and by a TEM Phillips® EM 420, 120 kV. Mass spectra were recorded with HIDEN® HPR-20QIC equipped with Bronkhorst® EL-FLOW Select mass flow meter/ controller.

Nanoparticle synthesis

An oven-dried 4ml microwave-borosilicate vial equipped with a Teflon stirring bar, a Teflon/silicon septum and a quartz inlet for a ruby-thermometer was filled with 500 mg of the ionic liquid. 50 mg of precursor (basic CuCO$_3$ 0.23 mmol, Ag$_2$CO$_3$ 0.18 mmol, NiCO$_3$6·H$_2$O 0.22 mmol, ZnCO$_3$ 0.40 mmol, Cu(OAc)$_2$·H$_2$O 0.25 mmol, AgOAc 0.30 mmol, Ni(OAc)$_2$·4H$_2$O 0.20 mmol, Zn(OAc)$_2$·2H$_2$O 0.23 mmol) was filled into the vial and stirred for 2.5 min on a conventional stirring plate to yield a homogeneous mixture. The vial was further equipped with a ruby-thermometer. The maximum irradiation power of the microwave was limited to 75 W when the reaction was about to start. The reaction parameters for the particle syntheses are summarised in the following table (Table 3.9).

Table 3.9: Reaction parameters for the nanoparticle syntheses in ionic liquids by microwave irradiation[a].

No.	type	IL	prec.	T [°C]	t [min]	d [nm]
1	Cu(0)	n-Bu$_4$POAc	CuCO$_3$	160	10	4.8 ($\pm$1.7)
2	Cu(0)	bmmim NTf$_2$	Cu(OAc)$_2$	235	3	4.9 ($\pm$1.1)
3	Ag(0)	n-Bu$_4$POAc	Ag$_2$CO$_3$	100	1.5	6.7 ($\pm$1.7)
4	Ag(0)	bmmim NTf$_2$	AgOAc	200	5	12.2 ($\pm$5.4)
5	Ni(II)O	n-Bu$_4$POAc	NiCO$_3$	200	10	5.8 ($\pm$1.7)
6	Ni(II)O	bmim NTf$_2$	Ni(OAc)$_2$	250	30	2.0 ($\pm$0.6)
7	Zn(II)O	n-Bu$_4$POAc	ZnCO$_3$	220	10	22.2 ($\pm$10.2)
8	Zn(II)O	bmmim NTf$_2$	Zn(OAc)$_2$	225	15	50.9 ($\pm$18.2)[b]
						189.3 ($\pm$61.5)[c]

[a] Reaction parameters: 500 mg IL, 50 mg precursor, 1000 rpm stirring, 75 W max. power. [b] ZnO nanorods diameter. [c] ZnO nanorods length.

3.3.4 Conclusion

The synthesis of copper, silver, nickel oxide and zinc oxide nanoparticles originating from eight inexpensive salt-precursors in two different ionic liquids – tetra-n-butylphosphonium acetate (n-Bu$_4$POAc) and 1-butyl-2,3-dimethylimidazolium N,N-bis (trifluoromethylsulfonyl)imid (bmmim NTf$_2$) – has been investigated. All reactions were carried out in a microwave for chemical reactions within 90 s to 30 min at temperatures between 100 °C and 250 °C resulting in small sized nanoparticles and nanorods. This clearly demonstrates the general approach of this synthetic protocol for nanostructures using simple ILs; both metal and metal oxide species particles can be obtained. Additionally, the acetate ion can act as nontoxic and environmentally friendly reducing agent, regardless whether it originates from the ionic liquid or the metal salt precursor. Furthermore, it should be emphasised that polarity and geometry differences of the ionic liquids clearly influence the crystal growth of the nanostructures.

3.3.5 Acknowledgements

3.3.6 Electronic Supporting Information

Fast track to nanomaterials: microwave assisted synthesis in ionic liquid media

Michael T. Kessler,[a] Maria K. Hentschel,[a] Christina Heinrichs,[a] Stefan Roitsch [b] and Martin H. G. Prechtl [a]*

[a] Department of Chemistry, Institute of Inorganic Chemistry, University of Cologne, Greinstraße 6, 50939 Cologne, Germany. E-mail: martin.prechtl@uni-koeln.de; Web: http://catalysis.uni-koeln.de; Fax: +49 221 4701788.
[b] Department of Chemistry, Institute of Physical Chemistry, University of Cologne, Luxemburger Str. 116, 50939 Cologne, Germany.
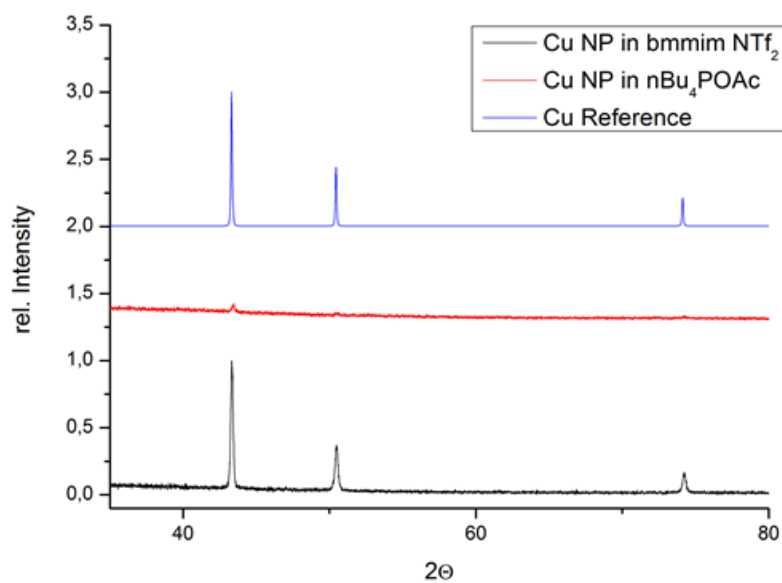
Figure 3.24: XRD-pattern of copper nanoparticles in n-Bu$_4$POAc (red) and bmmim NTf$_2$ (black).
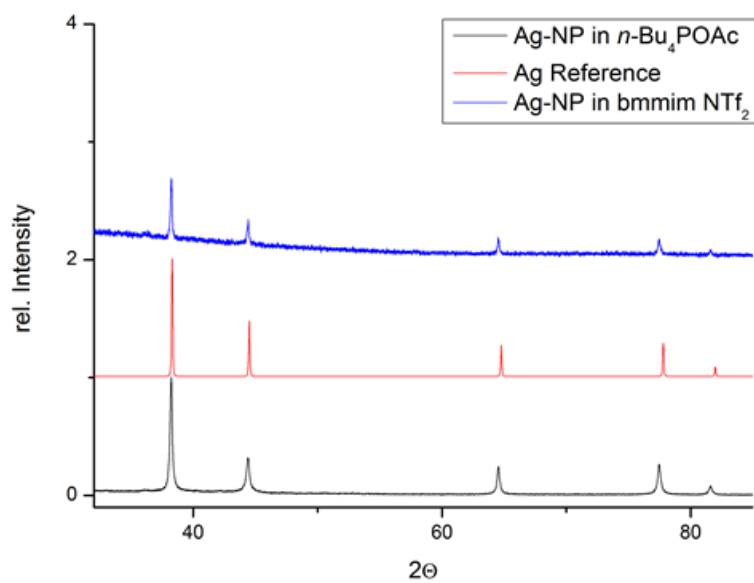
Figure 3.25: XRD-pattern of Ag nanoparticles in n-Bu$_4$POAc (black) and bmmim NTf$_2$ (blue).
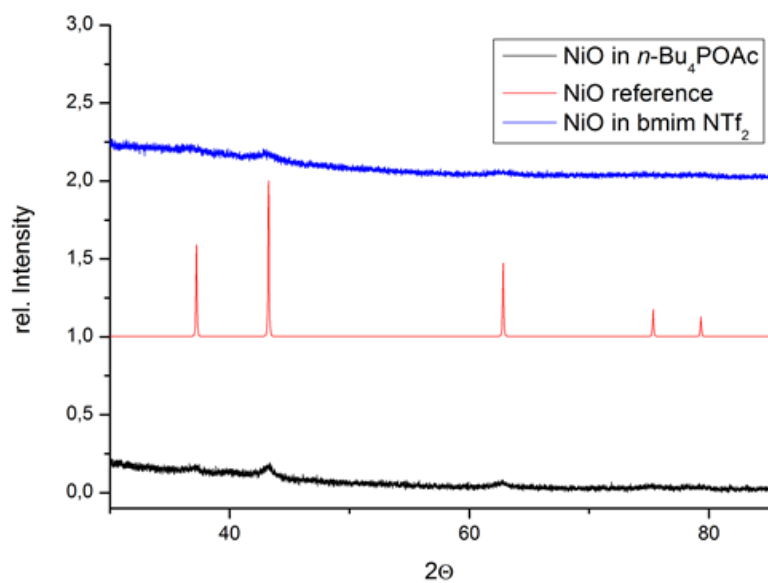
Figure 3.26: XRD-pattern of NiO nanoparticles in n-Bu$_4$POAc (black) and bmim NTf$_2$ (blue).
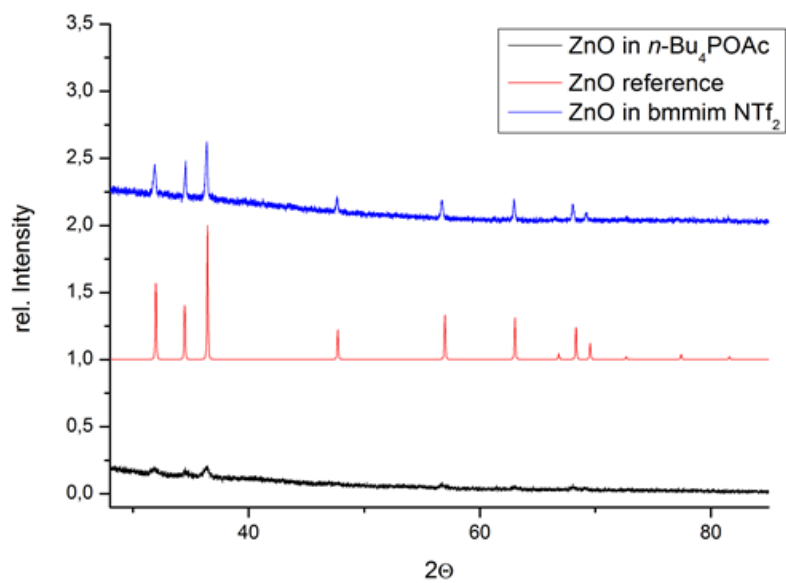
Figure 3.27: XRD-pattern of ZnO nanoparticles/nanorods in n-Bu$_4$POAc (black) and bmmim NTf$_2$ (blue).
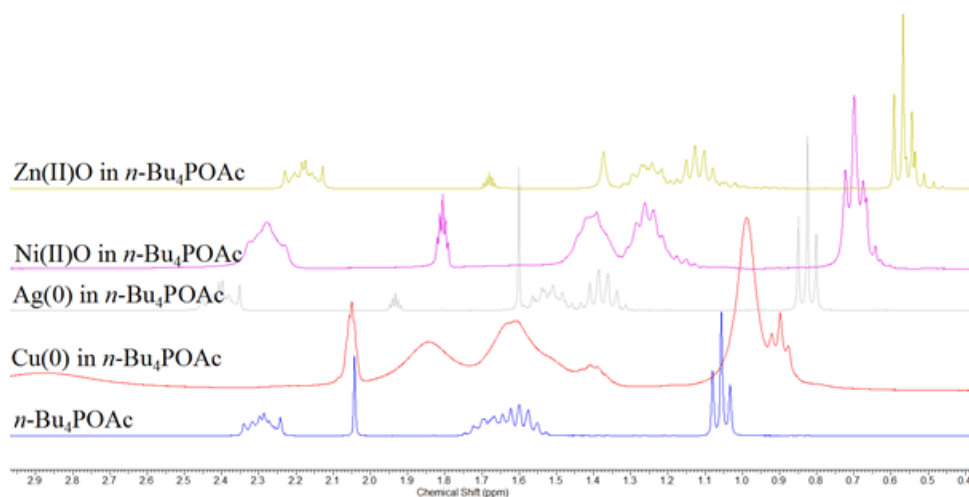
Figure 3.28: ^{1}H-NMR of the reaction mixture after the synthesis of Cu- (red), Ag- (grey), NiO- (pink) and ZnO (yellow) nanoparticles (offset: 0.15 ppm). A reference spectrum of n-Bu$_4$POAc (blue) is added.
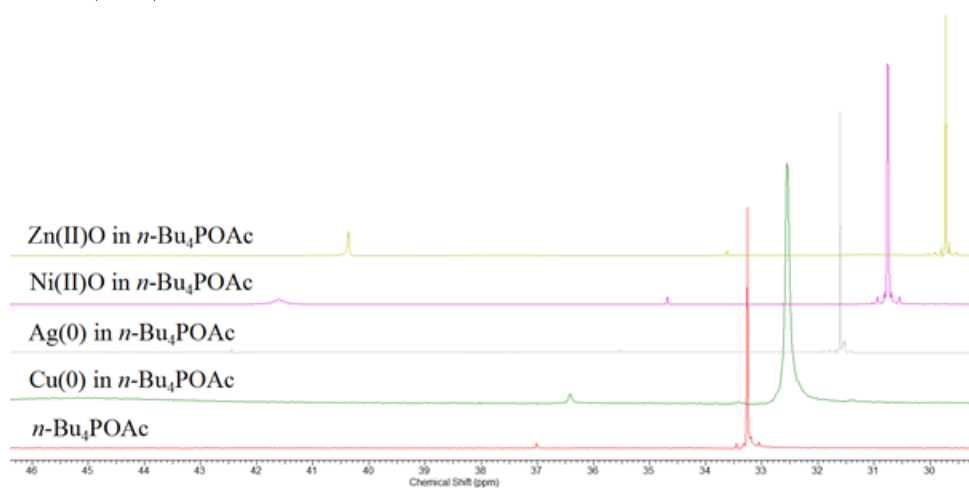
Figure 3.29: ^{31}P-NMR of the reaction mixture after the synthesis of Cu- (green), Ag- (grey), NiO- (pink) and ZnO (yellow) nanoparticles (offset: 1.0 ppm). A reference spectrum of n-Bu$_4$POAc (red) is added.
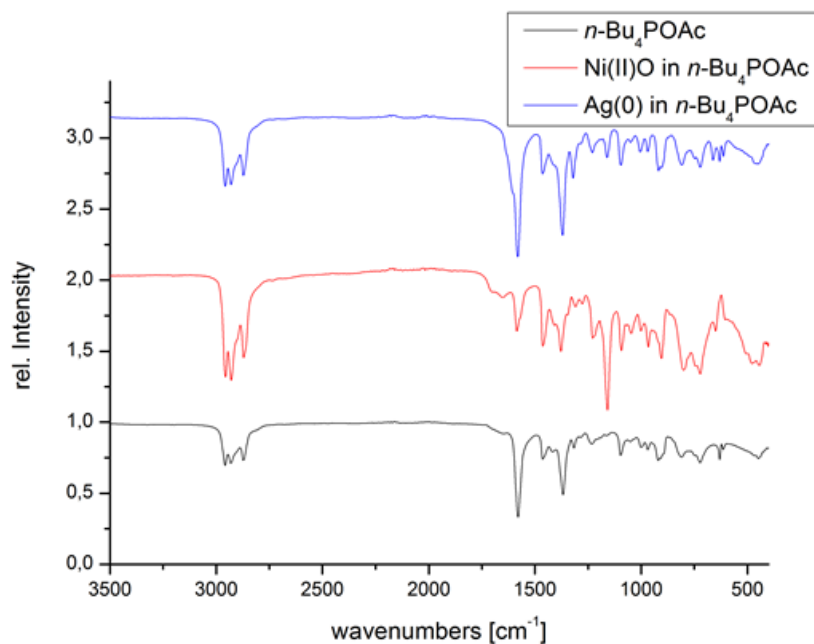
Figure 3.30: IR-spectra of pure *n*-Bu$_4$POAc (black) and the reaction mixtures of Ag-(blue) and NiO (red) nanoparticles in *n*-Bu$_4$POAc.
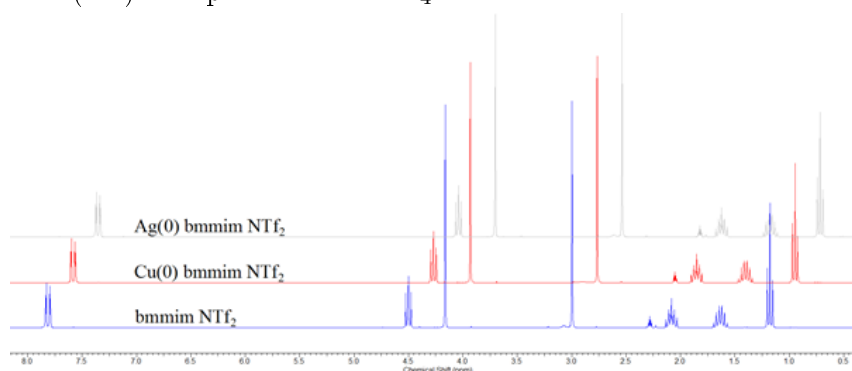
Figure 3.31: ^{1}H-NMR of selected reaction mixtures after the synthesis of Cu- (red) and Ag- (grey) nanoparticles (offset: 0.5 ppm). A reference spectrum of bmmim NTf$_2$ (blue) is added.
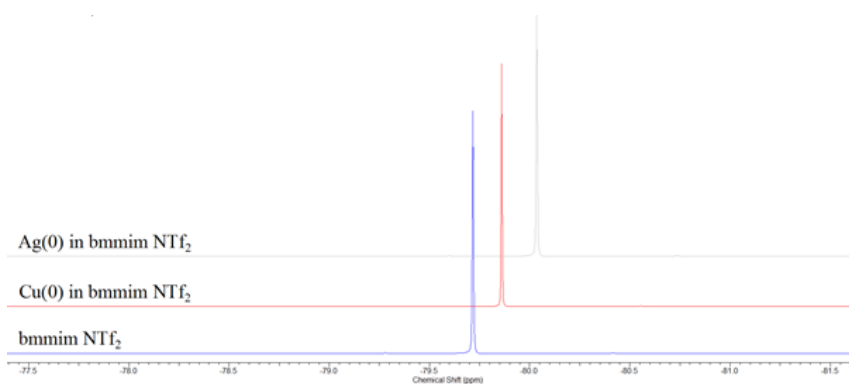
Figure 3.32: ^{19}F-NMR of selected reaction mixtures after the synthesis of Cu- (red) and Ag- (grey) nanoparticles (offset: 0.25 ppm). A reference spectrum of bmmim NTf$_2$ (blue) is added.
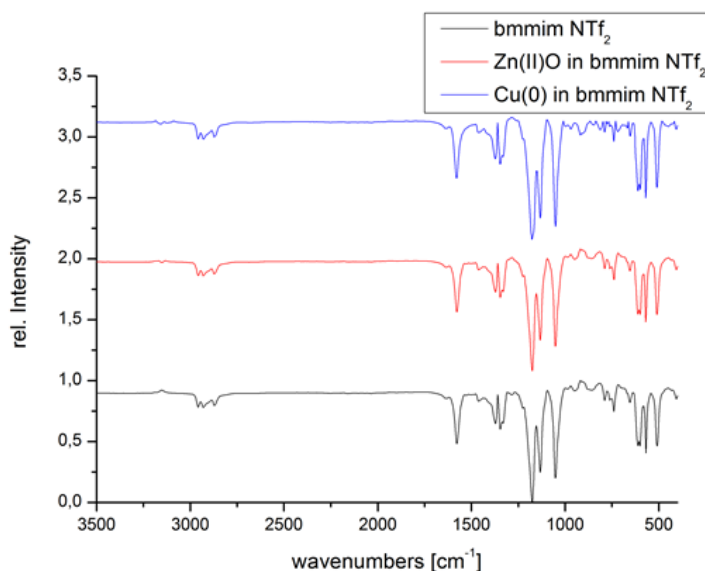
Figure 3.33: IR-spectra of pure bmmim NTf_2 (black) and the reaction mixtures of ZnO (red) and Cu(0) (blue) nanoparticles in bmmim NTf_2.
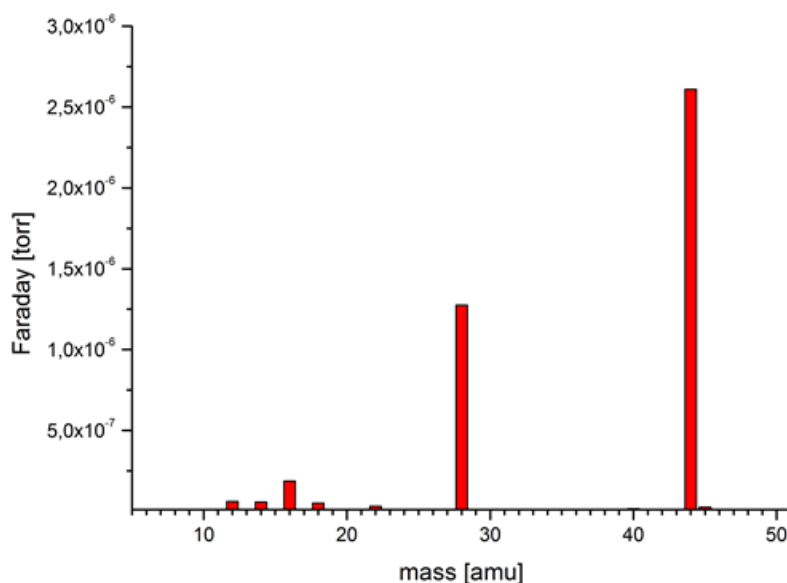
Figure 3.34: Gas-phase mass spectrogram of volatile compounds of the reductive decomposition of copper carbonate in n-Bu_4POAc.

Setup for gas-phase analyses

Experiments for gas phase analysis at elevated pressure were performed in a stainless steel autoclave purchased from Carl-Roth® with a direct connection to the MS-spectrometer via the mass flow controller. All reactions for the online gas-phase mass-spectrometry were carried out in dry 20ml screw cap vials equipped with a Teflon stirring bar and a perforated butyl/rubber septum. In comparison to the standard procedure the reaction batch was doubled in order to yield a significant amount of gaseous products.

Sample preparation for TEM analysis

A droplet of the nanoparticle dispersion embedded in IL was diluted with 2 ml acetone and a slight amount of this dispersion was placed in a holey carbon-coated copper grid. Particle size distributions were determined from the digital images obtained with a CCD camera. The NPs diameter was estimated from ensembles of 400 particles (800 counts) chosen in arbitrary areas of the enlarged micrographs. The diameters of the particles in the micrographs were measured using the software Lince Linear Intercept 2.4.2.

Sample preparation for XRD analysis

The nanoparticle dispersion was directly placed between two plastic disks as before transmission measurement. In case of a low viscosity the dispersion was dried at $40\,°C$ or at room-temperature under reduced pressure (10^{-2} mbar).

3.3.7   Notes and references

1. M. H. G. Prechtl, J. D. Scholten and J. Dupont, *J. Mol. Catal. A: Chem.*, **2009**, 313, 74–78.

2. P. G. Jessop, D. A. Jessop, D. B. Fu and L. Phan, *Green Chem.*, **2012**, 14, 1245–1259.

3. D. B. Zhao, Z. F. Fei, T. J. Geldbach, R. Scopelliti, P. J. Dyson, *J. Am, Chem. Soc.*, **2004**, 126, 15876–15882.

4. T. Y. Kim, J. H. Yeon, S. R. Kim, C. Y. Kim, J. P. Shim and K. S. Suh, *Phys. Chem. Chem. Phys.*, **2011**, 13, 16138–16141.

5. G. H. Hong and S. W. Kang, *Ind. Eng. Chem. Res.*, **2013**, 52, 794–797.

6. P. Migowski, G. Machado, S. R. Texeira, M. C. M. Alves, J. Morais, A. Traverse and J. Dupont, *Phys. Chem. Chem. Phys.*, **2007**, 9, 4814–4821.

7. R. R. Gandhi, S. Gowri, J. Suresh and M. Sundrarajan, *J. Mater. Sci. Technol.*, **2013**, 29(6), 533–538.

8. V. Calo, A. Nacci, A. Monopoli and P. Cotugno, *Angew. Chem., Int. Ed.*, **2009**, 48, 6101–6103.

9. V. Calo, A. Nacci, A. Monopoli and P. Cotugno, *Chem.–Eur. J.*, **2009**, 15, 1272–1279.

10. C. Amiens, B. Chaudret, M. Respaud and P. Lecante, *Actual. Chim.*, **2005**, 19–27.

11. L. M. Lacroix, S. Lachaize, F. Hue, C. Gatel, T. Blon, R. P. Tan, J. Carrey, B. Warot-Fonrose and B. Chaudret, *Nano Lett.*, **2012**, 12, 3245–3250.

12. W. Darwich, C. Gedig, H. Srour, C. C. Santini and M. H. G. Prechtl, *RSC Adv.*, **2013**, 3, 20324–20331.

13. M. H. G. Prechtl, P. S. Campbell, J. D. Scholten, G. B. Fraser, G. Machado, C. C. Santini, J. Dupont and Y. Chauvin, *Nanoscale*, **2010**, 2, 2601–2606.

14. M. T. Kessler, C. Gedig, S. Sahler, P. Wand, S. Robke and M. H. G. Prechtl, *Catal. Sci. Technol.*, **2013**, 3, 992–1001.

15. R. Venkatesan, M. H. G. Prechtl, J. D. Scholten, R. P. Pezzi, G. Machado and J. Dupont, *J. Mater. Chem.*, **2011**, 21, 3030–3036.

16. J. Dupont and J. D. Scholten, *Chem. Soc. Rev.*, **2010**, 39, 1780–1804.

17. J. Dupont and P. A. Z. Suarez, *Phys. Chem. Chem. Phys.*, **2006**, 8, 2441–2452.

18. J. Lopes and A. A. H. Padua, *J. Phys. Chem. B*, **2006**, 110, 3330–3335.

19. J. D. Scholten, B. C. Leal and J. Dupont, *ACS Catal.*, **2012**, 2, 184–200.

20. M. H. G. Prechtl and P. S. Campbell, *Nanotechnol. Rev.*, **2013**, 2, 577–595.

21. I. M. L. Billas, A. Chatelain and W. A. Deheer, *Science*, **1994**, 265, 1682.

22. M. Valden, X. Lai and D. W. Goodman, *Science*, **1998**, 281, 1647.

23. M. G. Bawendi, M. L. Steigerwald and L. E. Brus, *Annu. Rev. Phys. Chem.*, **1990**, 41, 477.

24. Y. Wang, *Acc. Chem. Res.*, **1991**, 24, 133.

25. T. Y. Kim, W. J. Kim, S. H. Hong, J. E. Kim and K. S. Suh, *Angew. Chem., Int. Ed.*, **2009**, 121, 3864.

26. B. Lim and Y. Xia, *Angew. Chem., Int. Ed.*, **2011**, 50, 76–85.

27. Y. Sun, Y. Yin, B. T. Mayers, T. Herricks and Y. Xia, *Chem. Mater.*, **2002**, 14, 4736–4745.

28. Y. Sun, B. Gates, B. Mayers and Y. Xia, *Nano Lett.*, **2002**, 2, 165–168.

29. J. Kim, S. W. Kang, S. H. Mun and Y. S. Kang, *Ind. Eng. Chem. Res.*, **2009**, 48, 7437.

30. K. I. Han, S. W. Kang, J. Kim and Y. S. Kang, *J. Membr. Sci.*, **2011**, 374, 43.

31. H. Wender, L. F. de Oliveira, P. Migowski, A. F. Feil, E. Lissner, M. H. G. Prechtl, S. R. Teixeira and J. Dupont, *J. Phys. Chem. C*, **2010**, 114, 11764–11768.

32. M. Ranjbar, S. Fardindoost, S. M. Mahdavi, A. I. Zad and N. Tahmasebi G, *Sol. Energy Mater. Sol. Cells*, **2011**, 95, 2335–2340.

33. M. H. G. Prechtl, J. D. Scholten and J. Dupont, *Molecules*, **2010**, 15, 3441–3461.

34. G. Demazeau, *J. Mater. Sci.*, **2008**, 43(7), 2104–2114.

35. M. K. Devaraju and I. Honma, *Adv. Energy Mater.*, **2012**, 2(3), 284–297.

36. C. H. Kuo and M. H. Huang, *Nano Today*, **2010**, 5(2), 106–116.

37. F. J. Douglas, D. A. MacLaren and M. Murrie, *RSC Adv.*, **2012**, 2(21), 8027–8035.

38. P. S. Vengsarkar and C. B. Roberts, *J. Phys. Chem. C*, **2013**, 117(27), 14362–14373.

39. D. K. Sahana, G. Mittal, V. Bhardwaj and M. Kumar, *J. Pharm. Sci.*, **2008**, 97(4), 1530–1542.

40. P. Singh, K. Kumaric, A. Katyal, R. Kalrad and R. Chandrab, *Spectrochim. Acta, Part A*, **2009**, 73, 218–220.

41. E. Rodil, L. Aldous, C. Hardacre and M. C. Lagunas, *Nanotechnology*, **2008**, 19, 105603.

42. E. Azaceta, N. T. Tuyena, D. F. Pickup, C. Rogerob, J. E. Ortega, O. Miguela, H.-J. Grandea and R. Tena-Zaera, *Electrochim. Acta*, **2013**, 96, 261–267.

43. I. Geukens, J. Fransaer and D. E. De Vos, *ChemCatChem*, **2011**, 3(9), 1431–1434.

44. B. Lim, T. Yu, J. Park, Y. Q. Zheng and Y. N. Xia, *Angew. Chem., Int. Ed.*, **2011**, 50(27), 6052–6055.

45. B. Ziolkowski, K. Bleek, B. Twamley, K. J. Fraser, R. Byrne, D. Diamond and A. Taubert, *Eur. J. Inorg. Chem.*, **2012**, 32, 5245–5251.

46. A. Banerjee, R. Theron and R. W. J. Scott, *Chem. Commun.*, **2013**, 49, 3227.

47. G. Fritz, V. Schadler, N. Willenbacher and N. J. Wagner, *Langmuir*, **2002**, 18(16), 6381–6390.

48. A. Pettersson, G. Marino, A. Pursiheimo and J. B. Rosenholm, *J. Colloid Interface Sci.*, **2000**, 228(1), 73–81.

49. F. Endres, *ChemPhysChem*, **2002**, 3(2), 144–154.

50. Y. Zhou, *Curr. Nanosci.*, **2005**, 1(1), 35–42.

51. P. Migowski and J. Dupont, *Chem.–Eur. J.*, **2007**, 13(1), 32–39.

52. A. Taubert and Z. Li, *Dalton Trans.*, **2007**, 7, 723–727.

53. M. Antonietti, D. B. Kuang, B. Smarsly and Z. Yong, *Angew. Chem., Int. Ed.*, **2004**, 43(38), 4988–4992.

54. M. T. Kessler, S. Robke, S. Sahler and M. H. G. Prechtl, *Catal. Sci. Technol.*, **2014**, 4, 102–108.

55. M. H. G. Prechtl, M. Scariot, J. D. Scholten, G. Machado, S. R. Teixeira and J. Dupont, *Inorg. Chem.*, **2008**, 47, 8995–9001.

56. C. C. Cassol, G. Ebeling, B. Ferrera and J. Dupont, *Adv. Synth. Catal.*, **2006**, 348, 243–248.

57. Y. G. Cui, I. Biondi, M. Chaubey, X. Yang, Z. F. Fei, R. Scopelliti, C. G. Hartinger, Y. D. Li, C. Chiappe and P. J. Dyson, *Phys. Chem. Chem. Phys.*, **2010**, 12, 1834–1841.

3.4 Molecular Palladium Precursors for Pd^0 Nanoparticle Preparation by Microwave Irradiation: Synthesis, Structural Characterization and Catalytic Activity

Frank Heinrich,[a] Michael T. Keßler,[a] Stephan Dohmen,[a] Mrityunjay Singh,[b] Martin H. G. Prechtl,[*a] and Sanjay Mathur[*a]

[a] Department of Chemistry, Chair of Inorganic and Materials Chemistry, University of Cologne, D-50939 Cologne, Germany
*E-mail: sanjay.mathur@uni-koeln.de and martin.prechtl@uni-koeln.de
[b] NASA Glenn Research Center, Ohio Aerospace Institute, Cleveland, OH 44135-3191, USA

Two new palladium complexes [Pd(MEA)$_2$Cl$_2$] (**1**) and [Pd(MEA)$_2$Br$_2$] (**2**) [MEA = (2-methoxyethyl)amine] were synthesized by the reaction of 2 equiv. of MEA with PdCl$_2$ or [(cod)PdBr$_2$] (cod = cycloocta-1,5-diene), respectively. Singlecrystal X-ray diffraction analysis of **1** and **2** revealed the formation of square-planar trans complexes with palladium coordinated by chloride/bromide ions and N-atoms of MEA bonded in a monodentate fashion. Given their molecular form and solubility, **1** and **2** act as intractable precursors to Pd nanoparticles by microwave-assisted synthesis. The influence of the reaction temperature, irradiation time and surfactant (PVP) concentration on the size (5–40 nm) of the resulting particles was studied by DLS (hydrodynamic diameter) and TEM analyses (particle size). The growth mechanism of the nanoparticles depended on the type of halide ligand. Powder X-ray diffractometry confirmed the formation of elemental Pd particles that were embedded in carbonized wood to examine their potential as a catalyst. The catalytic activity of these nanoscale particles was evaluated in carbon–carbon cross-coupling reactions by using Heck, Suzuki and Sonogashira reactions as benchmark models. The investigations included recycling experiments that resulted in total turnover numbers of 4321 (Heck), 6173 (Sonogashira) and 8223 (Suzuki).

3.4.1 Introduction

Palladium in the form of molecular complexes, nanoparticles and films is of significant interest due to its high catalytic activity and application in organic synthesis; for example, hydrogenation reactions or organic cross-coupling reactions (e.g. Heck, Stille, Suzuki and Sonogashira) are well known and widely described in the literature. Palladium based systems, which have been mostly obtained with ligands such as phosphanes, have been demonstrated as active reagents for homogeneous or heterogeneous catalysis with high

turnover numbers (TONs). Generally, the observed TONs are lower for heterogeneous catalysts. However, they are of potential interest due to the ease of purification of the resulting products and superior recycling efficiency when compared to the corresponding homogeneous systems. Nevertheless, a comparative evaluation between homogeneous and heterogeneous catalytic systems is not straightforward and is subject to a variety of physico-chemical parameters.[1]

Furthermore, palladium anchored on metal oxide (MO_x) substrates serve as excellent catalysts for the decomposition of volatile organic components (VOCs) and other environmental pollutants (NO_x, CO). In addition, Pd/MO_x heterostructures are well suited for the detection of toxic gases (CO, CH_4).[2] The extraordinary uptake of hydrogen in Pd structures has also led to new applications in the field of hydrogen storage and detection.[3]

Palladium nanoparticles (Pd NPs) are of current interest due to their large surface/volume ratio and the possible control over their size and shape, which influences their catalytic properties.[4,5] So far, many methods have been reported to prepare monodispersed Pd nanoparticles, which include chemical reduction of palladium salts or complexes[6] by reaction with molecular hydrogen, metal hydrides or by means of the polyol process,[5] or sonoelectrochemical methods[7] whereby different surfactants, polymers or ionic liquids have been used to prevent agglomeration and to impose a chemical control over the morphological features of the particles.[8]

Microwave irradiation of ionic or thermally labile precursors offers a facile, fast and green pathway to synthesize metal and metal oxide nanoparticles as the reaction durations are drastically reduced due to instantaneous heating of the reaction medium and formation of hot spots in the reaction mixture, which can be tuned by choosing solvents with desired polarity and dielectric properties.[9]
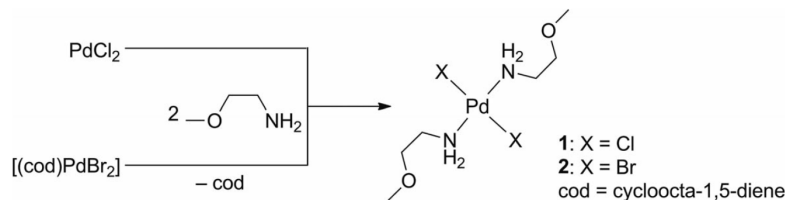
Figure 3.35: Syntheses of the palladium complexes **1** and **2**.

To this end, a number of ionic precursors, such as $PdCl_4{}^{2-}$, $PdCl_2$ and $Pd(OAc)_2$ as well as neutral complexes like $Pd_2(dba)_3$ (dba = dibenzylideneacetone), have been successfully used in the microwave-assisted synthesis of Pd nanoparticles.[10] The presence of a polar Pd complex in a polar solvent facilitates the interaction with the microwave field and results in a rapid heating and subsequent burst of decomposition reactions. The fast energy transfer and instantaneous decomposition of precursor species result in a brief nucleation stage producing well-dispersed particles with uniform size distribution.

We report here two new Pd complexes that exhibit lower decomposition temperatures and higher solubilities in common organic solvents compared to some other Pd precursors. Their ability to form palladium nanoparticles in the presence of PVP and ethanol by means of microwave-assisted decomposition has been tested and the influence of different reaction parameters and precursor configurations (Pd–Cl and Pd–Br units) on the size and shape of the particles was investigated. The Pd NPs were then embedded in carbonized wood and evaluated as recyclable precatalysts in ligand-free carbon–carbon cross-coupling reactions, namely the Heck, Suzuki and Sonogashira reactions.

3.4.2 Results and Discussion

Reaction of $PdCl_2$ or $[(cod)PdBr_2]$ (with cod = cycloocta- 1,5-diene) with 2 equiv. of (2-methoxyethyl)amine resulted in the formation of complexes **1** and **2** as orange and yellowish compounds, respectively (Figure 3.35). The products were characterized as discrete molecular species by single-crystal X-ray diffractometry, ^{1}H NMR spectroscopy, mass spectrometry, CHNS analysis and DSC/TGA analysis.

Single-crystal X-ray crystallography:

The molecular structures of **1** and **2** are isotypical (Figure 3.36). Both compounds crystallize in the monoclinic space group $P2_1/c$ where the unit cell of the dibromo derivative has a slightly higher cell volume (ca. 5.6%) due to the bulkier Br atoms. In addition to the halide atoms, two monodentate (2-methoxyethyl)amine molecules are coordinated to the Pd centre to complete the observed square-planar coordination around the central metal atom. The Pd–N distances are around 2.05 Å for both of the compounds, the Pd–Cl distance (**1**) was found to be 2.30 Å, while the Pd–Br distance (**2**) was 2.43 Å. The N–Pd–X [X = Cl (**1**), Br (**2**)] angles (89.18–90.82°) are very close to the optimal angle of 90°. Selected crystallographic data are given in Table 3.10.
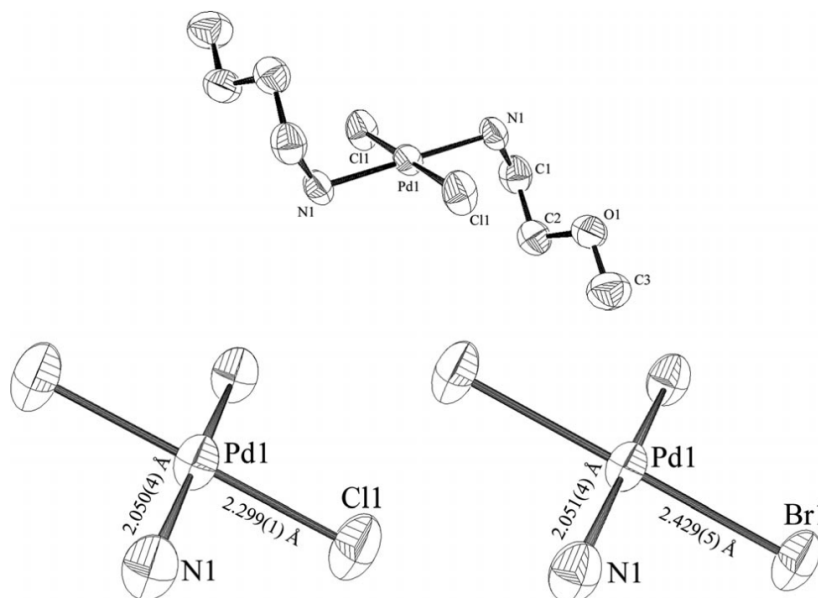
Figure 3.36: Molecular structure of **1** and coordination spheres of **1** and **2**. Ellipsoids are drawn with 50% probability level, hydrogen atoms are not depicted for clarity.

3.4.3 Thermal Properties

The thermal behaviour of **1** and **2** was analyzed by thermogravimetry and differential scanning calorimetry (TGA/DSC) measurements under air (Figure 3.37). Both **1** and **2** showed an endothermic feature without any significant weight loss up to 110 °C, which was attributed to the melting of the compounds, while at 200 °C the onset of decomposition was observed, which resulted in elemental palladium. The observed weight losses were very close to the theoretical values of 33% (calcd. 33%) for compound **1** and 27% (calcd. 26%) for compound **2**. No further weight reduction after 550 °C confirmed the formation of stable final products.

Table 3.10: Selected crystallographic data for **1** and **2**.

	1	2
Empirical formula	$C_6H_{18}Cl_2N_2O_2Pd$	$C_6H_{18}Br_2N_2O_2Pd$
Formula mass [g mol^{-1}]	327.52	416.44
Crystal system	monoclinic	monoclinic
Space group	P2$_1$c	P2$_1$c
a [Å]	8.566(2)	8.503(1)
b [Å]	8.605(1)	8.936(1)
c [Å]	8.987(2)	9.226(1)
β [°]	113.08(2)	113.34(2)
Z/V [Å^3]	2/609.4(2)	2/643.6(2)
Θ range [°]	2.58–29.61	3.31–28.08
T [K]	293(2)	293(2)
Index range	-11 <h <11	-11 <h <11
	-11 <k <11	-11 <k <11
	-12 <l <12	-12 <l <12
Total data collected	8395	6008
Unique data	1699	1555
Observed data	1070	1114
R$_{merg}$	0.0423	0.0539
μ [mm^{-1}]	1.936	7.627
R indexes [I>2σ(I)]	R$_1$ = 0.0427	R$_1$ = 0.0349
	wR$_2$ = 0.1012	wR$_2$ = 0.0792
R indexes (all data)	R$_1$ = 0.0719	R$_1$ = 0.0559
	wR$_2$ = 0.1177	wR$_2$ = 0.0841
Goof	0.992	1.031
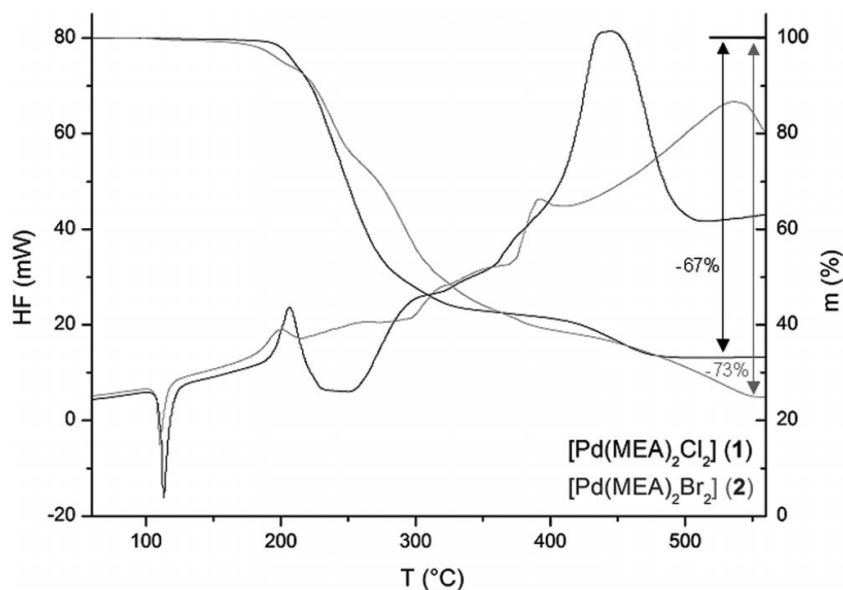
Figure 3.37: DSC/TGA plots for **1** and **2**.

3.4.4   Microwave-Assisted Synthesis of Pd Nanoparticles

Compounds **1** and **2** were used as precursors in the microwave assisted synthesis of Pd nanoparticles as they show low decomposition temperatures and good solubilities in common organic solvents. Exposure of the ethanolic solutions of **1** and **2** to microwave treatment induced the reduction reaction that led to elemental Pd. A remarkable colour change from yellow to dark brown during the microwave irradiation indicated the reduction of Pd^{II} to Pd^0, which sedimented in the form of a black powder; however, stable dispersions could be obtained by the addition of polyvinylpyrrolidone (PVP 40000), which acted as an efficient capping agent for the nanocrystals. As shown in the powder XRD pattern (Figure 3.38), elemental Pd in fcc phase was formed. The peaks at 40 °, 47 ° and 68 ° correspond to the 111, 200 and 220 lattice planes (JCPDS card no. 00-046-1043). According to the Scherrer equation a crystallite size of 8.7 nm ($\pm$0.9 nm) was obtained. The concentration of PVP, the reaction temperature and the time of microwave irradiation during the decomposition process were changed, and the influence of these changes on the particle size (hydrodynamic diameter) was analyzed by dynamic light scattering (DLS) measurements.
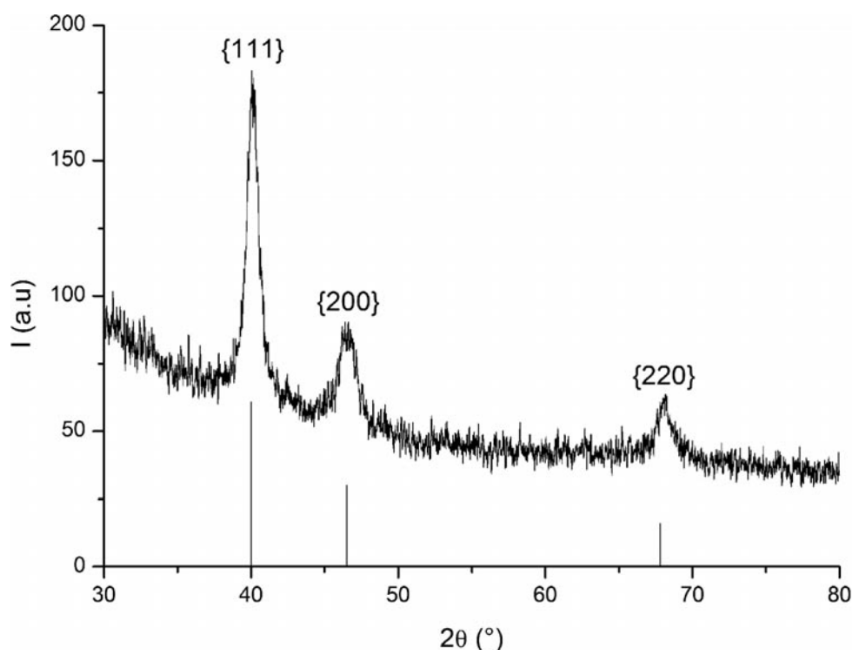
Figure 3.38: Powder XRD pattern of the as-synthesized Pd nanopar- ticles obtained from **1** with 20 mg of PVP, microwave irradiation time 5 min and temperature 150 °C.

Despite their isotypical crystal structures and similar decomposition profiles (TGA/DSC data), the microwave-assisted reduction of **1** and **2** led to palladium nanoparticles of different sizes. Apparently, the palladium–halogen bond becomes stronger in going from chloride to bromide, which results in a faster reduction of **1** under similar experimental conditions. Consequently, the faster growth of Pd nuclei leads to a faster formation of nanocrystals, as observed in the DLS measurements. In most of the reactions the particles are larger when complex **2** was used. The formation of Pd particles by microwave irradiation occurs at 130 °C for compound **1** and at 150 °C for compound **2** when applying a power of 150 W.
By enhancing the PVP/precursor ratio, the hydrodynamic diameter decreases in the case of compound **1** from about 48 nm (10 mg of PVP) to 37 nm (30 mg of PVP). In the case of compound **2**, these changes lead to an enhancement of the hydrodynamic diameter (from

47 to 54 nm) (Figure 3.39).
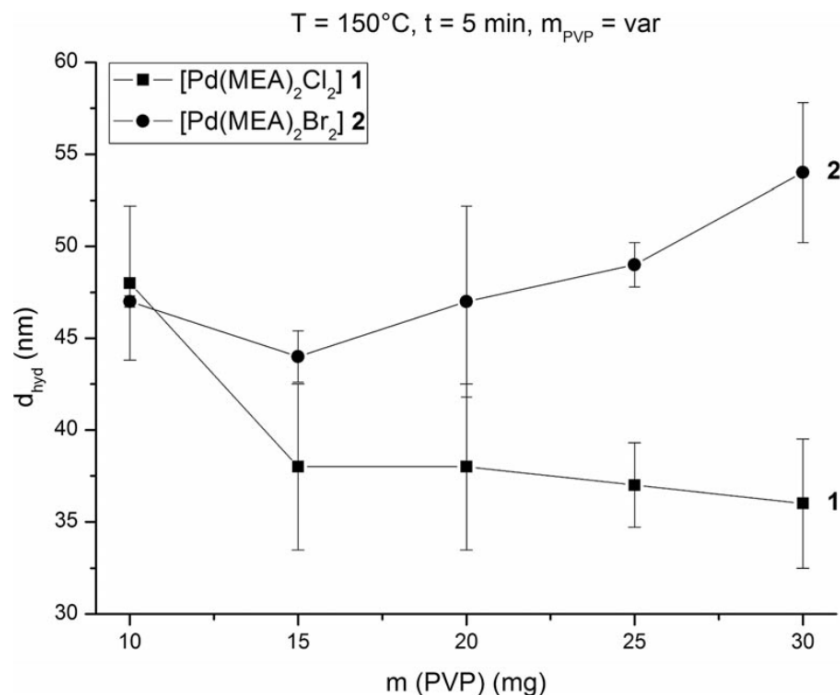
Figure 3.39: Mass of PVP vs. hydrodynamic diameter for Pd particles synthesized by using **1** and **2** with microwave irradiation time of 5 min and temperature of 150 °C.

The effect of the microwave irradiation time on the particle size did not exhibit a linear relationship. For compound **1**, after 3 and 4 min irradiation time the hydrodynamic diameters were in the range of 30–32 nm. After 5 min, the diameter increased to 37 nm and decreased to 33 nm at an irradiation time of 7 min. In the case of compound **2**, the hydrodynamic diameters increased from 42 to 63 nm on increasing the irradiation time from 3 min to 7 min, respectively, as shown in Figure 3.40.

Evidently, the synthesis temperature critically influences the size of the formed particles when the chloride-containing compound is used. At higher temperatures larger particles are formed (130 °C: 34 nm; 170 °C: 68 nm). At 110 °C no particles were obtained. Again the bromide-containing compound shows a different behavior. At temperatures lower than 150 °C no particles precipitated upon centrifugation. At 150 °C and 170 °C the hydrodynamic diameters of the particles are around 50 nm. It is well known that the growth mechanism of Pd particles is directly influenced by the halide ions present in the solution and, as reported by Xia *et al.*,[4,5] the addition of halide ions can change or rebuild the morphology of the as-formed nanoparticles. They observed that the adsorption of Br–ions on the surface of growing Pd nanoparticles promotes the formation of 100 facets. In their studies mainly nanocubes and nanobars of Pd were obtained, whereas upon using chloride-containing compounds and/or surfactants mainly polyhedral structures were observed. The shape of the resulting nanoparticles depends on the etching power of the halide ions; in the case of Ag NPs, which also crystallizes in the fcc phase, the presence of Cl^- ions produced Ag nanocubes, while the milder etchant Br^- enables the formation of bipyramidal particles.[5]

In addition, ions that are charged oppositely to the surface charge of NPs can strongly attenuate the influence of electrostatic double layer repulsion by neutralizing the surface
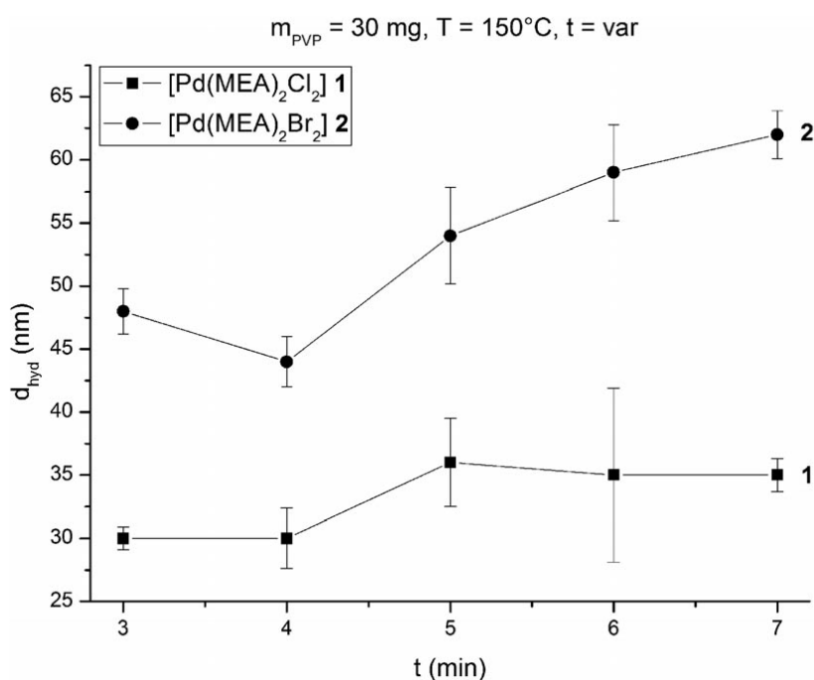
Figure 3.40: Irradiation time vs. hydrodynamic diameter for Pd particles synthesized by using **1** and **2** with a temperature of 150 °C and 30 mg PVP.

charge on the NPs, which can further affect the growth kinetics. Dyson *et al.* in the course of the nanoparticle synthesis that used palladium halides in imidazolium ionic liquids isolated stable palladium–carbene complexes with halide ligands in addition to palladium nanoparticles.[11e] This shows the influence of in situ complexation of ligands and their influence on the kinetics of the reduction, which affects the particle growth. The electron microscopy analysis revealed that the particles obtained from compound **1** at 130 °C showed a high degree of polydispersity. This temperature is too low to ensure spontaneous nucleation, and therefore the resulting particles show variable diameters and size-distribution. The particles obtained from **2** are less monodisperse than those obtained from compound **1**.
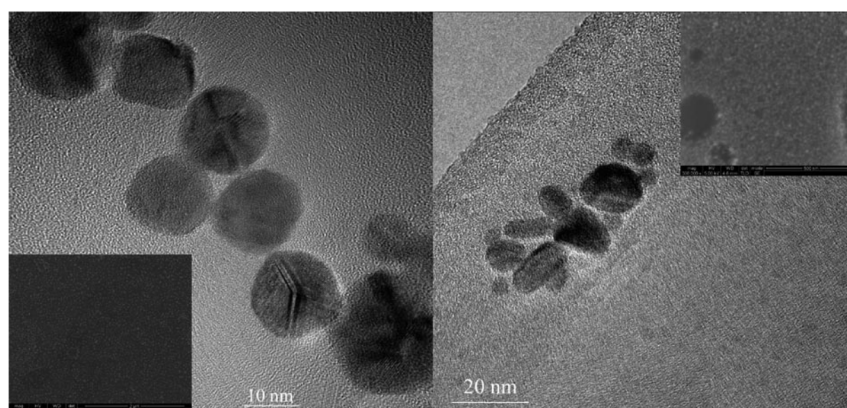
Figure 3.41: TEM and SEM images of Pd NPs derived from **1** (left) and **2** (right). Mass of PVP 30 mg, temperature 150 °C, power 150 W, irradiation time 5 min in both cases.

The particles do not have unique shapes but are elongated. The diameters of the

nanoparticles were between 5 and 40 nm, whereas the aspect ratio of the elongated structure was <10. TEM images confirmed the crystallinity of the particles in all of the measured samples (Figure 3.41).

3.4.5   Catalytic activity
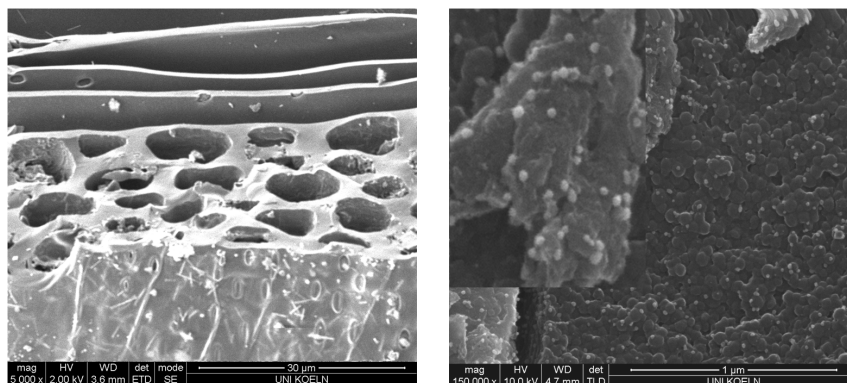
Figure 3.42: SEM images of empty wood channels (left) and wood channels decorated by Pd nanoparticles (right).

Palladium is known for its high catalytic activity in carbon–carbon cross-coupling reactions.[1,11] Traditionally, those reactions were carried out with defined palladium complexes or with palladium salts in the presence of phosphane, carbene or amine ligands.[11] In the last two decades it has been proven that ligand-free approaches involving molecular species and nanoparticles dissolved in a monophasic or biphasic reaction mixture play an important role in the catalytic cycle.[11]
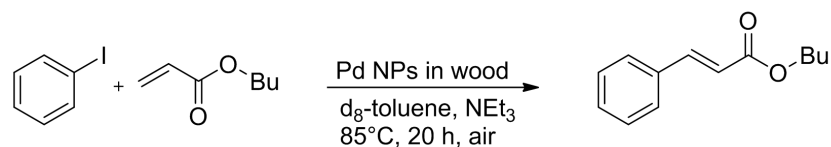
Scheme 3.7: Heck coupling reaction performed to test the efficacy of new heterogeneous catalysts.

It should be pointed out that the nanoparticles act as a reservoir for molecular species.[1c,11,12] The advantage of nanoparticle-based systems is their long-term stability compared to that of metal complexes. However, to make this property of nanoparticles useful in recyclable catalyst systems, the Pd NPs should be well immobilized in a liquid support or grafted onto a solid support.[1c]

In this manner the product phase can simply be separated from the catalyst by decantation or filtration. In the present work we embedded *in situ* synthesized palladium nanoparticles into carbonized cherry wood, which shows good structural features and means a very homogeneous distribution of channels. These channels could be filled with Pd NPs by decomposition of the dissolved palladium complexes **1** and **2** under microwave irradiation in the presence of pieces of wood. SEM measurements revealed that the wood was uniformly decorated with Pd nanoparticles (Figure 3.42). After impregnation of the wood with the PVP-protected palladium nanoparticles, the resulting material was evaluated in established carbon–carbon cross-coupling reactions to estimate their catalytic activity. The
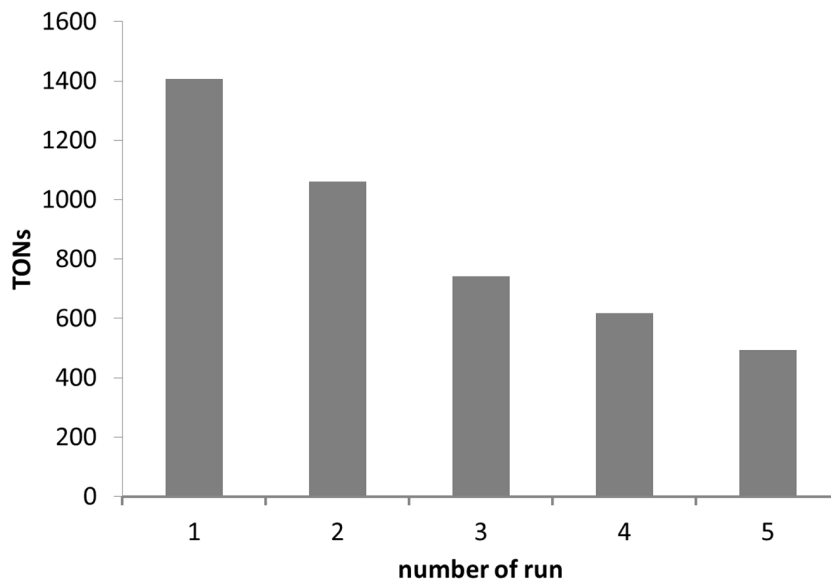
Figure 3.43: Recycling experiments in the Heck reaction.

Heck reaction is well-known to be promoted by Pd NPs as the catalyst reservoir.[1c,11,12] Therefore, we decided to couple iodobenzene with *n*-butyl acrylate in the presence of tri-ethylamine and PVP-Pd@wood (1.35 μmol Pd content; 0.14 wt.-% Pd) at 85 °C yielding butyl cinnamate in 57% (TON: 1407) in the first run (Scheme 3.7; Figure 3.43).
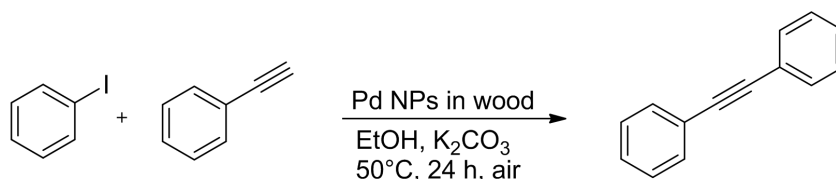
Scheme 3.8: Sonogashira coupling reaction.

The magic-number methodology was used for the calculation of the TONs based on the surface atoms of the metal nanoparticles.[13] A spherical crystallite of 8.7 nm ($\pm$0.9 nm) contains roughly 23485 atoms within 20 shells.
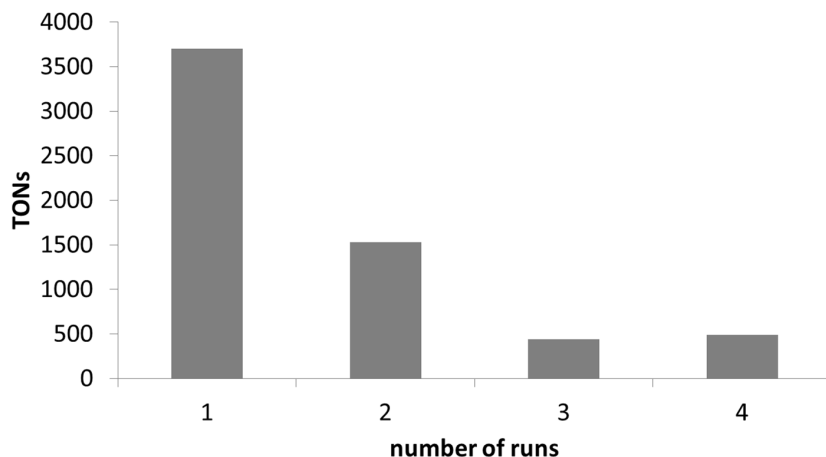
Figure 3.44: Recycling experiments in the Sonogashira reaction.

The surface shell contains 3500 atoms, and hence 15% of the atoms are surface atoms, which may potentially act as a catalyst reservoir. Figure 3.43 depicts the TONs of the recycling experiments in five runs taking only the surface atoms into account. The graphical sketch of the TONs may lead to the idea that strong catalyst leaching occurs during the consecutive recycling experiments. However, ICP-MS analysis of the catalyst material before and after the catalysis revealed that the palladium content does not change drastically, as will be discussed later (Suzuki reaction). After each run the catalyst material was separated from the formed ammonium salt and the product phase.

In the following recycling experiments the conversions decreased down to 494 TONs or 20% (Figure 3.43). Nevertheless, the very low Pd-loading gives remarkably high TONs in all of the runs (Figure 3.43) and a total TON for all runs of 4321. In further experiments we optimized the reaction conditions for C–C coupling reactions and performed the copper-free Sonogashira coupling of phenyl iodide and phenylacetylene in ethanol with potassium carbonate at 50 °C within 1 d (Scheme 3.8; Figure 3.44). In this case, the TON reached 3704 (75% conversion) in the initial run, the TONs dropped in every recycle and then stabilized in the third and fourth run to between 440 and 500.
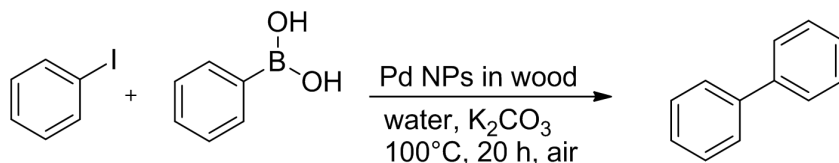
Scheme 3.9: Suzuki coupling reaction in water.

Furthermore, Suzuki reactions were performed with the PVP-Pd@wood catalyst in water as reaction media at 100 °C for 20 h (Scheme 3.9; Figure 3.45). The product is formed in the first two runs in high conversions (84–97%; 2074 and 2395 TONs) and can easily be isolated by extraction with *n*-pentane. The catalyst recycling shows remarkably high conversions in the first two runs in this biaryl coupling, and then the TONs decrease. The total TON over six runs reached 8223.
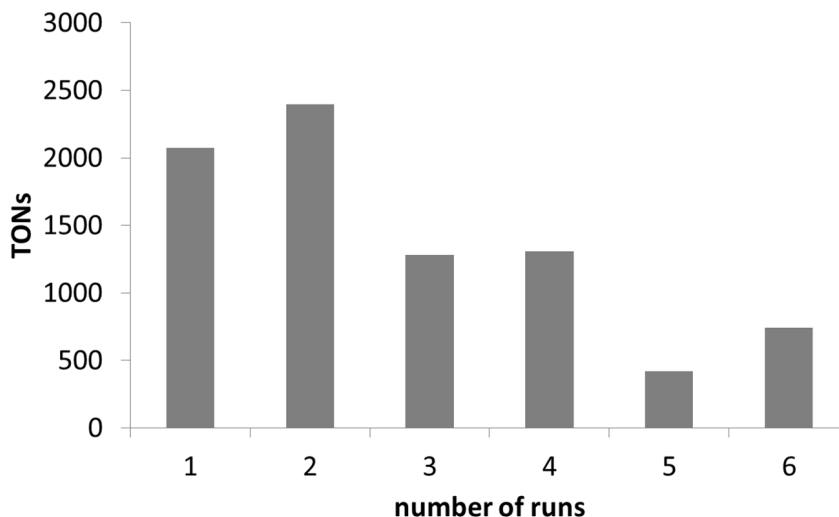
Figure 3.45: Recycling experiments in the Suzuki reaction in water.

ICP-MS analysis of the catalyst material before and after the catalysis reaction revealed that the palladium content does not change drastically. The prepared catalyst embedded onto wood contained 1.35 μmol palladium, and after the catalysis the palladium content was found to be 1.30 μmol. This indicates that the activity did not drop due to extensive metal leaching and that the deactivation must be related to another parameter. Considering the catalyst support, we assume that significant amounts of triethylammonium iodide that formed as byproduct may clog the pores and channels of the support material after each run. Consequently, fewer nanoparticles were available to act as the catalyst reservoir.

3.4.6 Conclusions

Two new palladium complexes were synthesized, characterized and used as precursors for the formation of Pd nanoparticles by means of microwave irradiation. DLS and SEM/TEM measurements show that the resulting shape and size of the crystalline particles is influenced by the halide content in the compounds. The particles were embedded into carbonized wood, and their catalytic activity was confirmed by Heck, copper-free Sonogashira and Suzuki reactions in recycling experiments. The total TONs reached under optimized conditions were 4321 (Heck), 6173 (Sonogashira) and 8223 (Suzuki). The deactivation of the catalyst material is probably related to salts that clog the pores and channels of the wooden matrices as no metal leaching was observed.

3.4.7 Experimental Section

General: [(cod)PdBr$_2$] was synthesized from K$_2$PdBr$_4$,[14] which was obtained from elemental palladium[15] according to literature procedures. The wooden templates were prepared by carbonization of wood (cherry wood) at 1000 °C in vacuo. All of the other chemicals were applied without further purification. ^{1}H-NMR spectra were recorded with a Bruker AVANCE II 300 spectrometer at 298 K (300.1 MHz, external standard TMS). C, H and N analyses were carried out with a HEKAtech Euro EA 3000 apparatus. Positive EI mass spectra were recorded with a Finnigan MAT 95 apparatus. Thermogravimetric measurements were performed with a STARe System by Mettler Toledo with TGA/DSC1

and Gas Controller GC100. For the synthesis of the Pd NPs a microwave CEM Discover and a centrifuge Eppendorf Centrifuge 5702 were used.

X-ray Crystallographic Analysis of Precursors: Single-crystal analysis was carried out with a STOE IPDS I and II with Mo-K$_\alpha$ irradiation. The structure was solved with SHELXS and SIR-92, the refinement was done with SHELXL and WinGX. For absorption correction STOE X-RED and STOE X-SHAPE were used. The structures were drawn with Ortep-III. CCDC-847018 (for **2**) and -847019 (for **1**) contain the supplementary crystallographic data for this paper. These data can be obtained free of charge from The Cambridge Crystallographic Data Centre via *www.ccdc.cam.ac.uk/data$_r$equest/cif*.

Characterization of Nanoparticles: The obtained Pd NPs were analyzed by powder X-ray diffractometry (STOE-STADI MP, Cu-K$_\alpha$ irradiation, $\lambda = 1.540598$ Å), SEM (Nano SEM 430 by FEI.), EDX (Apollo X by EDAX), TEM (Philips CM300 FEG/UT-STEM) and DLS (Zetasizer Nano-ZS by Malvern). The ICP-MS measurements were carried out by IWA, Institut für Wasser- und Abwasseranalytik GmbH, 52070 Aachen.

[Pd(MEA)$_2$Cl$_2$] (1): PdCl$_2$ (100 mg, 0.564 mmol) was suspended in THF (20 mL). (2-Methoxyethyl)amine (103 μL, 89 mg, 1.184 mmol) was added and the mixture stirred for 12 h. The solvent was evaporated, and the resulting orange solid was washed with *n*-pentane (3 x 10 mL) and recrystallized from THF. The yield was 163 mg (88%). ^{1}H NMR (300 MHz, room temp., CDCl$_3$): $\delta = 3.54$ (t, 2H, CH$_2$O), 3.35 (s, 3H, CH$_3$), 2.91 (m, 4H, CH$_2$N, NH$_2$) ppm. ^{13}C NMR (75 MHz, room temp., CDCl$_3$): $\delta = 71.1$ (CH$_2$O), 58.8 (CH$_3$), 44.8 (CH$_2$N) ppm. C$_6$H$_{18}$Cl$_2$N$_2$O$_2$Pd (327.55): calcd. C 22.00, H 5.54, N 8.55; found C 21.23, H 5.78, N 8.01. MS (EI$^+$, 20 eV, 140 °C): m/z(%) = 328 (2) [M]$^+$, 292 (5) [M – HCl]$^+$, 254(8) [M – 2 HCl]$^+$, 181 (3) [Pd(MEA)]$^+$, 76 (4) [MEA + H]$^+$, 75 (3) [MEA]$^+$, 45 (28) [C$_2$H$_5$O]$^+$, 44 (6) [C$_2$H$_6$N]$^+$, 30 (100) [CH$_4$N]$^+$.

[Pd(MEA)$_2$Br$_2$] (2): [(cod)PdBr$_2$] (200 mg, 0.534 mmol) was dissolved in THF (20 mL). (2-Methoxyethyl)amine (98 μL, 84 mg, 1.122 mmol) was added and the mixture stirred for 1 h. The solvent was evaporated, and the resulting orange-yellow solid was washed with *n*-pentane (3 x 10 mL) and recrystallized from THF. The yield was 195 mg (88%). ^{1}H NMR (300 MHz, room temp., CDCl$_3$): $\delta = 3.49$ (t, 2H, CH$_2$O), 3.35 (s, 3H, CH$_3$), 2.97 (t, 2H, CH$_2$N), 2.80 (br.s, 2H, NH$_2$) ppm. ^{13}C NMR (75 MHz, room temp., CDCl$_3$): $\delta = 71.1$ (CH$_2$O), 58.8 (CH$_3$), 45.7 (CH$_2$N) ppm. C$_6$H$_{18}$Br$_2$N$_2$O$_2$Pd (416.45): calcd. C 17.30, H 4.36, N 6.73; found C 17.31, H 4.52, N 6.36. MS (EI$^+$, 20 eV, 140 °C): m/z (%) = 337 (32) [M – Br]$^+$, 255 (9) [M–2Br–H]$^+$, 181 (3) [Pd(MEA)]$^+$, 76 (3) [MEA + H]$^+$, 75(2) [MEA]$^+$, 45 (26) [C$_2$H$_5$O]$^+$, 44 (6) [C$_2$H$_6$N]$^+$, 30 (100) [CH$_4$N]$^+$; [M]$^+$ could not be observed.

Pd Nanoparticles: In a typical synthesis precursor **1** (20 mg, 0.061 mmol) or **2** (25 mg, 0.061 mmol) was mixed with PVP 40000 (10–30 mg) and dissolved in ethanol (4 mL) in a microwave tube. The microwave treatment took place while stirring the mixture at 130–170 °C for 3–7 min. The resulting dark brownish solution was centrifuged at 11 krpm for 30–60 min, the surfactant was removed, ethanol (10 mL) was added to the residue, and the mixture was centrifuged again using the same parameters. This washing process was repeated three times. The particles could easily be redispersed in ethanol to form stable dispersions. For the impregnation of wood, small pieces of wood were directly added to the reaction mixture prior to decomposition.

Heck Reaction with Pd NPs: In a typical experiment iodobenzene ($55\,\mu$L, 0.5 mmol), *n*-butyl acrylate ($72\,\mu$L, 0.5 mmol), triethyl-amine ($80\,\mu$L, 0.6 mmol), PVP-Pd@wood
(98 mg; 0.14 wt.-% Pd) and [d$_8$]toluene (1 mL) were introduced into a 20 mL reaction vial in air. The mixture was stirred at 85 °C for 20 h. Then the conversion was determined directly by ^{1}H NMR spectroscopy by using hexamethyldisilane as the internal standard ($20\,\mu$L).

Sonogashira Reaction with Pd NPs: In a typical experiment phenyl acetylene ($110\,\mu$L, 1.0 mmol), iodobenzene ($120\,\mu$L, 1.1 mmol) and potassium carbonate (207 mg, 1.5 mmol) were added to ethanol (2 mL) and mixed with the PVP-Pd@wood (72 mg; 0.14 wt.-% Pd) in a 20 mL reaction vial in air. The mixture was stirred at 50 °C for 24 h. The product was extracted with pentane (30 mL) from the reaction mixture, diluted with water (2 mL), the organic layer was dried with MgSO$_4$, and the solvent was removed under vacuum. The product was analyzed, and the conversion was determined by ^{1}H NMR spectroscopy by using hexamethyldisilane as the internal standard ($20\,\mu$L).

Suzuki Reaction: In a typical experiment phenylboronic acid (91 mg, 0.75 mmol), iodobenzene ($55\,\mu$L, 0.5 mmol), and potassium carbonate (140 mg, 1.0 mmol) were added to water (3 mL) and mixed with PVP-Pd@wood (72 mg; 0.14 wt.-% Pd) in a 20 mL reaction vial in air. The mixture was stirred at 100 °C for 20 h. At room temperature a crystalline solid precipitated from the water. The product was extracted with pentane (30 mL) from the aqueous phase, the organic layer was dried with MgSO$_4$, and the solvent was removed under vacuum. The white solid was analyzed, and the conversion was determined by ^{1}H NMR spectroscopy by using hexamethyldisilazane as the internal standard ($20\,\mu$L).

3.4.8   Acknowledgements

1. a) C. Barnard, *Platinum Met. Rev.* **2008**, 52, 38–45; b) X. F. Wu, P. Anbarasan, H. Neumann, M. Beller, *Angew. Chem.* **2010**, 122, 9231; *Angew. Chem. Int. Ed.* **2010**, 49, 9047–9050; c) M. H. G. Prechtl, J. D. Scholten, J. Dupont, *Molecules* **2010**, 15, 3441–3461; d) R. Venkatesan, M. H. G. Prechtl, J. D. Scholten, R. P. Pezzi, G. Machado, J. Dupont, *J. Mater. Chem.* **2011**, 21, 3030–3036; e) M. Lamblin, L. Nassar-Hardy, J.-C. Hierso, E. Fouquet, F.-X. Felpin, *Adv. Synth. Catal.* **2010**, 352, 33–79.

2. a) Y. Liu, Z. Wu, Z. Sheng, H. Wang, N. Tang, J. Wang, *J. Hazard. Mater.* **2009**, 164, 542–548; b) M. S. Hegde, G. Madras, K. C. Patil, *Acc. Chem. Res.* **2009**, 42, 704–712; c) G. Centi, *J. Mol. Catal. A* **2001**, 173, 287–312; d) V. G. Papadakis, C. A. Pliangos, I. V. Yentekakis, X. E. Verykios, C. G. Vayenas, *Catal. Today* **1996**, 29, 71–75; e) M. V. Twigg, *Catal. Today* **2011**, 163, 33–41; f) H. H. Choi, I. Kim, G.-H. Kim, S. D. Kim, INEC: 2010 *3rd International Nanoelectronics Conference* **2010**, 1–2, 533–534; g) D.-J. Yang, I. Kamienchick, D. Y. Youn, A. Rothschild, I.-D. Kim, *Adv. Funct. Mater.* **2010**, 20, 4258–4264; h) J. Chen, K. Wang, R. Huang, T. Saito, Y. H. Ikuhara, T. Hirayama, W. Zhou, *IEEE T. Nanotechnol.* **2010**, 9, 634–639.

3. a) J.-S. Noh, J. M. Lee, W. Lee, *Sensors* **2011**, 11, 825–851; b) R. M. Penner, *MRS Bull.* **2010**, 35, 771–777; c) E. Sennik, N. Kilinc, Z. Z. Ozturk, *J. Appl. Phys.* **2010**, 108, 054317; d) S. R. Hunter, J. F. Patton, M. J. Sepaniak, P. G. Daskos, D. B. Smith, *Sensor Actuat. A: Phys.* **2010**, 163, 464–470; e) V. A. Vons, H. Leegwater, W. J. Legerstee, S. W. H. Eijt, A. Schmidt-Ott, *Int. J. Hydrogen Energy* **2010**, 35, 5479–5489.

4. a) Y. Xia, Y. Xiong, H. Cai, B. J. Wiley, J. Wang, M. J. Kim, *J. Am. Chem. Soc.* **2007**, 129, 3665–3675; b) Y. Xia, Y. Xiong, H. Cai, Y. Yin, *Chem. Phys. Lett.* **2007**, 440, 273–278; c) Y. Xia, Y. Xiong, J. M. McLellan, J. Chen, Y. Yin, Z.-Y. Li, *J. Am. Chem. Soc.* **2005**, 127, 17118–17127.

5. a) Y. Xia, Y. Xiong, J. Chen, B. Wiley, *J. Am. Chem. Soc.* **2005**, 127, 7332–7333; b) S. H. Im, Y. T. Lee, B. Wiley, Y. Xia, *Angew. Chem.* **2005**, 117, 2192; *Angew. Chem. Int. Ed.* **2005**, 44, 2154–2157.

6. a) H. Choo, B. He, K. Y. Liew, H. Liu, J. Li, *J. Mol. Catal. A* **2006**, 244, 217–228; b) D. Li, S. Komarneni, *J. Nanosci. Nanotechnology* **2008**, 8, 3930–3935.

7. Q. Shen, Q. Min, J. Shi, L. Jiang, J.-R. Zhang, W. Hou, J.-J. Zhu, *J. Phys. Chem. C* **2009**, 113, 1267–1273.

8. a) P.-F. Ho, K.-M. Chi, *Nanotechnology* **2004**, 15, 1059–1064; b) J. Dupont, J. D. Scholten, *Chem. Soc. Rev.* **2010**, 39, 1780–1804.

9. a) S. Mathur, L. Xiao, H. Shen, R. von Hagen, J. Pan, L. Belkoura, *Chem. Commun.* **2010**, 46, 6509–6511; b) M. N. Nadagouda, T. F. Speth, R. S. Varma, *Acc. Chem. Res.* **2011**, 44, 469–478.

10. a) T. Huang, Y. Yu, Y. Zhao, H. Liu, *Mater. Res. Bull.* **2010**, 45, 159–164; b) Y. X. Chen, B. L. He, H. F. Liu, *J. Mater. Sci. Technol.* **2005**, 21, 187–190; c) L. H. Du, Y. G. Wang, *Synth. Commun.* **2007**, 37, 217–222; d) A. da Conceicao Silva, J. D. Senra, L. C. S. Aguiar, A. B. C. Simas, A. L. F. de Souza, L. F. B. Malta, O. A. C. Antunes, *Tetrahedron Lett.* **2010**, 51, 3883–3885; e) D. L. Martins, H. M. Alvarez, L. C. S. Aguiar, *Tetrahedron Lett.* **2010**, 51, 6814–6817; f) Z. Du, W. Zhou, F. Wang, J. X. Wang, *Tetrahedron* **2011**, 67, 4914–4918.

11. a) M. T. Reetz, E. Westermann, *Angew. Chem.* **2000**, 112, 170; *Angew. Chem. Int. Ed.* **2000**, 39, 165–168; b) S. W. Kim, M. Kim, W. Y. Lee, T. Hyeon, *J. Am. Chem. Soc.* **2002**, 124, 7642–7643; c) A. Alimardanov, L. S. V. de Vondervoort, A. H. M. de Vries, J. G. de Vries, *Adv. Synth. Catal.* **2004**, 346, 1812–1817; d) M. T. Reetz, J. G. de Vries, *Chem. Commun.* **2004**, 1559–1563; e) Z. F. Fei, D. B. Zhao, D. Pieraccini, W. H. Ang, T. J. Geldbach, R. Scopelliti, C. Chiappe, P. J. Dyson, *Organometallics* **2007**, 26, 1588–1598.

12. a) C. C. Cassol, A. P. Umpierre, G. Machado, S. I. Wolke, J. Dupont, *J. Am. Chem. Soc.* **2005**, 127, 3298–3299; b) C. S. Consorti, F. R. Flores, J. Dupont, *J. Am. Chem. Soc.* **2005**, 127, 12054–12065; c) I. P. Beletskaya, A. N. Kashin, I. A. Khotina, A. R. Khokhlov, *Synlett* **2008**, 10, 1547–1552; d) C. Rangheard, C. D. Fernandez, P. H. Phua, J. Hoorn, L. Lefort, J. G. de Vries, *Dalton Trans.* **2010**, 39, 8464–8471.

13. A. P. Umpierre, E. de Jesus, J. Dupont, *ChemCatChem* **2011**, 3, 1413–1418.

14. G. Brauer, *Handbuch der präparativen anorganischen Chemie*, Ferdinand Enke Verlag, Stuttgart, **1981**, vol. 3, p. 1377.

15. P. Heimbach, M. Molin, *J. Organomet. Chem.* **1973**, 49, 483–494.

3.5   Coupling Reactions in Ionic Liquids

Chapter 6

Michael   T.   Keßler,[a]   Jackson   D.   Scholten,[b]   Frank   Galbrecht,[a]   and Martin H. G. Prechtl*[a]

[a] Universität zu Köln, Institut für Anorganische Chemie, Köln, Germany
[b] Universidade Federal do Rio Grande do Sul, Instituto da Quimica, Porto Alegre, Brazil

3.5.1   Introduction

In the last decade ionic liquids (ILs) have become very popular in the field of catalytic reactions under multiphase reaction conditions.[1−7] Their physico-chemical properties i.e. nonflammable, non-volatile, highly solvating, non-coordinating, tuneable polarity and good thermal stability make them highly attractive for biphasic reactions with water, organic solvents or supercritical fluids (scCO$_2$) as cosolvents.[8−9] Low melting organic salts are defined as IL (ionic liquid) with a melting point lower than $100\,°C$ (Figure 3.46).[7,10−11] The low melting points are related to a reduced lattice energy due to large ion pairs and low symmetry of cations.[8−9,12] These superior properties of ILs in comparison to volatile organic solvents make them feasible to reduce or suppress the hazards of common solvents in synthesis and catalysis.[13] Under optimized conditions the catalyst is immobilized in the IL phase and the substrates and products remain in the organic phase. Thus, the products can easily be separated and the catalyst is recycled. In absence of an organic (co)solvent the organic products can be easily extracted from the neat IL reaction mixture.

For task-specific applications the physico-chemical properties of ILs can be modified by tailoring the cation and/or anion structures.[14−18] In particular, ILs as solvents for transition metal catalysis are highly interesting because of the enhanced solubility of organometallic compounds in this solvent class. Therefore this 'catalyst–solvent couple' is quite promising for homogeneously catalyzed reactions. Interestingly, in certain cases, i.e. cross-coupling reactions, an anion-effect was observed regarding the selectivity or reaction pathway; therefore, the IL also plays a role as cocatalyst.[5,19] Other advantages of ILs for metalcatalyzed reactions are the solvation of the metal species, especially ionic complexes, which can be tuned by systematic tailoring the cation/anion pairs for optimized biphasic systems, where ILs are superior to water or organic solvents.[8] Other terms of selectivity in multiphase reactions can be influenced by the solubility/miscibility of reactants or intermediates in the catalyst phase. Thus, the catalytic activity and long-term stability of the catalyst is significantly optimized. One drawback in certain cases is the relatively high viscosity of ILs which may result in mass-transfer limitations in multiphase systems.[20] Especially, in the particular case of hydrogenation reactions, the reaction rate is influenced by the rather low solubility of hydrogen gas in IL. However, hydrogenation reactions in ILs are fast enough to be performed in these systems and the catalyst lifetime is prolonged impressively. Therefore, quite high total turnover numbers (TTONs) can be obtained.[20]
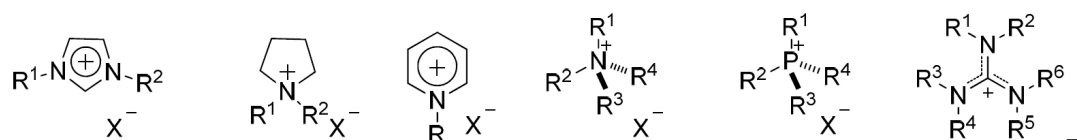
R = alkyl chains (C_1-C_{16}), aliphatic alcohols (butyl alcohol), ethers (butyl methyl ether), carboxylic acids (acetic acid), esters, nitriles (butyronitrile), amines (ethyl amine), glycol ether (triethylene glycol methyl ether), sulfonates (propanesulfonate), thiols (decanethiol), etc.

anions X⁻: CF_3SO_3, CH_3SO_3, $EtSO_4$, $(CF_3SO_2)_2N$ (NTf_2), halides, OAc, $PF_3(C_2F_5)_3$, PF_6, BF_4, amino acid carboxylates, camphersulfonate, etc.
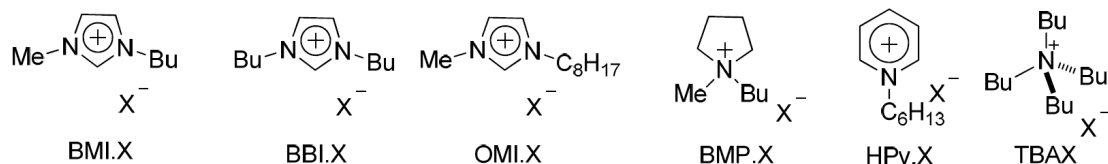
Figure 3.46: Selected examples for ILs with imidazolium, pyrrolidinium, pyridinium, ammonium, phosphonium and guanidinium cations. The side-chains are alkyl groups also carrying functionalities like alcoholic, ether, nitrile and other moieties. Usually weak coordinating anions are used as counterions such as BF_4, PF_6, NTf_2 [bis(trifluoromethanesulfonyl)imide], etc. On bottom selected cations discussed in this chapter with the used abbreviations: BMI = 1-butyl-3-methylimidazolium, BBI = 1,3- dibutylimidazolium, OMI = 1-methyl-3-octylimidazolium, BMP = N-butyl-N-methylpyrrolidinium, HPy = N-hexylpyridinium, TBA = tetrabutylammonium.

Besides hydrogenation reactions, carbon–carbon cross-coupling reactions are among the most investigated catalytic processes in ionic liquids as reaction media.[5] Most of the classical solvent systems used for cross-coupling reactions such as acetonitrile, DMF, NMP, DMAc, DMSO or chlorinated hydrocarbons are environmentally unfriendly.[21] Additionally, often sensitive and expensive compounds such as phosphanes are used as stabilizing ligands for the metal complexes. In particular, expensive and sensitive complexes often suffer from decomposition and metal/ligand leaching of the catalyst phase. Consequently, the catalyst phase is deactivated and the product is contaminated by ligand and metal impurities, which results in laborious product purification and difficult catalyst recycling. Catalyst immobilization in IL for the use in multiphase systems does not solve all problems of homogeneous and heterogeneous catalysis, but bridges a gap and helps to minimize the over-all number of problems in applied catalysis. To overcome these aspects, new approaches are currently under investigation using tailor-made solvents such as ionic liquids with functional groups (task-specific ILs).[14−16,18,22−25] The ILs as recyclable solvents have the potential to substitute the mentioned classical solvents. Furthermore, the functional groups as coordinating ligands for transition metals in task-specific ILs may substitute expensive and sensitive ligands. Thus, costs, by-products and catalyst leaching can be decreased due to higher selectivities, better catalyst immobilization, catalyst recovery and prolonged catalyst lifetime. In summary, the advantages of ILs for carbon–carbon cross-coupling reactions are as follows: facilitating catalyst recovery and separation of products, prolonged catalyst lifetime, thermal stability for high temperature application or low vapor pressure for application of reduced pressure during the reaction (work-up). Besides these aspects, certain combinations of cations and anions have been shown to influence the selectivity of organic reactions. For example, it is possible to distinguish between competing reactions like cross-coupling (Heck, Suzuki) versus homocoupling (Ullmann).[5,19] Since the

discovery, palladium-catalyzed cross-coupling reactions in the 1970s have been among the most investigated transition-metal catalyzed reactions.[26−30] The protocols use approaches with palladium complexes with phosphane and carbene ligands as well as palladacycles. Also palladium salts and zero-valent approaches, where palladium(0) species act as catalytically active species in absence of ligands.[31−36] For example, the Heck reaction using aromatic halides is catalyzed by myriad of Pd^{II} or Pd^0 sources.[1,21] And, this fact allows, at least for ligand free palladium sources, that soluble Pd nanoparticles (Pd-NPs) play a role as a reservoir of catalytically active species.[37−39] The present overview describes the application of several palladium sources in ILs in carbon–carbon cross-coupling reactions. The ILs act as stabilizing agents for the ionic metal complexes or π–π-stacking, salts or monodispersed metal NPs to prevent agglomeration.[20,24] Additionally, the IL forms a protective layer to avoid oxidation of sensitive ligands or the metal surface.[1,6] One disadvantage of using ILs in certain palladium-catalyzed coupling reactions is the fact that salts are formed as by-products in stoichiometric amount and they remain at least partially in the IL layer.[40] One approach in reaction engineering to overcome this problem is the application of so-called "switchable solvent", in particular amine/alcohol mixtures. These solvent mixtures can be reversibly converted into ILs by carrying out the reaction under carbon dioxide atmosphere ("ionic liquid mode"), resulting in alkylammonium alkyl carbonates. Theses carbonates decompose to the corresponding alcohols and CO_2 by simple exchange of the CO_2 atmosphere to a nitrogen/argon atmosphere ("organic solvent mode").[40−42] In this way, the product is separated from the polar IL phase in the first step (under CO_2); afterwards the inorganic salts are separated by precipitation from solution by converting the IL into an organic solvent mixture under nitrogen or argon. The first reports of palladium catalyzed coupling reactions go back to the 1970s and were honored in 2010 with the Nobel Prize in Chemistry.[43] More systematic and mechanistic studies of this reaction class have been conducted in more than three decades by numerous research groups worldwide and new findings are published every week.[43] The following sections cover a brief summary of wellknown coupling reactions like Heck-type, Suzuki, Stille, Sonogashira, Negishi, Buchwald-Hartwig and Ullmann reactions carried out in ILs using: (i) metal complexes, (ii) metal salts as well as classical supported metal catalysts and (iii) metal(0) nanoparticles (Scheme 3.10).

3.5.2 Metal Complexes

The previously described problems in palladium-catalyzed reactions are strongly connected to the classical polar solvents (DMSO, DMF, DMAc, acetonitrile, methanol, etc.) often used in C–C coupling reactions. Many cross-coupling products are important in the synthesis of natural products and in the production of fine chemicals. However, this reaction class often suffered from various limitations and hence hampered a larger industrial exploitation. The mentioned solvents are quite polar, strongly solvating, some have high boiling points, and miscible with a broad range of solvents. Thus, they provoke the formation of emulsions in combination with apolar solvents. Therefore, these solvents are unsuitable for multiphase catalysis and difficult to separate and recycle by extraction or distillation. These drawbacks can be overcome by substituting these solvents with tailor-made ionic liquids of tunable polarity. On one hand the ILs contain regions of high polarity; on the other hand due to the ionic character certain ILs are neither miscible with apolar solvents nor with water. This indicates their suitability for biphasic and even liquid systems with three phases (hydrocarbons/IL/water). The mentioned IL properties help to dissolve and recycle the catalyst, suppress the tendencies for decomposition of the catalyst and leaching, allows product isolation by phase separation, and in certain cases the selectivity can be

R' $\diagdown$, base, -HX

Heck → R' $\diagup$ R   R' = aryl, alkenyl, alkyl

R—BE$_2$, base, -HX

Suzuki → R—R'   R' = aryl, alkenyl
BE$_2$ = borylester, boronic acid

R'—Sn(R)$_3$

Stille → R—R' + XSn(R)$_3$ R' = aryl, alkenyl, alkyl

R'—≡ , base, -HX

Sonogashira → R—≡—R'   R' = aryl, alkenyl

R—X   R—X **[Pd-cat.]** **ILs**

Ullmann → R—R   R' = aryl

R = aryl, (alkenyl), (allyl), (alkynyl)
X = I, Br, Cl, OTf

R'R''NH, base, -HX

Buchwald-Hartwig → R—N(R')(R'')   R' = aryl, alkyl, H
R'' = aryl, alkyl

[Pd-cat.]:
Phosphine/NHC-complexes,
Pd salts, Pd-NPs,
Pd/C, Pd/Al$_2$O$_3$, etc.

R—Zn-X'

Negishi → R—R'   R' = aryl, alkenyl, allyl, alkyl

ILs:
cations:
tetraalkylammonium, imidazolium,
pyridinium, pyrrolidinium,
phosphonium, guanidinium, etc.
anions:
CF$_3$SO$_3$, CH$_3$SO$_3$, EtSO$_4$, N(CF$_3$SO$_2$)$_2$,
halides, OAc, PF$_3$(C$_2$F$_5$)$_3$, PF$_6$, BF$_4$, etc.

Scheme 3.10: Overview about palladium-catalyzed cross-coupling reactions in ILs.

controlled for one or another reaction (cross-coupling vs. homocoupling).

Mizoroki-Heck Reaction

One of the most investigated reactions is the Heck coupling which has been reviewed several times.[27,44−46] *Kaufmann* and coworkers reported a Heck-coupling reaction with the use of ionic liquids in 1996.[47] This reaction procedure showed good performance of 51–99% yield in the synthesis of trans-cinnamates (Scheme 3.11). The ionic liquid seems to stabilize the palladium catalyst which did not precipitate in most of the reactions. *Böhm* and *Herrmann* studied chloroarenes which showed an improved activity and stability of almost any known catalyst system in ILs compared to conventional solvents.[48] The reaction of bromobenzene with styrene, for example, gave only 20% conversion in DMF, whereas the yield could be increased up to 99% using diiodobis(1,3-dimethylimidazolium-2-ylidene)palladium(II) for Heck reactions carried out in ILs which were reviewed in detail by *Molnár*.[44]

Good to excellent yields even with twelve reuses of the catalyst have been reported. This shows significantly the potential of ILs as reaction media in Heck couplings. ILs may be considered as a non-innocent solvent for the Heck reaction.[48−49] However, the reaction is feasible with various catalysts. In an early study, *Seddon* and their coworkers applied PdCl$_2$ and Pd(OAc)$_2$Ar$_3$P as catalyst in a Heck reaction carried out in BMI.PF$_6$ (1-butyl-3- methylimidazolium hexafluorphosphate) or HPy.PF$_6$ (N-hexylpyridinium hexafluorphosphate).[50] The product could easily be isolated using a three-phase system of IL–hexane–water. The product was soluble in the organic phase whereas the catalysts remained in the IL and the salt was removed through the aqueous phase (Scheme 3.12).
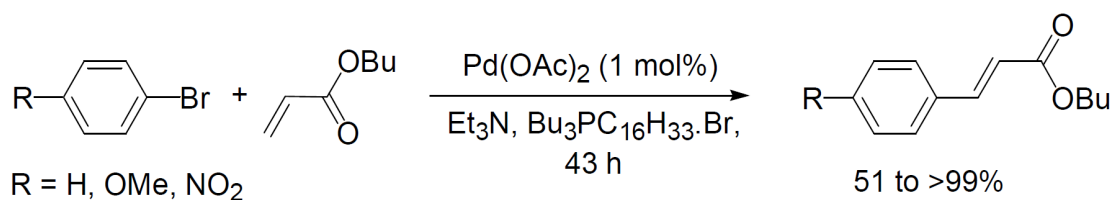
Scheme 3.11: Heck Reaction in molten tetraalkylammonium and tetraalkylphosphonium bromides.
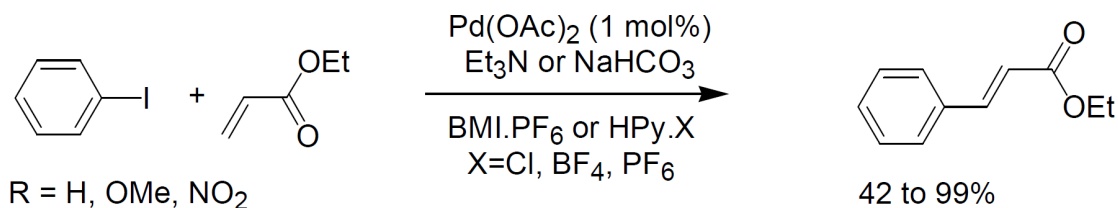
Scheme 3.12: Heck Reaction according to *Earle* and *Seddon*.[50]

A wide range of Pd^0 and Pd^{II} catalysts have been applied in the Heck reaction including $PdCl_2$ and $Pd(OAc)_2$. Furthermore, palladacycles such as trans-di(μ-acetato)-bis[o-(di-otolylphosphano) benzyl]-dipalladium(II) and 1,3-dimesitylimidazol-2-ylidene-palladium(0)-(η^2,η^2)-1,1,3,3-tetramethyl-1,3-divinyl disiloxane are also potential catalysts in the Heck reaction.[51] ILs based on guanidine (GILs) and acetic acid shows high efficiency in the Heck reaction.[52] The reaction of bromobenzene and styrene showed high yields and TON applying $Pd(OAc)_2$ and $PdCl_2$ in this case. The active species in this procedure is formed during the formation of the IL by reaction with acetic acid. The reaction of the amine with HPF_6 formed an inactive IL where the formation of palladium black was observed indicating decomposition of the catalyst. According to *Shreeve* and coworkers ILs play a dual role by immobilizing the palladium species and as a coordinating ligand. For example, the complex in Figure 3.47 was synthesized by the reaction of the depicted IL containing a 2,2'-biimidazole (BIIM) moiety with $PdCl_2$.[53]
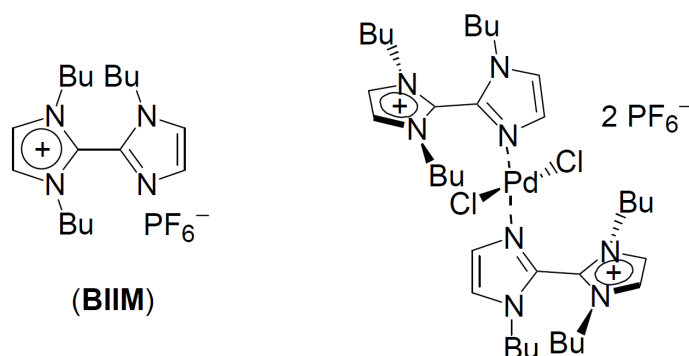
Figure 3.47: Palladium complex (right) with the 2,2'-biimidazole ligand BIIM (left).

This catalytic system was tested in the reaction of iodobenzene with methyl acrylate in ten consecutive runs (changing to non-activated chlorobenzene after the fifth cycle). The reactants were added to a preformed solution of 2 mol% $PdCl_2$ in IL (Scheme 3.13).[53] The

catalyst–ionic liquid solution was recovered simply by washing with water to remove the salt and drying under vacuum. The recycled catalytic system was reused at least ten times without significant loss of activity (81% yield in cycle ten). The benefit of this system is that the ionic catalyst is well-immobilized and does not leach to the organic phase during the extraction of the product.
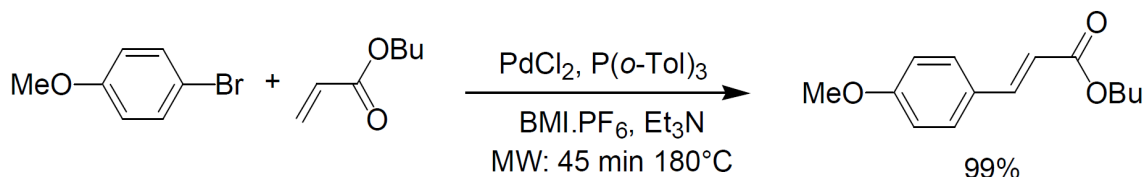
Scheme 3.13: The use in Heck coupling of *Shreeve's* system with the 2,2'-biimidazole ligand (Figure 3.47).[53]

Shreeve and coworkers extended the catalyst–IL system to various ILs, e.g. pyridylfunctionalized ILs. High efficiency and excellent stability of such catalytic system were shown by continuous catalyst recycling of up to 13 runs and 92% yield in the last run.[54−55] Microwave as a heat source in Heck reactions has been studied by *Vallin* and coworkers.[56] Palladium sources such as $PdCl_2$, $Pd(OAc)_2$ and Pd/C (2 mol%) were used in these studies with common phosphane ligands (4 mol%) in $BMI.PF_6$ with conversions between 43% and 99%. The best catalytic system for the reaction of 4-bromoanisole and *n*-butyl acrylate was found to be the combination of P(o-tol)$_3$ and $PdCl_2$ which gave a yield of 99% (Scheme 3.14).
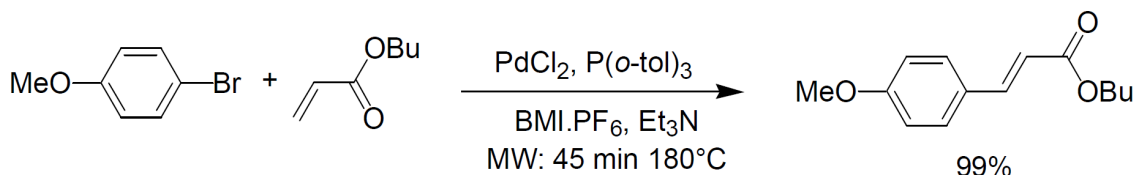
Scheme 3.14: Microwave-assisted Heck coupling.

Recyclability studies of the catalytic ionic system have been made and the catalyst system could be reused at least five times. The authors predicted that formed palladium black was redissolved upon microwave-assisted heating. The Heck coupling in ILs gives a good choice of controlled regioselectivity by choosing appropriate ligands or ILs. Scheme 3.15 shows the synthesis of arylated-γ,δ-unsaturated ketones.[57]
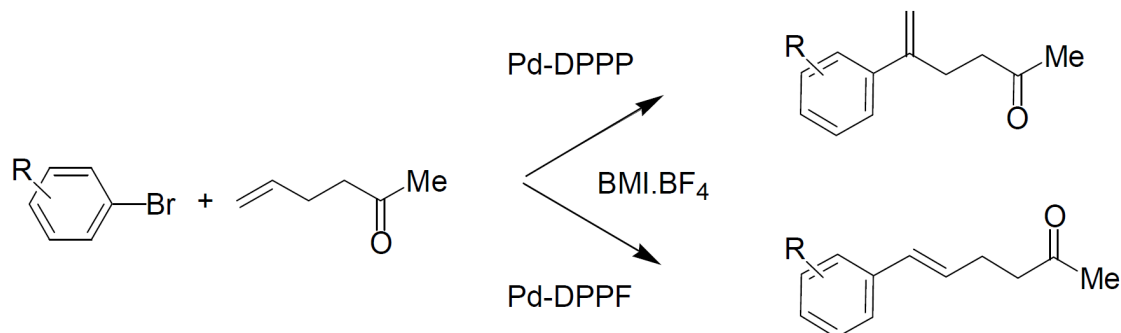
Scheme 3.15: Synthesis of γ-arylated and δ-arylated γ,δ-unsaturated ketones.

The use of 1,3-bis(diphenylphosphano)propane palladium Pd-DPPP gave mainly branched γ- arylated products while the use of 1,1'-bis(diphenylphosphano)ferrocene DPPF affords mainly the (E)-type δ-arylated γ,δ-unsaturated ketones. The Heck reaction of enol ethers bearing an electron-donating group gives a mixture of α- and β-substituted products if the reaction is carried out in common solvents. Nevertheless, the reaction of vinyl ethers with aryl halides in BMI.BF$_4$ gives over 99% of the α-substituted isomer.[58] This high selectivity has been observed in the reaction of electron-rich olefins with aryl halides in BMI.BF$_4$ compared to 75% in organic solvents (Scheme 3.16).
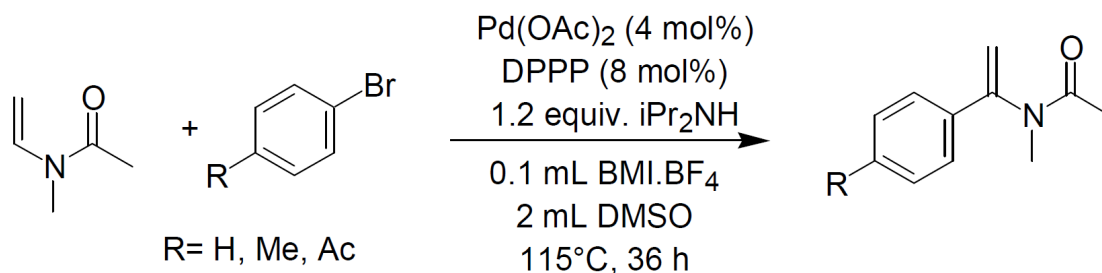
Scheme 3.16: Reaction of electron-rich olefins with aryl halides.

The reaction rate has been improved by using BMI.Br with the effect attributed to the formation of 1-butyl-3-methylimidazol-2-ylidene (BMIy) complexes of palladium [PdBr(μ-Br)(BMIy)]$_2$ and [PdBr$_2$(BMIy)$_2$] only observed in the bromide based system.[58–59] *Xiao* and coworkers studied the regioselective Heck reaction of heteroaryl halides such as halopyridines, bromoquinolines and bromothiophenes with the electron-rich vinyl ether and allyl alcohols in IL in comparison to common solvents (Scheme 3.17).[60] The Heck reaction in BMI.BF^4 gave exclusively α-substituted products in good to excellent yields of 69–95%.
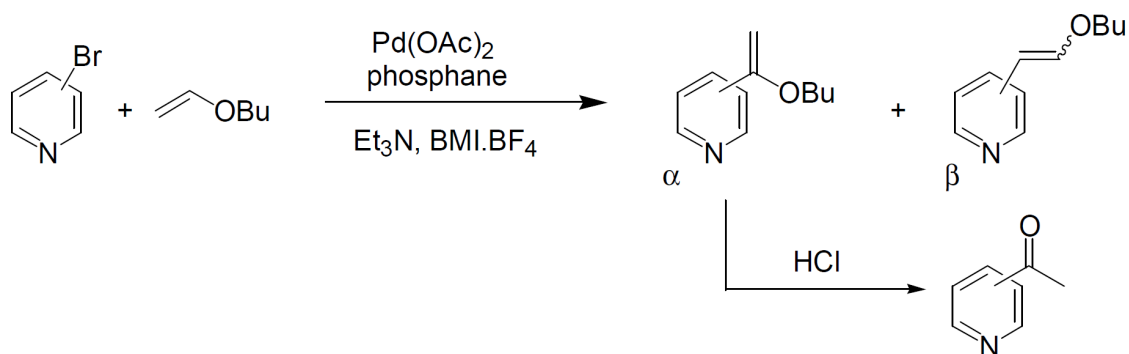
Scheme 3.17: Regioselective Heck reaction of heteroaryl halides.[60]

Besides the well-known parameters e.g. choice of the base, ligands, etc. a few pieces of information are discussed here to give some hints for the survey of suitable experimental procedures. Commonly used Pd^0 and Pd^{II} catalysts are based on palladacycles, Pd(OAc)$_2$ and PdCl$_2$. Palladium catalysts prepared by reaction with ILs (e.g. *Shreeve's* complex) seems to be potential candidates for stable and efficient catalyst–IL–systems.[53] A halide effect in the Heck reaction has been observed and discussed.[61] It has been found that the presence of halide ions can accelerate the Heck reaction showing the greatest improvement with iodide followed by bromide and then chloride. Interestingly the authors found an unexpected activity in an upscaling experiment and attributed this acceleration to impurities remained in the IL. Another important observation was the stability of the palladium cat-

alyst. Halide-free and chloride-assisted reactions of iodobenzene and methyl acrylate show deposition of palladium black on the sides of the reaction vessels whereas no decomposition was observed with addition of bromide or iodide.

Sonogashira Coupling
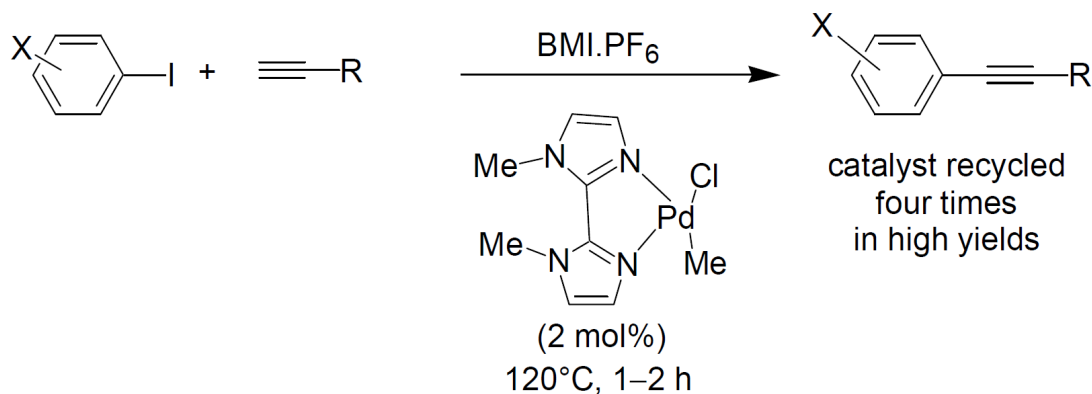
Scheme 3.18: Sonogashira coupling in IL.

The Sonogashira coupling reaction is an established synthetic pathway for alkynylation of arenes. This reaction procedure is gaining much interest as it opens a pathway to materials which are potential candidates for application in nonlinear optical electronic devices and it is also a key step in natural product synthesis.[62−63] Sonogashira couplings are traditionally performed by reacting terminal alkynes with aryl halides or triflates and palladium as catalyst in the presence of Cu salts and phosphane ligands. Alkynylation reactions being active without copper have recently been developed (so-called Heck-type alkynylation). However, procedures have been reported in the last years utilizing ILs for the Sonogashira coupling reactions.[64−67] ILs as reaction medium are of interest as procedures were developed in the absence of copper and phosphane ligands. [(Bis-imidazole)Pd(CH$_3$)Cl] catalyzes the coupling reaction efficiently in the absence of Cu salts or bulky phosphane ligands (Scheme 3.18). The catalyst could be recycled four times in high yields which show the efficiency of this catalyst system.[65]
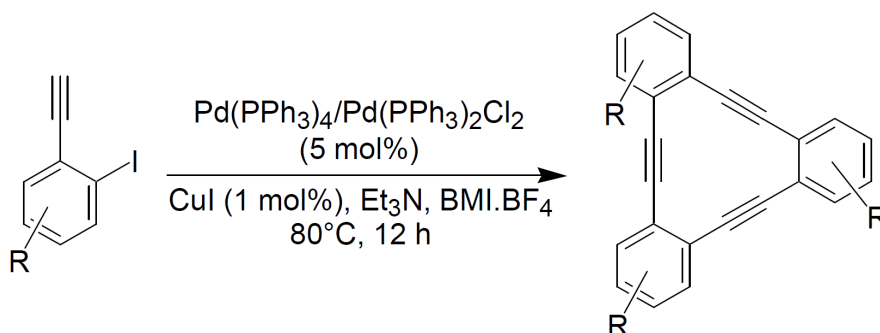
Scheme 3.19: Synthesis of tribenzohexadehydro[12]annulene in BMI.BF$_4$ via Sonogashira coupling.

PdCl$_2$[P(OPh)$_3$]$_2$ has been applied in the cross-coupling and carbonylative coupling of terminal alkynes with aryl iodides with good performance.[66] Compared to the reac-

tion in toluene the process with the use of ILs is faster. In ILs $BMI.PF_6$ or $OMI.PF_6$ the catalyst was recycled and used in four consecutive catalytic cycles and showed no significant loss of catalytic activity. In the absence of aryl iodide the same catalytic system catalyzed head-to-tail dimerization of phenylacetylene to the corresponding 1,3-diphenylenyne, trans-$PhC\equiv C-C(Ph)=CH_2$, in a yield of 85%. The synthesis of tribenzo-hexadehydro[12]annulene and its derivatives have been reported under Sonogashira conditions in $BMI.BF_4$ (Scheme 3.19). Homocoupling could be minimized by reducing the amount of Cu salt.[68] Copper-free Sonogashira coupling reactions with the use of $PdCl_2(PPh_3)_2$ can be performed in $BMI.PF_6$ in good to high yields (Scheme 3.20). The application of this reaction was also performed in a microflow system.[67]

$$Ar\text{-}I \quad + \quad H\!\!=\!\!\!=\!\!\!=\!\!R \xrightarrow[\substack{BMI.PF_6\,,\,60°C,\,2\,h \\ iPr_2NH\ or\ piperidine}]{Pd(PPh_3)_2Cl_2\ (5\ mol\%)} Ar\!\!=\!\!\!=\!\!\!=\!\!R$$

R = alkyl, aryl

(85–97 %)
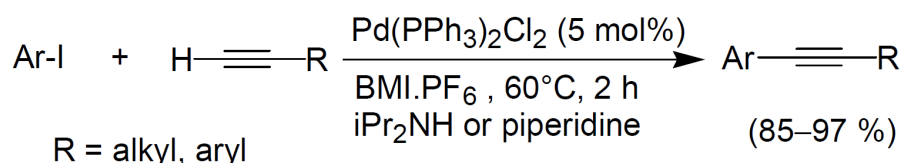
Catalyst Screening:
5 mol% $Pd(PPh_3)_4$/CuI, 91%; 2 mol% $Pd(PPh_3)_4$, 13%;
2 mol% $PdCl_2(PPh_3)_2$, 96%;
1 mol% $PdCl_2(PPh_3)_2$, 96%, (80°C);
10 mol% $Pd(OAc)_2$/PPh_2, 83%; $Pd(OAc)_2$, 61%;
$PdCl_2$, 57%; $PdCl_2(NCPh)_2$, 63%; $PdCl_2(NCMe)_2$, 56%

Scheme 3.20: Copper-free alkyne-coupling.

Ryu and coworkers found that the use of piperidine as a base in place of diisopropylamine was particularly useful to create a copper-free reaction system. Recycling studies were carried out. After separation of the products from the catalyst by extracting with *n*-hexane, the resulting ionic liquid layer was washed with water to remove ammonium salts. The resulting ionic liquid contains the palladium catalyst and was reused several times. After four cycles the yield decreased from 96% (first cycle) to 63%. Different palladium complexes were tested in the reaction of iodobenzene and phenylacetylene in $BMI.PF_6$. The conversion depends on the different palladium complexes used in the reaction for two hours at 60 °C (Scheme 3.20). *Shreeve* and co-workers applied a pyrazole-functionalized ionic liquid in combination with the corresponding pyrazole Pd^{II} complexes to the Sonogashira cross-coupling (Scheme 3.21).[69] Recycling studies has been performed with the consecutive reaction of various iodoarenes. The yields are high (87–95%) in six recycles and imply no effect of the substituents (R = 1. H, 2. Me, 3. MeO, 4. F, 5. NO_2, 6. 2-iodothiophene).

The choice of the experimental procedure is hard to predict. New reaction components have to be tested to achieve the most suitable conditions. Nevertheless, a few pieces of information for the survey to a practicable procedure are described here. Ligands, co-catalysts and other additives can change the results dramatically. The most commonly used complexes are $Pd(PPh_3)_4$ or $Pd(PPh_3)_2Cl_2$. The number of cycles the catalysts can be reused seems to be limited to give satisfying yields over more than four cycles. This problem seems to be solved utilizing more complex catalysts either as carbapalladacycles or preformed catalyst with functionalized ILs. One reason can be the stability and solubility in the IL.
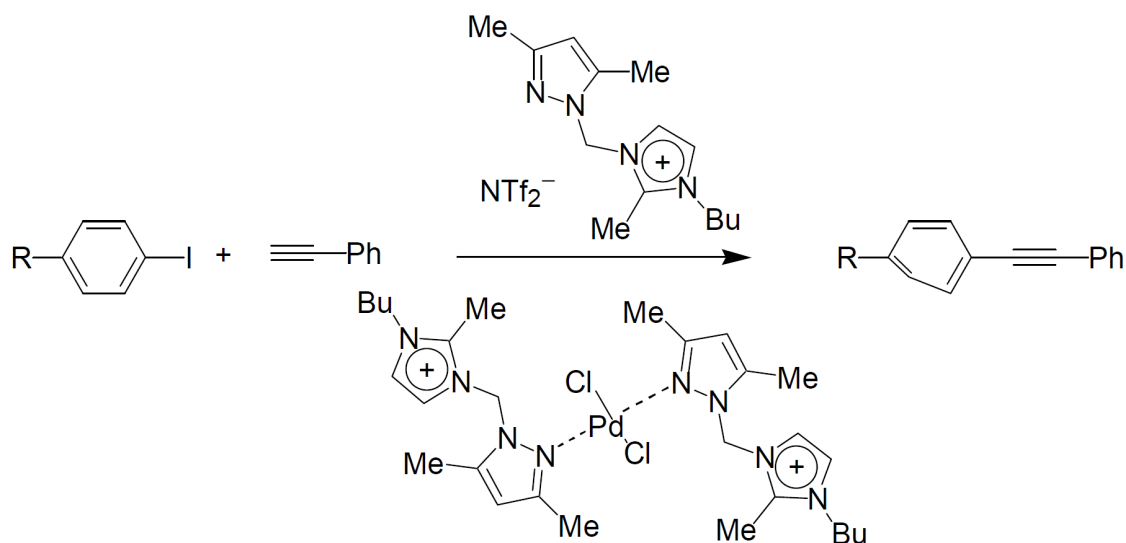
Scheme 3.21: Pyrazole Pd^{II} complex applied to Sonogashira coupling.

Phosphane-free coupling procedures have been described and show high yield in their first cycles. One promising catalyst system applied by *Shreeve* and coworkers utilizing the palladium catalyst in IL shows no difference in the reactivity even after six cycles (Scheme 3.21). This implies that the work-up procedure in other cases can result in lower activities. Copper(I) cocatalyst accelerates the reaction but copper-free procedures show no significant difference in reaction times or yields.

The well-known reactivity of the aryl halides Ar-I »Ar-Br >Ar-Cl is significant and in ILs this trend keeps the same. *Alper* and coworkers illustrate this trend in the reaction of aryl halides and acetylenes containing electron-withdrawing substituents in which case the rate of the coupling is faster than the reoxidation of Pd^{0}.[65] Reactions of compounds with electron rich substituents were found to proceed more slowly. In addition, steric effects in the Sonogashira coupling also influence the reaction. Inorganic bases gave very low yields, which may be due to solubility problems. Typically Et$_3$N, piperidine or iPr$_2$NH are used in procedures carried out in ILs.

Careful purge of oxygen and drying applied in the synthesis procedures seem to suppress homocoupling and thereby give high yields. Catalyst recycling can be made by extracting the reaction mixture with, e.g., diethyl ether and subsequent washing of the IL solution containing the Pd^{II} catalyst with water to remove excess base and the salt formed and, finally, using an appropriate drying of the IL at reduced pressure at 60 °C.

Suzuki-Miyaura-Coupling

The Suzuki cross-coupling reaction is an important and well established method for carbon–carbon bond formation.[70] The use of ILs as a reaction media for Suzuki cross-coupling reactions under homogeneous conditions have been reported in several publications.[44,71]

Utilizing Pd(PPh$_3$) in IL BMI.BF$_4$ reduced the reaction time in the reaction of bromobenzene with phenylboronic acid from six hours to ten minutes with an increased yield of 93% (conv. 88%) compared to a conventional Suzuki coupling procedure. The easy work-up and recovery of the catalyst system are major advantages of this procedure (Scheme 3.22).[72]

Suzuki coupling procedures without the use of phosphane ligands at ambient temperature
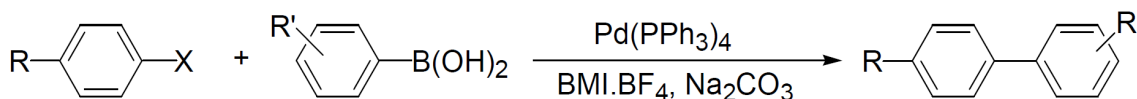
Scheme 3.22: Suzuki coupling in ILs.[72]

under ultrasonic irradiation have been reported.[73] 1,3-Dibutylimidazolium tetrafluoroborate BBI.BF$_4$ and methanol as co-solvent were applied in this procedure. The major drawback in this procedure was the formation of Pd black which indicates a decomposition of the catalyst. This problem could be overcome by using a bis-carbene palladium complex (Figure 3.48).[73] This catalytic system was reused for three times with decreasing catalytic activity (82% first run 80% and 75% third run), which maybe due to loss of the catalyst during the work-up procedure because of its solubility in organic solvents.
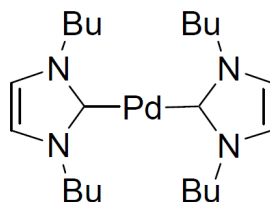
Figure 3.48: Bis-NHC (N-heterocyclic carbene) palladium complex.

The use of ionic phosphane ligands in the Suzuki coupling has been reported and showed high activities and high yields even after ten reuses of the catalyst system based on DPPC.PF$_6$ [DPPC = 1,1'-bis(diphenylphosphano)cobaltocenium] and PdCl$_2$ in BMI.PF$_6$.[74] The typical experimental setup started with heating PdCl$_2$ and DPPC.PF$_6$ at 110 °C in IL BMI.PF$_6$ for approx. two hours. The reactants were then added to this solution and heated again for 0.5–3 h followed by extraction with diethyl ether or hexane. No leaching of Pd catalyst was found indicating a good complexation in the IL. The authors noted that the catalyst showed no significant loss in the activity even after 140 uses. PdCl$_2$-DPPF in a control reaction showed reduced activity of the catalytic system after six runs starting with a yield of 90% and giving a yield of 40% in the last run.
The triethylammonium-tagged diphenylphosphane Pd^{II} complex (Figure 3.49) confirmed this strategy. Suzuki couplings of aryl bromides and arylboronic acids in BMP.NTf$_2$ gave high yields of 84–99% within short reaction times.[75] 15% of homocoupled product was found carrying out the reaction on air. This catalyst system showed slightly decreasing yields after recycling but only a low level of leached Pd was detected (<10 ppb).

Imidazole complexes as catalyst precursors in 1-butyl-3methylimidazolium-based ILs are stable and recyclable catalyst systems for the coupling of iodo- and bromoarenes with phenylboronic acids.[76–77] A key step in this protocol was the initiation of the catalytic system by heating the palladium source in the ionic liquid. The catalyst system (CH$_3$CN)$_2$PdCl$_2$/[BMI] showed high activities in BMP.NTf$_2$ and BMI.BF$_4$.

Negishi Coupling

The Negishi coupling has also been carried out utilizing ILs. A biphasic IL/toluene system was used to couple aryl- and benzylzinc halides with aryl halides.[78] As palladium source [Pd(dba)$_2$] and ionic phosphane (IP) was used. Moderate to high yields of 70–92% have
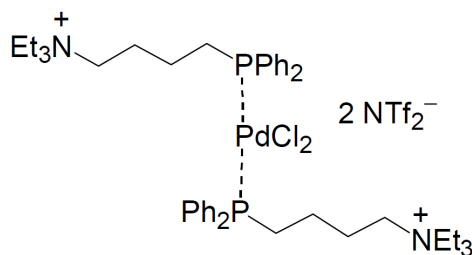
Figure 3.49: Triethylammonium-tagged diphenylphosphane Pd^{II} complex.

been reported (Scheme 3.23). The catalytic system showed lower yields in recycling and even with longer reaction times after the third cycle.
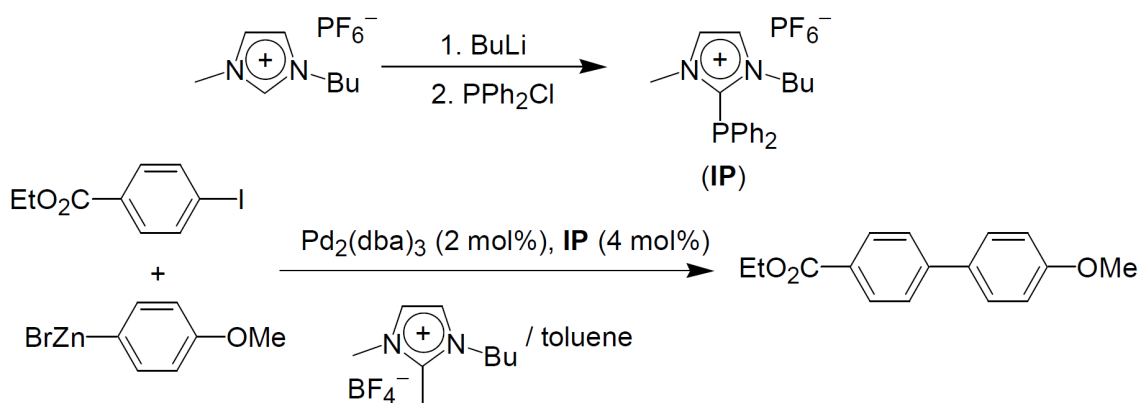
Scheme 3.23: Synthesis of ionic phosphane IP and its use in Negishi coupling.

Tsuji-Trost Coupling

A biphasic Tsuji-Trost coupling procedure has been developed utilizing methylcyclohexane and BMI.Cl as the solvent in the presence of triphenylphosphane trisulfonate (Scheme 3.24).[79] An increased catalytic activity was found due to the higher solubility of the substrates compared to the aqueous system. Greater selectivity has been reported where the formation of cinnamyl alcohol and phosphonium salts could be suppressed in this protocol. Moreover, a coupling procedure through nucleophilic substitution of allylic compounds in the reaction of 3-acetoxy-1,3-diphenylpropene with dimethyl malonate in BMI.BF$_4$ gave 91% yield within 5 h reaction time at room temperature.[80] The catalyst system was based on PdCl$_2$ in the presence of phosphane ligand and K$_2$CO$_3$ as the base whereas the catalyst system could be recycled.

3.5.3 Metal Salts and Metal on Solid Support

There is no doubt that C–C coupling reactions catalyzed by metal precursors constitute one of the most important synthetic methods in chemistry. Among the metal catalysts employed for this transformation, Pd-based precursors are far the most used mainly due to their superior activity when compared to other metals.[81−82] In this context, several coupling reactions catalyzed by Pd metal salts dissolved in organic solvents have been explored
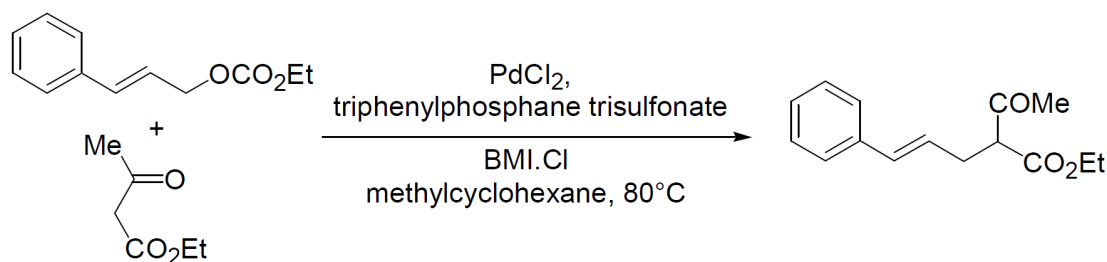
Scheme 3.24: Tsuji-Trost reaction in IL.[79]

in recent years. However, it is commonly accepted that the true catalysts, in general, are not the Pd salts but molecular palladium(0) species or metal nanoparticles (NPs) generated *in situ* that act as catalytically active species.[31−32,34−36] In particular, ionic liquids (ILs) emerged as an alternative reaction medium for coupling reactions not only due to their attractive physicochemical properties, but also because they can stabilize these generated Pd^0 species avoiding the aggregation into the inactive bulk material.[2,5] In fact, the presence of Pd NPs was confirmed by XAFS measurements during Heck reaction performed in ILs.[83] Moreover, it was demonstrated by a physical separation method that palladium atoms detached from the NP surface are the probable catalytic active species.[84−85] More examples of the in situ formation of metal NPs in ILs during coupling reactions can be found in this chapter and in other related reviews in literature.[10,29,86−87]

Mizoroki-Heck Reaction

As an example for the use of metal salts dispersed in ILs during the Mizoroki-Heck reaction is the effective application of Pd(OAc)$_2$ or PdCl$_2$ as catalysts for the coupling of aryl halides or benzoic anhydride with alkenes in pyridinium- and imidazolium-based ILs (Scheme 3.25a).[50] The coupling of iodobenzene and ethyl acrylate catalyzed with Pd(OAc)$_2$ achieved moderate to high yields depending on the IL and reaction conditions used. Moreover, PdCl$_2$ dissolved in a pyridinium IL gives a high yield of trans-*n*-butyl cinnamate during the reaction of benzoic anhydride and *n*-butyl acrylate. It is important to mention again that the multiphase nature of reactions performed in ILs provides beneficial conditions for product separation and catalyst recycling.
Pd^{II} or Pd^0 metal precursors in Bu$_4$N.Br (TBAB) IL shown to be active catalytic systems during the Heck reaction of chloroarenes and olefins.[48] The efficiency of the method was proved by the better performance of IL as reaction medium giving reasonably good product yields when compared to classical organic solvents. Indeed, the coupling of chlorobenzene and styrene to produce stilbene was successfully catalyzed with ligand-free PdCl$_2$ in IL (Scheme 3.25b).
A regioselective Heck arylation of electron-rich olefins and aryl halides catalyzed by palladium acetate could be reached in BMI.BF$_4$.[58−59] The reaction proceeded with high regioselectivity to provide the α-arylated olefin. In fact, for all aryl halides tested, superior α/β product ratios of 99/1 were detected (Scheme 3.25c). It is noteworthy, that the presence of IL did not require the use of aryl triflates, and for aryl halides, the addition of silver salts, which until then were necessary conditions to obtain good regioselectivities. It was also supposed that the reaction proceeds via an ionic pathway and the IL effect may be related to the stabilization of ionic species where the dissociation of halide anion from palladium was favored. Similarly, the coupling of aryl bromides with hydroxyalkyl vinyl

ethers catalyzed by $Pd(OAc)_2$ generates cyclic ketals in IL (Scheme 3.25d).[88] Once again, the Pd-IL system showed high selectivity for the α-arylation (α/β >99/1), which was followed by a cyclization step to form the ketals. Moreover, this system could be recycled for at least eight runs without significant loss in activity.

Guanidinium-based ILs have also been employed as efficient reaction media in Heck processes.[52] The coupling of several aryl halides and olefins catalyzed by $PdCl_2$ in guanidinium IL was effectively achieved in short times and high yields of the trans product (Scheme 3.25e). Some important advantages on the use of this IL can be mentioned. In addition to be the solvent of the reaction, the IL can act as a strong base, since there is an equilibrium into the organic base and acetic acid at high temperature. Furthermore, it acts as a ligand to stabilize the active palladium species during reaction. As a result, the addition of an external base or ligand is not necessary in this case. Substituted benzofurans were synthesized by an intramolecular Heck reaction catalyzed by $PdCl_2$ in IL.[89] For example, orthoiodobenzyl allyl ether was transformed into 3-methylbenzofuran in moderate yield (71%) in the presence of $BMI.BF_4$ IL (Scheme 3.25f). During recycling experiments, a slight loss in activity of the catalyst system was observed after the fourth run.

As an alternative to conventional systems, microwave irradiation was used in Heck reactions performed in $BMI.PF_6$.[56] The best catalytic system for the coupling of substituted aryl halides and butyl acrylate was based on $PdCl_2$ in IL. Under controlled microwave heating, moderate to excellent yields were attained in the reaction of bromoanisole and n-butyl acrylate (Scheme 3.25g), in which the use of a phosphane ligand slightly improves the catalyst activity. In contrast, only poor results were observed when the classical supported metal catalyst Pd/C was tested. Under phosphane-free conditions, $PdCl_2$ was able to promote the reaction between iodobenzene and n-butyl acrylate, where the IL phase could be recycled up to five times without significant loss in activity.

Silica-supported palladium catalysts were prepared as another strategy to obtain satisfactory results in the Heck coupling reactions.

For this purpose, an interesting approach based on the immobilization of $Pd(OAc)_2$ in amorphous silica aimed by an IL was developed.[90] Results showed that $BMI.PF_6$ was the best IL for the immobilization of the Pd salt in the IL layer inside of the silica pores. In addition, this catalyst was efficient to promote the Heck coupling of aryl halides and olefins in organic solvents, mainly in the case of iodobenzene and cyclohexyl acrylate, where up to 99% in yield was attained (Scheme 3.25h). Moreover, the catalyst could be recycled maintaining a high activity even after six runs.

An efficient application of classical heterogeneous catalysts was also described for Heck reactions.[91] In fact, the coupling of iodoarenes and ethyl acrylate works well in the presence of Pd/C in $BMI.PF_6$, and the IL was reused for six runs (Scheme 3.25i). However, when bromoarenes were tested, the yield dropped considerably, which is very similar to the results observed in independent experiments for a system using microwave irradiation.[56]
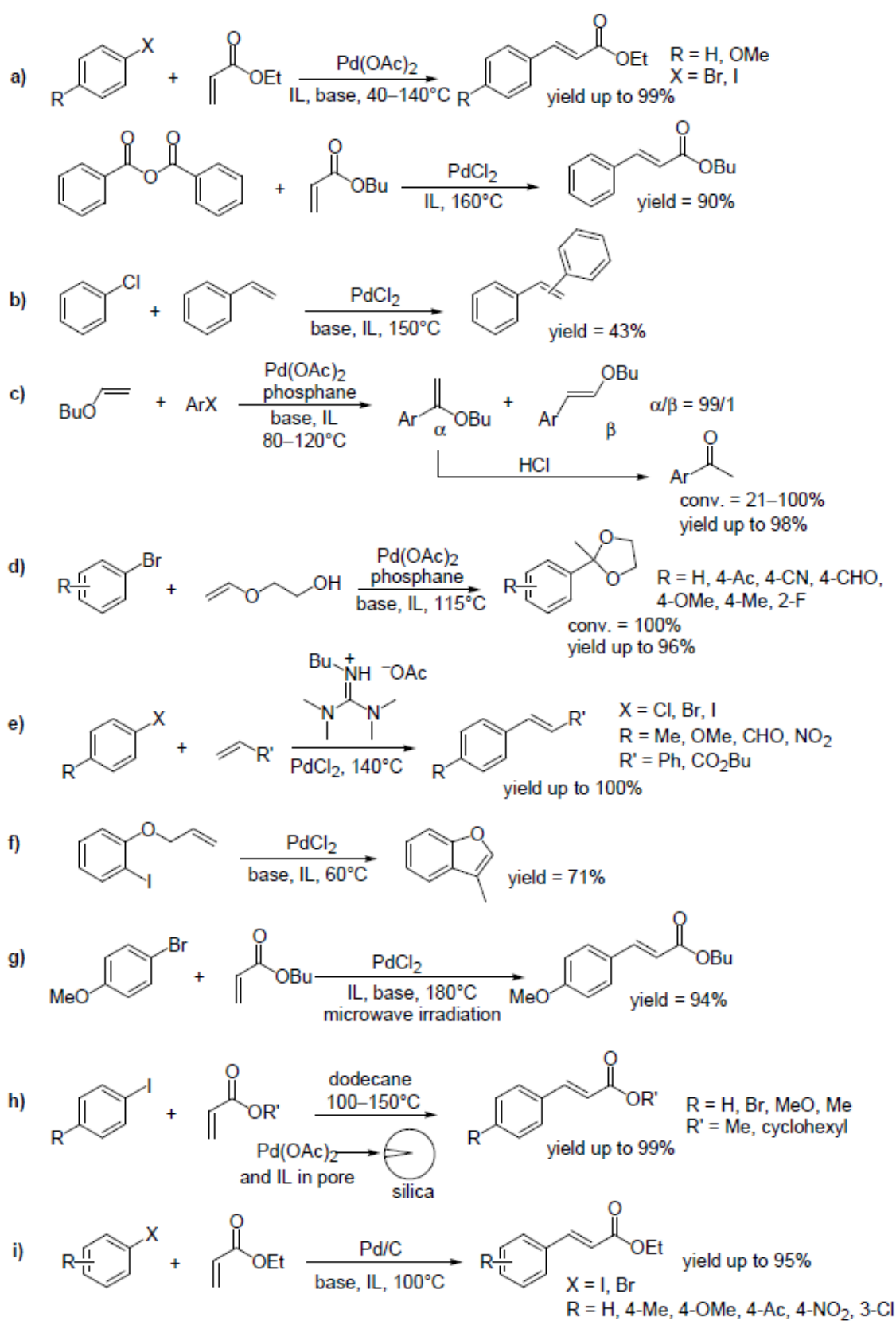
Scheme 3.25: Heck reactions promoted by metal salts as catalyst precursors in ILs (BMI.X with X = BF$_4$, PF$_6$) except reaction c.[48,50,52,56,58−59,88−91]

Suzuki-Miyaura Reaction

It is well-known that Suzuki-Miyaura reaction is another important method in C–C coupling synthesis. This reaction has also been carried out in ILs in the presence of Pd salts or supported metals as catalysts. For example, the use of 2,2'-bisimidazolium-based ILs in palladium-catalyzed Suzuki reaction was described.[92] In this case, a mono-quaternary IL was adopted as solvent and ligand for the PdCl$_2$ catalyst on the coupling of phenylboronic acid and bromobenzene, providing an isolated yield of 83% after product purification (Scheme 3.26a). On the other hand, changing the aryl halide to chlorobenzene does not afford good results, only 15% of yield was detected under the same conditions. Noteworthy, the catalytic system was recycled for at least 14 runs without loss in activity, suggesting a strong interaction between the catalyst and IL that prevents catalyst leaching after work-up procedures.
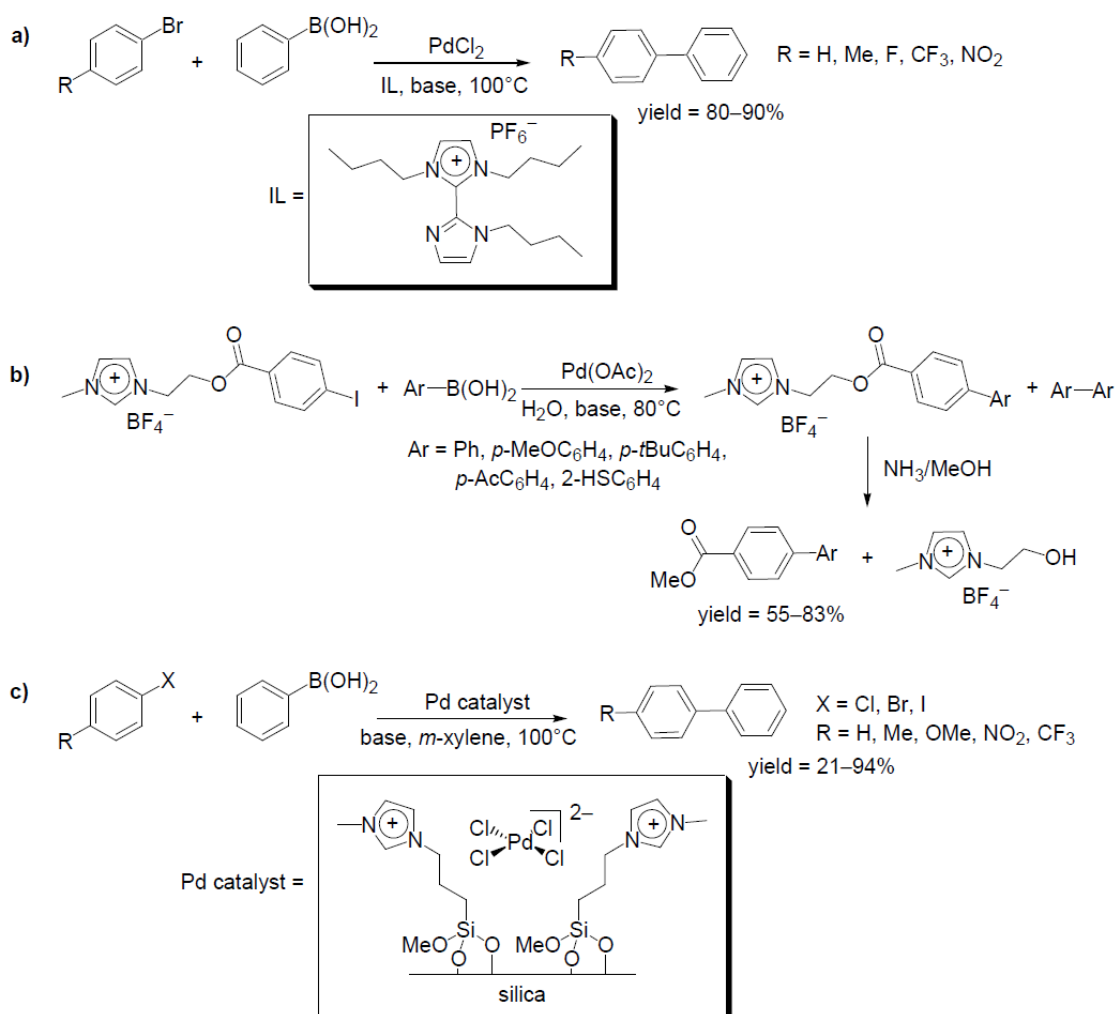
Scheme 3.26: Selected examples of Suzuki cross-coupling reactions catalyzed by metal salts in ILs.[92−94]

Interestingly, the Suzuki reaction was selected to demonstrate and explore the ability of IL to act as soluble supports in organic processes.[93] Indeed, the reaction of an IL-supported benzoate compound with arylboronic acids catalyzed by Pd(OAc)$_2$ gave both

excellent yields and purity of biaryl products after a cleavage step with ammonia/methanol (Scheme 3.26b). Remarkably, the reaction works better with the IL-supported benzoate compound than methyl *p*-iodobenzoate substrate. This result was attributed to the better solubility of the IL-based substrate in the aqueous medium, the beneficial effect of the positive charge from IL moiety on the reaction rate, or the loss of methyl *p*-iodobenzoate by sublimation.

The immobilization of a Pd salt onto a silica support modified with imidazolium IL fragments appears to be another convenient route to prepare a competent catalyst for Suzuki crosscoupling reactions.[94] A simple covalent attachment of 1-methyl-3-(3-trimethoxysilylpropyl) imidazolium chloride to silica, and then mixing with $PdCl_2$ led to the supported catalyst. Due to its good activity compared to other catalysts tested, this supported material proved to be a suitable promoter for the reaction between phenylboronic acid and bromobenzene in *m*-xylene (89% yield of product; Scheme 3.26c). Notably, the product yield can be increased up to 94% depending on the conditions used. Recycling experiments showed that the system is active until the third run, but the activity decreased considerably in the fourth and fifth recycles.

Stille Reaction

Since the Stille reaction corresponds to an important process for C–C bond formation, some examples using ILs as alternative solvents had been reported. For this purpose, a series of ILs based on different cations was investigated in order to identify the role of IL properties in the efficiency of Stille reaction.[95] Although ligands improve the efficiency of coupling process, a ligandless reaction between iodobenzene with tributylvinylstannane (Scheme 3.27a) promoted by $Pd(OAc)_2$ works well in two imidazolium-based ILs $BMI.NTf_2$ and $BM_2I.NTf_2$ (BM_2I = 1-butyl-2,3-dimethylimidazolium), as well as in pyrrolidinium-based IL $BMP.NTf_2$ and pyridinium-based IL $HPy.NTf_2$. In particular, a conversion of 94% was attained in this coupling reaction when performed in $BM_2I.NTf_2$ IL. However, the transfer of alkyl group to the iodobenzene substrate was difficult in IL. In the case of ligandless condition, the hydrophobic IL $BMI.C_8H_{17}SO_4$ ($C_8H_{17}SO_4$ = octylsulfate) showed the best performance as solvent for the coupling of tetramethylstannane with iodobenzene catalyzed by $Pd(OAc)_2$.

The idea of employing IL-supported materials was successfully applied in Stille C–C coupling transformation.[96] In fact, the reaction of IL-supported organotin reagents with substituted aryl bromides was evaluated under several conditions. Among the catalytic systems investigated, $Pd(OAc)_2$ without additional ligand demonstrated the high activity (93% of conversion) in the coupling of 3-bromopyridine and IL-supported dibutylphenylstannane group (Scheme 3.27b). As expected, the increase in temperature from 35 °C to 100 °C affords total conversion in a short reaction time. This system was competent even when other types of organotin fragments and aryl bromides were used. Noteworthy, this concept does not require the use solvent, ligand, or additives in the reaction.

In summary, this section reviews some remarkable works on the use of metal salts dissolved in ILs as catalytic system for Heck, Suzuki and Stille coupling reactions. It is important to highlight that only selected studies using metal salts as catalysts which did not clearly indicate the formation of metal nanoparticles were discussed herein.

3.5.4 Metal Nanoparticles

Carbon–carbon or carbon–heteroatom cross-coupling reactions in chemical synthesis are usually carried out using palladium complexes or palladium salts. A new and upcoming
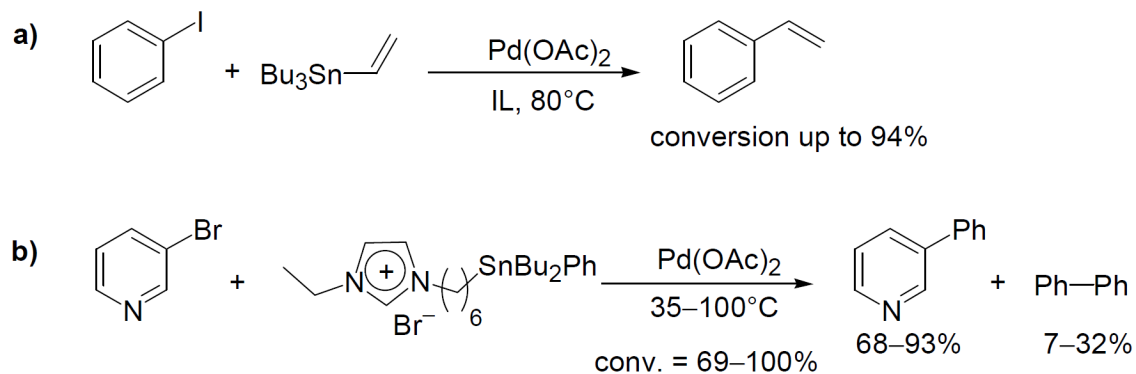
Scheme 3.27: Stille coupling in ILs using metal salts as catalysts precursors.[95−96]

methodology is the usage of transition metal nanoparticles as cheap and easily synthesizable catalysts [37]. Nanocatalysis stands for a frontier between homogeneous and heterogeneous catalysis that permits new applications and new prospects, which cannot be realized by traditional catalysis.

In spite of the high price, the metal of choice for C-C cross-coupling reactions is palladium [28]. There are several ways of synthesizing palladium NPs ranging from reductive methods, thermal or sonochemical decomposition to laser ablation, physical vapor deposition (PVD), or microwave synthesis [97−100]. Nowadays, the synthesized palladium NPs have a narrow size distribution around 1–10 nm and provide high activities for cross-couplings. Usual precursors for the synthesis of palladium NPs are metal salts such as $Pd(OAc)_2$, $PdCl_2$, or $Na_2[PdCl_4]$ [28,37,101]. Very useful are zero-valent precursors such as $Pd(dba)_2$, $Pd(COD)_2$, and palladium metal in terms of targets, foils, or ablation plates [102]. After decomposition of the precursor, mainly volatile by-products are produced, which can be easily removed from the reaction mixture. The first examples of the synthesis of palladium NPs by decomposition of Pd^0 sources came up in the early 1970s and were further developed in the following 20 years by different workgroups [97,98,102].

Very famous reaction (co)media for the synthesis of palladium NPs are ionic liquids, which provide a large variety of parameters to control shape and size [10]. They can also be optimized in order to enhance the catalytic performance of the NP/IL dispersion. Ionic liquids provide a large variety of liquid ranges, good thermal and chemical stability, negligible vapor pressure, and the potential of recycling (see below)[8]. One of the most interesting properties of ILs is their ability to stabilize nanoparticles and protect them from agglomeration [1,4,8]. A protective layer of anions is weakly but sufficiently bonded to the partially positively charged surface of the nanoparticles. In addition, the steric interaction of the bulky coordination sphere of the IL suppresses attractive interaction between the nanoparticles sterically and electrostatically, thereby hindering agglomeration of the NPs to bulk metal (Figure 3.50) [4,5,20,103].Furthermore, ILs prevent oxidation and hydrolysis of the nanoscale catalyst surface by the formation of the protective shell.

Moreover, ionic liquids are also used successfully in recycling experiments of nanoscale catalysts [5]. One of the major drawbacks of molecular palladium species for catalysis is the difficulty concerning their recovery from the reaction media. Usually they are lost in the end of the reaction and/or contaminate the product. Phosphane ligands are among the most popular ligands for homogeneous catalysis but are very often toxic and sensitive to air and moisture. Palladium clusters and particles in ionic liquids are usually ligand free and circumvent the complex problems that come along with the use of molecular ligand-stabilized palladium species. In fact, palladium NPs are not determined as the
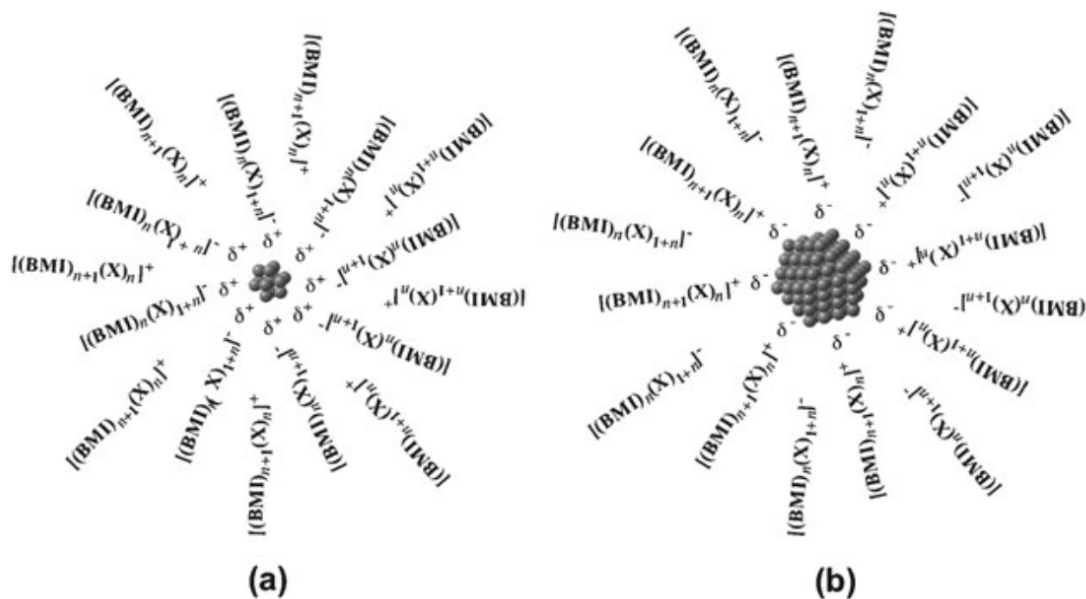
Figure 3.50: Electrosteric shielding of metal nanoparticles by ionic liquids [4]. (Reproduced (adapted) with permission from Ref. [4]. Copyright 2010 The Royal Society of Chemistry.)

catalytically active species; rather, they act as catalyst reservoir [5,101]. For instance, the reaction substrates coordinate to the surface of the palladium NPs and leach out molecular Pd^0 species that undergo oxidative addition and enter into the catalytic cycle (Figure 3.51). After reductive elimination, the Pd^0 species is regenerated and can form new nanoparticles due to Ostwald ripening (although agglomeration of large nanoparticles is inhibited by the electrosteric shielding of the IL) or undergo a further catalytic cycle.

NP/IL dispersions are highly suitable for multiphase systems [5,6]. That is why, there were several attempts to recycling experiments with palladium nanoparticles dispersed in an ionic liquid. Another cosolvent, such as water or commonly used organic solvents that are insoluble in each other, acts as the second phase for reagents and additives. The reaction takes place at the interface between catalytic phase and reactant phase. In bi- and multiphase systems, the catalytic phase can be separated easily, purified if necessary, and reused. C-C cross-coupling reactions that are usually performed with the use of Pd/IL dispersions are Heck, Suzuki, Sonogashira, and Ullmann reactions. They show significant improvements in comparison to classical homogeneous and heterogeneous catalysis and are presented in the following subsections.

3.5.5 The Mizoroki–Heck Reaction with PdNPs in ILs

Because of its versatility, the Mizoroki–Heck coupling is one of the most famous reactions in synthetic chemistry [26,27,29]. The academic and industrial community is highly interested in further developing the Heck reaction due to its possible applications for the synthesis of products that are in great demand. Usually an unsaturated organic halide reacts catalytically driven with alkenes in the presence of a base. Typical representatives of palladium catalysts are palladium complexes or palladium salts and, as a new and upcoming method for palladium catalysis, the use of palladium nanoparticles and their precursors [101,104]. The formation of palladium nanoparticles in imidazolium ILs proceeds (i) via
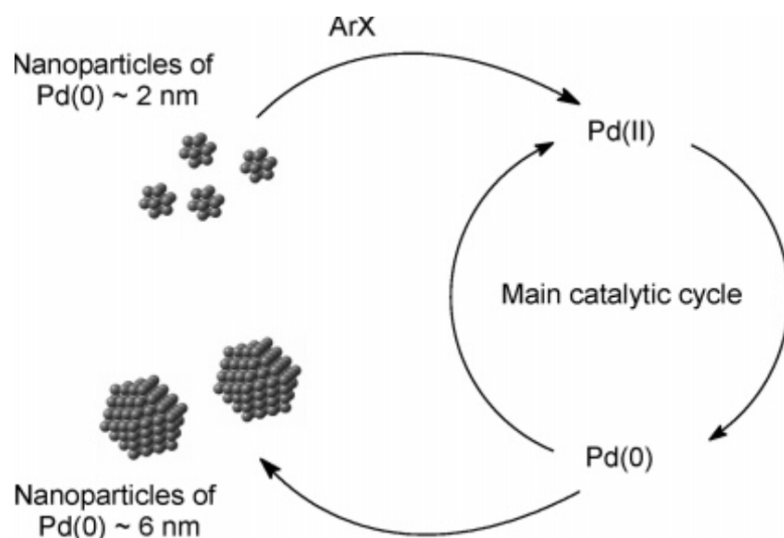
Figure 3.51: Catalytic species and catalyst reservoirs in the Heck reaction catalyzed by palladium nanoparticles [101]. (Reproduced (adapted) with permission from Ref. [101]. Copyright 2005 American Chemical Society.)

an N-heterocyclic carbene intermediate that is reduced to elemental palladium to form nanoparticles (Figure 3.52) [105−108]. Besides this, it is also possible that (ii) Pd^{II} species are directly leached out from the nanoparticles' surface by oxidative addition as well as (iii) Pd^0 is generated by reductive elimination resembling a nanoparticle (Ostwald ripening).
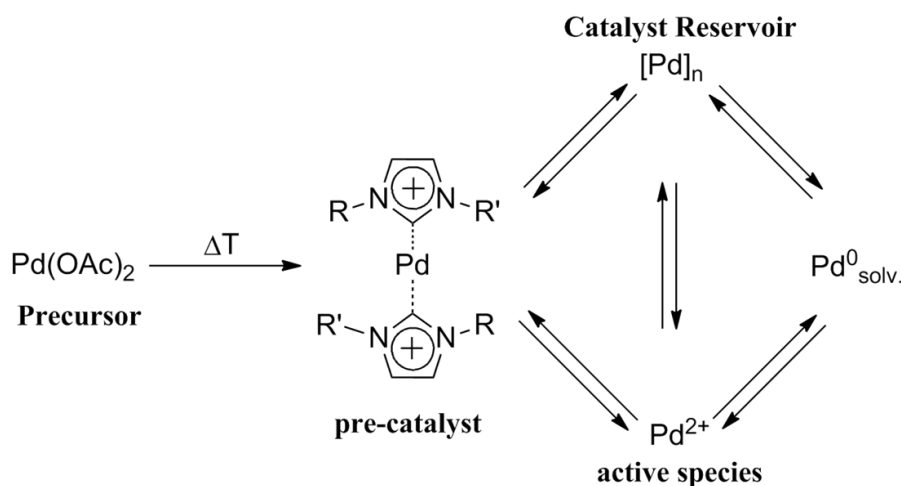
Figure 3.52: Equilibrium between precatalyst, active palladium species, and nanoparticles as the catalyst reservoir.

In fact, there is evidence for the high catalytic activity of palladium biscarbene complexes in Heck couplings ascertained by *Xiao* and coworkers [105] and *Welton* and coworkers [106]. As a result of the nonpolar reactants in Heck reactions, the catalysis is mostly performed in classical organic solvents, but other reaction media are also popular. In the past few years, a wide range of ionic liquids have been used as a mediator for Heck reactions with great prosperity. One of the major advantages is the selectivity of the coupled alkenes:

preferentially the trans-product is formed in high yields, as *Deshmukh et al.* found for the reaction of iodobenzenes with several alkenes, even at temperatures as low as 30 °C [109]. Furthermore, ionic liquids such as the quaternary ammonium IL used by *Reetz et al.* [36,110] or methylimidazolium IL developed by *Dyson* and coworkers [23] act as stabilizing agents, as well as an imidazolium polymer/IL composite (Scheme 3.28), and allow also the coupling of less reactive aryl bromides.
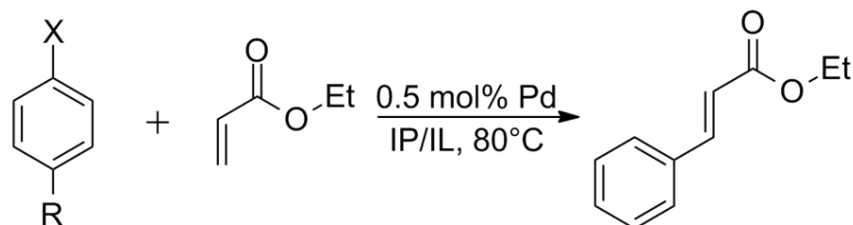
Scheme 3.28: Heck vinylation of substituted aryl halides with low Pd loadings performed by *Dyson* and coworkers [23].

It is necessary to point out that the Heck reaction under ambient conditions cannot be performed with classical organic solvents [109]. Thus, the application of nanoparticles in ionic liquids seems to be essential for this kind of coupling under the above-mentioned conditions. Furthermore, ILs may establish a multiphase catalytic system with a single catalytic phase and one reactant phase in a classical organic solvent [5,6]. The ability to immobilize nanoparticles in the ionic liquid is crucial for considering them as recyclable and therefore environmentally benign. There are several co-solvents for the reactant phase conceivable ranging from polar to apolar solvents.

Interestingly, it is not necessary to synthesize palladium nanoparticles in situ in an ionic liquid in order to use them as catalyst (reservoir). *Calo et al.* showed that small nanoparticles can be redispersed in ILs such as tetrabutylammonium bromide (TBAB) [111,112]. They are also capable of catalyzing Heck reactions with tetrabutylammonium acetate (TBAAc) used as a base. Another possibility is the immobilization of palladium nanoparticles on silica or sepiolite as well as SiO_x and Al_2O_3 particles [113]. They can act as good and reusable catalysts for Heck-type reactions also in ILs. Furthermore, *Teuma* and coworkers presented a Heck coupling utilizing functionalized carbon nanotubes (fCNTs) bearing palladium nanoparticles in an ionic liquid [114]. Interestingly, there was no need for a supplementary base in this setup.

Corma et al. presented a method to synthesize palladium nanoparticles immobilized on polyoxometallate ionic liquid (POM-IL) nanoparticles [115]. These POMIL particles can act as a good recyclable catalyst in nonpolar media as well as for gasphase reactions. Another promising method for Heck reactions is the immobilization of palladium nanoparticles on poly(divinylbenzene) (PDVB) as a copolymer for 1-aminoethyl-3-vinylimidazolium bromide (VAIm·Br) [116]. The IL is grafted on the copolymer that causes a multiple enhancement of the catalytic activity of the palladium particles in the Heck reaction as recently described by *Han* and coworkers.

One of the major goals in Heck-type nanocatalysis is a smooth reaction of deactivated coupling partners such as aryl chlorides and deactivated olefins. Up to now, there is only scarce information about the coupling of these compounds, especially concerning nanocatalysis. In 2009, *Calo et al.* showed an impressive way of performing the Heck reaction within a few minutes with the help of TBAB/TBAAc [111]. This Heck reaction does not proceed with other ILs, such as imidazolium ILs or pyridinium-derived ILs.

3.5.6 Suzuki–Miyaura Reaction

Next to the Heck reaction there is another very important cross-coupling reaction, which is one of the most famous reactions in organic chemistry. The Suzuki–Miyaura coupling – besides the Ullmann reaction – is the most common to synthesize biaryls. Biaryls are key intermediates for industrial targets such as drugs, liquid crystals, or agricultural chemicals [117]. That is the reason why the application of metal nanoparticles in Suzuki reaction has attracted very much interest for industrial production and is used as a benchmark for nanocatalyst testing. Palladium nanoparticles derived from palladium salts such as $Pd(OAc)_2$, dispersed in tetraalkylammonium ILs, especially tetrabutylammonium ionic liquids, are the most promising catalysts for Suzuki couplings. Tetrabutylammonium base (TBA-OH) is preferentially used during the catalysis [118]. Nanoparticle stabilization is crucial for the high yields in this reaction. High concentrations of tetraalkylammonium ions in the IL phase – derived from the IL itself and the base – as well as longer alkyl side chains of the ILs significantly increase nanoparticle stability. It is possible to perform the reaction even at temperatures as low as $70\,^\circ\mathrm{C}$ within 3–4 h in good to excellent yields [118]. Guanidinium-based ionic liquids are another interesting stabilizing medium. *Li* and co-workers presented a method utilizing hexaalkylguanidinium ionic liquids (GIL) that mediate Suzuki couplings in water as the cosolvent with remarkable efficiency and also good recyclability [119]. Interestingly, this system enables the use of iodo-, bromo-, and chloroarenes, which is up to now not common in cross coupling reactions due to the low reactivity of chloroarenes.

The stabilization and activity of palladium nanocrystals are mainly affected by shielding effects of the surrounding ionic liquid. Very low catalyst loadings of only 0.05 mol% Pd were satisfactory in the reaction protocol of *Peng* and coworkers [120]. The reaction is carried out without any inert reaction atmosphere in a water/ethanol mixture at $70\,^\circ\mathrm{C}$. 3-(2,3-Dihydroxypropyl)-1-vinylimidazolium chloride is copolymerized with styrene to support the Pd nanoparticles. The catalyst can be reused several times without significant loss of activity.
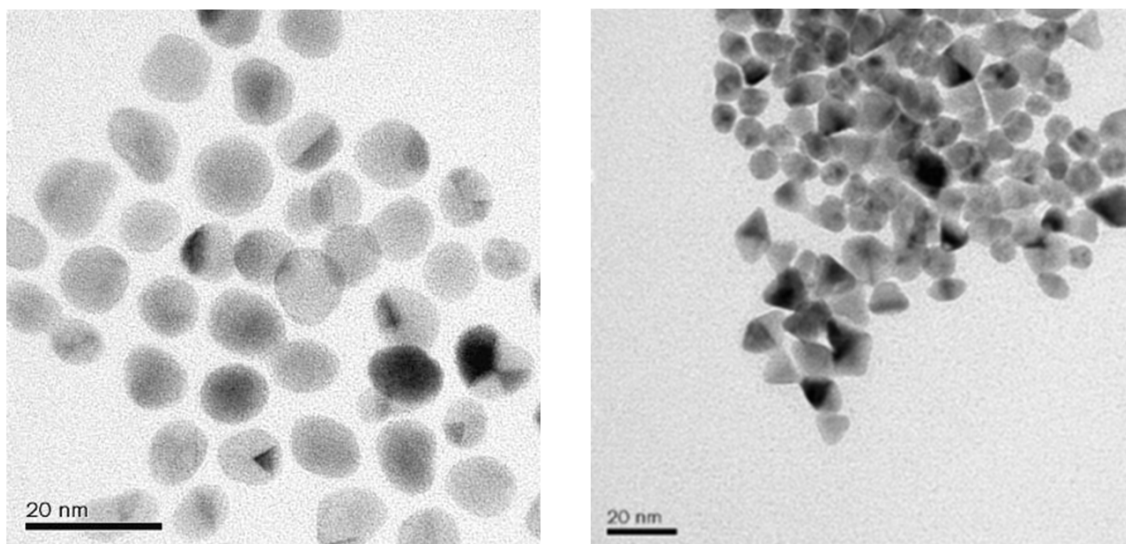
Figure 3.53: Pd nanoparticles with anion-depending shapes synthesized by *Kerton* and *Kalviri* [121]. (Reproduced with permission from Ref. [121]. Copyright 2011 The Royal Society of Chemistry.)

Kerton and *Kalviri* presented a phosphonium-based ionic liquid for Pd nanocrystallite support [121]. Trihexyl(tetradecyl)phosphonium chloride was used as the decomposition medium of the precursor $Pd(OAc)_2$ and as the stabilizing agent of small palladium nanoparticles formed in the range of 7 nm. The nanoparticle dispersion was used as a very effective coupling catalyst for the Suzuki reaction of 4-bromotoluene and phenylboronic acid. The shape of the nanoparticles was shown to depend basically on the precursor anion (Figure 3.53). $PdCl_2$ gave truncated octahedrons, whereas $Pd(OAc)_2$ provides triangular shapes. The effect on the catalyst activity could not yet be clarified.

Besides palladium acetate, $Pd(COD)Cl_2$ is reduced by hydrogen in $BMI·PF_6$ to form starlike nanoparticle self-organization. In Suzuki reaction, these particles exhibit very good activity in IL suspension (total conversion within 60 min at 100 °C). The catalytic layer of the biphasic system could be recycled up to 10 times without significant loss of activity. In contrast, the isolated Pd powder shows no appreciable activity [122].

An upcoming method to immobilize palladium nanoparticles is the use of onedimensional grown structures such as nanowires or dendrimers. *Hagiwara et al.* presented a highly active palladium catalyst immobilized on nanoscale silica dendrimers with the help of ILs (SILC). In this ligand-free approach in $EtOH/H_2O$ solution, the catalyst could be easily recycled by simple centrifugation in excellent yields up to 93% (TON 176000 of a single run), and in similar systems with 10 subsequent runs [123,124].
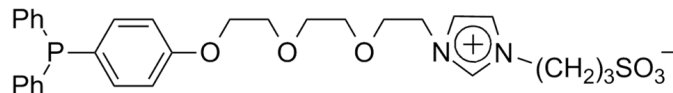
Figure 3.54: Phosphane-functionalized zwitterionic ionic liquid synthesized by *Akiyama et al.* [125].

Zwitterionic liquids (ZILs) are also very capable in surface protecting of nanoparticles due to their strong polarity. *Akiyama et al.* presented a phosphane with zwitterionic liquid based on imidazolium sulfonate linked to ethylene glycol (Figure 3.54). The protected nanoparticles are stable in aqueous medium even with high electrolyte loadings and act as efficient catalyst in Suzuki couplings[125].

An easy synthesis and simple preparation of a catalyst phase were presented by *Safavi et al.* They incorporated palladium nanoparticles into a silica xerogel with the help of a (2-phosphinite)propylmethyl imidazolium hexafluorophosphate IL [126].

3.5.7   Stille Reaction

The Stille coupling is a very famous C-C cross-coupling reaction. Due to the toxicity of most organotin reagents, chemists try to avoid the usage of these coupling reagents. However, there are still certain reactions that can only be realized in satisfactory amounts with the Stille reaction. Analogous to the Heck and Suzuki reactions, the catalytically active species in Stille couplings are molecular palladium complexes that are leached out of nanoparticles [5]. Several ionic liquids based on pyridinium, imidazolium, pyrrolidinium [14,17], and tetraalkylammonium ions [118] were used as protecting agents and as solvents [5,14,27]. *Dyson* and coworkers presented ionic liquids containing nitrile functionalities, which were used in several cross-coupling reactions, such as Stille reaction [16,18]. The catalytic phase could be recovered about nine times without a loss of activity, which can be explained by the exceptional shielding of the nanoparticle by the nitrile group (Figure 3.55).

Furthermore, for nitrile functionalized ILs the leaching of molecular palladium species into the organic layer was remarkably lower in comparison to the alkyl-functionalized ILs; this is particularly true for imidazolium ILs. The conversions of Stille reactions in CN-functionalized ILs are constant at 90% even after several recycling steps. Other factors influencing product yields, leaching, and reaction parameters are, for instance, the viscosity of the IL and the solubility of metal salts in the ILs.

Furthermore, ion pairing effects play a crucial role in substrate conversions [14]. One focus in research is the use of aryl chlorides, which is quite challenging. Aryl chlorides are usually unreactive or at least deactivated in comparison to aryl bromides or iodides. Their low prices, however, make couplings with aryl chlorides a worthwhile target in chemical research. *Calo et al.* used tetraalkylammonium ionic liquids with incorporated palladium nanoparticles and tetrabutylammonium acetate as base for Stille reactions. Bromo- and iodoarenes were coupled in excellent yields and low catalyst loadings (2.5 mol%). Even chloroarenes could be coupled in good to excellent yields, which makes this reaction remarkably interesting concerning recycling experiments [111]. *Dyson*, *Li*, and coworkers also published a Stille reaction with an imidazolium polymer/IL composite. The

Figure 3.55: Electrostatic surface shielding by nitrile functionalities of imidazolium or other ionic liquids.

nanoparticle shielding is very effective and makes the precatalyst dispersion stable for months. Stille reactants, catalysts, and additives – such as bases – can be stored without undergoing degradation. Good to excellent yields could be obtained with catalytically active phases, which were already several months old and with a low palladium loading of about 0.5 mol%. The phases showed very good recycling capabilities with no significant loss of activity after five runs [23].

3.5.8 Buchwald-Hartwig Reaction

One of the most famous carbon–heteroatom cross-coupling reactions is the Buchwald–Hartwig reaction. Usually aryl halides or pseudohalides are coupled with amines with the help of palladium catalysts. Up to now, there are only few examples for nanoscale palladium catalysis in ionic liquids, even though there would be a tremendous industrial interest. *Cacchi* and coworkers presented a combination of Heck and Buchwald–Hartwig reactions [127]. The reactions are completely independent, in terms of their mechanistic point of view. The reaction proceeds in a mixture of molten TBAAc/TBAB to give 4-aryl-2-quinolones, a chemical target that is in great demand for antibiotic synthesis [128]. There is only one last example for nanoparticle catalysis in phosphonium-based ionic liquids presented by *De Vos* and coworkers. However, they used nanoscale nickel particles as catalyst [129].

3.5.9 Sonogashira Reaction

Couplings of aryl halides with substituted acetylenes can be performed with the Sonogashira reaction. Usually organocopper compounds are used for the transmetallation step. The oxidative addition of the aryl halides takes place at the surface of the palladium particle, analogously to the Heck and Suzuki couplings. Palladium nanowires were synthesized by *Zhang* and coworkers as the palladium source for a Sonogashira reaction [130]. A thiol-functionalized ionic liquid was used as reaction medium (Scheme 3.29), $NaBH_4$ acted as reductive agent, and gold colloids served as seeds for the nanowire growth. Iodobenzene and phenylacetylene were coupled in quantitative yield within 12 h at temperatures as low as 75 °C. CuI was used as copper source in order to generate the organocopper compound and PPh_3 for further stabilization of the molecular Pd^{II} species.
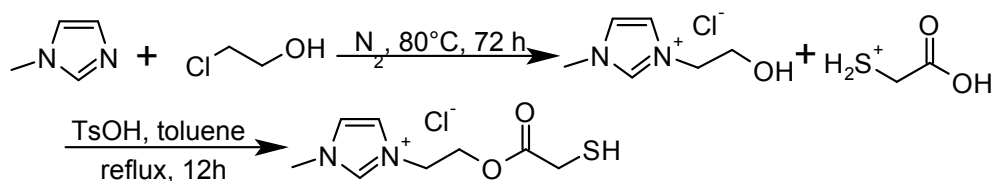
Scheme 3.29: Synthesis of thiol-functionalized ionic liquid by *Zhang* and coworkers [130].

Corma et al. synthesized palladium nanoparticles in $BMI \cdot PF_6$ as well as in $BMI \cdot Cl$ with poly(ethylene glycol) (PEG) for further stabilization [131]. As precursor, they used 40-hydroxyacetophenone oxime complex of Pd^{II}, which is a well-known and highly active palladium complex for cross-coupling reactions. After thermal decomposition, small nanoparticles (2–5 nm) could be collected. Neither a copper source nor a further stabilizing ligand is necessary in this method, which makes it promising for a recyclable multiphase catalyst system. Unfortunately, the obtained yields were (with a few exceptions) rather moderate, which is due to the low solubility of the utilized base (CsOAc) in the ionic liquids.

3.5.10 Ullmann Reaction

In contrast to the Suzuki reaction, the Ullmann reaction is a homo coupling of aryl halides to produce biaryl compounds. Although the Suzuki reaction is more famous than the Ullmann reaction, because of the possibility to work copper free and the very high reaction temperatures required for the original reaction protocol, there are still some examples left, which make the Ullmann reaction interesting for chemical synthesis. The use of palladium nanoparticles and a reductive additive (usually aldehydes) makes the copper compound dispensable. One alternative is proposed by *Calo et al.* [19]: tetraalkylammonium-based ILs interestingly act as reaction medium (TBAB), base, and ligand (TBAAc), which make them crucial for this type of synthesis. The reaction proceeds under comparably mild conditions at 130 °C with total conversion within 2 h. The possible reactants are not restricted to aryl halides, but vinyl and heteroaryl halides may also be reacted. Average to good conversions (70–90 %) were already obtained at temperatures as low as 40–90 °C.
An electrochemical attempt was performed by *Rothenberg* and coworkers for a room-temperature catalyzed Ullmann reaction [132]. At first palladium nanoparticles with the

size of 2.5 nm ($\pm$0.5 nm) were generated in an electrochemical cell (Pd anode and Pt cathode). In a mixture of water and OMI·BF$_4$ as a recyclable solvent, aryl bromides and iodides (no aryl chlorides) were coupled by applying an electric current of about 1.0–1.6 V at 10 mA. Water is crucial for the catalytic cycle, because a two-electron oxidation of water regenerates the Pd^0 species. Within 8–24 h, the yields varied between 20 and 99 % at room temperature.

3.5.11   Summary and Outlook

In summary, palladium-catalyzed coupling reactions carried out in ionic liquid media represent quite efficient and recyclable catalyst phases. Detailed reaction insights have been obtained in several studies about Heck, Suzuki, and Stille reactions with palladium complexes, salts, classical heterogeneous catalysts, and nanoparticles. Moreover, related couplings such as Sonogashira and Ullmann were also discussed. The experimental insights about the catalytic systems are collected in the related sections. These results allow us to describe a generalized conclusion regarding recyclability, activity, yields, and selectivity of the IL-based catalyst systems. The discussed systems are classified in different types: palladium complexes, palladium salts, classical solid catalysts, and palladium nanoparticles that are applied under quasi-homogeneous reaction conditions providing good yields for Heck coupling. Furthermore, immobilized complexes are highly efficient for Suzuki and Sonogashira reactions. Solid catalysts based on silica, alumina, or carbon exhibit good performance in the mentioned reactions. Presumably, this may be related to porosity of the support with the Pd particles grafted on the surface. The incorporation of functional groups into the IL enhances the stabilizing properties; thus, the long-term stability of the catalyst material is optimized. Here, amino, N-heterocyclic, nitrile, ether, and alcoholic OH groups are highly suitable in combination with soluble palladium species. These groups act like ligands and enhance the efficiency and stability of molecular and solid (or anchored) palladium catalysts in recycling experiments. Here, one may distinguish between catalyst systems giving high yields, high selectivity, or high total TONs in recycling experiments. These systems are often based on nanoparticles or anchored complexes. This implies that both approaches give access to highly active catalysts. On the other hand, major general trends of activity and stability cannot easily be predicted in comparison to molecular and solid catalysts. Moreover, most of the shown catalysts are only tested for a few different reactions and reaction conditions. Therefore, only a few general conclusions can be made: Effective catalysts are usually well immobilized, have low metal leaching, and stay in equilibrium between the solid phase (anchored ligands, supported metals, or metal NPs) and solvated molecular Pd species, hence dissolved complexes. Therefore, the efficiency of catalysis depends not only on the type of active species, but also on the support material, in the present case the type of ionic liquid and ionic ligands. The combination of the suitable Pd precursor with an appropriate IL resulting in stable metal species is the first step for good performance (high yields, high selectivity, low catalyst leaching, high recyclability). Moreover, for easy-to-use applications, it is favorable to work with catalysts that are robust for prolonged time in the presence of air and moisture. These aspects are most important for continuous recycling experiments, and this point is crucial, for example, in industrial applications with high TTONs. For further optimization, more in-depth studies about selective catalyst poisoning, kinetic studies, and reaction insights into multiphase catalysis are required to guarantee the development of new catalysts for best efficiency, robustness, and lower "homeopathic" catalyst loadings. The approach to embed and protect Pd NPs or molecular species with ILs gives a good access for particle size control and to prevent agglomeration to Pd black. Moreover, the ILs are suitable to anchor ligand in side chains

or they may also act as the base.

For future perspectives, one may assume that several other coupling reactions using traditionally Pd complexes will be transferred to IL-based systems, and most likely also in combination with Pd NPs as catalyst reservoir. This might lead to easy recyclability, robustness, and long-term stability of the catalyst phase.

3.5.12   Abbreviations

BBI 1,3-dibutylimidazolium
BIIM 2,2'-biimidazole
BMIy 1-butyl-3-methylimidazol-2-ylidene
BMP N-butyl-N-methylpyrrolidinium
DMAc N,N-dimethylacetamide
DMF N,N-dimethylformamide
DMSO dimethyl sulfoxide
DPPC 1,10-bis(diphenylphosphano)cobaltocenium
DPPF 1,10-bis(diphenylphosphano)ferrocene
fCNT functionalized carbon nanotube
HPy N-hexylpyridinium
IL ionic liquid
IP ionic phosphane
NMP N-methyl-2-pyrrolidone
NPs nanoparticles
NTf$_2$ bis(trifluoromethanesulfonyl)imide
OMI 1-methyl-3-octylimidazolium
Pd NP Pd nanoparticle
Pd-DPPP 1,3-bis(diphenylphosphano)propane palladium
PDVB poly(divinylbenzene)
PEG poly(ethylene glycol)
POM-IL polyoxometallate ionic liquid
PVD physical vapor deposition
TBAAc tetrabutylammonium acetate
TBAB tetrabutylammonium bromide
TTON total turnover number
ZIL zwitterionic liquid

3.5.13   References

1. Scholten, J.D., Leal, B.C., and Dupont, J. (2012) *ACS Catal.*, 2, 184–200.

2. Prechtl, M.H.G., Scholten, J.D., and Dupont, J. (2011) *Ionic Liquids: Applications and Perspectives* (ed. A.Kokorin), InTech, Vienna, pp. 393–414.

3. Dupont, J., Scholten, J.D., and Prechtl, M. H.G. (2012) in *Handbook of Green Chemistry – Green Processes*, vol. 8 (eds M. Selva and P.T. Anastas), Wiley-VCH Verlag GmbH, Weinheim, in press.

4. Dupont, J. and Scholten, J.D. (2010) *Chem. Soc. Rev.*, 39, 1780–1804.

5. Prechtl, M.H.G., Scholten, J.D., and Dupont, J. (2010) *Molecules*, 15, 3441–3461.

6. Migowski, P. and Dupont, J. (2007) *Chem. Eur. J.*, 13, 32–39.

7. Dupont, J., de Souza, R.F., and Suarez, P.A.Z. (2002) *Chem. Rev.*, 102, 3667–3691.

8. Dupont, J. and Suarez, P.A.Z. (2006) *Phys. Chem. Chem. Phys.*, 8, 2441–2452.

9. Dupont, J. (2004) *J. Braz. Chem. Soc.*, 15, 341–350.

10. Hallett, J.P. and Welton, T. (2011) *Chem. Rev.*, 111, 3508–3576.

11. Welton, T. (1999) *Chem. Rev.*, 99, 2071–2083.

12. Krossing, I., Slattery, J.M., Daguenet, C., Dyson, P.J., Oleinikova, A., and Weingärtner, H. (2006) *J. Am. Chem. Soc.*, 128, 13427–13434.

13. Welton, T. (2011) *Green Chem.*, 13, 225–225.

14. Cui, Y.G., Biondi, I., Chaubey, M., Yang, X., Fei, Z.F., Scopelliti, R., Hartinger, C. G., Li, Y.D., Chiappe, C., and Dyson, P.J. (2010) *Phys. Chem. Chem. Phys.*, 12, 1834–1841.

15. Yang, X., Fei, Z.F., Geldbach, T.J., Phillips, A.D., Hartinger, C.G., Li, Y.D., and Dyson, P.J. (2008) *Organometallics*, 27, 3971–3977.

16. Fei, Z.F., Zhao, D.B., Pieraccini, D., Ang, W.H., Geldbach, T.J., Scopelliti, R., Chiappe, C., and Dyson, P.J. (2007) *Organometallics*, 26, 1588–1598.

17. Chiappe, C., Pieraccini, D., Zhao, D.B., Fei, Z.F., and Dyson, P.J. (2006) *Adv. Synth. Catal.*, 348, 68–74.

18. Zhao, D.B., Fei, Z.F., Geldbach, T.J., Scopelliti, R., and Dyson, P.J. (2004) *J. Am. Chem. Soc.*, 126, 15876–15882.

19. Calo, V., Nacci, A., Monopoli, A., and Cotugno, P. (2009) *Chem. Eur. J.*, 15, 1272–1279.

20. Prechtl, M.H.G., Scariot, M., Scholten, J. D., Machado, G., Teixeira, S.R., and Dupont, J. (2008) *Inorg. Chem.*, 47, 8995–9001.

21. Calo, V., Nacci, A., and Monopoli, A. (2006) *Eur. J. Org. Chem.*, 3791–3802.

22. Zhao, D.B., Fei, Z.F., Scopelliti, R., and Dyson, P.J. (2004) *Inorg. Chem.*, 43, 2197–2205.

23. Yang, X., Fei, Z.F., Zhao, D.B., Ang, W.H., Li, Y.D., and Dyson, P.J. (2008) *Inorg. Chem.*, 47, 3292–3297.

24. Prechtl, M.H.G., Scholten, J.D., and Dupont, J. (2009) *J. Mol. Catal. A: Chem.*, 313, 74–78.

25. Venkatesan, R., Prechtl, M.H.G., Scholten, J.D., Pezzi, R.P., Machado, G., and Dupont, J. (2011) *J. Mater. Chem.*, 21, 3030–3036.

26. Beletskaya, I.P. and Cheprakov, A.V. (2000) *Chem. Rev.*, 100, 3009–3066.

27. Liu, Y.,Wang, S.S., Liu, W.,Wan, Q.X., Wu, H.H., and Gao, G.H. (2009) *Curr. Org. Chem.*, 13, 1322–1346.

28. Moreno-Manas, M. and Pleixats, R. (2003) *Acc. Chem. Res.*, 36, 638–643.

29. Phan, N.T.S., Van Der Sluys, M., and Jones, C.W. (2006) *Adv. Synth. Catal.*, 348, 609–679.

30. Yin, L.X. and Liebscher, J. (2007) *Chem. Rev.*, 107, 133–173.

31. Bedford, R.B. (2003) *Chem. Commun.*, 1787–1796.

32. de Vries, A.H.M., Mulders, J., Mommers, J.H.M., Henderickx, H.J.W., and de Vries, J.G. (2003) *Org. Lett.*, 5, 3285–3288.

33. de Vries, A.H.M., Mulders, J., Willans, C. E., Schmieder-van de Vondervoort, L., Parlevliet, F.J., and de Vries, J.G. (2003) *Abstr. Pap. Am. Chem. Soc.*, 225, 60-ORGN.

34. de Vries, A.H.M., Parlevliet, F.J., Schmieder-van de Vondervoort, L., Mommers, J.H.M., Henderickx, H.J.W., Walet, M.A.M., and de Vries, J.G. (2002) *Adv. Synth. Catal.*, 344, 996–1002.

35. Reetz, M.T. and de Vries, J.G. (2004) *Chem. Commun.*, 1559–1563.

36. Reetz, M.T., Westermann, E., Lohmer, R., and Lohmer, G. (1998) *Tetrahedron Lett.*, 39, 8449–8452.

37. Reetz, M.T. and Westermann, E. (2000) *Angew. Chem.*, 112, 170–173; *Angew. Chem., Int. Ed.*, 39, 165–166 (2000).

38. Rocaboy, C. and Gladysz, J.A. (2003) *New J. Chem.*, 27, 39–49.

39. Tromp, M., Sietsma, J.R.A., van Bokhoven, J.A., van Strijdonck, G.P.F., van Haaren, R.J., van der Eerden, A.M.J., van Leeuwen, P., and Koningsberger, D.C. (2003) *Chem. Commun.*, 128–129.

40. Hart, R., Pollet, P., Hahne, D.J., John, E., Llopis-Mestre, V., Blasucci, V., Huttenhower, H., Leitner, W., Eckert, C. A., and Liotta, C.L. (2010) *Tetrahedron*, 66, 1082–1090.

41. Liu, Y.X., Jessop, P.G., Cunningham, M., Eckert, C.A., and Liotta, C.L. (2006) *Science*, 313, 958–960.

42. Jessop, P.G., Heldebrant, D.J., Li, X.W., Eckert, C.A., and Liotta, C.L. (2005) *Nature*, 436, 1102–1102.

43. Wu, X.F., Anbarasan, P., Neumann, H., and Beller, M. (2010) *Angew. Chem.*, 122, 9231-9234; *Angew. Chem., Int. Ed.*, 49, 9047-9050 (2010).

44. Molnar, A. (2011) *Curr. Org. Synth.*, 8, 172–186.

45. Olivier-Bourbigou, H., Magna, L., and Morvan, D. (2010) *Appl. Catal. A: Gen.*, 373, 1–56.

46. Liu, S. and Xiao, J. (2007) *J. Mol. Catal. A: Chem.*, 270, 1–43.

47. Kaufmann, D.E., Nouroozian, M., and Henze, H. (1996) *Synlett*, 1091–1092.

48. Böhm, V.P.W. and Herrmann, W.A. (2000) *Chem. Eur. J.*, 6, 1017–1025.

49. Herrmann, W.A. and Böhm, V.P.W. (1999) *J. Organomet. Chem.*, 572, 141–145.

50. Carmichael, A.J., Earle, M.J., Holbrey, J. D., McCormac, P.B., and Seddon, K.R. (1999) *Org. Lett.*, 1, 997–1000.

51. Selvakumar, K., Zapf, A., and Beller, M. (2002) *Org. Lett.*, 4, 3031–3033.

52. Li, S.H., Lin, Y.J., Xie, H.B., Zhang, S.B., and Xu, J.N. (2006) *Org. Lett.*, 8, 391–394.

53. Xiao, J.C., Twamley, B., and Shreeve, J.M. (2004) *Org. Lett.*, 6, 3845–3847.

54. Wang, R., Xiao, J.C., Twamley, B., and Shreeve, J.M. (2007) *Org. Biomol. Chem.*, 5, 671–678.

55. Wang, R.H., Twamley, B., and Shreeve, J. M. (2006) *J. Org. Chem.*, 71, 426–429.

56. Vallin, K.S.A., Emilsson, P., Larhed, M., and Hallberg, A. (2002) *J. Org. Chem.*, 67, 6243–6246.

57. Mo, J., Ruan, J.W., Xu, L.J., Hyder, Z., Saidi, O., Liu, S.F., Pei, W., and Xiao, J.L. (2007) *J. Mol. Catal. A: Chem.*, 261, 267–275.

58. Xu, L.J., Chen,W.P., Ross, J., and Xiao, J. L. (2001) *Org. Lett.*, 3, 295–297.

59. Mo, J., Xu, L.J., and Xiao, J.L. (2005) *J. Am. Chem. Soc.*, 127, 751–760.

60. Pei, W., Mo, J., and Xiao, J.L. (2005) *J. Organomet. Chem.*, 690, 3546–3551.

61. Handy, S.T. and Okello, M. (2003) *Tetrahedron Lett.*, 44, 8395–8397.

62. Paterson, I., Davies, R.D.M., and Marquez, R. (2001) *Angew. Chem.*, 113, 623–627; *Angew. Chem., Int. Ed.*, 40, 603–607 (2001).

63. Wolff, J.J., Siegler, F., Matschiner, R., and Wortmann, R. (2000) *Angew. Chem.*, 112, 1494–1498; *Angew. Chem., Int. Ed.*, 39, 1436–1437 (2000).

64. Kmentova, I., Gotov, B., Gajda, V., and Toma, S. (2003) *Monatsh. Chem.*, 134, 545–549.

65. Park, S.B. and Alper, H. (2004) *Chem. Commun.*, 1306–1307.

66. Sans, V., Trzeciak, A.M., Luis, S., and Ziolkowski, J.J. (2006) *Catal. Lett.*, 109, 37–41.

67. Fukuyama, T., Shinmen, M., Nishitani, S., Sato, M., and Ryu, I. (2002) *Org. Lett.*, 4, 1691–1694.

68. Li, Y., Zhang, J.Y., Wang, W.K., Miao, Q., She, X.G., and Pan, X.F. (2005) *J. Org. Chem.*, 70, 3285–3287.

69. Wang, R.H., Piekarski, M.M., and Shreeve, J.M. (2006) *Org. Biomol. Chem.*, 4, 1878–1886.

70. Miyaura, N. and Suzuki, A. (1979) *J. Chem. Soc., Chem. Commun.*, 866–867.

71. Singh, R., Sharma, M., Mamgain, R., and Rawat, D.S. (2008) *J. Braz. Chem. Soc.*, 19, 357–379.

72. Mathews, C.J., Smith, P.J., and Welton, T. (2000) *Chem. Commun.*, 1249–1250.

73. Rajagopal, R., Jarikote, D.V., and Srinivasan, K.V. (2002) *Chem. Commun.*, 616–617.

74. Ren, Y., Yu, G.A., Guan, J.T., and Liu, S.H. (2007) *Appl. Organomet. Chem.*, 21, 1–4.

75. Lombardo, M., Chiarucci, M., and Trombini, C. (2009) *Green Chem.*, 11, 574–579.

76. Mathews, C.J., Smith, P.J., and Welton, T. (2004) *J. Mol. Catal. A: Chem.*, 214, 27–32.

77. McLachlan, F., Mathews, C.J., Smith, P.J., and Welton, T. (2003) *Organometallics*, 22, 5350–5357.

78. Sirieix, J., Ossberger, M., Betzemeier, B., and Knochel, P. (2000) *Synlett*, 1613–1615.

79. de Bellefon, C., Pollet, E., and Grenouillet, P. (1999) *J. Mol. Catal. A: Chem.*, 145, 121–126.

80. Chen, W.P., Xu, L.J., Chatterton, C., and Xiao, J.L. (1999) *Chem. Commun.*, 1247–1248.

81. Molnar, A. (2011) *Chem. Rev.*, 111, 2251–2320.

82. Trzeciak, A.M. and Ziolkowski, J.J. (2007) *Coord. Chem. Rev.*, 251, 1281–1293.

83. Hamill, N.A., Hardacre, C., and McMath, S.E.J. (2002) *Green Chem.*, 4, 139–142.

84. Gaikwad, A.V., Holuigue, A., Thathagar, M.B., ten Elshof, J.E., and Rothenberg, G. (2007) *Chem. Eur. J.*, 13, 6908–6913.

85. Thathagar, M.B., ten Elshof, J.E., and Rothenberg, G. (2006) *Angew. Chem.*, 118, 2952-2956; *Angew. Chem., Int. Ed.*, 45, 2886–2890 (2006).

86. Parvulescu, V.I. and Hardacre, C. (2007) *Chem. Rev.*, 107, 2615–2665.

87. Bellina, F. and Chiappe, C. (2010) *Molecules*, 15, 2211–2245.

88. Hyder, Z., Mo, J., and Xiao, J.L. (2006) *Adv. Synth. Catal.*, 348, 1699–1704.

89. Xie, X.G., Chen, B., Lu, J.P., Han, J.J., She, X.G., and Pan, X.F. (2004) *Tetrahedron Lett.*, 45, 6235–6237.

90. Hagiwara, H., Sugawara, Y., Isobe, K., Hoshi, T., and Suzuki, T. (2004) *Org. Lett.*, 6, 2325–2328.

91. Hagiwara, H., Shimizu, Y., Hoshi, T., Suzuki, T., Ando, M., Ohkubo, K., and Yokoyama, C. (2001) *Tetrahedron Lett.*, 42, 4349–4351.

92. Xiao, J.C. and Shreeve, J.M. (2005) *J. Org. Chem.*, 70, 3072–3078.

93. Miao, W. and Chan, T.H. (2003) *Org. Lett.*, 5, 5003–5005.

94. Sasaki, T., Tada, M., Zhong, C.M., Kume, T., and Iwasawa, Y. (2008) *J. Mol. Catal. A: Chem.*, 279, 200–209.

95. Chiappe, C., Imperato, G., Napolitano, E., and Pieraccini, D. (2004) *Green Chem.*, 6, 33–36.

96. Louaisil, N., Phuoc Dien, P., Boeda, F., Faye, D., Castanet, A.-S., and Legoupy, S. (2011) *Eur. J. Org. Chem.*, 143–149.

97. Bönnemann, H., Brijoux,W., and Joussen, T. (1990) *Angew. Chem.*, 102, 324–326; *Angew. Chem., Int. Ed. Engl.*, 29, 273–275 (1990).

98. Bönnemann, H., Brijoux, W., Brinkmann, R., Dinjus, E., Joussen, T., and Korall, B. (1991) *Angew. Chem.*, 103, 1344–1346; *Angew. Chem., Int. Ed. Engl.*, 30, 1312–1314 (1991).

99. Marquardt, D., Xie, Z.L., Taubert, A., Thomann, R., and Janiak, C. (2011) *Dalton Trans.*, 40, 8290–8293.

100. Oda, Y., Hirano, K., Yoshii, K., Kuwabata, S., Torimoto, T., and Miura, M. (2010) *Chem. Lett.*, 39, 1069–1071.

101. Cassol, C.C., Umpierre, A.P., Machado, G., Wolke, S.I., and Dupont, J. (2005) *J. Am. Chem. Soc.*, 127, 3298–3299.

102. Takahashi, Y., Ito, T., Sakai, S., and Ishii, Y. (1970) *J. Chem. Soc. D: Chem. Commun.*, 1065–1066.

103. Prechtl, M.H.G., Campbell, P.S., Scholten, J.D., Fraser, G.B., Machado, G., Santini, C.C., Dupont, J., and Chauvin, Y. (2010) *Nanoscale*, 2, 2601–2606.

104. Reetz, M.T. and Lohmer, G. (1996) *J. Chem. Soc., Chem. Commun.*, 1921–1922.

105. Xu, L.J., Chen,W.P., and Xiao, J.L. (2000) *Organometallics*, 19, 1123–1127.

106. Mathews, C.J., Smith, P.J., Welton, T., White, A.J.P., and Williams, D.J. (2001) *Organometallics*, 20, 3848–3850.

107. Dupont, J. and Spencer, J. (2004) *Angew. Chem.*, 116, 5408–5409; *Angew. Chem., Int. Ed.*, 43, 5296–5297 (2004).

108. Lebel, H., Janes, M.K., Charette, A.B., and Nolan, S.P. (2004) *J. Am. Chem. Soc.*, 126, 5046–5047.

109. Deshmukh, R.R., Rajagopal, R., and Srinivasan, K.V. (2001) *Chem. Commun.*, 1544–1545.

110. Reetz, M.T., Breinbauer, R., and Wanninger, K. (1996) *Tetrahedron Lett.*, 37, 4499–4502.

111. Calo, V., Nacci, A., Monopoli, A., and Cotugno, P. (2009) *Angew. Chem.*, 121, 6217–6219; *Angew. Chem., Int. Ed.*, 48, 6101–6103 (2009).

112. Calo, V., Nacci, A., Monopoli, A., Laera, S., and Cioffi, N. (2003) *J. Org. Chem.*, 68, 2929–2933.

113. Tao, R.T., Miao, S.D., Liu, Z.M., Xie, Y., Han, B.X., An, G.M., and Ding, K.L. (2009) *Green Chem.*, 11, 96–101.

114. Rodriguez-Perez, L., Pradel, C., Serp, P., Gomez, M., and Teuma, E. (2011) *ChemCatChem*, 3, 749–754.

115. Corma, A., Iborra, S., Xamena, F.X.L.I., Monton, R., Calvino, J.J., and Prestipino, C. (2010) *J. Phys. Chem. C*, 114, 8828–8836.

116. Liu, G., Hou, M.Q., Song, J.Y., Jiang, T., Fan, H.L., Zhang, Z.F., and Han, B.X. (2010) *Green Chem.*, 12, 65–69.

117. Balanta, A., Godard, C., and Claver, C. (2011) *Chem. Soc. Rev.*, 40, 4973–4985.

118. Calo, V., Nacci, A., Monopoli, A., and Montingelli, F. (2005) *J. Org. Chem.*, 70, 6040–6044.

119. Lin, L., Li, Y.C., Zhang, S.B., and Li, S.H. (2011) *Synlett*, 1779–1783.

120. Wang, J.Y., Song, G.H., and Peng, Y.Q. (2011) *Tetrahedron Lett.*, 52, 1477–1480.

121. Kalviri, H.A. and Kerton, F.M. (2011) *Green Chem.*, 13, 681–686.

122. Durand, J., Teuma, E., Malbosc, F., Kihn, Y., and Gomez, M. (2008) *Catal. Commun.*, 9, 273–275.

123. Hagiwara, H., Sasaki, H., Tsubokawa, N., Hoshi, T., Suzuki, T., Tsuda, T., and Kuwabata, S. (2010) *Synlett*, 1990–1996.

124. Hagiwara, H., Ko, K.H., Hoshi, T., and Suzuki, T. (2007) *Chem. Commun.*, 2838–2840.

125. Akiyama, T., Ibata, C., and Fujihara, H. (2010) *Heterocycles*, 80, 925–931.

126. Safavi, A., Maleki, N., Iranpoor, N., Firouzabadi, H., Banazadeh, A.R., Azadi, R., and Sedaghati, F. (2008) *Chem. Commun.*, 6155–6157.

127. Battistuzzi, G., Bernini, R., Cacchi, S., De Salve, I., and Fabrizi, G. (2007) *Adv. Synth. Catal.*, 349, 297–302.

128. Nelson, J.M., Chiller, T.M., Powers, J.H., and Angulo, F.J. (2007) *Clin. Infect. Dis.*, 44, 977–980.

129. Geukens, I., Fransaer, J., and De Vos, D.E. (2011) *ChemCatChem*, 3, 1431–1434.

130. Gao, S.Y., Zhang, H.J.,Wang, X.M., Mai, W.P., Peng, C.Y., and Ge, L.H. (2005) *Nanotechnology*, 16, 1234–1237.

131. Corma, A., Garcia, H., and Leyva, A. (2005) *Tetrahedron*, 61, 9848–9854.

132. Pachon, L.D., Elsevier, C.J., and Rothenberg, G. (2006) *Adv. Synth. Catal.*, 348, 1705–1710.

3.6 Palladium Catalysed Aerobic Dehydrogenation of C-H Bonds in Cyclohexanones

Michael T. Keßler, and Martin H.G. Prechtl*[a]

Dedicated to Professor Hans-Josef Altenbach on the occasion of his 65th birthday

[a] M. T. Keßler, Dr. M. H. G. Prechtl
University of Cologne
Institute for Inorganic Chemistry
Greinstr. 6, 50939 Köln (Germany)
Fax: (+49) 221-470-1788
E-mail: martin.prechtl@uni-koeln.de
Homepage: http://catalysis.uni-koeln.de
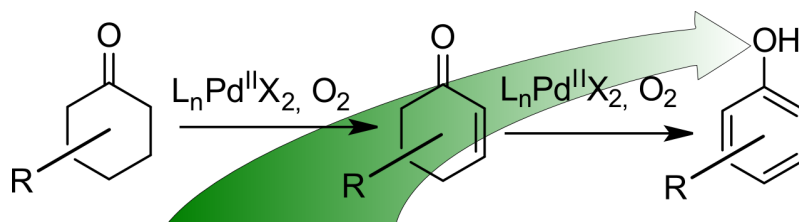
Two steps to aromaticity: Aromatic compounds such as phenols represent a common structural motive in nature and they are of great demand in chemical synthesis. Due to the lack of possibilities to substitute the aromatic ring system in meta position phenols were rather expensive and their production environmentally unfriendly. The advances in catalytic aerobic dehydrogenation stand for a new approach to make them easily available from cyclohexanones.

The transformation of cycloalkanes into aromatic compounds, such as phenols, is a fundamental reaction in organic chemistry. Phenols have a wide spread of applications in fields ranging from polymers to pharmaceuticals, as electronic materials in final products or intermediates in chemical synthesis.[1] Their unique properties originate from the manifold opportunities to substitute these compounds along the aromatic ring system regioselectively. Electrophilic aromatic substitution (S_eAr) is a very simple and versatile method to synthesise substituted aromatic rings.[2] Owing to electronic effects the S_eAr mechanism results only in *ortho-* and *para-*substituted products and fails to generate *meta-*substituted derivatives. There are different approaches to introduce a hydroxyl group at the *meta-*position. One option is the condensation of a ketone with a 1,3-dicarbonyl component, forming a substituted phenol.[3] This method is, however, limited to nitro-substituted dicarbonyl compounds and suffers from low yields, as described by *Bamfield* and *Gordon*.[3] Another possibility is a two-step synthesis through the borylation and subsequent oxidation of a cyclic carbonyl mediated by a Ir[COD]-type catalyst.[4] The substrates are limited,

however, to halogenated arenes; the corresponding phenols result in moderate to good yields. In contrast to the catalytic borylation step, the oxidation requires a stoichiometric oxidant, which leads to a phenol in a two-step dehydrogenation. The low yields, use of a stoichiometric reagent as a hydrogen acceptor,[5−7] harsh reaction conditions[5] and long reaction time[6] are undesirable, especially for synthesis on a technical scale. In addition, nearly all catalytic attempts, for example with iridium complexes, failed because of their limitation to unsubstituted arenes or the stoichiometric consumption of the catalyst. *Yi* and co-workers presented a Ru-catalysed method for the dehydrogenative aromatisation of carbonyl compounds and amines.[8] The ruthenium-μ-oxo-μ-hydroxo-hydride-complex presented exhibits a moderate turnover number for the conversion of cyclic carbonyls to the corresponding phenols. Despite the positive catalytic activity, the overall consumption of hydrogen acceptor (*tert*-butylethylene) and the reaction temperature (200 °C) were too high and made this reaction intolerant towards labile functional groups. *Hirao* and *Mori* succeeded in the dehydrogenative aromatisation of an α,β-unsaturated cyclohexenone mediated by a $VO(OR)Cl_2$ oxidant.[9] Based on these developments, *Hirao* and *Moriuchi* presented a vanadium-catalysed dehydrogenation of a variety of substituted cyclohexenones in 2009.[10] The catalyst used in this reaction was the commercially available NH_4VO_3 or $VOSO_4$ with Bu_4NBr/HBr and trifluoroacetic acid (TFA) additives; the oxidative species was molecular dioxygen. Under an argon atmosphere there was no significant conversion of the cyclohexenone to the corresponding phenol. The combination of oxidative bromination from a bromine source, a Brønsted acid, and molecular oxygen in the vanadium-catalysed dehydrogenation to arenes, alkenes, and alkynes, had already been reported.[11] Although this catalytic approach maintains yields of up to 90%, it still suffers from the large amounts of additives required (300–1000 mol%). Recently, *Stahl* and co-workers presented a catalytic approach for the dehydrogenation of cyclohexanones with a loading of 3–5 mol% palladium trifluoroacetate [$Pd(TFA)_2$], *p*-toluenesulfonic acid (TsOH) and 2-(N,N-dimethylamino)pyridine.[12] As shown in Table 3.11, they dehydrogenated 3-methylcyclohex-2-ene (1) and 3-methylcyclohexanone (2) to obtain *meta*-cresole in quantitative yield after 24 h (Table 3.11; Entry 5). Molecular oxygen (1 atm), a highly desirable oxidant from chemical, environmental, and economic perspectives, was used at 80 °C and generated water as an easily removable by-product.[13] The major advantage of the catalytic conversion of cyclohexanones into phenols is the ready availability of the reactants. Diels–Alder reactions, aldol condensations, Robinson annulations and numerous other reactions are commonly used to generate cyclohexanones because of their atom economy and typically mild reaction conditions.

Further investigation of the possible reactants revealed the extensive benefit of this catalytic dehydrogenation reaction. Several alkyl- and aryl-substituted cyclohexenones and cyclohexanones were converted into the corresponding phenols in good to excellent yields, which only decreased in cases of *para*-bromo- or iodo-substituted derivatives. In addition to the alkyl and aryl groups, this reaction tolerates many other functional groups in the saturated ring system, for example, carbonic acids, halides or alkoxy groups.[12] The reaction pathway in Scheme 3.30 includes a primary dehydrogenation to derivatives of 2-cyclohexenone and a secondary dehydrogenation to 2,4-cyclohexadienone, which rearranges to the corresponding phenol. Both dehydrogenation steps consist of an initial palladium insertion and subsequent β-hydride elimination. A HX species is thereby eliminated, leaving behind a Pd^0 catalyst. The direct oxidation of Pd^0 by dioxygen is, however kinetically inhibited,[14] as described in a preliminary model by *Bianchi* and *Bortolo*.[15] An intermediate η_2-peroxo palladium complex is formed,[16] although a hydroperoxopalladium(II)-species would also be conceivable.[19,20] The η_2-peroxo intermediate can be stabilised by a

Table 3.11: Yields (determined by GC) of the dehydrogenation of 3-methylcyclohex-2-ene **1** and 3-methylcyclohexanone **2**.

Entry	Catalyst	Ligand	Additive	Yield from	
				1	2
1	Pd(OAc)$_2$	-	-	30	40
2	Pd(TFA)$_2$	^{2NHMe}py	-	72	22
3	Pd(TFA)$_2$	^{2NH2}py	TsOH	65	45
4	Pd(TFA)$_2$	^{2NMe2}py	TsOH	74	79
5	Pd(TFA)$_2$ 5 mol%	^{2NMe2}py	TsOH	100	84

Reaction cnditions: 3 mol% catalyst loading, 6 mol% ligand [^{2NHMe}py = 2-methylaminopyridine; ^{2NH2}py = 2-aminopyridine; ^{2NMe2}py = 2-(N,N-dimethylamino)pyridine], 12 mol% TsOH, 1 atm O$_2$, in DMSO, 80 °C, 24 h.

large number of different pyridine-derived ligands, which are not oxidised by dioxygen. The eliminated HX compound adds to the palladium centre and leaves behind H$_2$O$_2$ as depicted in Scheme 3.30. The utilised TsOH is used to protonate the amine group of the 2-(N,N-dimethylamino)pyridine and increase the electron deficiency of the pyridine, which is crucial for the phenol yield (Table 3.11, Entries 3–5).[19] The 2-(N,N-dimethylamino)pyridine is the preferentially used ligand because it is stable towards molecular oxygen and resists undesired ligand decomposition (Entries 4 and 5).[20]
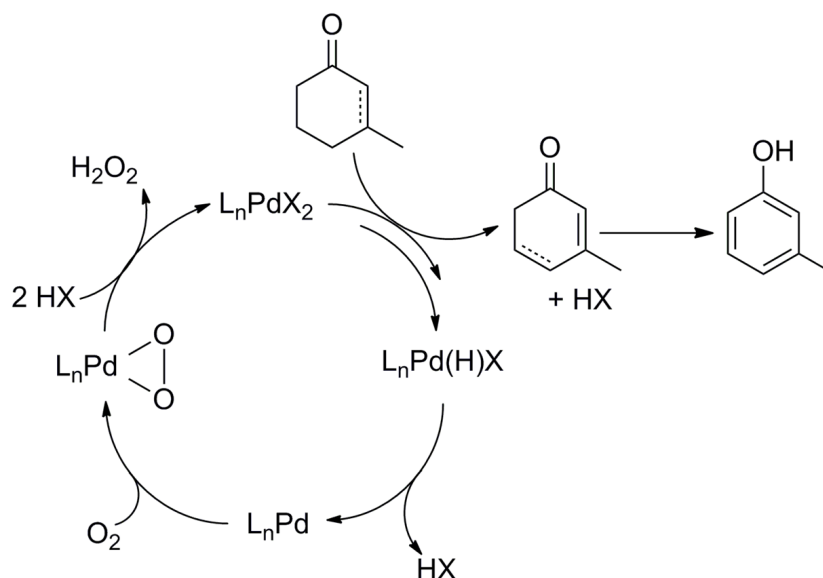
Scheme 3.30: Catalytic cycle of the Pd-mediated dehydrogenation of substituted cyclohexanones.

More recently, *Diao* and *Stahl* presented a method to synthesise cyclic enones with a similar reaction mechanism by dehydrogenation of cyclic ketones, which follows the primary dehydrogenation step described here.[21] In conclusion, the palladium-catalysed dehydrogenative oxidation of a variety of substituted cyclohexanones and cyclohexenones yields the corresponding phenols in good to excellent conversions using molecular oxygen as the

terminal oxidant. This process is also beneficial for application on an industrial scale.

3.6.1   Acknowledgements

1. J. H. P. Tyman in *Synthetic and Natural Phenols*, Elsevier, New York, **1996**.

2. G. A. Olah, *Acc. Chem. Res.* **1971**, 4, 240–248.

3. P. Bamfield, P. F. Gordon, *Chem. Soc. Rev.* **1984**, 13, 441–448.

4. R. E. Maleczka Jr., F. Shi, D. Holmes, M. R. Smith III, *J. Am. Chem. Soc.* **2003**, 125, 7792–7793.

5. P. F. Schuda, W. A. Price, *J. Org. Chem.* **1987**, 52, 1972–1979.

6. D. R. Buckle in *Encyclopedia of Reagents for Organic Synthesis* (Ed.: D. Crich), Wiley-VCH, New York, **2011**.

7. J. Muzart, J. P. Pete, *J. Mol. Catal. A-Chem.* **1982**, 15, 373–376.

8. C. S. Yi, D. W. Lee, *Organometallics* **2009**, 28, 947–949.

9. T. Hirao, M. Mori, Y. Ohshiro, *Chem. Lett.* **1991**, 20, 783–784.

10. T. Moriuchi, K. Kikushima, T. Kajikawa, T. Hirao, *Tetrahedron Lett.* **2009**, 50, 7385–7387.

11. K. Kikushima, T. Moriuchi, T. Hirao, *Chem. Asian J.* **2009**, 4, 1213–1216.

12. Y. Izawa, D. Pun, S. S. Stahl, *Science* **2011**, 333, 209–213.

13. S. S. Stahl, *Angew. Chem.* **2004**, 116, 3480–3501; *Angew. Chem. Int. Ed.* **2004**, 43, 3400–3420.

14. a) M. O. Unger, R. A. Fouty, *J. Org. Chem.* **1969**, 34, 18–21; b) J. M. Davidson, C. Triggs, *Chem. Ind.-London* **1967**, 31, 1361; c) H. Itatani, H. Yoshimoto, *Chem. Ind.-London* **1971**, 24, 674–675.

15. a) D. A. Bianchi, R. N. Bortolo, R. N. D. Aloisio, M. N. Ricci, S. C. Soattini (Enichem S. p. A.), EP0-808-796A1, **1997**; b) D. Bianchi, R. Bortolo, R. D. Aloisio, M. Ricci, *Angew. Chem.* **1999**, 111, 734–736; *Angew. Chem. Int. Ed.* **1999**, 38, 706–708; c) D. Bianchi, R. Bortolo, R. D. Aloisio, M. Ricci, *J. Mol. Catal. A-Chem.* **1999**, 150, 87–94; d) D. Bianchi, R. Bortolo, R. D Aloisio, C. Querci, M. Ricci, *Stud. Surf. Sci. Catal.* **1999**, 126, 481–484; e) R. Bortolo, D. Bianchi, R. D. Aloisio, C. Querci, M. Ricci, *J. Mol. Catal. A Chem.* **2000**, 153, 25–29.

16. G. Wilke, H. Schott, P. Heimbach, *Angew. Chem.* **1967**, 79, 62–62; *Angew. Chem. Int. Ed. Engl.* **1967**, 6, 92–93.

17. T. Hosokawa, S.-I. Murahashi, *Acc. Chem. Res.* **1990**, 23, 49–54.

18. T. Nishimura, Y. Maeda, N. Kakiuchi, S. Uemura, *J. Chem. Soc. Perkin Trans.* 1 **2000**, 4301–4305.

19. Y. Izawa, S. S. Stahl, *Adv. Synth. Catal.* **2010**, 352, 3223–3229.

20. L. H. Heitman, R. Narlawar, H. de Vries, M. N. Willemsen, D. Wolfram, J. Brussee, A. P. IJzerman, *J. Med. Chem.* **2009**, 52, 2036–2042.

21. T. Diao, S. S. Stahl, *J. Am. Chem. Soc.* **2011**, 133, 14566–14569.

3.7 Nanoparticle Syntheses and Applications as Catalysts

3.7.1 Synthesis of Pd/Cu bimetallic nanoparticles in ionic liquids
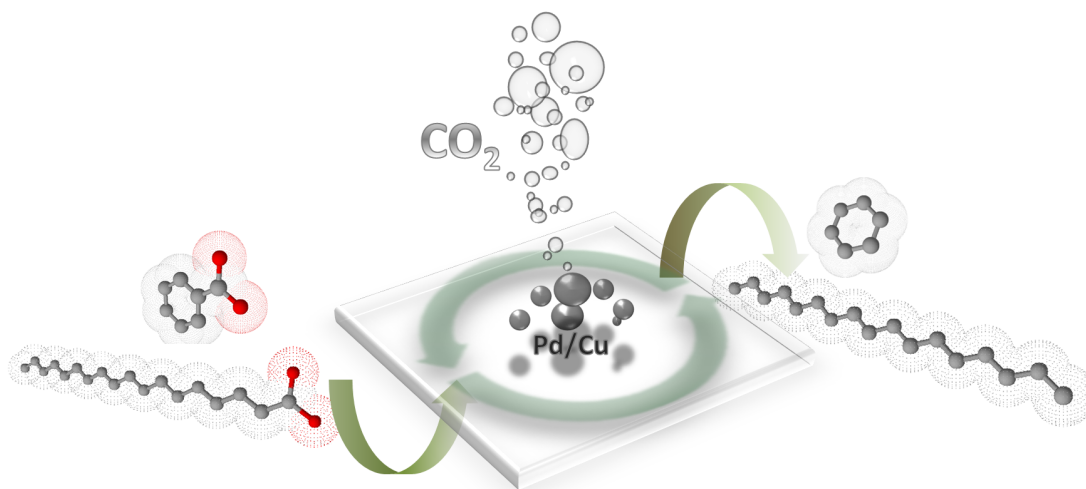
Since the synthesis of palladium particles from $Pd(OAc)_2$ and copper particles from $Cu(OAc)_2$ is possible, the attempt for the synthesis of bimetallic Pd/Cu is presented here. Blended metal particles often show a different behavior in catalytic applications, in catalytic activity, in shape or morphology. The Pd/Cu particles were synthesized by using $Pd(OAc)_2$ and $Cu(OAc)_2 \cdot H_2O$ as catalyst precursors.
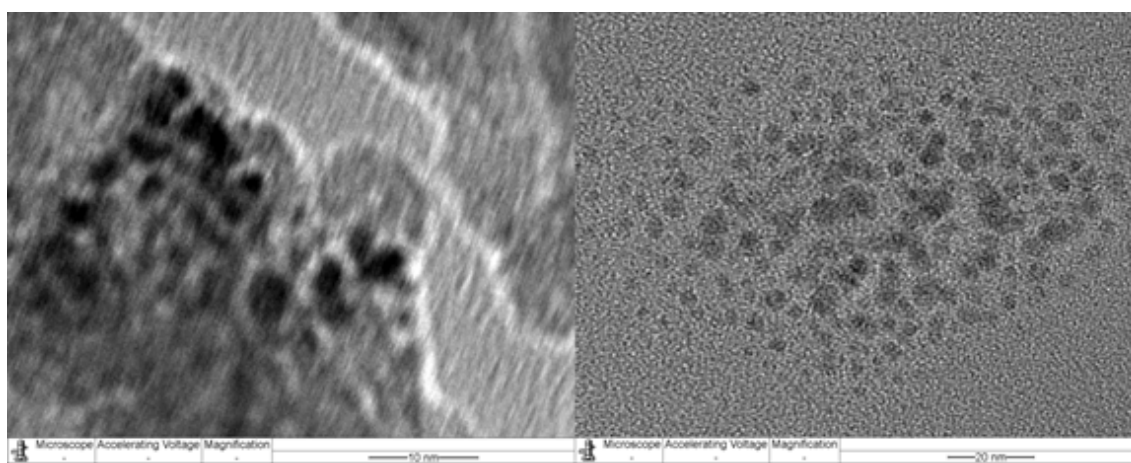
Figure 3.56: TEM pictures of Pd/Cu particles in n-Bu$_4$POAc (left, scale bar 10 nm) and bmmim NTf$_2$ (right, scale bar 20 nm).

The $Pd(OAc)_2$ was blended with $Cu(OAc)_2 \cdot H_2O$ to give a molar 2:1 mixture, which was not taken arbitrarily, but seems to be the most active ratio concerning decarboxylation reactions (see later). The particles in both ionic liquids have been synthesized within 24 h at 200 °C. The particles synthesized in n-Bu$_4$POAc show a higher tendency to build up aggregates, than those synthesized in bmmim NTf$_2$ as can be seen in the TEM picture in Figure 3.56 and they are not as homogeneously distributed on the carbon grid. On the other hand, the particles obtained in n-Bu$_4$POAc are slightly smaller. The HR-TEM pictures in Figure 3.57 and Figure 3.58 reveal an overall size of the Pd/Cu nanoparticles of 4-8 nm, whereas the particles obtained in bmmim NTf$_2$ show a higher degree of polydispersity with a mean diameter of 4-12 nm.
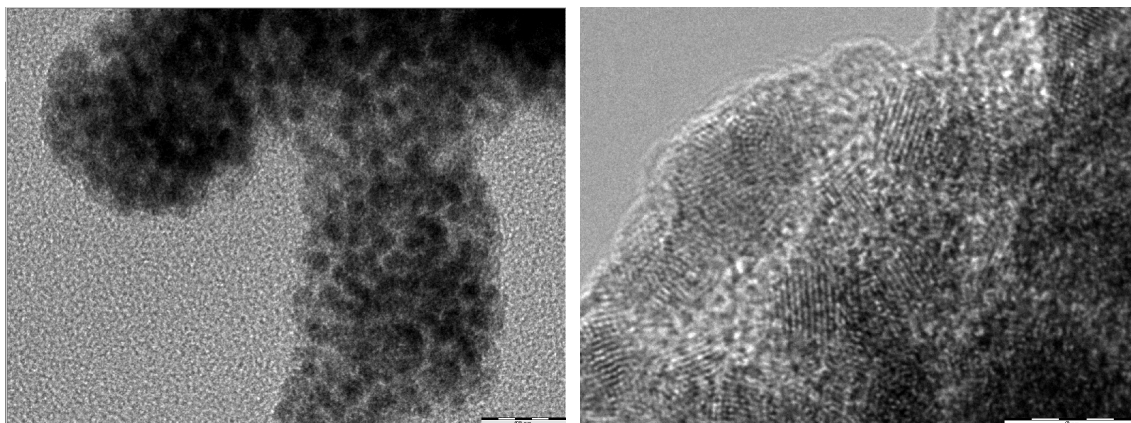
Figure 3.57: HR-TEM picture of Pd/Cu particles in *n*-Bu$_4$POAc (scale bar 10 nm).

Figure 3.58: HR-TEM picture of Pd/Cu particles in *n*-Bu$_4$POAc (scale bar 5 nm).

XAS-Analyses of Pd/Cu particles in ionic liquids

The EXAFS/XANES measurements of Pd/Cu particles have already been discussed in the Masters thesis of Maria K. Hentschel (University of Cologne) in a different context.
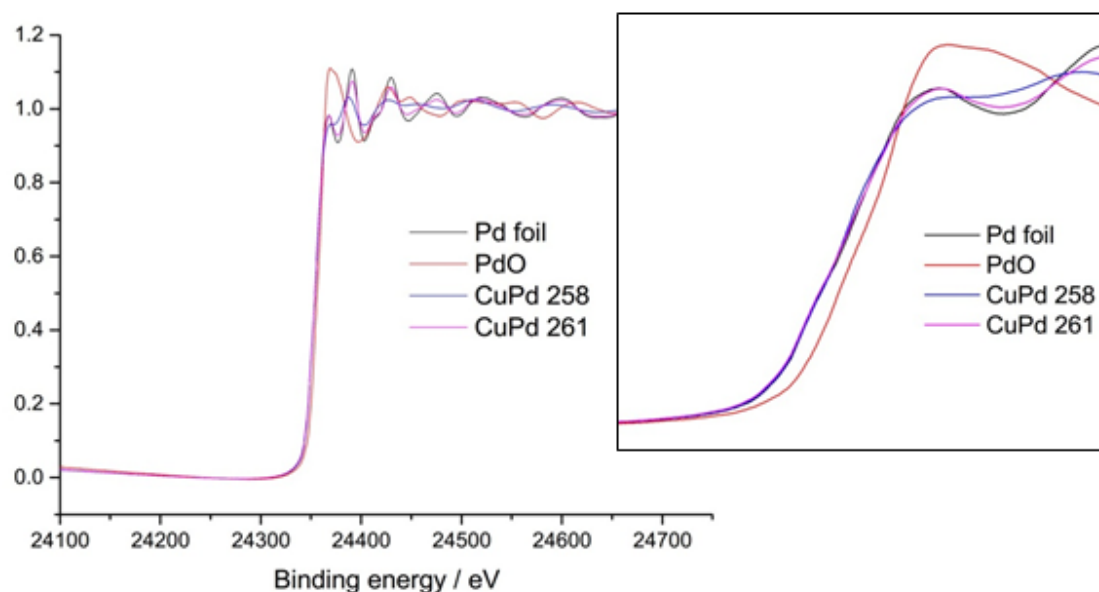
Figure 3.59: XANES-spectra of Pd/Cu in *n*-Bu$_4$POAc (CuPd 258) and of Pd/Cu in NTf$_2$ (CuPd 261). References of Pd-oxide (PdO) and pure palladium (Pd foil) are also displayed. A magnification of the absorption edge is displayed in the inset.

Two different X-ray absorption spectra have been taken from both particle types, either synthesized in *n*-Bu$_4$POAc or bmmim NTf$_2$. Firstly, XANES (X-ray Absorption Near Edge Structure) spectra have been analyzed. In the first instance, the absorption edge for X-ray irradiation and promotion of inner core electrons is specific for each element. In case of palladium the absorption-edge is located at 24360 eV and represents the overall binding energy of K-shell electrons (and therefore the X-ray photon energy). This energy is eminently influenced by the atoms electronic surrounding, thus influencing the energy levels of unoccupied electronic states.

Figure 3.60: EXAFS wave functions extracted from XANES spectra of Pd/Cu in *n*-Bu$_4$POAc (CuPd 258) and of Pd/Cu in NTf$_2$ (CuPd 261) as well as of Pd-oxide (PdO) and pure palladium (Pd foil).
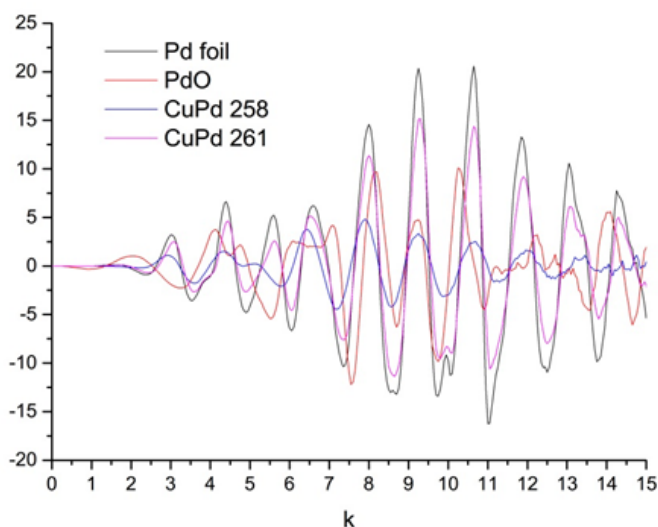
Both samples show a high similarity to pure palladium (see reference Pd foil in Figure 3.59) and a lower similarity to PdO, indicating that both palladium and copper rather stay in metallic state. A slight shift of electron density from copper (EN = 1.9) to palladium (EN = 2.2) thus cannot be excluded. This similarity to metallic Pd is also indicated by comparing the k-space values of the EXAFS measurement. The EXAFS k-space values give rise to the near atomic surrounding of the probe element (here Pd) in both samples by measuring the (single) scattering of the photoelectron emissions.

Figure 3.61: Fourier transformed EXAFS spectra and extracted r-space values of Pd/Cu in *n*-Bu$_4$POAc (CuPd 258) and of Pd/Cu in bmmim NTf$_2$ (CuPd 261) as well as of PdO and palladium foil.
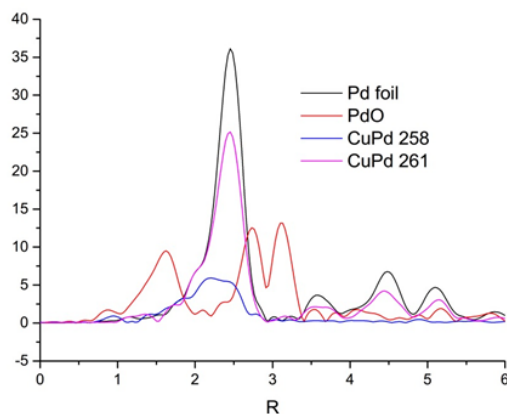
They show no significant similarity to PdO but more similarity to pure palladium. Despite this, the spectra of Pd/Cu in *n*-Bu$_4$POAc (CuPd 258) and of Pd/Cu in bmmim NTf$_2$ (CuPd 261) show differences even amongst themselves (Figure 3.60). This can be confirmed in the Fourier transformed EXAFS (FT-EXAFS) spectra of both samples, too (Figure 3.61). The surroundings of the Pd atoms in both particle samples seem to vary and not surprisingly are different from pure Pd, due to Cu doping. The difference to PdO is obvious now.

Nevertheless, a contamination with oxygen cannot be excluded yet. One can clearly see, that the spectrum of Pd/Cu in bmmim NTf$_2$ (CuPd 261) resembles the Pd reference more than its counterfeit in *n*-Bu$_4$POAc. This can be explained by different levels of Cu doping. With the k- and R-space values the coordination number (CN) of the Pd atoms in

Table 3.12: Calculated coordination numbers (CN) and atom-atom distances for both Pd/Cu samples in comparison to Pd.

sample		CN	r [Å]	σ^2	R
Pd	Pd-Pd	12	2.74±0.01	0.006±0.001	0.771
Pd/Cu	Pd-Pd	7.97±1.99	2.67±0.03	0.017±0.004	0.0001
n-Bu$_4$POAc	Pd-Cu	3.71±0.63	2.59±0.02	0.008±0.001	
Pd/Cu	Pd-Pd	9.78±3.45	2.73±0.02	0.007±0.002	0.195
bmmim NTf$_2$	Pd-Cu	1.33±2.31	2.59±0.14	0.005±0.009	

both samples can be calculated. The comparison of the CN in Table 3.12 demonstrates the difference between Pd/Cu in bmmim NTf$_2$ and in n-Bu$_4$POAc. Whereas in n-Bu$_4$POAc palladium is surrounded by 3.7±0.6 copper atoms, in bmmim NTf$_2$ Pd is only surrounded by 1.3±2.3 Cu atoms. This might be due to either a less Cu doping in bmmim NTf$_2$ or due to a core-shell separation of Cu and Pd in the particle (Pd core means high CN, Cu shell means low CN).

Decarboxylation reactions of benzoic- and fatty acids

Deoxygenation of stearic acid with Pd/Cu nanoparticles in n-Bu$_4$POAc

In this section, the as-synthesised Pd/Cu nanoparticles in n-Bu$_4$POAc are used as deoxygenation catalysts for stearic acid.
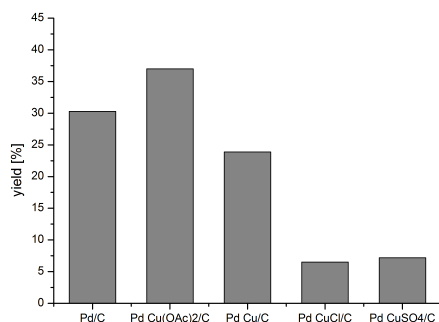
Figure 3.62: Yields of five immobilized catalysts for the deoxygenation of stearic acid using commercially available Pd/C as support.

For comparative reasons commercially available Pd on carbon was used as catalyst and as catalyst support where only the additional copper must be appended. A selection of the best results are presented here (for details please find Table 5.13 in the Experimental part). Already pure commercially available Pd on carbon shows a significant catalytic activity (30.3%) which can be seen in Figure 3.62. It could be improved further by adding Cu^{2+} originating from Cu(OAc)$_2$ to a maximum yield of 37.0%. Other Cu(II) sources like CuSO$_4$·5H$_2$O did not increase, but decrease the yield (7.2%) equally to the added Cu(I) species originating from CuCl (6.5%). In case of elemental copper (hydrogen reduced Cu(OAc)$_2$) the yield decreased slightly to 23.9%.

The as-prepared Pd/Cu particles in n-Bu$_4$POAc are used for the deoxygenation of

Figure 3.63: Comparison of yields of deoxygenated stearic acid catalysed by commercially available Pd/C, Pd/C with Cu^{2+} and Pd/Cu catalyst in n-Bu_4POAc (under air and under nitrogen).
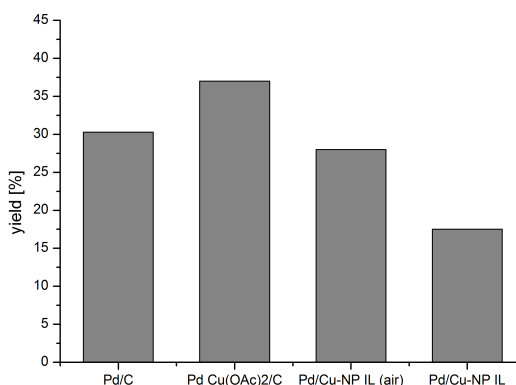
stearic acid and compared to the outcome of deoxygenation reactions conducted with supported Pd/Cu catalysts. In comparison to the previously shown results the overall yield of alkanes and alkenes in those reactions catalysed by Pd/Cu catalyst in n-Bu_4POAc is significantly lower. The yield the reactions conducted without inert atmosphere (e.g. nitrogen) was higher (28%) in comparison to those conducted under nitrogen (17.5%) (see Figure 3.63). In fact, this is the only reaction where the absence of inert conditions seems to improve the yield.
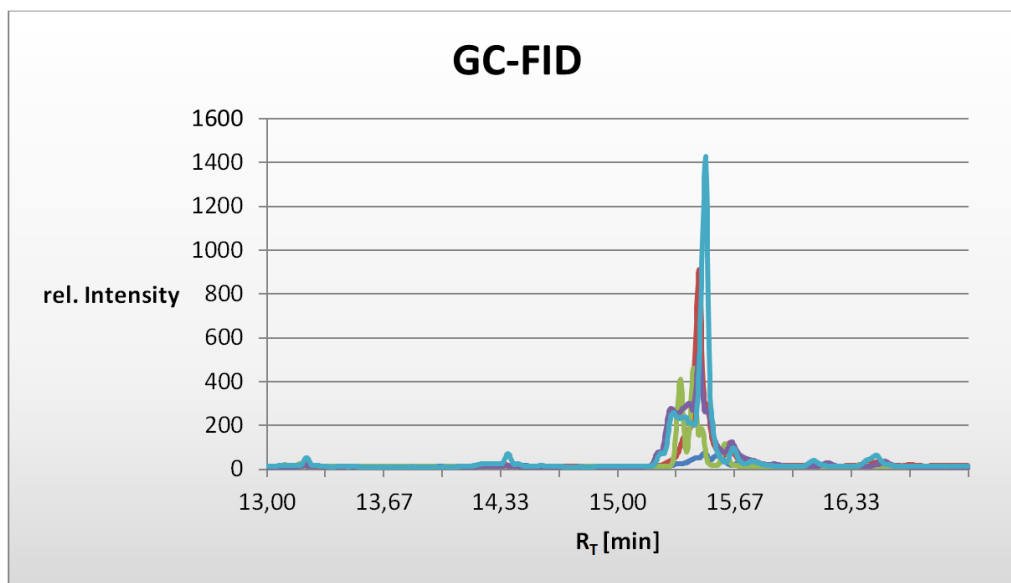
Figure 3.64: Chromatograms of the deoxygenation reactions of stearic acid using Pd/Cu in IL (N_2, green), Pd/Cu in IL (air, violet), Pd/C (red), Pd/C Cu^{2+} (blue).

Usually a dark black and waxy solid is formed which is in all probability carbon black resulting from coking of the stearic acid. The yield of alkanes and alkenes in those reactions is usually below 7% after 2 h. In order to compare the outcome of the catalyses with the above shown catalysts the four corresponding chromatograms are shown in (Figure 3.64). Obviously, mainly C_{17}-alkanes and alkenes are produced (RT = 15.2-15.6 min) and only minor amounts of C_{18} (RT = 16.3 min), C_{16} (RT = 14.3 min) and C_{15} (RT = 13.3 min) products can be found (ratio$_{(C15:C16:C17:C18)}$ = 2.2 : 2.2 : 95.0 : 0.6). Although the

selectivity towards C_{17} products is very high, all the catalysts show a lower selectivity between alkanes and alkenes as can be seen in Figure 3.65.
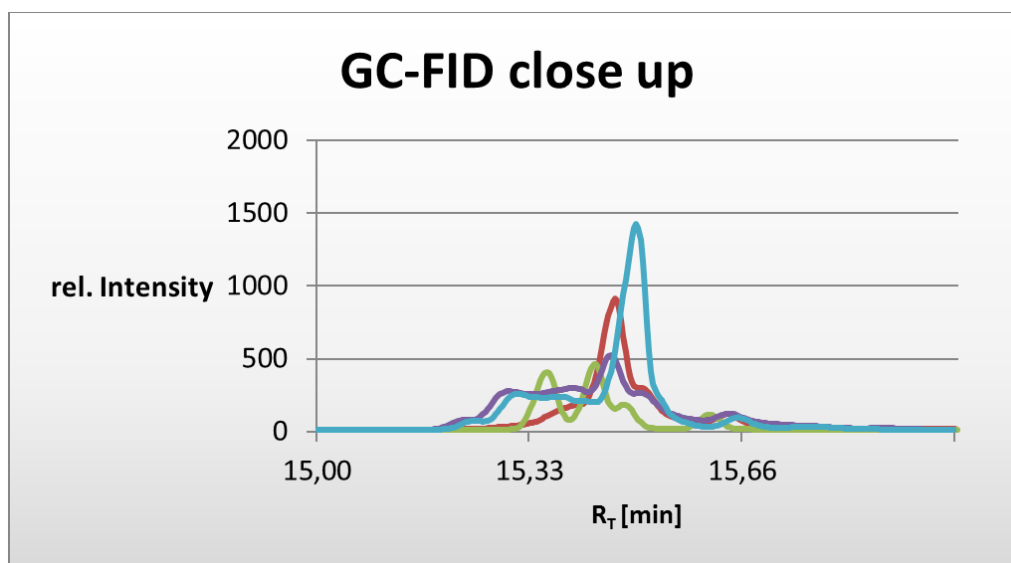
Figure 3.65: GC-FID close up on chromatograms showing mainly C_{17}-products (RT = 15.2-15.6 min) with Pd/Cu in IL (N_2, green), Pd/Cu in IL (air, violet), Pd/C (red), Pd/C Cu^{2+} (blue).

In some cases the C_{17} products seem to be contaminated with minor amounts of C_{18}-aldehydes (less than 3%). Due to this, it cannot be excluded, that also in the other fractions (C_{15}, C_{16}) small amounts of corresponding aldehydes are present. It is still not clear if a non-sufficient deoxygenation takes place (e.g. decarbonylation as a side-reaction) or if re-oxidation takes place.

Table 3.13: Overview about some selected examples for the deoxygenation of stearic acid, concerning the overall yield of C_{17}-alkanes and alkenes and the selectivity between them. N/A means, that the yield of the final products was too low in order to determine exactly the ratio of alkenes and alkanes.

catalyst	loading [mol%]	temp. [°C]	gas	time [h]	yield [%]	ratio (alkane:alkene)
Pd/C	10	350	N_2	2	30.3	4.0 : 96.0
Pd Cu(OAc)$_2$	5, 5	350	N_2	2	37.0	11.6 : 88.4
Pd/Cu-NP IL	10, 5	350	air	2	28.0	9.6 : 90.4
Pd Cu/C	10, 5	350	N_2	2	23.9	5.9 : 94.1

Furthermore, there is not only one alkene isomer present, but at least two (presumably 1-heptadecene, 2-heptadecene), which can also be seen in Figure 3.65. There is no trend observable in the selectivity of the catalysts towards alkanes or alkenes (see Table 3.13). At least there is a hint, that at lower overall yields the amount of alkane is slightly increased, whereas at higher overall yields, the amount of alkenes is strongly dominating. One possible reason for the decreasing yield of alkanes and alkenes by using the IL as stabilising agent for the catalyst might be thermal degradation of the used ionic liquid. At reaction

temperatures of about 350 °C *n*-Bu$_4$POAc tends to undergo elimination reactions. On the one hand, the ionic liquid cannot stabilise the as-prepared nanoparticles during elimination reactions, leading to agglomeration and aggregation of the nanoparticles. On the other hand, the resulting tributylphosphine might coordinate to the remaining active sites even lowering the activity of the catalyst. A support or ionic liquid with higher temperature stability seems to be of practical use.

Decarboxylation of benzoic acids with Pd/Cu catalyst in ionic liquids
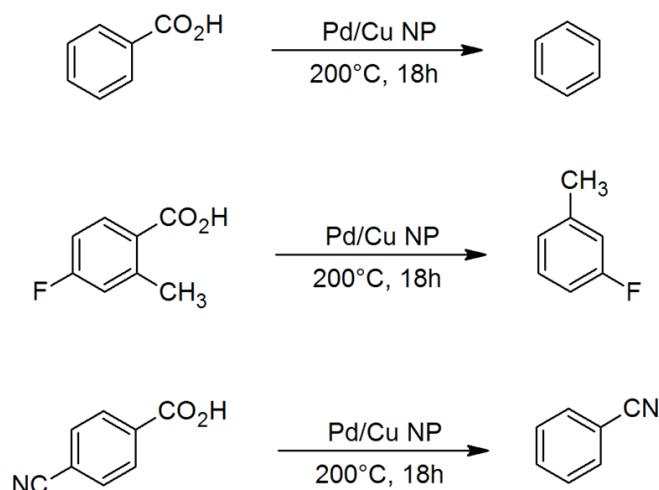
Scheme 3.31: Decarboxylation reactions of benzoic acid, 4-fluoro-2-methyl benzoic acid and 4-cyanobenzoic acid.

As Cu$_2$O nanoparticles, presented in chapter 3.1 are not active catalysts for the decarboxylation of all kinds of benzoic acids, Pd/Cu catalysts seem to be highly promising, since those have shown their use in deoxygenation reactions of rather nonreactive fatty acids. In order to determine the catalytic activity of the bimetallic catalyst three substrates with different functional groups (excluding NO$_2$-groups in ortho position) were considered for test reactions. Yields of about 40% of the corresponding arene could be achieved with Pd/Cu nanoparticles in *n*-Bu$_4$POAc (see Table 3.14, Entry 1,3,4). Nevertheless, 4-cyanobenzoic acid is still not decarboxylated in satisfying yields (see Table 3.14, Entry 5+6). The shown reactions have also been conducted in bmmim NTf$_2$ with Pd/Cu nanoparticles as catalytic phase. All benzoic acids tend to evaporate at these high temperatures and recrystallized on the cold glass wall. Therefore no conversion of benzoic acid decarboxylation was detectable in bmmim NTf$_2$. The higher polarity of *n*-Bu$_4$POAc compared to bmmim NTf$_2$ seems to suppress the evaporation of the benzoic acids and therefore the reaction can only take place in the phosphonium based ionic liquid.

Table 3.14: Overview about the decarboxylation reactions of benzoic acids with Pd/Cu catalyst (10 mol%) in two different ionic liquids. The reaction temperature was 200 °C.

substrate	IL	gas	time [h]	yield [%]
Benzoic acid	n-Bu$_4$POAc	N$_2$	18	40.2
Benzoic acid	n-Bu$_4$POAc	air	18	9.0
4-fluoro-2-methyl benzoic acid	n-Bu$_4$POAc	N$_2$	18	40.4
4-fluoro-2-methyl benzoic acid	n-Bu$_4$POAc	air	18	44.1
4-cyano benzoic acid	n-Bu$_4$POAc	N$_2$	18	6.3
4-cyano benzoic acid	n-Bu$_4$POAc	air	18	6.3
Benzoic acid	bmmim NTf$_2$	N$_2$	18	-
4-fluoro-2-methyl benzoic acid	bmmim NTf$_2$	N$_2$	18	-
4-cyano benzoic acid	bmmim NTf$_2$	N$_2$	18	-

3.7.2 Regioselective deuterodecarboxylation of 2-nitrobenzoic acids
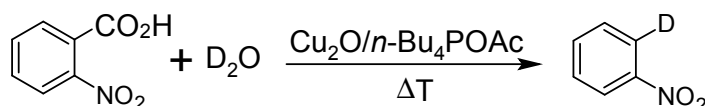
Scheme 3.32: Regioselective deuteration of 2-nitrobenzoic acid with Cu$_2$O nanoparticles in n-Bu$_4$POAc.

Besides decarboxylation reactions and consecutive protonation reactions, 2-nitrobenzoic acids can also be selectively mono-deuterated via decarboxylation/ deuteration. The deuterium source of choice is D$_2$O (deuteriumoxide). The reaction must be conducted under exclusion of water in order to prevent a competitive protodecarboxylation. In comparison to the protodecarboxylation, the yield of mono-deuterated nitrobenzene (*o*-deutero-nitrobenzene) after 24 h is slightly lower (82%) (see Table 3.15).

Table 3.15: Comparison of protodecarboxylation and deuterodecarboxylation of 2-nitrobenzoic acid.

IL	T [°C]	t [h]	yield nitrobenzene d$_1$ [%]	yield nitrobenzene [%]
n-Bu$_4$POAc	120	24	82	100

This might be due to isotope effects (proton/deuteron) slowing down the reaction or due to water impurities in the D$_2$O (HDO, H$_2$O). Since the replaced carboxylate group is located adjacent to the nitro group the deuteron labeling of the arene-product is highly regioselective.

3.7.3 Decarboxylative Cross-Coupling reaction
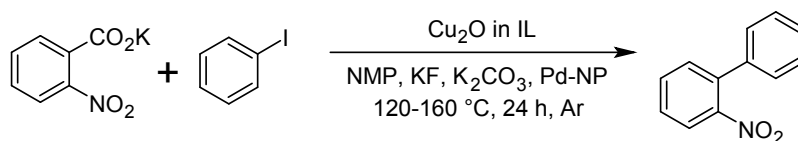
Scheme 3.33: Decarboxylative cross-coupling of potassium 2-nitrobezoate with iodobenzene in n-Bu$_4$POAc.

Since the proto- and deuterodecarboxylation reactions can be catalyzed by Cu$_2$O nanoparticles in n-Bu$_4$POAc in good to excellent yields, this prescription can be extended to decarboxylative cross-coupling reactions. The decarboxylation of the benzoic acid and the generation of the aryl cuprate is the rate determining step and therefore iodobenzene was chosen as the coupling partner, because it is known to couple easily with other organometal compounds, e.g. in *Suzuki-* or *Heck* reactions. The sole use of Cu$_2$O nanoparticles in n-Bu$_4$POAc, does not lead to a coupling of iodobenzene with the generated aryl-Cu compound. An aqueous workup leads to a mixture of 2-nitrobenzene and non-converted iodobenzene (Table 3.16, Entry 1). The addition of Pd nanoparticles does not lead to a significant improvement of yield (Entry 2, 18%). Since aprotic and polar solvents are well-known to support the homogeneously catalyzed decarboxylative cross-coupling, *N*-methyl-pyrrolidone (NMP) is added as co-solvent to the reaction mixture. By this and by changing the ionic liquid medium to C$_3$CNmpyrr NTf$_2$, the yield of 2-nitrobiphenyl is increased to 45.5% (Entry 3). Another aprotic polar solvent, DMSO, does not increase the yield in comparable extent. The maximum yield was 24.1% (Entry 4). Mesitylene, as a nonpolar co-solvent, hampers the conversion to 2-nitrobiphenyl completely (Entry 5).

Table 3.16: Decarboxylative cross-coupling reactions with variation of co-solvents.

Entry	IL	catalyst	co-catalyst	co-solvent	yield of 2-nitrobiphenyl [%]
1	n-Bu$_4$POAc	Cu$_2$O-NP	-	-	n.d.
2	n-Bu$_4$POAc	Cu$_2$O-NP	Pd-NP	-	18.0
3	C$_3$CNmpyrrNTf$_2$	Cu$_2$O-NP	Pd-NP	NMP	45.5
4	C$_3$CNmpyrrNTf$_2$	Cu$_2$O-NP	Pd-NP	DMSO	24.1
5	C$_3$CNmpyrrNTf$_2$	Cu$_2$O-NP	Pd-NP	mesitylene	n.d.

3.7.4 Investigation of the IL/Cu$_2$O-NP phase after amination reactions

The catalytic phase consisting of Cu$_2$O nanoparticles incorporated in n-Bu$_4$POAc showed very good catalytic performance for protodecarboxylation reactions even after ten consequtive reaction steps. In contrast, the IL/Cu$_2$O-NP phase did not show any catalytic activity in recycling experiments for the amination reaction of iodobenzene with aqueous ammonia solution. The assumption, that the active copper species was leached out of the reaction mixture during the extraction process was not confirmed, as ICP-OES investigation of the extracted reaction product showed. The amount of extracted copper in the

crude product was between $0.041\,\mu$mol and $0{,}00029\,\mu$mol (corresponding to 0.082% of the initially used catalyst precursor).
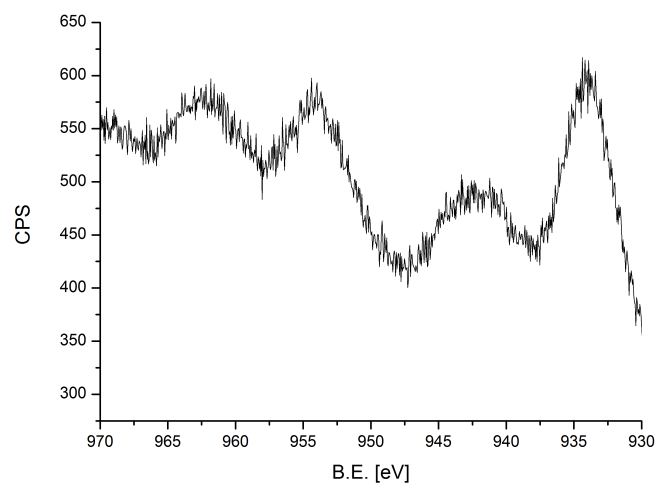
Figure 3.66: XPS of Cu_2O-NP after the amination of iodobenzene with aqueous ammonia solution. The peak at 943 eV indicates the presence of Cu(II).

Further investigation of the catalyst residue in the ionic liquid with XPS analysis showed, that large amounts of Cu(I) (at least on the particle's surface) are oxidized under basic conditions to Cu(II) (Figure 3.66, peak at $943\,$eV)[205] which is not active in amination reactions at the applied reaction conditions. Obviously the ionic liquid does not suppress the oxidation of the particles sufficiently.

4 | Summary and Outlook

In this work, nanoscale catalysts incorporated in ionic liquids or immobilized on new supports as well as their application for a broad choice of chemical reactions have been presented.

To establish a recyclable catalyst system, which is not depending on cost intensive platinum-group metals, Cu_2O nanoparticles have been synthesized in n-Bu_4POAc and in $(n$-$Bu_4P)_2SO_4$. The resulting nanoparticles showed an average diameter of 5.5 nm (± 1.2 nm) and 8.0 nm (± 2.7 nm), respectively, and were homogeneously divided within the solvent. The protodecarboxylation of a variety of 2-nitrobenzoic acids, which is usually conducted with Cu(I) or Ag(I) phosphine complexes,[206,207] could be realized with Cu_2O nanoparticles in both phosphonium ionic liquids. The best results were achieved in n-Bu_4POAc (representing a simple and comparatively cheap ionic liquid) due to the smaller particle diameter of the Cu_2O catalyst. The yields of the corresponding nitro arenes reached in some cases up to 99%. Depending on the electronic effects of functional groups or steric hindering, the yields droped down to 10%. However, the catalytic phase could be recycled and reused up to ten times. A regio-selective deuteration of 2-nitrobenzoic acid was presented in the complementary part of this work. In principle, this represents a deuterodecarboxylation, following the same reaction mechanism as the protodecarboxylation. The deuterating agent was D_2O.

Due to this encouraging results, a further reaction which is well known in homogeneous catalysis or with palladium nanoparticles, the *Buchwald-Hartwig* coupling, was established with Cu_2O nano catalysts for the fist time in an ionic liquid medium. A palladium free approach with Cu_2O nanoparticles in n-Bu_4POAc led to excellent results for the amination of aryl halides (mainly iodides), which is in no way inferior to popular homogeneously driven catalyses. Primary and secondary amines coupled smoothly with aryl halides with good to excellent yields (57-99%). Even ammonia, the most desirable amination substrate, could be coupled with iodobenzene with 92% yield. Unsurprisingly, the yields dropped for coupling reactions with aryl bromides and chlorides, respectively. Although there was no significant leaching of the catalytic copper species detectable (below 0.001% per reaction), the recycling of the catalytic phase was not possible. Due to the basic environment, the Cu^+ catalyst was oxidized to Cu^{2+} (proven by XPS), which does not show any catalytic activity in recycling experiments. It has to be pointed out, that both, the protodecarboxylation and the *Buchwald-Hartwig* reaction, were performed without the necessity of ligands, further additives or inert conditions, due to the use of the ionic liquid as reaction medium. Additionally, the ionic liquid fills the role of the solvent, the reducing medium, the nanoparticles' stabilizer and the base. In fact, this compensates the higher cost of the IL in comparison to classical solvents by far.

Since the syntheses of nanoparticles originating from acetate and carbonate precursors is very convincing, a more generalized method for the synthesis of transition metal(-oxide)

nanostructures was established in here. Copper-, silver-, nickeloxide- and zincoxide nanostructures were synthesized in n-Bu$_4$POAc originating from their carbonate precursors. The same could be realized in bmmim NTf$_2$ with acetate precursors. All nanoparticles were synthesised via microwave heating, a time and resource saving method which is especially suitable with ionic liquids as ionic reaction medium. The as-obtained copper particles had an average diameter of 4.8 nm ($\pm$1.7 nm) in n-Bu$_4$POAc and 4.9 nm ($\pm$1.1 nm) in bmmim NTf$_2$. The silver particles had an average size of 6.7 nm ($\pm$1.7 nm) in n-Bu$_4$POAc and 12.2 nm ($\pm$5.5 nm) in bmmim NTf$_2$. Oxide particles of nickel and zinc have also been synthesized. The nickel oxide particles showed a diameter of 5.8 nm ($\pm$1.7 nm) in n-Bu$_4$POAc and 2.0 nm ($\pm$0.6 nm) in bmim NTf$_2$, whereas the zinc oxide nanoparticles were 22.2 nm ($\pm$10.2 nm) in n-Bu$_4$POAc. In bmmim NTf$_2$ the zinc oxide formed nanorods with an average length of 189.3 nm ($\pm$61.5 nm) and a mean diameter of 50.9 nm ($\pm$18.2 nm). It has been possible to show, that the acetate ion is the main reductive agent, no matter if it is part of the IL or the precursor. It clearly shows the versatility of this "acetate"-route.

Furthermore, palladium nanoparticles anchored in the pores of carbonized wood were presented as effective catalysts for C-C cross coupling reactions in the course of this work. This publication was developed in collaboration with Dr. *F. Heinrich*, who has already presented the synthesis of the particle precursor and the particle incorporation into the carbonized wood in his PhD thesis. n-Butylacrylate was coupled with iodobenzene in a *Heck* reaction with 57% yield. In recycling experiments the yield dropped to 20% in the fifth run. In the *Suzuki* reaction phenylboronic acid was coupled with iodobenzene yielding 84% biphenyl. After the sixth run (33% yield) the catalyst was deactivated. The third test reaction was the *Sonogashira* reaction of phenylacetylene and iodobenzene yielding 75% of tolane (1,2-diphenylacetylene). Four consecutive runs could be performed with a yield of 10% in the last recycling step. This showed, that carbonized wood is a very promising though inexpensive immobilization substrate for nanoparticles, which can be used as recyclable catalyst. Since there is no significant leaching of the Pd species occurring (proven by ICP-MS), the deactivation of the catalyst seems to arise from salt sedimentation in the pores of the carbonized wood.

Although platinum group metals are expensive catalysts, their use in catalysis is still indispensable due to their high catalytic activity. Even today there are certain reactions which can only be convincingly performed by palladium catalysts, like the aerobic dehydrogenation which has been introduced in a reviewing publication during this work. The highlight article summarizes the development of the syntheses of functionalized arenes. Nowadays, the state of the art method is the aerobic dehydrogenation of cyclohexanone derivatives to yield substituted phenols, which is catalyzed by palladium complexes. An emerging economical factor for the use of an expensive catalyst is the possibility to reuse or recycle it. As recycling is the most challenging issue for homogeneous catalysts, nanoparticles can easily be recycled, no matter if they are incorporated in an ionic liquid (see protodecarboxylation) or immobilized on a support (see C-C cross coupling reactions). Moreover, a comprehensive overview about Pd catalyzed reactions has been given, which confirms the versatile use of palladium in catalysis and the outstanding activity of palladium nanoparticle catalysts, but also the demand to substitute noble metal catalysts with more abundant transition metals.

Finally, the ongoing and, up to now, unpublished work has been presented in the last part of this work. This includes the synthesis of Pd/Cu bimetalic nanoparticles in n-Bu$_4$POAc, the deoxygenation reactions of stearic acid with bimetallic Pd/Cu nanoparticles as catalysts as well as their comparison to well known palladium and/or copper catalysts immobilized on carbon supports. The same catalyst has been used for the decarboxylation of deacti-

vated benzoic acids. Both reactions showed promising yields in the range of 28-40%. Based on the succes of the protodecarboxylation reaction, the decarboxylative cross-coupling of 2-nitrobenzoic acid and iodobenzene catalyzed by Cu_2O nanoparticles has been presented and its dependency on aprotic polar co-solvents like NMP and DMSO. It could be shown, that pure ionic liquid medium does not support the synthesis of 2-nitrobiphenyl and that the best results could be obtained with NMP as co-solvent (45.5%). Nonpolar co-solvents, like mesitylene, did not yield any coupling products at all.

In future work, the application of the bimetallic Pd/Cu nanocatalyst should be extended. On the one hand, the yields concerning the decarboxylation of benzoic acids must be increased. Furthermore, their application for decarboxylative cross-coupling reactions seems to be at hand, since these particles bear both active catalysts. On the other hand, the choice of the ionic liquid is, as could be demonstrated in the course of this work, crucial for the reaction outcome. Phosphonium ionic liquids usually suffer from Hofman elimination reactions at higher temperatures (>200 °C), especially under basic conditions. Triphenyl-alkyl-phosphonium based ionic liquids could be an alternative, since they show a lower temperature sensitivity - fine tuning and design of the cation can also make the toxic co-solvent N-methyl-pyrrolidone dispensable and could simplify the whole reaction workup.

In sum, nanoscale catalysis is presented as an alternative for classical homogeneous and heterogeneous catalysis. As mentioned in the introduction, the focus was threefold: Examples for ionic liquids, nanoparticles and their successful application for catalyses have been experimentally presented and substantiated by thorough literature reviews.

5 | Experimental

5.1 Analytics

^{1}H-, ^{13}C-, ^{19}F- and ^{31}P-NMR spectra were recorded on a Bruker® AVANCE II 300 spectrometer at the Institute of Inorganic Chemistry (University of Cologne) at 298 K (300.1 MHz, 75 MHz, 272 MHz, 121 MHz, internal standard hexamethyldisilane HMDS for ^{1}H- and ^{13}C-NMR).

IR spectra were measured on a Bruker® alpha Platinum ATR with a diamond-ATR-module in a glove box under argon atmosphere (Institute of Inorganic Chemistry - University of Cologne).

The obtained nanoparticle powders were analyzed by powder X-ray diffractometry with a STOE®-STADI MP, Cu-K$_\alpha$ radiation, $\lambda = 1.540598$ Å (Institute of Inorganic Chemistry - University of Cologne). The diffractometer has been calibrated with a Si-standard.

Cu_2O nanoparticles were analyzed by a TEM Phillips® EM 420, 120 kV (dechema Institute, Frankfurt am Main). (HR-)TEM measurements of Pd/Cu nanoparticles have been taken by JOEL® JEM-2100 with a maximum electron acceleration voltage of 200 kV (Institute of Chemical and Biomolecular Engineering, National University of Singapore). Cu-, Ag-, NiO- and ZnO nanostructures were analyzed on a TEM Zeiss LEO 912 with a maximum electron acceleration voltage of 120 kV (Institute of Physical Chemistry - University of Cologne).

ICP-OES measurements for determining the leaching of Cu were performed on an AMETEK® Spectro Arcos equipped with an ESI® SC4-DX auto-sampler and run using the Spectro® Smart Analyser Vision software (Instiute of Geology, University of Cologne).

Gas phase mass spectrogramms were recorded with HIDEN® HPR-20QIC equipped with a Bronkhorst® EL-FLOW Select massflow controller (Institute of Inorganic Chemistry - University of Cologne). Argon was used as carrier gas in selected samples.

GC-FID analyses haven been done on a Agilent® 7890A GC-system with Agilent® HP-5 column (30 m length, 250 μm diameter). Used methods were LWJ EG with the following parameters: $T_{Start} = 40\,°C$, ramp: $10\,°C/min$, $T_{End} = 350\,°C$, hold: 10 min and EG 12-31 with parameters as follows: $T_{Start} = 40\,°C$, ramp: $20\,°C/min$, $T_{End} = 280\,°C$, hold: 3 min. Yields and conversions were calculated by using the effective carbon number method[208] and by adding n-dodecane as internal standard (Institute of Chemical and Biomolecular Engineering, National University of Singapore).

HPLC analysis was performed on an Agilent® 1200 series with an Agilent® ZDRBAX Eclipse Plus C$_{18}$ column 4.6 x 150 mm; 5 μm (Institute of Chemical and Biomolecular Engineering, National University of Singapore).

GC-MS analyses were performed on an Agilent® 7890A GC with an Agilent® 5975C MSD-deector. The used method was "MiKeD" with the following parameters: T$_{Start}$ = 40 °C, ramp: 20 °C/min, T$_{End}$ = 210 °C, hold: 1 min (Institute of Chemical and Biomolecular Engineering, National University of Singapore).

XPS measurements were performed on a Surface Science Intruments® ESCA M-Probe spectrometer with monochromatic Al-K$_\alpha$ irradiation (E = 1486.708 eV, λ = 8.34 Å) with a maximum power of 200 W, a maximum emission current of 20 mA and a resolution of 0.8 eV. The pass energy was 158.0 eV and 22.9 eV for high resolution measurements, respectively. Charge compensation has been achieved by a low energy electron flood gun of 0–10 eV in combination with a magnetic immersion lense. Data processing was conducted with CasaXPS software of Casa Software® Ltd.

Pd K edge X-ray absorption spectra (XAS) of the Pd/Cu catalysts and reference samples (Pd foil, and PdO) were recorded at the BL01B1 beam line at the SPring-8 (Japan Synchrotron Radiation Research Institute, Hyogo, Japan) in the transmission mode at ambient temperature. A Si (111) double crystal monochromator was used to obtain a monochromatic X-ray beam. The monochromator was calibrated at the shoulder peak of the absorption edge of an X-ray absorption near edge structure (XANES) spectrum of Cu foil. Pd K-edge XAS of the catalysts and reference samples (Pd foil and PdO) were also recorded in the same manner except for the use of a Si (311) double crystal monochromator. The monochromator was calibrated at the inflection point of the XANES spectrum of the metal powder/foil. In both cases, higher harmonics were removed by changing glancing angles of collimation and focusing mirrors. Data reduction was carried out with Athena and Artemis included in the Ifeffit and Demeter package. For curve-fitting analysis on extended X-ray absorption fine structure (EXAFS) spectra, each theoretical scattering path, was generated with FEFF 6.0L, and amplitude reduction factors were estimated by the curve-fitting on the reference metal samples. The k^3-weighted EXAFS oscillation in the range of 3.0-13 Å^{-1} was Fourier transformed, and curve-fitting analyses were performed in the range 1.4-2.8 Å in R space.

5.1.1   Sample Preparation for Analysis

For ICP-OES analysis two identical reaction samples were prepared. The reaction of iodobenzene with ammonia was investigated. The reaction mixtures were extracted with *n*-pentane according to the procedure for amination reactions. *n*-pentane was removed under reduced pressure, and the residue was digested in 2 ml of 65% HNO$_3$ at 90 °C for 3 h to give a clear yellow solution. The crude solution was allowed to cool to room-temperature and diluted with H$_2$O to 1:50 and 1:100 (sample 1), as well as to 1:50 and 1:500 (sample 2). Every sample was measured three times and the emissions were compared to a reference material and a blank probe. The characteristic spectral lines at 224.7 nm and 324.7 nm were used to determine the amount of leached copper-catalyst.

For TEM investigations a droplet (2-3 mg) of the corresponding as-prepared NPs embedded in IL was dispersed in 3-5 ml acetone, *iso*-propanol or CH$_2$Cl$_2$ and a slight amount of this dispersion was placed on a holey carbon-coated copper grid. The prepared grid

was immediately introduced into the pre-vacuum chamber of the TEM. Particle size distributions were determined from the digital images obtained with a CCD camera. The NPs diameter was estimated from ensembles of 400-500 particles (800-1000 counts) chosen in arbitrary areas of the enlarged micrographs. The diameters of the particles in the micrographs were measured using the software Sigma Scan Pro5 and Lince Linear Intercept 2.4.2. For HR-TEM investigations, the grids were prepared analogously in a N_2 containing glove box.

Sample preparation for HR-TEM-analysis: A small amount of the as-synthesised Pd/Cu catalyst (2-3 mg) was diluted with 1.5 ml CH_2Cl_2 in an oven dried HPLC-Vial to give a clear and transparent solution with a slightly brown colour. 2-4 droplets of this dispersion were given onto a carbon coated copper grid and stored under dust-free conditions.

For powder XRD analysis (transmission mode) of pure nanoparticle composition, the nanoparticle dispersion was dispersed in 10 ml acetone and centrifuged to yield a dark brown precipitate, which was filtered off and washed three times with acetone. The powder was dried under vacuum and prepared between two plastic disks before measurement. For powder XRD analysis (transmission mode) of the incorporated nanoparticles, the nanoparticle dispersion was directly prepared between two plastic disks before measurement.

For XPS analysis of copper(I,II)oxide nanoparticles, the as-obtained particles were washed twice with water and three times with ethyl acetate and filtered. The resulting black powder was dried under reduced pressure (10^{-3} mbar) for at least 48 h. For measurement, the powder was placed onto a silicon wafer.

5.1.2 General Reaction Conditions

All reactions (where not otherwise stated) have been conducted under inert atmosphere (N_2, Ar) with standard *Schlenk* techniques or were prepared in a glove-box (N_2, Ar). All microwave reactions were carried out in a Monowave 300 microwave (Anton Paar®) with a maximum power of 850 W at 2.45 MHz. The microwave was equipped with a ruby thermometer and an IR-reference thermometer as well as a stirring unit. Reactions can be carried out up to a maximum pressure of 30 bar and a maximum temperature of 300 °C. Reaction-mixtures were handled without precautions against water/moisture or air/oxygen in 4 ml microwave-borosilicate vials equipped with a Teflon/silicon septum and a quartz inlet for the thermometer.
All used chemicals have been used without further or additional filtration, separation or purification.
All glass-reaction tubes and stirring bars have been thoroughly cleaned with HNO_3/HCl for two hours at 85 °C to remove possible metal-contamination. Further cleaning was achieved with KOH/HCl/H_2O baths. They were stored at 80 °C in a dry-oven when not in use.
Small samples were taken from each (successful) reaction, labeled and stored in a refrigerator at -30 °C in tight closed HPLC-vials for later characterization.

5.2 Syntheses of Ionic Liquids

5.2.1 1-Butyl-3-methylimidazolium chloride (bmim Cl)
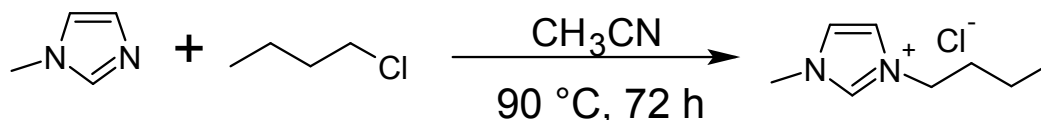
In a 250 ml three-necked round bottom flask, equipped with a stirring bar and a dropping funnel, 10 ml (9.7 g, 0.118 mol) 1-methylimidazole was dissolved in 25 ml acetonitrile. 13.5 ml (12.0 g, 0.13 mol) 1-chlorobutane was added and the reaction mixture was heated to 90 °C for 72 h under vigorous stirring. After cooling to room-temperature and removing of the solvent under vacuum, a crystalline to waxy yellowish solid was obtained. This was recrystallized from acetonitrile and further washed five times with 35 ml ethyl acetate to yield a white and crystalline but hygroskopic powder which was dried under reduced pressure (10^{-4} mbar) for 12 h and stored under argon.[209]

Yield: 17.73 g (0.102 mol) 86%

^{1}H-NMR (300 MHz, CDCl$_3$) δ [ppm]: 10.64 (s, NC$\underline{H}$N, 1H), 7.68 (d, ^{3}J$_{H-H}$ = 9.58 Hz, NC$\underline{H}$C$\underline{H}$N, 2H), 4.35 (t, ^{3}J$_{H-H}$ = 7.31 Hz, NC$\underline{H}_2$, 2H), 4.15 (s, C$\underline{H}_3$N, 3H), 1.91 (quint, ^{3}J$_{H-H}$ = 7.48 Hz, NCH$_2$C$\underline{H}_2$, 2H), 1.36 (sext, ^{3}J$_{H-H}$ = 7.50 Hz, C$\underline{H}_2$CH$_3$, 2H), 0.96 (t, ^{3}J$_{H-H}$ = 7.42 Hz, C$\underline{H}_3$CH$_2$, 3H).

^{13}C-NMR (75 MHz, Acetone-d$_6$) δ [ppm]: 136.32 (CH$_3$NCHC$\underline{H}$N), 124.05 (CH$_3$NC$\underline{H}$CHN), 122.48 (N$\underline{C}$HN), 120.13 (N$\underline{C}$H$_2$(CH$_2$)$_2$CH$_3$, 48.07 (N$\underline{C}$H$_3$), 35.08 (NCH$_2$$\underline{C}H_2CH_2CH_3$), 25.09 (N(CH$_2$)$_2$$\underline{C}H_2CH_3$), 13.87 (N(CH$_2$)$_3$$\underline{C}H_3$).

IR $\tilde{\nu}$ [cm^{-1}] = 3160-2814 (m), 1580 (s), 1475 (w), 1391 (s), 1321 (w), 1179 (m), 815 (m), 740 (m), 640 (m), 614 (m).

5.2.2 1-Butyl-3-methylimidazolium *N,N*-bis(trifluoromethyl)sulfonylimide (bmim NTf$_2$)

In a 250 ml one-necked round bottom flask, equipped with a stirring bar, 10 g (65 mmol) 1-butyl-3-methylimidazolium chloride was dissolved in 30 ml water to yield a clear solution. 18,6 g (65 mmol) lithium *N,N*-bis(trifluoromethyl)sulfonyl imide was added stepwise. The solution immediately turned into a turbid suspension. After 24 h of vigorous stirring, the reaction mixture had separated into two phases. The aqueous phase was removed and the crude ionic liquid was washed thoroughly three times with water (3 x 15 ml) and diethylether (3 x 15 ml). The viscous clear liquid was dried under reduced pressure (10^{-4} mbar) and stored under argon.[210]

Yield: 21.9 g (52 mmol) 90%

^{1}H-NMR (300 MHz, CDCl$_3$) δ [ppm]: 8.76 (s, NC$\underline{H}$N, 1H), 7.33 (d, $^3J_{H-H}$ = 9.58 Hz, NC$\underline{H}$C$\underline{H}$N, 2H), 4.18 (t, $^3J_{H-H}$ = 7.31 Hz, NC$\underline{H}_2$, 2H), 3.95 (s, C$\underline{H}_3$N, 3H), 1.86 (quint, $^3J_{H-H}$ = 7.48 Hz, NCH$_2$C$\underline{H}_2$, 2H), 1.38 (sext, $^3J_{H-H}$ = 7.50 Hz, C$\underline{H}_2$CH$_3$, 2H), 0.97 (t, $^3J_{H-H}$ = 7.42 Hz, C$\underline{H}_3$CH$_2$, 3H).

^{13}C-NMR (75 MHz, Acetone-d$_6$) δ [ppm]: 123.33 (CH$_3$NCH$\underline{C}$HN), 122.23 (CH$_3$N$\underline{C}$HCHN), 117.69 (N$\underline{C}$HN), 49.88 (N$\underline{C}$H$_2$(CH$_2$)$_2$CH$_3$), 36.32 (N$\underline{C}$H$_3$), 31.86 (NCH$_2$$\underline{C}H_2CH_2CH_3$), 19.31 (N(CH$_2$)$_2$$\underline{C}H_2CH_3$), 13.17 (N(CH$_2$)$_3$$\underline{C}H_3$).
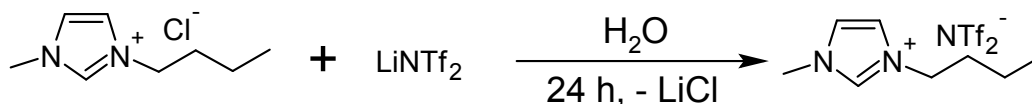
^{19}F-NMR (282 MHz, Acetone-d$_6$) δ [ppm]: -79.07.

IR $\tilde{\nu}$ [cm^{-1}] = 2960-2870 (w), 1532 (w), 1460 (w), 1370 (m), 1186 (s), 1163 (s), 1140 (s), 765 (w), 730 (m), 630 (s), 586 (s), 490 (s).

5.2.3   *n*-Butyl-methylsulfonate
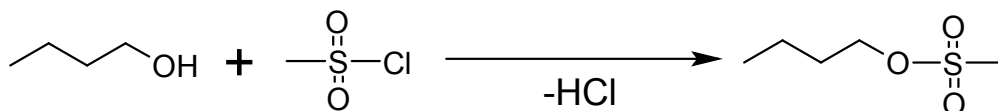
In an oven-dried 100 ml round bottom narrow neck flask, equipped with a stirring bar and a dropping funnel, 10 ml (14.8 g, 154 mmol) methane sulfonic acid was added (within 30 min) to 14.9 ml (12.1 g, 163 mmol) *n*-butanol under vigorous stirring and under argon atmosphere. After the vivid reaction diminished the reaction mixture was stirred for further 18 h at 60 °C. The product mixture was fractionally distilled (head temp.: 115 °C, 2.0 x 10^{-2} mbar) to yield *n*-butyl-methylsulfonate as a clear liquid.[211]

Yield: 13.13 g (86.5 mmol) 56%

^{1}H-NMR (300 MHz, CDCl$_3$) δ [ppm]: 4.15 (t, $^3J_{H-H}$ = 6.03 Hz, SOC$\underline{H}_2$(CH$_2$)$_2$CH$_3$, 2H), 2.93 (s, SC$\underline{H}_3$, 3H), 1.66 (quint, $^3J_{H-H}$ = 7.50 Hz, SOCH$_2$C$\underline{H}_2$CH$_2$CH$_3$, 2H), 1.37 (sext, $^3J_{H-H}$ = 7.23 Hz, SO(CH$_2$)$_2$C$\underline{H}_2$CH$_3$, 2H), 0.88 (t, $^3J_{H-H}$ = 7.49 Hz, SO(CH$_2$)$_3$C$\underline{H}_3$, 3H).

^{13}C-NMR (75 MHz, CDCl$_3$) δ [ppm]: 70.0 (s, SO$\underline{C}$H$_2$(CH$_2$)$_2$CH$_3$), 37.1 (s, S$\underline{C}$H$_3$), 30.9 (s, SOCH$_2$$\underline{C}H_2CH_2CH_3$), 18.5 (s, SO(CH$_2$)$_2$$\underline{C}H_2CH_3$), 13.3 (s, SO(CH$_2$)$_3$$\underline{C}H_3$).

5.2.4   1-Butyl-3-methylimidazolium methylsulfonate (bmim OMs)

In a 250 ml round bottom flask, equipped with a stirring bar, 10 ml (9.7 g, 118 mmol) 1-methylimidazole was dissolved in 50 ml *iso*-propanol. 19.78 g (130 mmol) *n*-butyl-

methylsulfonate was dissolved in 25 ml *iso*-propanol and slowly added to the solution. After 96 h a colourless and crystalline precipitate formed, which was filtered to yield a clear hygroscopic and crystalline solid. The crude product was dried under reduced pressure (10^{-4} mbar) and stored under argon.[211]

Yield: 14.70 g (96.6 mmol) 82%

^{1}H-NMR (300 MHz, CDCl$_3$) δ [ppm]: 7.59 (s, NC$\underline{H}$N, 1H), 7.36 (d, ^{3}J$_{H-H}$ = 9.58 Hz, NC$\underline{H}$C$\underline{H}$N, 2H), 4.13 (t, ^{3}J$_{H-H}$ = 7.31 Hz, NC$\underline{H}_2$, 2H), 3.93 (s, C$\underline{H}_3$N, 3H), 2.72 (s, SC$\underline{H}_3$, 3H), 1.78 (quint, ^{3}J$_{H-H}$ = 7.48 Hz, NCH$_2$C$\underline{H}_2$, 2H), 1.35 (sext, ^{3}J$_{H-H}$ = 7.50 Hz, C$\underline{H}_2$CH$_3$, 2H), 0.95 (t, ^{3}J$_{H-H}$ = 7.42 Hz, C$\underline{H}_3$CH$_2$, 3H).

^{13}C-NMR (75 MHz, Acetone-d$_6$) δ [ppm]: 123.06 (CH$_3$NCH$\underline{C}$HN), 121.30 (CH$_3$N$\underline{C}$HCHN), 120.99 (N$\underline{C}$HN), 48.46 (N$\underline{C}$H$_2$(CH$_2$)$_2$CH$_3$), 39.49 (S$\underline{C}$H$_3$), 35.62 (N$\underline{C}$H$_3$), 31.75 (NCH$_2$$\underline{C}H_2CH_2CH_3$), 19.59 (N(CH$_2$)$_2$$\underline{C}H_2CH_3$), 13.51 (N(CH$_2$)$_3$$\underline{C}H_3$).
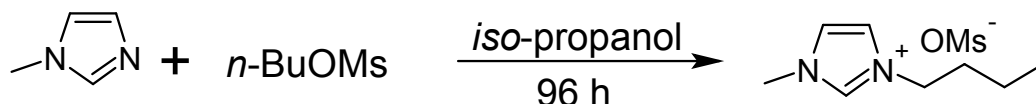
5.2.5   1-Butyl-3-methylimidazolium acetate (bmim OAc)
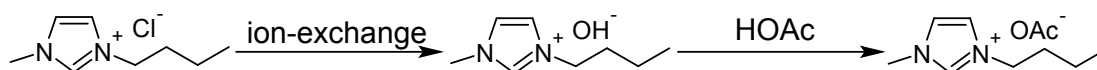
5 g (28.7 mmol) 1-butyl-3-methylimidazolium chloride was dissolved in 10-15 ml water and converted into the corresponding 1-butyl-3-methylimidazolium hydroxide aqueous solution via an ion exchange column filled with AMBERLITE ion exchange resin. The alkaline aqueous solution was checked with HNO$_3$/AgNO$_3$ for chloride residues and the ion exchange was repeated accordingly as appropriate. The solution was neutralised with acetic acid and the water content removed *in vacuo*. The final product was a colourless and highly hygroscopic solid.[212]

Yield: 5.29 g (26.7 mmol) 93%

^{1}H-NMR (300 MHz, D$_2$O) δ [ppm]: 8.70 (s, NC$\underline{H}$N, 1H), 7.43 (d, ^{3}J$_{H-H}$ = 9.58 Hz, NC$\underline{H}$C$\underline{H}$N, 2H), 4.15 (t, ^{3}J$_{H-H}$ = 7.31 Hz, NC$\underline{H}_2$, 2H), 3.85 (s, C$\underline{H}_3$N, 3H), 1.99 (s, COC$\underline{H}_3$, 3H), 1.79 (quint, ^{3}J$_{H-H}$ = 7.48 Hz, NCH$_2$C$\underline{H}_2$, 2H), 1.26 (sext, ^{3}J$_{H-H}$ = 7.50 Hz, C$\underline{H}_2$CH$_3$, 2H), 0.85 (t, ^{3}J$_{H-H}$ = 7.42 Hz, C$\underline{H}_3$CH$_2$, 3H).

^{13}C-NMR (75 MHz, Acetone-d$_6$) δ [ppm]: 177.23 ($\underline{C}$OCH$_3$), 135.91 (N$\underline{C}$HN), 123.48 (CH$_3$NCH$\underline{C}$HN), 122.33 (CH$_3$N$\underline{C}$HCHN), 49.30 (N$\underline{C}$H$_2$(CH$_2$)$_2$CH$_3$), 34.3 (N$\underline{C}$H$_3$), 31.2 (NCH$_2$$\underline{C}H_2CH_2CH_3$), 21.01 (CO$\underline{C}H_3$), 19.0 (N(CH$_2$)$_2$$\underline{C}H_2CH_3$), 12.7 (N(CH$_2$)$_3$$\underline{C}H_3$).

5.2.6   1-Butyl-2,3-dimethylimidazolium chloride (bmmim Cl)

1,2-Dimethylimidazole should be recrystallized from toluene if its purity is below 98%. In a 250 ml three-necked round bottom flask, equipped with a stirring bar and a dropping funnel, 28.8 g (0.3 mol) 1,2-dimethylimidazole was dissolved in 50 ml *iso*-propanol. 33.8 ml (30.1 g, 0.33 mol) 1-chlorobutane was added and the reaction mixture was heated to 70 °C for 96 h. After cooling to room-temperature and removal of the solvent, a resinous yellow solid was obtained. This was recrystallized twice from acetonitrile. The crude product was dissolved in *iso*-propanol and poured into 300 ml ethyl acetate. The fine powder was washed three times with ethyl acetate to yield a colourless, crystalline and hygroscopic powder which was dried under reduced pressure (10^{-4} mbar) for 12 h and stored under argon.[213]

Yield: 41.5 g (0.209 mol) 69%

^{1}H-NMR (300 MHz, D_2O) δ [ppm]: 7.60 (d, $^3J_{H-H}$ = 9.58 Hz, NCH̲CH̲N, 2H), 4.39 (t, $^3J_{H-H}$ = 7.31 Hz, NCH̲$_2$, 2H), 3.89 (s, CH̲$_3$N, 3H), 2.76 (s, NCCH̲$_3$N, 3H), 2.58 (t, $^3J_{H-H}$ = 7.48 Hz, CH$_2$CH̲$_3$, 3H), 2.24 (quint, $^3J_{H-H}$ = 7.48 Hz, NCH$_2$CH̲$_2$, 2H), 1.97 (sext, $^3J_{H-H}$ = 7.50 Hz, CH̲$_2$CH$_3$, 2H).

^{13}C-NMR (75 MHz, D_2O) δ [ppm]: 123.3 (CH$_3$NCHC̲HN), 120.3 (CH$_3$NC̲HCHN), 117.9 (NC̲HN), 47.9 (NC̲H$_2$(CH$_2$)$_2$CH$_3$), 34.3 (NC̲H$_3$), 31.2 (NCH$_2$C̲H$_2$CH$_2$CH$_3$), 19.0 (N(CH$_2$)$_2$C̲H$_2$CH$_3$), 12.7 (N(CH$_2$)$_3$C̲H$_3$), 10.4 (NCC̲H$_3$N).

IR $\tilde{\nu}$ [cm^{-1}] = 3110-2890 (s), 1730 (w), 1670 (w), 1590 (m), 1530 (m), 1480 (s), 1410 (s), 1350 (m), 1260 (s), 1240 (m), 1145 (m), 1130 (m), 1042 (m), 832 (s), 762 (m), 660 (m).

5.2.7 1-Butyl-2,3-dimethylimidazolium *N,N*-bis(trifluoromethyl)-sulfonyl imide (bmmim NTf$_2$)

In a 250 ml round bottom flask, equipped with a stirring bar, 10 g (49.3 mmol) 1-butyl-2,3-dimethylimidazolium chloride was dissolved in 20 ml water to yield a clear slightly yellow solution. 15.8 g (55 mmol) lithium *N,N*-bis(trifluoromethyl)sulfonyl imide was added stepwise. The solution immediately turned into a turbid suspension. After 24 h of vigorous stirring, the reaction mixture had separated into two phases. The aqueous phase was discarded and the crude ionic liquid was washed thoroughly three times with water (3 x 20 ml) and with 25 ml of a diethylether/*n*-pentane mixture. The high viscous, but clear liquid was dried under reduced pressure (10^{-4} mbar) and stored under argon.[210]

Yield: 16.8 g (38.8 mmol) 78%

^{1}H-NMR (300 MHz, CDCl$_3$) δ [ppm]: 7.58 (d, $^3J_{H-H}$ = 9.58 Hz, NCH̲CH̲N, 2H), 4.27 (t, $^3J_{H-H}$ = 7.31 Hz, NCH̲$_2$, 2H), 3.93 (s, CH̲$_3$N, 3H), 2.77 (s, NCCH̲$_3$N, 3H), 1.87-1.85 (quint, NCH$_2$CH̲$_2$, 2H), 1.40 (sext, CH̲$_2$CH$_3$, 2H), 0.95 (t, $^3J_{H-H}$ = 7.40 Hz, CH̲$_3$CH$_2$, 3H).

^{13}C-NMR (75 MHz, Acetone-d$_6$) δ [ppm]: 123.3 (CH$_3$NCHC̲HN), 120.3 (CH$_3$NC̲HCHN), 117.9 (NC̲HN), 47.9 (NC̲H$_2$(CH$_2$)$_2$CH$_3$), 34.3 (NC̲H$_3$), 31.2 (NCH$_2$C̲H$_2$CH$_2$CH$_3$), 19.0 (N(CH$_2$)$_2$C̲H$_2$CH$_3$), 12.7 (N(CH$_2$)$_3$C̲H$_3$), 8.7 (NCC̲H$_3$N).

^{19}F-NMR (282 MHz, Aceton-d$_6$) δ [ppm]: -79.91.

IR $\tilde{\nu}$ [cm^{-1}] = 2960-2870 (m), 1580 (s), 1460 (w), 1370 (s), 1250 (w), 1110 (m), 930 (m), 810 (m), 750 (m), 630 (m), 440 (m).

5.2.8 1-Butyl-2,3-dimethylimidazolium methylsulfonate (bmmim OMs)

1,2-Dimethylimidazole should be recrystallised from toluene if its purity is below 98%. In a 500 ml round bottom flask 5 g (52 mmol) 1,2-dimethylimidazole was dissolved in 100 ml *iso*-propanol. 8.74 g (57.5 mmol) *n*-butyl-methylsulfonate was dissolved in 50 ml *iso*-propanol and slowly added to the solution. After 96 h a crystalline precipitate formed, which was filtered to yield a colourless hygroscopic and crystalline solid. The crude product was dried under reduced pressure (10^{-4} mbar) and stored under argon.[211]

Yield: 10.7 g (40.5 mmol) 78%

^{1}H-NMR (300 MHz, D$_2$O) δ [ppm]: 7.47 (d, $^{3}J_{H-H}$ = 9.57 Hz, NCHCHN, 2H), 4.15 (t, $^{3}J_{H-H}$ = 7.32 Hz, NCH$_2$, 2H), 3.95 (s, CH$_3$N, 3H), 2.74 (s, NCCH$_3$N, 3H), 2.67 (s, SCH$_3$, 3H), 1.80 (m, NCH$_2$CH$_2$, 2H), 1.40 (m, CH$_2$CH$_3$, 2H), 0.97 (t, $^{3}J_{H-H}$ = 7.40 Hz, CH$_3$CH$_2$, 3H).

^{13}C-NMR (75 MHz, Acetone-d$_6$) δ [ppm]: 122.02 (CH$_3$NCHCHN), 120.68 (CH$_3$NCHCHN), 47.91 (NCH$_2$(CH$_2$)$_2$CH$_3$), 38.52 (SCH$_3$), 34.50 (NCH$_3$), 31.01 (NCH$_2$CH$_2$CH$_2$CH$_3$), 18.95 (N(CH$_2$)$_2$CH$_2$CH$_3$), 12.78 (N(CH$_2$)$_3$CH$_3$), 8.76 (NCCH$_3$N).

IR $\tilde{\nu}$ [cm^{-1}] = 3210-2860 (w), 1720 (w), 1670 (w), 1610 (w), 1230 (s), 1070 (s), 750 (s), 580 (s), 540 (s).

5.2.9 1-Butyl-2,3-dimethylimidazolium acetate (bmmim OAc)

5 g (24.9 mmol) 1-butyl-2,3-dimethylimidazolium chloride was dissolved in 10-15 ml water and converted into the corresponding 1-butyl-2,3-dimethylimidazolium hydroxide aqueous solution via an ion exchange column filled with AMBERLITE ion exchange resin. The alkaline aqueous solution was checked with HNO$_3$/AgNO$_3$ for chloride residues and the ion exchange was repeated accordingly as appropriate. The solution was neutralised with acetic acid and the water content removed *in vacuo*. The final product was a slightly yellow and highly hygroscopic solid.[212]

Yield: 2.33 g (10.96 mmol) 44%

^{1}H-NMR (300 MHz, D$_2$O) δ [ppm]: 7.25 (d, $^{3}J_{H-H}$ = 9.58 Hz, NCHCHN, 2H), 4.02 (t, $^{3}J_{H-H}$ = 7.68 Hz, NCH$_2$, 2H), 3.68 (s, CH$_3$N, 3H), 2.49 (s, NCCH$_3$, 3H), 1.83 (s,

COC$\underline{H}_3$, 3H), 1.70 (quint, $^3J_{H-H} = 7.48$ Hz, NCH$_2$C$\underline{H}_2$, 2H), 1.25 (sext, $^3J_{H-H} = 7.50$ Hz, C$\underline{H}_2$CH$_3$, 2H), 0.84 (t, $^3J_{H-H} = 7.42$ Hz, C$\underline{H}_3$CH$_2$, 3H).

5.2.10   1-Cyanopropyl-3-methylimidazolium chloride (C$_3$CNmim Cl)

In a 500 ml three-necked round bottom flask, equipped with a stirring bar and a dropping funnel, 12.5 ml (12.2 g, 0.15 mol) 1-methylimidazole was dissolved in 40 ml acetonitrile. 15.4 ml (16.9 g, 165 mmol) 4-chlorobutyronitrile was added and the reaction mixture heated to 90 °C for 72 h. After cooling to room-temperature and removal of the solvent, a resinous yellow solid was obtained. This was recrystallized twice from acetonitrile and washed three times with 50 ml ethyl acetate to yield a colourless and crystalline, but hygroscopic powder which was dried under reduced pressure (10^{-4} mbar) for 12 h and stored under argon.[65]
Yield: 22.18 g (0.12 mol) 81%
^{1}H-NMR (300 MHz, CDCl$_3$) δ [ppm]: 9.12 (s, NC$\underline{H}$N, 1H), 7.72 (d, $^3J_{H-H} = 9.47$ Hz, CH$_3$NC$\underline{H}$C$\underline{H}$N, 2H), 4.25 (t, $^3J_{H-H} = 7.31$ Hz, NC$\underline{H}_2$, 2H), 3.85 (s, C$\underline{H}_3$N, 3H), 2.57 (t, $^3J_{H-H} = 7.48$ Hz, C$\underline{H}_2$CN, 2H), 2.15 (quint, $^3J_{H-H} = 7.42$ Hz, NCH$_2$C$\underline{H}_2$, 2H).

5.2.11   1-Cyanopropyl-3-methylimidazolium *N,N*-bis(trifluoromethyl)-   sulfonyl imide (C$_3$CNmim NTf$_2$)

In a 100 ml round bottom flask, equipped with a stirring bar, 10 g (54 mmol) 1-cyanopropyl-3-methylimidazolium chloride was dissolved in 30 ml water to yield a clear solution. 15.78 g (55 mmol) lithium *N,N*-bis(trifluoromethyl)sulfonyl imide was added. After 18 h of vigorous stirring, the reaction mixture separated into two phases. The aqueous phase was decanted and the crude ionic liquid was washed twice with water (20 ml) and three times with 30 ml of a diethylether/*n*-pentane mixture (1:1). The slightly viscous, but clear liquid was dried under reduced pressure (10^{-4} mbar) and stored under argon.[65]
Yield: 20.83 g (48.5 mmol) 90%
^{1}H-NMR (300 MHz, Acetone-d$_6$) δ [ppm]: 9.12 (s, NC$\underline{H}$N, 1H), 7.73 (d, $^3J_{H-H} = 9.47$ Hz, CH$_3$NC$\underline{H}$C$\underline{H}$N, 2H), 4.25 (t, $^3J_{H-H} = 7.31$ Hz, NC$\underline{H}_2$, 2H), 3.85 (s, C$\underline{H}_3$N, 3H), 2.57 (t, $^3J_{H-H} = 7.48$ Hz, C$\underline{H}_2$CN, 2H), 2.15 (quint, $^3J_{H-H} = 7.42$ Hz, NCH$_2$C$\underline{H}_2$, 2H).
^{13}C-NMR (75 MHz, Acetone-d$_6$) δ [ppm]: 124.25 (CH$_3$N$\underline{C}$H), 122.35 (CH$_3$N($\underline{C}$H)$_2$), 48.12 (N$\underline{C}$H$_3$), 36.05 (N$\underline{C}$H$_2$), 25.59 (NCH$_2$$\underline{C}H_2$), 13.81 (CN$\underline{C}H_2$).
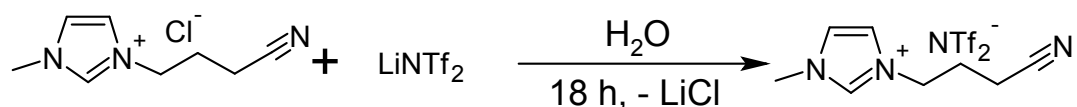
5.2.12 1-Cyanopropyl-3-methylimidazolium acetate (C$_3$CNmim OAc)
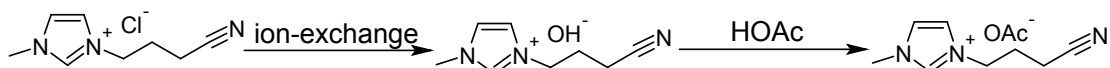
5 g (27 mmol) 1-cyanopropyl-3-methylimidazolium chloride was dissolved in 10-15 ml water and converted into the corresponding 1-cyanopropyl-3-methylimidazolium hydroxide aqueous solution via an ion exchange column filled with AMBERLITE ion exchange resin. The alkaline aqueous solution was checked with HNO$_3$/AgNO$_3$ for chloride residues and the ion exchange was repeated accordingly as appropriate. The solution was neutralised with acetic acid and the water content removed *in vacuo*. The final product was a colourless, waxy and highly hygroscopic solid. Yield: 3.67 g (17.6 mmol) 65%

^{1}H-NMR (300 MHz, Aceton-d$_6$) δ [ppm]: 8.72 (s, NC<u>H</u>N, 1H), 7.43 (d, [3]J_{H-H} = 9.47 Hz, CH$_3$NC<u>H</u>C<u>H</u>N, 2H), 4.26 (t, [3]J_{H-H} = 7.31 Hz, NC<u>H</u>$_2$, 2H), 3.81 (s, C<u>H</u>$_3$CO, 3H), 2.51 (t, [3]J_{H-H} = 7.48 Hz, C<u>H</u>$_2$CN, 2H), 2.18 (quint, [3]J_{H-H} = 7.42 Hz, NCH$_2$C<u>H</u>$_2$, 2H), 1.81 (s, NC<u>H</u>$_3$).

^{13}C-NMR (75 MHz, Acetone-d$_6$) δ [ppm]: 123.93 (CH$_3$N(<u>C</u>H)$_2$), 122.22 (CH$_3$N(<u>C</u>H)$_2$), 47.98 (N<u>C</u>H$_3$), 35.72 (N<u>C</u>H$_2$), 25.04 (NCH$_2$<u>C</u>H$_2$), 23.47 (CO<u>C</u>H$_3$), 13.70 (CN<u>C</u>H$_2$).

5.2.13 1-Cyanopropyl-2,3-dimethylimidazolium chloride (C$_3$CNmmim Cl)
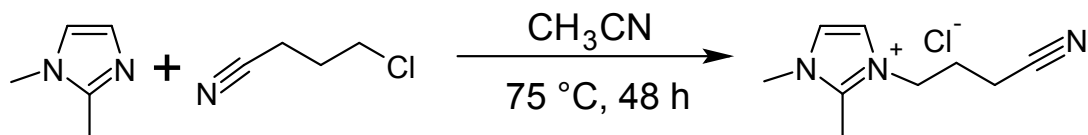
1,2-Dimethylimidazole should be recrystallized from toluene if its purity is below 98%. In a 500 ml three-necked round bottom flask, equipped with a stirring bar and a dropping funnel, 7.42 g (75 mmol) 1,2-dimethylimidazole was dissolved in 75 ml acetonitrile. 7.65 ml (8.41 g, 81.2 mmol) 4-chlorobutyronitrile was added and the reaction mixture heated to 75 °C for 48 h. After cooling to room temperature and removal of the solvent and all volatiles, a resinous and slightly yellow solid was obtained. This was recrystallized twice from acetonitrile and washed three times with 50 ml ethyl acetate to yield a colourless, crystalline and hygroscopic powder which was dried under reduced pressure (10^{-4} mbar) for 12 h and stored under argon.[65]

Yield: 10.64 g (53.2 mmol) 71%

^{1}H-NMR (300 MHz, D$_2$O) δ [ppm]: 7.39 (d, [3]J_{H-H} = 9.52 Hz, CH$_3$NC<u>H</u>C<u>H</u>N, 2H), 4.26 (t, [3]J_{H-H} = 7.31 Hz, NC<u>H</u>$_2$, 2H), 3.77 (s, C<u>H</u>$_3$N, 3H), 2.61 (s, NCC<u>H</u>$_3$N, 3H), 2.60 (t, [3]J_{H-H} = 7.48 Hz, C<u>H</u>$_2$CN, 2H), 2.21 (quint, [3]J_{H-H} = 7.42 Hz, NCH$_2$C<u>H</u>$_2$, 2H).

^{13}C-NMR (75 MHz, D$_2$O) δ [ppm]: 144.75 (<u>C</u>N), 122.61 (CH$_3$N<u>C</u>H), 120.69

(CH$_3$NCH<u>C</u>H), 102.38 (N<u>C</u>CH$_3$N), 46.62 (N<u>C</u>H$_3$), 34.84 (N<u>C</u>H$_2$), 24.80 (NCH$_2$<u>C</u>H$_2$), 13.81 (CN<u>C</u>H$_2$), 9.03 (NC<u>C</u>H$_3$N).

5.2.14   1-Cyanopropyl-2,3-dimethylimidazolium *N,N*-bis(tri-fluoromethyl)sulfonyl imide (C$_3$CNmmim NTf$_2$)
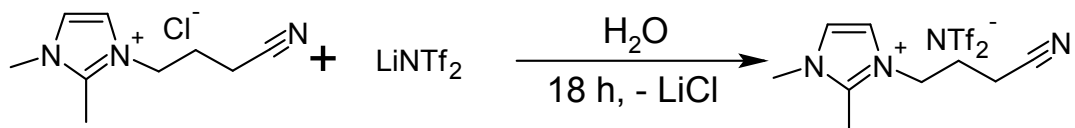
In a 250 ml round bottom flask, equipped with a stirring bar, 10 g (50 mmol) 1-cyanopropyl-2,3-dimethylimidazolium chloride was dissolved in 30 ml water to yield a clear solution. 15.78 g (55 mmol) solid lithium *N,N*-bis(trifluoromethyl)sulfonyl imide was added. After 18 h of vigorous stirring and additional 15 min the reaction mixture had separated into two phases. The aqueous phase was decanted and the crude ionic liquid was washed twice with water (2 x 30 ml) and three times with a (1:1) mixture of diethylether/*n*-pentane (3 x 15 ml). The slightly viscous, but clear liquid was dried under reduced pressure (10^{-3} mbar) and stored under argon.[65]

Yield: 20.44 g (46 mmol) 92%

^{1}H-NMR (300 MHz, CDCl$_3$) δ [ppm]: 7.26 (d, $^3J_{H-H}$ = 9.54 Hz, CH$_3$NC<u>H</u>C<u>H</u>N, 2H), 4.18 (t, $^3J_{H-H}$ = 7.31 Hz, NC<u>H</u>$_2$, 2H), 3.71 (s, C<u>H</u>$_3$N, 3H), 2.54 (s, NCC<u>H</u>$_3$N, 3H), 2.44 (t, $^3J_{H-H}$ = 7.48 Hz, C<u>H</u>$_2$CN, 2H), 2.11 (quint, $^3J_{H-H}$ = 7.42 Hz, NCH$_2$C<u>H</u>$_2$, 2H).

^{19}F-NMR (282 MHz, CDCl$_3$) δ [ppm]: -79.4.

IR $\tilde{\nu}$ [cm^{-1}] = 1320 (w), 1220 (s), 1210 (m), 1080 (s), 740 (w), 680 (m), 660 (m), 510 (m).

5.2.15   1-Butyl-pyridinium chloride (bpy Cl)
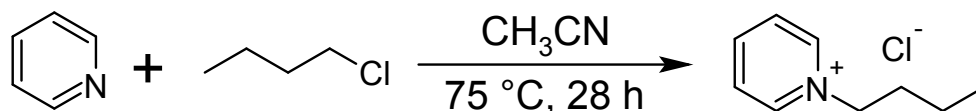
In a 250 ml three-necked round bottom flask, equipped with a stirring bar and a dropping funnel, 10 ml (9.63 g, 125 mmol) pyridine was mixed with 50 ml acetonitrile. 15.6 ml (13.9 g, 150 mmol) 1-chlorobutane was added and the reaction mixture heated to 75 °C for 28 h. After cooling to room-temperature the crude product starts to crystallise in long needles. After removing of the solvent the crude product was recrystallised from acetonitrile to yield hygroscopic and clear needles which have been dried under reduced pressure (10^{-3} mbar) for 2 h and stored under argon.[214]

Yield: 27.6 g (0.1 mol) 81%

^{1}H-NMR (300 MHz, D$_2$O) δ [ppm]: 8.82 (d, $^3J_{H-H}$ = 7.31 Hz, NC<u>H</u>$_{arom}$, 2H), 8.53 (t,

$^3J_{H-H}$ = 7.48 Hz, (CH)$_2$C$\underline{H}$(CH)$_2$, 1H), 8.06 (t, $^3J_{H-H}$ = 7.28 Hz, CHC$\underline{H}$CHC$\underline{H}$CH, 2H), 4.60 (t, $^3J_{H-H}$ = 6.54 Hz, NC$\underline{H}_2$, 2H), 1.99 (quint, $^3J_{H-H}$ = 6.14 Hz, NCH$_2$C$\underline{H}_2$, 2H), 1.34 (sext, $^3J_{H-H}$ = 6.14 Hz, C$\underline{H}_2$CH$_3$, 2H), 0.92 (t, C$\underline{H}_3$CH$_2$, $^3J_{H-H}$ = 6.54 Hz, 3H).
^{13}C-NMR (75 MHz, D$_2$O) δ [ppm]: 145.4 (N(C$\underline{H}_2$)$_2$), 144.19 (N(CH$_2$)$_2$C$\underline{H}_2$), 128.22 (N(CH$_2$)$_2$(C$\underline{H}_2$)$_2$), 61.76 (NC$\underline{H}_2$), 32.57 (NCH$_2$C$\underline{H}_2$), 18.71 (N(CH$_2$)$_2$C$\underline{H}_2$), 12.52 (C$\underline{H}_3$).

5.2.16   1-Butyl-pyridinium *N,N*-bis(trifluoromethyl)sulfonyl imide (bpy NTf$_2$)
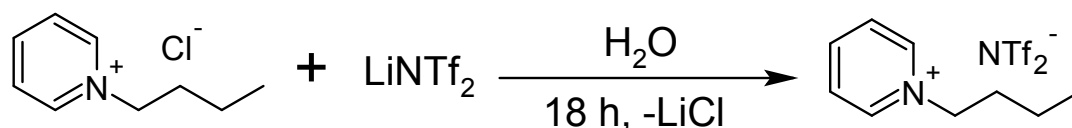
In a 100 ml one-necked round bottom flask, equipped with a stirring bar, 10 g (58.5 mmol) 1-butyl-pyridinium chloride was dissolved in 25 ml water to yield a clear solution. 17.93 g (62.5 mmol) lithium *N,N*-bis(trifluoromethyl)sulfonyl imide was added stepwise. The solution immediately turned into a turbid suspension. After 18 h of vigorous stirring, the reaction mixture had separated into two phases. The aqueous phase was removed and the crude ionic liquid was washed thoroughly three times with water (3 x 30 ml) and three times with diethylether (3 x 15 ml). The highly viscous and clear liquid was dried under reduced pressure (10^{-4} mbar) for 24 h and stored under argon.[214]
Yield: 22.89 g (55 mmol) 94%
^{1}H-NMR (300 MHz, Acetone d$_6$) δ [ppm]: 9.17 (d, $^3J_{H-H}$ = 7.31 Hz, NC$\underline{H}_{arom}$, 2H), 8.73 (t, $^3J_{H-H}$ = 7.48 Hz, (CH)$_2$C$\underline{H}$(CH)$_2$, 1H), 8.24 (t, $^3J_{H-H}$ = 7.28 Hz, CHC$\underline{H}$CHC$\underline{H}$CH, 2H), 4.84 (t, $^3J_{H-H}$ = 6.54 Hz, NC$\underline{H}_2$, 2H), 2.12 (quint, $^3J_{H-H}$ = 6.14 Hz, NCH$_2$C$\underline{H}_2$, 2H), 1.46 (sext, $^3J_{H-H}$ = 6.14 Hz, C$\underline{H}_2$CH$_3$, 2H), 0.98 (t, C$\underline{H}_3$CH$_2$, $^3J_{H-H}$ = 6.54 Hz, 3H).
^{13}C-NMR (75 MHz, Acetone d$_6$) δ [ppm]: 205.56 (s, C$\underline{F}_3$), 145.80 (s, N(C$\underline{H}_2$)$_2$), 144.48 (s, N(CH$_2$)$_2$C$\underline{H}_2$), 128.54 (s, N(CH$_2$)$_2$(C$\underline{H}_2$)$_2$), 61.88 (s, NC$\underline{H}_2$), 33.20 (s, NCH$_2$C$\underline{H}_2$), 19.12 (s, N(CH$_2$)$_2$C$\underline{H}_2$), 12.74 (s, C$\underline{H}_3$).
^{19}F-NMR (282 MHz, Aceton d$_6$) δ [ppm]: -79.89.

5.2.17   1-Cyanopropylpyridinium chloride (C$_3$CNpy Cl)
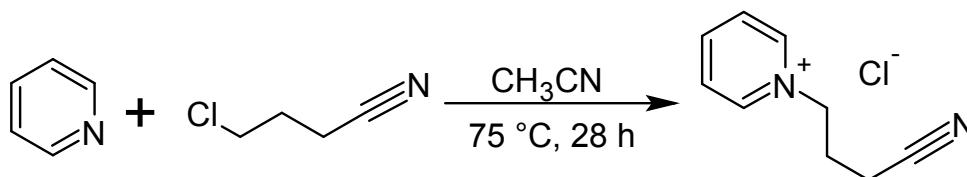
In a 250 ml three-necked round bottom flask, equipped with stirring bar and a dropping funnel, 20.1 ml (20.01 g, 0.25 mol) pyridine was dissolved in 75 ml acetonitrile. 31.05 g

(0.3 mol) 4-chlorobutyronitrile was added and the reaction mixture heated to 75 °C for 28 h. After cooling to room temperature the crude product started to crystallise in brownish needles. After removing of the solvent the crude product was recrystallised from acetonitrile to yield a hygroscopic solid which was further dried under reduced pressure (10^{-3} mbar) for 18 h and stored under argon.[214]

Yield: 31.92 g (178 mmol) 70%

^{1}H-NMR (300 MHz, D$_2$O) δ [ppm]: 8.82 (d, ^{3}J$_{H-H}$ = 7.31 Hz, NC$\underline{H}_{arom}$, 2H), 8.50 (t, ^{3}J$_{H-H}$ = 7.48 Hz, (CH)$_2$C$\underline{H}$(CH)$_2$, 1H), 8.02 (t, ^{3}J$_{H-H}$ = 7.28 Hz, CHC$\underline{H}$CHC$\underline{H}$CH, 2H), 4.86 (t, ^{3}J$_{H-H}$ = 6.54 Hz, NC$\underline{H}_2$, 2H), 2.58 (t, ^{3}J$_{H-H}$ = 6.14 Hz, C$\underline{H}_2$CN, 2H), 2.35 (quint, ^{3}J$_{H-H}$ = 5.66 Hz, C$\underline{H}_2$CH$_2$CN, 2H).

^{13}C-NMR (75 MHz, D$_2$O) δ [ppm]: 146.72 (N($\underline{C}$H$_2$)$_2$), 144.48 (N(CH$_2$)$_2$$\underline{C}H_2$), 128.54 (N(CH$_2$)$_2$($\underline{C}H_2$)$_2$), 57.89 (N$\underline{C}H_2$), 26.23 (NCH$_2$$\underline{C}H_2$), 13.81 ($\underline{C}H_2$CN).

5.2.18   1-Cyanopropylpyridinium acetate (C$_3$CNpy OAc)
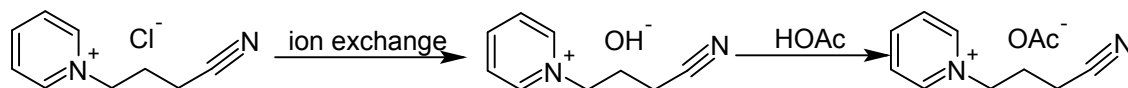
5 g (27.3 mmol) 1-cyanopropylpyridinium chloride was dissolved in 10-15 ml water and converted into the corresponding 1-cyanopropylpyridinium hydroxide aqueous solution via an ion exchange column filled with AMBERLITE ion exchange resin. The alkaline aqueous solution was checked with HNO$_3$/AgNO$_3$ for chloride residues and the ion exchange was repeated accordingly as appropriate. The solution was neutralised with acetic acid and the water content removed *in vacuo*. The final product was a colourless, waxy and highly hygroscopic solid.[214]

Yield: 2.31 g (11.2 mmol) 41%

^{1}H-NMR (300 MHz, D$_2$O) δ [ppm]: 8.89 (d, ^{3}J$_{H-H}$ = 7.31 Hz, NC$\underline{H}_{arom}$, 2H), 8.56 (t, ^{3}J$_{H-H}$ = 7.48 Hz, (CH)$_2$C$\underline{H}$(CH)$_2$, 1H), 8.08 (t, ^{3}J$_{H-H}$ = 7.28 Hz, CHC$\underline{H}$CHC$\underline{H}$CH, 2H), 4.73 (t, ^{3}J$_{H-H}$ = 6.54 Hz, NC$\underline{H}_2$, 2H), 2.63 (t, ^{3}J$_{H-H}$ = 6.14 Hz, C$\underline{H}_2$CN, 2H), 2.40 (quint, ^{3}J$_{H-H}$ = 5.66 Hz, C$\underline{H}_2$CH$_2$CN, 2H), 1.95 (s, COC$\underline{H}_3$, 3H).

^{13}C-NMR (75 MHz, D$_2$O) δ [ppm]: 146.33 (N($\underline{C}$H$_2$)$_2$), 144.51 (N(CH$_2$)$_2$$\underline{C}H_2$), 128.66 (N(CH$_2$)$_2$($\underline{C}H_2$)$_2$), 119.90 (CO$\underline{C}H_3$), 60.27 (N$\underline{C}H_2$), 26.07 (NCH$_2$$\underline{C}H_2$), 13.85 ($\underline{C}H_2$CN).

5.2.19   *N*-Cyanopropyl-*N*-methyl-pyrrolidinium chloride (C$_3$CNmpyrr Cl)
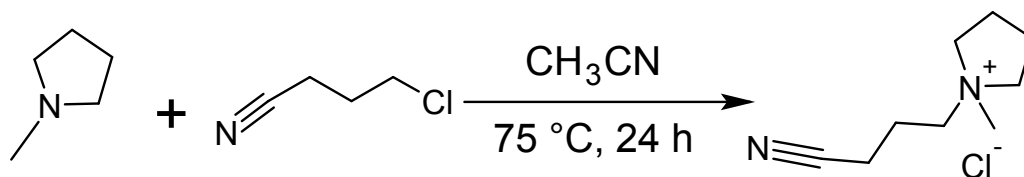
In a 250 ml round bottom flask, equipped with a stirring bar, 13.0 ml (10.65 g, 125 mmol) N-methyl-pyrrolidine was dissolved in 40 ml acetonitrile. 14.19 ml (15.54 g, 0.15 mol) 4-chlorobutyronitrile was added and the reaction mixture heated to 75 °C for 24 h under continuous stirring. After cooling to room temperature the crude product started to crystallise to give a yellowish-white solid. After removal of the surplus solvent the crude product was recrystallised twice from acetonitrile and washed three times with 25 ml diethylether to yield a hygroscopic and white solid, which was dried under reduced pressure (10^{-3} mbar) for 2 h and stored under argon.[62]

Yield: 17.21 g (66.3 mmol) 73%

^{1}H-NMR (300 MHz, rt, D$_2$O) δ [ppm]: 3.61-3.29 (m, NC$\underline{H}_2$C$\underline{H}_2$, 4H), 3.02 (s, NC$\underline{H}_3$, 3H), 2.43 (t, NC$\underline{H}_2$, 2H), 2.26-1.97 (m, NCH$_2$C$\underline{H}_2$C$\underline{H}_2$CN, 4H).

5.2.20 *N*-Cyanopropyl-*N*-methyl-pyrrolidinium *N,N*-bis(trifluoromethyl)sulfonyl imide (C$_3$CNmpyrr NTf$_2$)
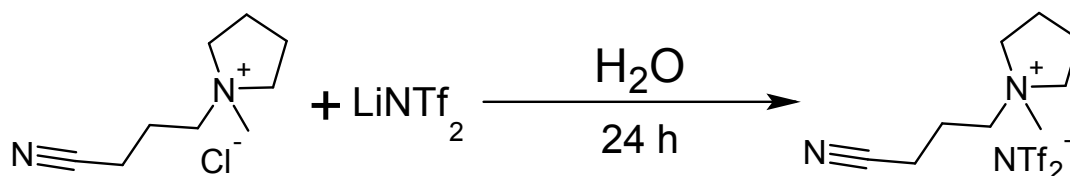
In a 250 ml round bottom flask, equipped with a stirring bar, 10 g (53 mmol) N-cyanopropyl-N-methyl-pyrrolidinium chloride was dissolved in 50 ml water. 17.93 g (73 mmol) solid lithium N,N-bis(trifluoromethyl)sulfonyl imide was added into the clear solution stepwise. The solution immediately turned into a turbid suspension. After 24 h of vigorous stirring, the reaction mixture had separated into two phases. The aqueous phase was removed and the crude ionic liquid was washed intensively three times with water and another three times with a diethylether/*n*-pentane mixture (1:1). The high viscous, but clear liquid was further dried under reduced pressure (10^{-4} mbar) and stored under argon.[62]

Yield: 19.4 g (50.0 mmol) 89%

^{1}H-NMR (300 MHz, CDCl$_3$) δ [ppm]: 3.61-3.29 (m, NC$\underline{H}_2$C$\underline{H}_2$, 4H), 3.02 (s, NC$\underline{H}_3$, 3H), 2.43 (t, NC$\underline{H}_2$, 2H), 2.26-1.97 (m, NCH$_2$C$\underline{H}_2$C$\underline{H}_2$CN, 4H).

^{19}F-NMR (282 MHz, CDCl$_3$) δ [ppm]: -79.3.

5.2.21 *N*-Butyl-*N*-methyl-pyrrolidinium acetate (bmpyrr OAc)
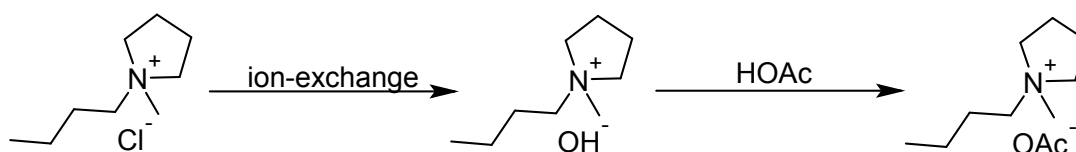
5 g (24.8 mmol) *N*-butyl-*N*-methyl-pyrrolidinium chloride was dissolved in 12 ml distilled water and converted into the corresponding *N*-butyl-*N*-methyl-pyrrolidinium hydrox-

ide aqueous solution via an ion exchange column filled with AMBERLITE ion exchange resin. The alkaline aqueous solution was checked with $HNO_3/AgNO_3$ for chloride residues and the ion exchange was repeated accordingly as appropriate. The solution was neutralised with acetic acid and the water content removed *in vacuo*. The final product was a colourless and highly hygroscopic solid. Yield: 2.69 g (13.39 mmol) 53%

¹H-NMR (300 MHz, D_2O) δ [ppm]: 3.37 (m, $NCH_2(C\underline{H}_2)_2CH_2$, 4H), 3.20 (m, $NC\underline{H}_2$, 2H), 2.91 (s, $COC\underline{H}_3$, 3H), 2.08 (m, $N(C\underline{H}_2)_2$, 4H), 1.79 (s, $NC\underline{H}_3$, 3H), 1.66 (quint, $^3J_{H-H}$ = 6.14 Hz, $NCH_2C\underline{H}_2$, 2H), 1.26 (sext, $^3J_{H-H}$ = 6.02 Hz, $N(CH_2)_2C\underline{H}_2$, 2H), 0.83 (t, $^3J_{H-H}$ = 7.32 Hz, $CH_2C\underline{H}_3$, 3H).

¹³C-NMR (75 MHz, D_2O) δ [ppm]: 64.17 ($N(\underline{C}H_2)_2$), 48.05 ($O\underline{C}H_3$), 25.10 ($N\underline{C}H_2$), 23.35 ($N\underline{C}H_3$), 21.27 ($NCH_2\underline{C}H_2$), 19.25 ($\underline{C}H_2CH_3$), 12.75 ($\underline{C}H_3CH_2$).

5.2.22 Tetra-*n*-butyl-phosphonium acetate (*n*-Bu₄POAc)
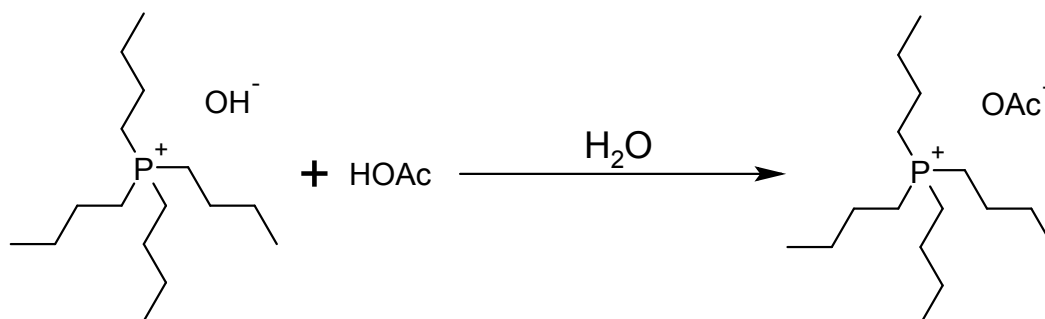
In a 100 ml round bottom flask, 50 ml 40 wt% tetra-*n*-butyl-phosphonium hydroxide solution (72.4 mmol *n*-Bu₄POH) is mixed with 4.12 ml (72.4 mmol) of 99% acetic acid under vigorous stirring. After further stirring for 25 min the residual water is removed under reduced pressure (10^{-3} mbar) at 60 °C. The resulting ionic liquid is further dried under reduced pressure (10^{-3} mbar) for 72 h leaving a hygroscopic waxy solid behind.
Yield 20.8 g (68.8 mmol, 95%)

¹H-NMR (300 MHz, D_2O) δ [ppm]: 2.25–2.09 (m, $PC\underline{H}_2$, 8H), 1.93 (s, $COC\underline{H}_3$, 3H), 1.61–1.32 (m, $PCH_2C\underline{H}_2C\underline{H}_2$, 16H), 0.94–0.82 (t, $CH_2C\underline{H}_3$, 12H).

¹³C-NMR (75 MHz, D_2O) δ [ppm]: 173.8 ($\underline{C}OCH_3$), 26.5 ($\underline{C}H_3CO$), 24.8 ($P(CH_2)_2\underline{C}H_2CH_3$), 24.1 ($PCH_2\underline{C}H_2$), 19.1 ($P\underline{C}H_2$), 13.8 ($P(CH_2)_3\underline{C}H_3$).

³¹P-NMR (121 MHz, D_2O) δ [ppm]: 33.25.

IR $\tilde{\nu}$ [cm⁻¹] = 2960-2860 (w), 1580 (m), 1380(m), 1345 (m), 1160 (s), 1126 (s), 1050 (s), 610 (m), 570 (m).

ESI-MS high resolution, positive ion mode $C_{16}H_{36}P^+$ calculated mass = 259.2549142 amu, measured mass = 259.25460 amu (deviation -1.23 ppm).

5.2.23 Tetra-*n*-butyl-phosphonium sulphate ((n-Bu$_4$P)$_2$SO$_4$)
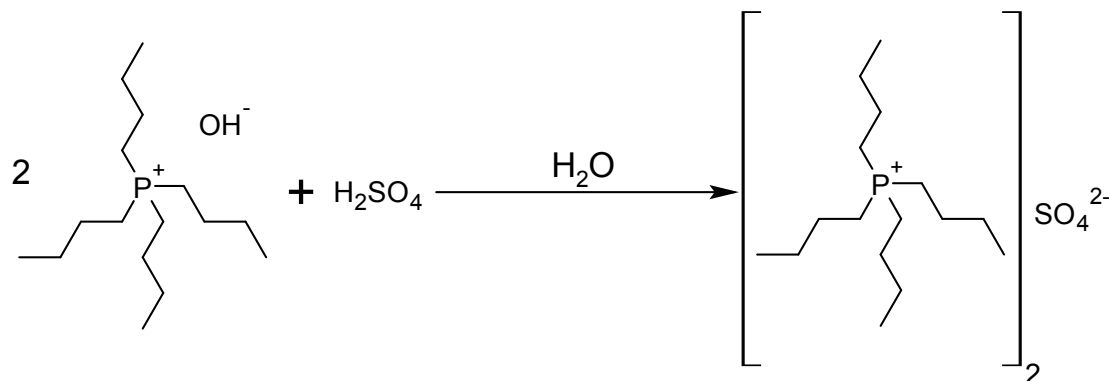
In a 100 ml round bottom flask, 50 ml 40 wt% tetra-*n*-butyl-phosphonium hydroxide solution (72.4 mmol, n-Bu$_4$POH) is mixed with 4.12 ml (72.4 mmol) of 10% sulphuric acid solution under vigorous stirring. After stirring for 25 min the residual water is removed under reduced pressure (10^{-3} mbar) at 60 °C. The resulting ionic liquid is further dried under reduced pressure for 72 h. The final product was a white solid.

Yield: 27.8 g (71.7 mmol, 99%)

^{1}H-NMR (300 MHz, D$_2$O) δ [ppm]: 2.25–2.09 (m, PC$\underline{\text{H}}_2$, 8H), 1.61–1.32 (m, PCH$_2$C$\underline{\text{H}}_2$C$\underline{\text{H}}_2$, 16H), 0.90 (t, CH$_2$C$\underline{\text{H}}_3$, 12H).

^{13}C-NMR (75 MHz, D$_2$O) δ [ppm]: 24.8 (P(CH$_2$)$_2$$\underline{\text{C}}H_2CH_3$), 24.1 (PCH$_2$$\underline{\text{C}}H_2$), 19.1 (P$\underline{\text{C}}H_2$), 13.8 (P(CH$_2$)$_3$$\underline{\text{C}}H_3$).

^{31}P-NMR (121 MHz, D$_2$O) δ [ppm]: 33.25.

IR $\tilde{\nu}$ [cm^{-1}] = 2960-2860 (w), 1580 (m), 1380(m), 1345 (m), 1160 (s), 1126 (s), 1050 (s), 610 (m), 570 (m).

ESI-MS high resolution, positive ion mode C$_{16}$H$_{36}$P$^+$ calculated mass = 259.2549142 amu, measured mass = 259.25460 amu (deviation -1.13 ppm).

5.2.24 Tri-*n*-butyl-3-cyanopropyl-phosphonium chloride (C$_3$CNn-Bu$_3$PCl)

In an oven dried 130 ml schlenktube, equipped with a Teflon stirring bar, 5 ml (4.1 g, 20.2 mmol) tri-*n*-butyl phosphine was mixed with 25 ml toluene (anhydrous) in a glove box. Later 3.1 g (30 mmol) 4-chlorobutyronitrile was added under vigorous stirring and the schlenktube heated to 65 °C for 48 h. After cooling to room temperature a two phase system established immediately. The organic phase (toluene/4-chlorobutyronitrile) was discarded and the crude ionic liquid washed twice with *n*-pentane and dried under reduced pressure (10^{-3} mbar) at 50 °C for 48 h.

Yield: 3.65 g (11.9 mmol) 59%

^{1}H-NMR (300 MHz, D$_2$O) δ [ppm]: 3.10 (t, PC$\underline{\text{H}}_2$, 2H), 2.89 (t, C$\underline{\text{H}}_2$CN, 2H), 2.67 (m,

C<u>H</u>$_2$CH$_2$CN, 2H), 1.61 (quint, PCH$_2$C<u>H</u>$_2$, 6H), 1.18 (sext, C<u>H</u>$_2$CH$_3$, 6H), 1.13 (t, C<u>H</u>$_3$, 9H), 0.98 (t, PC<u>H</u>$_2$, 6H).

^{13}**C-NMR** (75 MHz, D$_2$O) δ [ppm]: 118.84 (<u>C</u>N), 23.93 (P<u>C</u>H$_2$CH$_2$CH$_2$CH$_3$, 3C) , 23.7 (PCH$_2$<u>C</u>H$_2$CH$_2$CH$_3$, 3C), 18.88 (P<u>C</u>H$_2$CH$_2$CH$_2$CN), 18.87 (PCH$_2$CH$_2$<u>C</u>H$_2$CH$_3$, 3C), 18.73 (PCH$_2$<u>C</u>H$_2$CH$_2$CN), 18.28 (PCH$_2$CH$_2$<u>C</u>H$_2$CN), 13.4 (<u>C</u>H$_3$).

^{31}**P-NMR** (121 MHz, D$_2$O) δ [ppm]: 33.3.

IR $\tilde{\nu}$ [cm^{-1}] = 2970-2860 (s), 1580 (s), 1410(m), 1360 (m), 1225 (m), 1125 (s), 1005 (s), 810 (m), 721 (w), 644 (w).

5.2.25 Tri-*n*-butyl-3-cyanopropyl-phosphonium acetate (C$_3$CN*n*-Bu$_3$POAc)

2 g (6.52 mmol) tri-*n*-butyl-3-cyanopropyl-phosphonium chloride was dissolved in 10-15 ml water and converted into the corresponding Cyanopropyl-tri-*n*-butyl-phosphonium hydroxide aqueous solution via an ion exchange column filled with AMBERLITE ion exchange resin. The alkaline aqueous solution was checked with HNO$_3$/AgNO$_3$ for chloride residues and the ion exchange was repeated accordingly as appropriate. The solution was neutralised with acetic acid and the water content removed *in vacuo*. Yield: 1.52 g (4.95 mmol) 76 %

^{1}**H-NMR** (300 MHz, D$_2$O) δ [ppm]: 2.89-2.73 (m, PC<u>H</u>$_2$, COC<u>H</u>$_3$, 5H), 2.33 (m, C<u>H</u>$_2$CH$_2$CN, 6H), 2.06 (sext, PCH$_2$C<u>H</u>$_2$, 6H), 1.52 (m, C<u>H</u>$_2$CH$_3$, 6H), 0.97 (t, C<u>H</u>$_3$, 9H).

^{31}**P-NMR** (121 MHz, D$_2$O) δ [ppm]: 33.3.

IR $\tilde{\nu}$ [cm^{-1}] = 2960-2860 (m), 1580 (s), 1370(s), 1345 (m), 1160 (w), 760 (m), 722 (m).

ESI-MS high resolution, positive ion mode C$_{16}$H$_{33}$NP$^+$ calculated mass = 270.2345131 amu, measured mass = 270.23425 (deviation -0.97 ppm).

5.3 Nanoparticle Syntheses

5.3.1 Cu$_2$O Nanoparticles

Cu$_2$O nanoparticles were synthesized in an oven-dried 25 ml crimp top or screw top vial equipped with a butyl-rubber septum and a glass stirring bar. 1 mmol copper precursor

was suspended in 1 g IL and heated to 120-160 °C for 3-18 h while stirring at 500 rpm in a vial holder (see Table 5.1). The resulting precipitate was a brownish red dispersion of Cu_2O nanoparticles in IL. The as-obtained particles in IL could be easily dispersed in acetone, ethanol or *iso*-propanol.

Table 5.1: Various ionic liquids as reaction media for the synthesis of Cu_2O nanoparticles.

Entry	precursor	IL	T [°C]	type	d [nm]
1	$CuCO_3$	bmmim NTf_2	120	bulk	bulk
2	$CuCO_3$	bmim NTf_2	120	n.d.	n.d.
3	$CuCO_3$	bpy NTf_2	120	n.d.	n.d.
4	$CuCO_3$	C_3CNmim NTf_2	120	n.d.	n.d.
5	$CuCO_3$	n-Bu_4POAc	120	Cu_2O	5.5 ($\pm$1.2)
6	$CuCO_3$	$(n$-$Bu_4P)_2SO_4$	120	n.d.	n.d.
7	$CuCO_3$	$(n$-$Bu_4P)_2SO_4$	160	Cu_2O	8.0 ($\pm$2.7)
8	$Cu(NO_3)_2$	n-Bu_4POAc	160	n.d.	n.d.
9	$Cu(OAc)_2$	n-Bu_4POAc	160	n.d.	bulk
10	CuI	n-Bu_4POAc	160	n.d.	n.d.
11	CuF_2	n-Bu_4POAc	160	n.d.	n.d.
12	$CuCO_3$	C_3CNmmim NTf_2	120	n.d.	n.d.*
13	$CuCO_3$	bpy NTf_2	120	n.d.	n.d.*

* These results have not been published.

5.3.2 Microwave Syntheses of Cu, Ag, NiO and ZnO Nanoparticles

$$CuCO_3$$
$$Ag_2CO_3$$
$$NiCO_3 \xrightarrow[h\nu]{n\text{-}Bu_4POAc}$$
$$ZnCO_3$$

$$Cu\text{-}NP$$
$$Ag\text{-}NP$$
$$NiO\text{-}NP$$
$$ZnO\text{-}NP$$

An oven-dried 4 ml microwave borosilicate vial equipped with a stirring bar, a Teflon/silicon septum and a quartz inlet for a ruby-thermometer was filled with 500 mg of n-Bu_4POAc. 10 wt% (50 mg) of precursor (basic $CuCO_3$ 0.23 mmol, Ag_2CO_3 0.18 mmol, $NiCO_3 \cdot 6H_2O$ 0.22 mmol or $ZnCO_3$ 0.40 mmol) was filled into the vial and stirred for 2.5 min on a conventional stirring plate to yield a homogeneous mixture. The vial was further equipped with a ruby-thermometer. The maximum irradiation power of the microwave was limited to 75 W when the reaction was about to start.

$$\text{Cu(OAc)}_2$$
$$\text{AgOAc}$$
$$\text{Ni(OAc)}_2 \quad \xrightarrow[\text{h}\nu]{\text{bm(m)im NTf}_2}$$
$$\text{Zn(OAc)}_2$$

Cu-NP
Ag-NP
NiO-NP
ZnO-NP

An oven-dried 4 ml microwave-borosilicate vial equipped with a Teflon stirring bar, a Teflon/silicon septum and a quartz inlet for a ruby-thermometer was filled with 500 mg of bmmim NTf_2. 10 wt% (50 mg) of precursor (Cu(OAc)$_2$·H_2O 0.25 mmol, AgOAc 0.30 mmol or Zn(OAc)$_2$·$2H_2O$ 0.23 mmol) was filled into the vial and stirred for 2.5 min on a conventional stirring plate to yield a homogeneous mixture (see Table 5.2). Ni(OAc)$_2$·H_2O (0.20 mmol) was mixed with bmim NTf_2 due to a better solubility. The vial was equipped with a ruby-thermometer. The maximum irradiation power of the microwave was limited to 75 W when the reaction was about to start.

Table 5.2: Reaction parameters for the nanoparticle syntheses in ionic liquids by microwave irradiation[a].

Entry	type	IL	precursor	T [°C]	t [min]	d [nm]
1	Cu(0)	n-Bu$_4$POAc	CuCO$_3$	160	10	4.8 ($\pm$1.7)
2	Cu(0)	bmmim NTf$_2$	Cu(OAc)$_2$	235	3	4.9 ($\pm$1.1)
3	Ag(0)	n-Bu$_4$POAc	Ag$_2$CO$_3$	100	1.5	6.7 ($\pm$1.7)
4	Ag(0)	bmmim NTf$_2$	AgOAc	200	5	12.2 ($\pm$5.4)
5	Ni(II)O	n-Bu$_4$POAc	NiCO$_3$	200	10	5.8 ($\pm$1.7)
6	Ni(II)O	bmim NTf$_2$	Ni(OAc)$_2$	250	30	2.0 ($\pm$0.6)
7	Zn(II)O	n-Bu$_4$POAc	ZnCO$_3$	220	10	22.2 ($\pm$10.2)
8	Zn(II)O	bmmim NTf$_2$	Zn(OAc)$_2$	225	15	50.9 ($\pm$18.2)[b]
						189.3 ($\pm$61.5)[c]

[a] Reaction parameters: 500 mg IL, 50 mg precursor, 1000 rpm stirring, 75 W max. power. [b] ZnO nanorods diameter. [c] ZnO nanorods length.

5.3.3 Syntheses of Supported Pd, Cu and Pd/Cu Catalysts

$$\text{Pd(OAc)}_2 \atop \text{MX}_n \quad \xrightarrow[\substack{\text{impregnation} \\ 80\,°C}]{\text{"carbon"}} \quad \text{Pd}^{2+}\text{M}^{n+}\text{/C} \quad \xrightarrow[250\text{-}300\,°C]{\text{H}_2} \quad \text{Pd}^0\text{M}^0\text{/C}$$

M = Cu, Ni
n = 1,2
X = Cl, OAc; X$_2$ = SO$_4$

The precursor salt (Pd(OAc)$_2$ (7.0 mg, 0.035 mmol), Cu(OAc)$_2$·H_2O (7.0 mg, 0.035 mmol), CuSO$_4$·$5H_2O$ (8.7 mg, 0.035 mmol), CuCl (3.5 mg, 0.035 mmol) or Ni(OAc)$_2$·$4H_2O$ (8.7 mg, 0.035 mmol)) was dissolved in 1 ml of a 1:1 mixture of acetone and

water or in petrol ether. For complete dissolution the mixture was placed in an ultrasonic bath at 45 °C for 30 min. Then the carbon support (activated Carbon 78 mg, MWCNT 50 mg or Pd/C 10wt% 52 mg) was added and the mixture was placed again in the ultrasonic bath for 30 min. Then the fitting of the vial was removed and the solvent was removed at 80 °C in an oven. Where appropriate, the as-dried compound was placed in a 50 cm quartz tube equipped with glass wool and under constant hydrogen flow (30 ml/min) reduced at 250-300 °C for 1 h.

5.3.4 Pd/Cu Bimetallic Nanoparticles in n-Bu$_4$POAc

$$Pd(OAc)_2 \ + \ Cu(OAc)_2 \ \xrightarrow[\text{200 °C, 24 h, N}_2]{\text{n-Bu}_4\text{POAc}} \ Pd/Cu\text{-NP}$$

In an oven-dried quartz tube equipped with Teflon fastening and a glass stirring bar 0.07 mmol Pd(OAc)$_2$ (14.6 mg) and 0.035 mmol Cu(OAc)$_2$·H$_2$O (7.0 mg) were mixed with 950 mg n-Bu$_4$POAc. The tube was sealed under nitrogen and heated to 200 °C within 30 min for 24 h to yield a dark brown mixture.

5.3.5 Syntheses of Pd/Cu Bimetallic Nanoparticles in bmmim NTf$_2$

$$Pd(OAc)_2 \ + \ Cu(OAc)_2 \ \xrightarrow[\text{200 °C, 24 h, N}_2]{\text{bmmim NTf}_2} \ Pd/Cu\text{-NP}$$
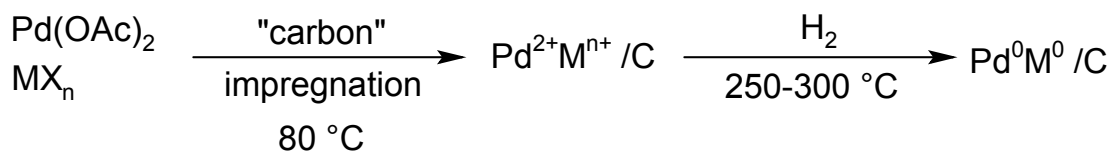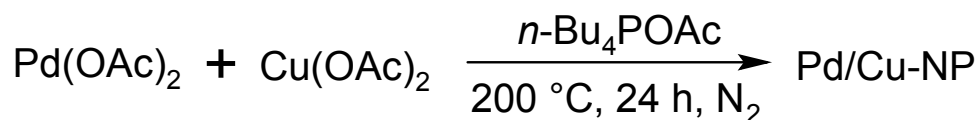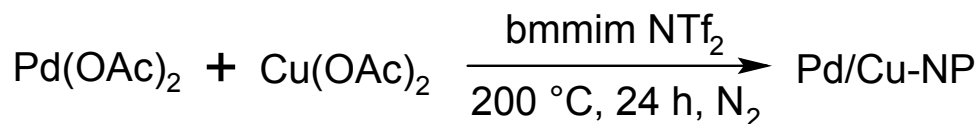
In an oven-dried quartz tube equipped with Teflon fastening and a glass stirring bar 0.07 mmol Pd(OAc)$_2$ (14.6 mg) and 0.035 mmol Cu(OAc)$_2$·H$_2$O (7.0 mg) were mixed with 1 g bmmim NTf$_2$. The tube was sealed under nitrogen and heated to 200 °C within 30 min for 24 h to yield a dark brown mixture.

5.4 Nanocatalyses

5.4.1 *Heck* Reactions with Pd-NP Immobilized on Wood
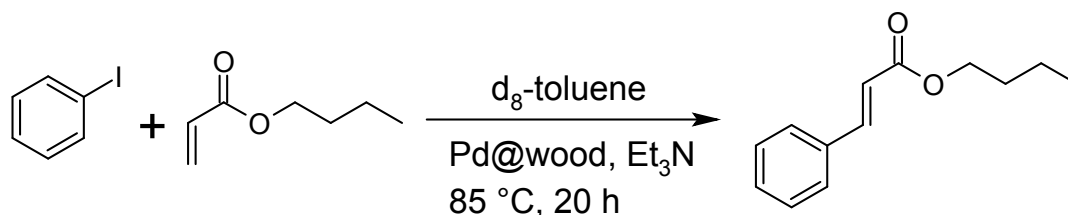
An oven dried 20 ml reaction vial was loaded with iodobenzene (55 μl, 0.5 mmol), *n*-butyl acrylate (72 μl, 0.5 mmol), triethyl amine (80 μl, 0.6 mmol), PVP-Pd@wood (98 mg, 0.14 wt.-% Pd) and toluene-d$_8$ (1 ml). The mixture was stirred at 85 °C for 20 h. Then the conversion was determined directly by ^{1}H-NMR spectroscopy by using hexamethyldisilane as internal standard (20 μl) (see Table 5.3). For recycling of the catalyst, the wood was rinsed twice with water (5 ml) and ethanol (5 ml) and immediately used for the next reaction.

Table 5.3: Recycling experiments in *Heck* reactions catalyzed by Pd-NP on carbonized wood.

	run 1	run 2	run 3	run 4	run 5
yield [%]	57	44	32	27	20
TON	1407	1087	795	664	494

5.4.2 *Sonogashira* Reactions with Pd-NP Immobilized on Wood
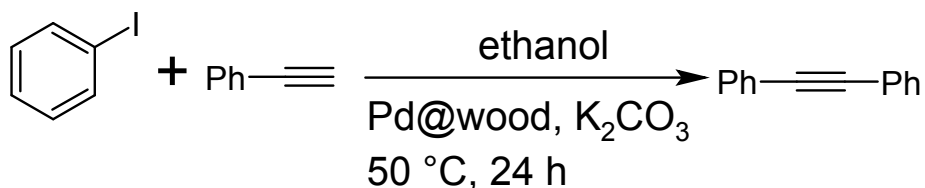
110 μl phenylacetylene (1.0 mmol), 120 μl iodobenzene (1.1 mmol) and 207 mg potassium carbonate (1.5 mmol) were added to ethanol (2 ml) and mixed with the PVP-Pd@wood (72 mg, 0.14 wt.-% Pd) in a 20 ml reaction vial in air. The mixture was stirred at 50 °C for 24 h. The product was extracted three times with *n*-pentane (3 x 10 ml). The organic phase was washed with water (2 ml), separated from the aqueous phase and dried over MgSO$_4$. Finally, the solvent was removed under reduced pressure. The product was analysed, and the conversion was determined by ^{1}H-NMR spectroscopy by using hexamethyldisilane as internal standard (20 μl) (see Table 5.4). For recycling of the catalyst, the wood was rinsed twice with water (5 ml) and ethanol (5 ml) and immediately used for the next reaction.

Table 5.4: Recycling experiments in *Sonogashira* reactions catalyzed by Pd-NP on carbonized wood.

	run 1	run 2	run 3	run 4
yield [%]	75	34	9	10
TON	3704	1671	440	500

5.4.3 *Suzuki* Reactions with Pd-NP Immobilized on Wood
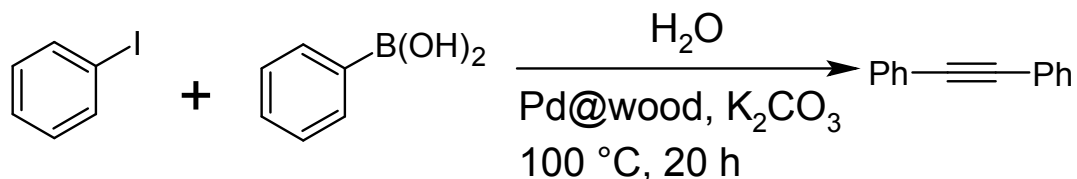
Phenylboronic acid (91 mg, 0.75 mmol), iodobenzene (55 μl, 0.5 mmol), and potassium carbonate (140 mg, 1.0 mmol) were added to water (3 ml) and mixed with PVP-Pd@wood (72 mg; 0.14 wt.-% Pd) in a 20 ml reaction vial in air. The mixture was stirred at 100 °C for 20 h. At room temperature a crystalline solid precipitated in the aqueous solution. The product was extracted with *n*-pentane (3 x 10 ml) from the aqueous phase, the organic layer was dried over MgSO$_4$, and the solvent was removed under reduced pressure. The white solid was analyzed, and the conversion was determined by ^{1}H-NMR spectroscopy by using hexamethyldisilane as internal standard (20 μl) (see Table 5.5). For recycling of the catalyst, the wood was rinsed twice with water (5 ml) and ethanol (5 ml) and immediately used for the next reaction.

Table 5.5: Recycling experiments in *Suzuki* reactions catalyzed by Pd-NP on carbonized wood.

	run 1	run 2	run 3	run 4	run 5	run 6
yield [%]	84	97	57	58	20	33
TON	2074	2395	1416	1436	501	824

5.4.4 Decarboxylation of Nitrobenzoic Acids with Cu$_2$O Nanoparticles
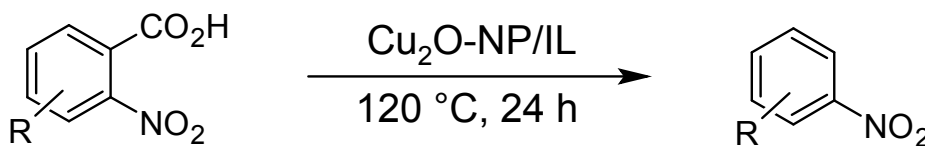
The Cu$_2$O nanoparticle dispersion obtained from the reductive decomposition in *n*-Bu$_4$POAc (chapter 5.3.1) was cooled to room temperature (see Nanoparticle synthesis). 1 mmol of the corresponding nitro-benzoic acid was then added to the dispersion and heated to 120 °C for 24 h. After cooling to room temperature the reaction mixture was extracted with 3 x 10 ml *n*-pentane. The organic phase was separated and the solvent removed under reduced pressure. The residue was analyzed by ^{1}H-NMR (internal standard: hexamethyl-disilane, 0.1 mmol, 20 μl, see Table 5.7).

For recycling experiments 167 mg (1 mmol) 2-nitrobenzoic acid was used as decarboxy-lation substrate. After extraction of nitro benzene (product) the reaction mixture was

Table 5.6: Variation of the reaction conditions and ionic liquid media in the protodecarboxylation of 2-nitrobenzoic acid.

Entry	Cu source	IL	Additives	T [°C]	yield[a] [%]
1	Cu_2O-NPs[a]	n-Bu_4POAc	-	80	1
2	Cu_2O-NPs[a]	n-Bu_4POAc	-	120	61
3	Cu_2O-NPs[a]	n-Bu_4POAc	KF, K_2CO_3	120	59
4	Cu_2O-NPs[a]	n-Bu_4POAc	KF	120	58
5	Cu_2O-NPs[a]	n-Bu_4POAc	K_2CO_3	120	55
6	Cu_2O-NPs[b]	n-Bu_4POAc	-	120	100
7	Cu_2O-NPs[c]	$(n$-$Bu_4P)_2SO_4$	-	160	51
8	$CuCO_3$[d]	bmim OMs	-	120	39
9	$Cu(OAc)_2$[d]	bmim OMs	-	120	24
10	$Cu(NO_3)_2$[d]	bmim OMs	-	160	39
11	$CuCO_3$[d]	C_3CNmim OAc	-	120	23
12	$CuCO_3$[d]	C_3CNpyOAc	-	120	17 *
13	$CuCO_3$[d]	bmmim OMs	-	120	15 *
14	Cu_2O[e]	n-Bu_4POAc	-	120	20

Reaction conditions: [a] 1 mmol 2-nitrobenzoic acid, Cu_2ONPs ($35mol\%_{Surface}$) in 1 g IL. [b] With Cu_2O-NPs ($105\ mol\%_{Surface}$) [c] Cu_2O-NPs ($17.5\ mol\%_{Surface}$) in 1 g IL. [d] 1 mmol 2-nitrobenzoic acid, 1 mmol Cu-source in 1 g IL. [e] Commercial copper(I)oxide. Reaction time 24 h. *unpublished results

Table 5.7: Substrate screening for protodecarboxylation reactions of different 2-nitrobenzoic acids in n-Bu_4POAc with Cu_2O nanoparticles.

Entry	benzoic acid	yield[a] [%]
1	2-nitrobenzoic acid	100
2	2,4-dinitrobenzoic acid	24
3	4-trifluoromethyl-2-nitrobenzoic acid	32
4	4-carboxyl-2-nitrobenzoic acid	10
5	3-methyl-2-nitrobenzoic acid	30
6	4-chloro-2-nitrobenzoic acid	65
7	4-fluoro-2-nitrobenzoic adid	40
8	5-amino-2-nitrobenzoic acid	10
9	5-chloro-2-nitrobenzoic acid	21
10	5-methoxy-2-nitrobenzoic acid	15
11	5-methyl-2-nitrobenzoic acid	26

[a] yield of the corresponding arene.

reloaded with 1 mmol 2-nitrobenzoic acid and the reaction conducted again as described above (see Table 5.8)

In chemo-selectivity experiments (see Table 5.9) 1 mmol of a second benzoic acid was

Table 5.8: Recycling experiments of the protodecarboxylation of 2-nitrobenzoic acid

Entry	Cu$_2$O-NPs^a n-Bu$_4$POAc	Cu$_2$O-NPs^b n-Bu$_4$POAc	yield [%] Cu$_2$O-NPs^c n-Bu$_4$POAc	CuCO$_3$ bmim OMs	Ag$_2$CO$_3$ bmim OMs
1	61	55	100	5	38
2	96	100	100	17	12
3	79	100	100	23	9
4	39	100	60	39	8
5	36	84	100	-	
6	36	45	100	-	
7	25	32	100	-	
8	10	21	100	-	
9	-	6	100	-	
10	-	-	15	-	

^{a} 1 mmol CuCO$_3$ precursor ^{b} 2 mmol CuCO$_3$ precursor ^{c} 3 mmol CuCO$_3$ precursor.

added to the reaction mixture.

Table 5.9: Chemo-selectivity of the nanoscale protodecarboxylation in the presence of a selection of different benzoic acid derivatives.

Entry	Acid A	Acid B	yield [%] A:B	sel. [%] A:B
1	2-nitrobenz.	4-nitrobenz.	57:0	100:0
2	2-nitrobenz.	2-chloro-4-nitrobenz.	39:0	100:0
3	2-nitrobenz.	2-methoxybenz.	50:0	100:0
4	2-nitrobenz.	4-cyanobenz.	48:0	100:0
5	2-nitrobenz.	2-chloro-4-fluorobenz.	23:0	100:0
6	2-nitrobenz.	4-methoxybenz.	47:0	100:0
7	2-nitrobenz.	2-sulfonylbenz.	78:0	100:0
8	2-nitrobenz.	4-aminobenz.	62:0	100:0

5.4.5   Amination Reactions of Aryl Halides with Cu$_2$O Nanoparticles
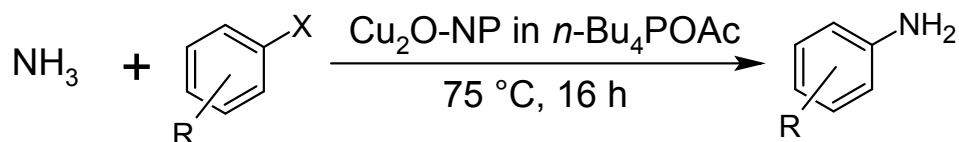
The as-prepared Cu$_2$O nanoparticle dispersion (chapter 5.3.1) was allowed to cool to room temperature in a 25 ml crimp-top vial. Then 1 mmol aryl halide and 1 ml of an aqueous ammonia solution (NH$_3$ (20 wt%) 12 mmol) were added under vigorous stirring.

Table 5.10: Variation of primary amines and ammonia for the *Buchwald-Hartwig* amination of iodobenzene.

Entry	amine	cat.load [mol%]	yield [%]
1	NH_3	10	100
2	CH_3-NH_2	10	65
3	CH_3-NH_2	5	65
4	*n*-Bu-NH_2	5	71
5	*iso*-Bu-NH_2	5	95
6	*c*Hex-NH_2	5	77
7	*n*-Oct-NH_2	5	90
8	*iso*-Pr-NH_2	5	99
9	*tert*-Bu-NH_2	5	57
10	$C_6H_5NH_2$	5	65

The vial was closed with a new crimp cap and heated to $75\,°C$ for $16\,h$. The reaction mixture was cooled to room temperature and extracted with *n*-pentane (3 x 5 ml). The organic phases were combined, dried over $MgSO_4$ and the solvent was evaporated under reduced pressure. The residue was analysed using ^{1}H-NMR techniques (internal standard: hexamethyldisilane, $0.1\,mmol$, $20\,\mu l$, see Table 5.10).
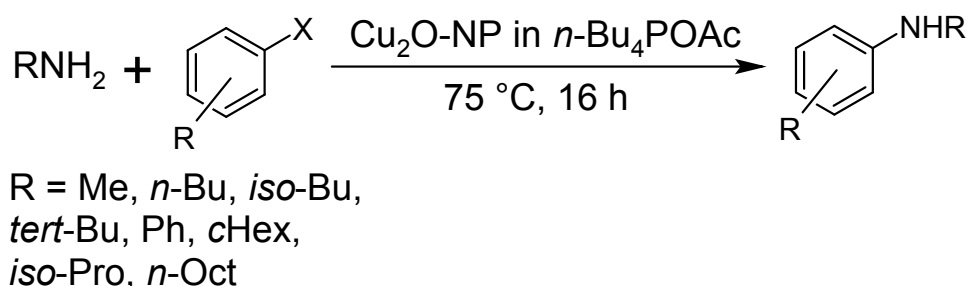
The as-prepared Cu_2O nanoparticle dispersion (chapter 5.3.1) was allowed to cool down to room temperature in the 25 ml crimp-top vial. Then 1 mmol aryl halide and 1 ml of a primary amine (CH_3-NH_2(40 wt%) 12.9 mmol, *n*-Bu-NH_2 10.1 mmol, *iso*-Bu-NH_2 10.6 mmol, *c*Hex-NH_2 8.7 mmol, *n*-Oct-NH_2 6.0 mmol, *iso*-Pr-NH_2 11.6 mmol, *tert*-Bu-NH_2 9.5 mmol or C_6H_5-NH_2) were added under vigorous stirring. The vial was closed with a new crimp cap and heated to $75\,°C$ for $16\,h$. The reaction mixture was cooled to room temperature and extracted with *n*-pentane (3 x 5 ml). The organic phases were combined and washed with 2 ml water. The aqueous phase was discarded and the organic phase was dried over $MgSO_4$ and the solvent was evaporated under reduced pressure. The residue was analysed using ^{1}H-NMR techniques (internal standard: hexamethyldisilane, $0.1\,mmol$, $20\,\mu l$, see Table 5.10).

Table 5.11: Variation of secondary amines for the *Buchwald-Hartwig* amination of iodobenzene.

Entry	amine	cat.load [mol%]	yield [%]
1	Et_2NH	5	65
2	n-Bu_2NH	5	16
3	piperidine	5	99
4	Ph_2NH	5	0
5	morpholine	5	99
6	L-proline	5	33
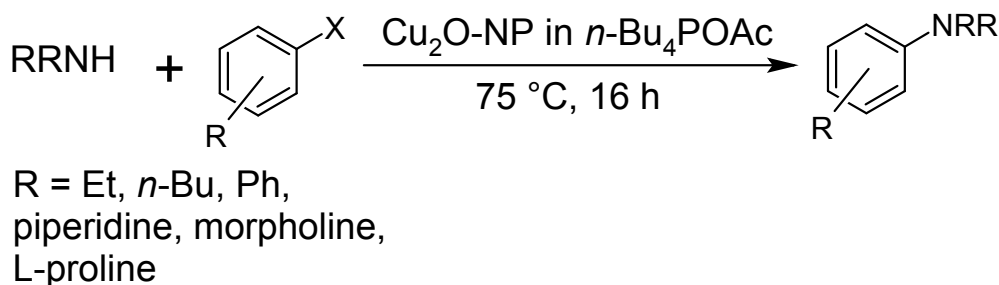
RRNH + (aryl halide, X) → (product, NRR)

Cu_2O-NP in n-Bu_4POAc

75 °C, 16 h

R = Et, *n*-Bu, Ph,
piperidine, morpholine,
L-proline

The as-prepared Cu_2O nanoparticle dispersion (chapter 5.3.1) was allowed to cool down to room temperature in the 25 ml screw-top vial. Then 1 mmol aryl halide and 1 ml of a secondary amine (Et_2NH 9.6 mmol, n-Bu_2NH 5.9 mmol, piperidine 10.1 mmol, Ph_2NH 6.9 mmol, morpholine 11.5 mmol or L-Prolin 11.7 mmol) were added with vigorous stirring. The vial was closed and heated to 75 °C for 16 h. The reaction mixture was cooled to an ambient temperature and extracted with *n*-pentane (3 x 5 ml). The organic phases were combined, dried over $MgSO_4$ and the solvent was removed under reduced pressure. The residue was analysed using ^{1}H-NMR (internal standard: hexamethyldisilane, 0.1 mmol, 20 μl, see Table 5.11 and Table 5.12).

Table 5.12: Variation of aryl halides for the coupling with ammonia, diethylamine and piperidine at optimized reaction parameters.

Entry	aryl-X	amine	cat.load [mol%]	yield [%]
1	C_6H_5Br	NH_3	10	12
2	3-iodoanisole	NH_3	5	92
3	4-iodotoluene	NH_3	10	79
4	1,2-dichlorobenzene	Et_2NH	5	0
5	C_6H_5Br	Et_2NH	5	10
6	2-iodophenol	Et_2NH	5	0
7	2-iodoanisole	Et_2NH	5	0
8	3-iodoanisole	Et_2NH	5	24
9	2-iodotoluene	Et_2NH	5	0
10	4-iodotoluene	Et_2NH	5	33
11	3-iodoanisole	piperidine	5	93
12	4-iodotoluene	piperidine	5	85

5.4.6 Deoxygenation of Stearic Acid with Pd/Cu Bimetallic Catalysts
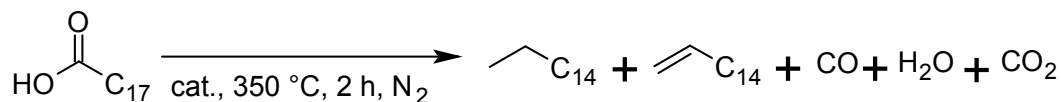
All deoxygenation reactions were carried out under nitrogen atmosphere. In addition, each reaction was carried out under air (without nitrogen atmosphere) as a control experiment. 0.7 mmol stearic acid (200 mg) was mixed with the catalyst in an oven-dried quartz tube with Teflon fastening and a glass stirring bar in a glove-box. The reaction mixture was heated in a tube oven with a 25 min ramp up to 350 °C for 2 h. The crude light brown product was allowed to cool to room temperature and dissolved in 4 ml CH_2Cl_2 and refluxed for 20 min. After cooling to room temperature the internal standard *n*-dodecane was added (50 μl, 39.04 mg, 0.23 mmol) and the whole mixture filled up to 10 ml with a mixture of CH_2Cl_2 and MeOH (3:1). Finally the mixture was centrifuged for 3 min at 5000 min^{-1}. About 1 ml was taken as sample for GC-FID analysis to determine the yield (see Table 5.13) or HPLC analysis to determine the conversion of stearic acid and filtered through a 200 μm syringe filter directly before injection.

Table 5.13: Overview about selected examples for the deoxygenation of stearic acid within 2 h, concerning the overall yield of C_{17}-alkanes and alkenes and the selectivity between them.

Entry	catalyst	loading [mol%]	temp. [°C]	gas	yield [%]	ratio [alkane:alkene]
1	$Cu(OAc)_2$	10	350	N_2	2.4	N/A
2	$Pd(OAc)_2$	10	350	N_2	4.8	N/A
3	CuCl	10	350	N_2	4.4	N/A
4	Pd^{2+} Cu^{2+}	5, 5	350	N_2	5.2	95.6 : 4.4
5	$Co(OAc)_2$	10	300	N_2	0.1	N/A
6	Pd Cu (Cu^{2+})/C	5, 5	350	N_2	8.6	16.1 : 83.9
7	Pd Ni (Ni^{2+})/C	5, 5	350	N_2	30.9	5.5 : 94.5
8	Pd^{2+} Cu^{2+}_{MWCNT}	5, 5	350	N_2	22.5	6.8 : 93.2
9	Pd Cu^{2+}/C	5, 5	350	N_2	9.3	7.5 : 92.5
10	Pd/C	10	350	N_2	30.3	4.0 : 96.0
11	Pd/C Cu^{2+}	10, 5	350	N_2	37.0	11.6 : 88.4
12	Pd/C Cu	10, 5	350	N_2	23.9	5.9 : 94.1
13	Pd/C Cu^+	10, 5	350	N_2	6.5	13.3 : 86.7
14	Pd/C Cu^{2+}_{SO4}	10, 5	350	N_2	7.2	25.5 : 74.5
15	Pd/Cu-NP IL	10, 5	350	air	28.0	9.6 : 90.4
16	Pd/Cu-NP IL	10, 5	350	N_2	17.5	9.8 : 90.2

5.4.7 Decarboxylation Reactions of Benzoic Acid Derivatives with Pd/Cu Bimetallic Particles
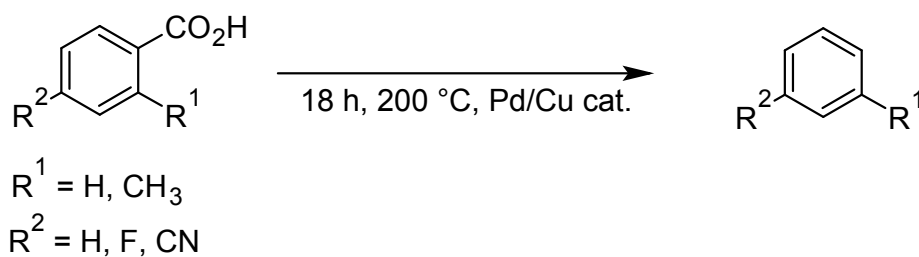
The as synthesized Pd/Cu catalyst in n-Bu$_4$POAc or bmmim NTf$_2$ (chapter 5.2.4) was mixed with 1 mmol of benzoic acid (122 mg), 4-fluoro-2-methyl benzoic acid (154 mg) or 4-cyanobenzoic acid (147 mg), respectively. In control experiments the glass tube was evacuated and purged with nitrogen gas and closed in the glove box. The mixture was heated to 200 °C for 18 h. After cooling to room temperature, the mixture was dissolved in 3 ml CH_2Cl_2 and further 7 ml of a mixture of CH_2Cl_2 and MeOH (3:1). 50 μl n-dodecane (39.04 mg, 0.23 mmol) was added as internal standard. Finally the mixture was centrifuged for 3 min at 5000 min^{-1} and filtered through a 200 μm syringe filter prior to analysis with GC-FID and GC-MS (see Table 5.14).

Table 5.14: Overview about the decarboxylation reactions of benzoic acids with Pd/Cu catalyst (10 mol%) in two different ionic liquids. The reaction temperature was 200 °C.

Entry	substrate	IL	gas	time [h]	yield [%]
1	Benzoic acid	n-Bu$_4$POAc	N$_2$	18	40.2
2	Benzoic acid	n-Bu$_4$POAc	air	18	9.0
3	4-fluoro-2-methyl benzoic acid	n-Bu$_4$POAc	N$_2$	18	40.4
4	4-fluoro-2-methyl benzoic acid	n-Bu$_4$POAc	air	18	44.1
5	4-cyano benzoic acid	n-Bu$_4$POAc	N$_2$	18	6.3
6	4-cyano benzoic acid	n-Bu$_4$POAc	air	18	6.3
7	Benzoic acid	bmmim NTf$_2$	N$_2$	18	-
8	4-fluoro-2-methyl benzoic acid	bmmim NTf$_2$	N$_2$	18	-
9	4-cyano benzoic acid	bmmim NTf$_2$	N$_2$	18	-

5.4.8 Regioselective Deutero-decarboxylation of 2-Nitrobenzoic Acid
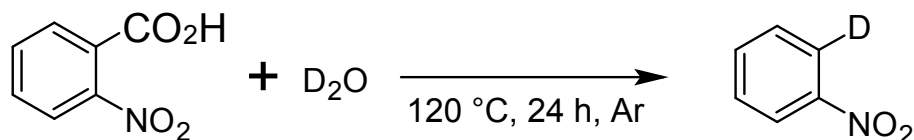
Cu$_2$O nanoparticles dispersed in anhydrous n-Bu$_4$POAc (chapter 5.3.1) were further dried under reduced pressure (10^{-3} mbar) at 50 °C, flushed with argon and introduced into a glove box. 1 mmol (167 mg) of 2-nitrobenzoic acid was added to the dispersion. 1 ml D$_2$O was added with a syringe and the mixture was heated to 120 °C for 24 h. After cooling to room temperature the reaction mixture was extracted with 3 x 10 ml n-pentane. The organic phase was separated, dried over MgSO$_4$ and the solvent removed under reduced pressure. The residue was analysed by ^{1}H-NMR (internal standard: hexamethyldisilane, 0.1 mmol, 20 μl).

5.4.9 Decarboxylative Cross-Coupling Reaction
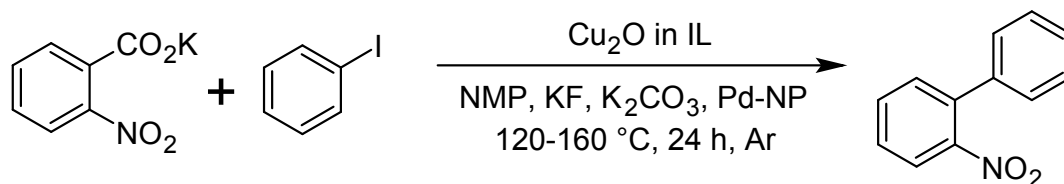
Cu$_2$O nanoparticles dispersed in IL were further dried under reduced pressure (10^{-3} mbar) at 50 °C, flushed with argon and introduced into a glove box. 205 mg (1 mmol) potassium 2-nitrobenzoate and 500 mg powdered molecular sieve (3Å) was mixed with the nanopar-

ticle dispersion and 1 ml *N*-methyl-pyrrolidone (NMP). The reaction mixture was heated to 160 °C for 3 h. After cooling to room temperature, 4.5 mg (0.02 mmol) Pd(OAc)$_2$, 87 mg (1 mmol) potassium fluoride, 3 ml NMP and 165 μl (1.5 mmol) iodobenzene were added. Then the reaction mixture was heated to 120 °C for 21 h. After cooling to room temperature the mixture was diluted with 1N hydrochloric acid and extracted five times with 15 ml ethyl acetate. The combined organic phases were washed with brine and dried with MgSO$_4$. Finally the organic solvent was evaporated under reduced pressure. The residue was analysed by ^{1}H-NMR (internal standard: hexamethyldisilane, 0.1 mmol, 20 μl).

Table 5.15: Decarboxylative cross-coupling reactions with variation of co-solvents.

Entry	IL	catalyst	co-catalyst	co-solvent	yield of 2-nitrobiphenyl [%]
1	*n*-Bu$_4$POAc	Cu$_2$O-NP	-	-	n.d.
3	*n*-Bu$_4$POAc	Cu$_2$O-NP	Pd-NP	-	18.0
3	C$_3$CNmpyrrNTf$_2$	Cu$_2$O-NP	Pd-NP	NMP	45.5
4	C$_3$CNmpyrrNTf$_2$	Cu$_2$O-NP	Pd-NP	DMSO	24.1
5	C$_3$CNmpyrrNTf$_2$	Cu$_2$O-NP	Pd-NP	mesitylene	n.d.

Reaction conditions: All reactions were carried out under argon atmosphere. Catalyst loading: 2 mol% Pd(OAc)$_2$ for the synthesis of Pd nanoparticles, 1 mmol CuCO$_3$ for the synthesis of Cu$_2$O nanoparticles.

6 | Concluding Remarks

6.1 List of Publications

The following publications are part of this work and listed in chronological order:

- <u>M. T. Keßler</u>, M. H. G. Prechtl*, "Palladium Catalysed Aerobic Dehydrogenation of C-H Bonds in Cyclohexanones", *ChemCatChem* **2012**, 4, 326-327.

- F. Heinrich, <u>M. T. Keßler</u>, S. Dohmen, M. Singh, M. H. G. Prechtl*, S. Mathur*, "Molecular Palladium Precursors for Pd^0 Nanoparticle Preparation by Microwave Irradiation: Synthesis, Structural Characterization and Catalytic Activity" *Eur. J. Inorg. Chem.* **2012**, 36, 6027-6033.

- <u>M. T. Keßler</u>, J. D. Scholten, F. Galbrecht, M. H. G. Prechtl*, "*Coupling Reactions in Ionic Liquids*" in *"Palladium-Catalyzed Cross-Coupling Reactions - Practical Aspects and Future Developments"* **2013**, ch. 6, p. 201-231, Wiley-VCH, Weinheim.

- <u>M. T. Keßler</u>, C. Gedig, S. Sahler, P. Wand, S. Robke, M. H. G. Prechtl*, "Recyclable Nanoscale Copper(I) Catalyst in Ionic Liquid Media for Selective Decarboxylative C-C Bond Cleavage" *Catal. Sci. Technol.* **2013**, 3, 992-1001.

- <u>M. T. Keßler</u>, S. Robke, S. Sahler, M. H. G. Prechtl*, "Ligand-free copper(I) oxide nanoparticle-catalysed amination of aryl halides in ionic liquids" *Catal. Sci. Technol.* **2014**, 4, 102-108.

- <u>M. T. Keßler</u>, M. K. Hentschel, C. Heinrichs, S. Roitsch, M. H. G. Prechtl*, "Fast track to nanomaterials: Microwave assisted ionothermal synthesis in ionic liquid media" *RSC Adv.* **2014**, 4, 14149-14156.

Besides the last-mentioned articles, the following publications are not included in this thesis:

- <u>M. T. Keßler</u>, J. D. Scholten, M. H. G. Prechtl*, "*Metal Catalysts immobilised in Ionic Liquids: A Couple with Opportunities for Fine Chemicals Derived from Biomass*" in "Catalytic Hybrid Materials, Composites, and Organocatalysts" **2013**, ch. 10, 243-264, Elsevier, Amsterdam.

- T. N. Gieshoff, A. Welther, <u>M. T. Keßler</u>, M. H. G. Prechtl*, A. Jacobi v. Wangelin*, "Stereoselective iron-catalyzed alkyne hydrogenation in ionic liquids" *Chem. Commun.* **2014**, 50, 18, 2261-2264.

- S. Sahler, S. Sturm, <u>M. T. Keßler</u>, M. H. G. Prechtl*, "The Role of Ionic Liquids in Hydrogen Storage" *Chem. Eur. J.* **2014**, 20, 29, 8934–8941.

6.2   Reprint Permissions and Copyrights

JOHN WILEY AND SONS LICENSE
TERMS AND CONDITIONS

Aug 04, 2014

This is a License Agreement between Michael Keßler ("You") and John Wiley and Sons ("John Wiley and Sons") provided by Copyright Clearance Center ("CCC"). The license consists of your order details, the terms and conditions provided by John Wiley and Sons, and the payment terms and conditions.

All payments must be made in full to CCC. For payment instructions, please see information listed at the bottom of this form.

License Number	3441840960590
License date	Aug 04, 2014
Licensed content publisher	John Wiley and Sons
Licensed content publication	Wiley oBooks
Licensed content title	Coupling Reactions in Ionic Liquids
Book title	Palladium-Catalyzed Coupling Reactions: Practical Aspects and Future Developments
Licensed copyright line	Copyright © 2013 Wiley-VCH Verlag GmbH & Co. KGaA
Licensed content author	Michael T. Keßler,Jackson D. Scholten,Frank Galbrecht,Martin H. G. Prechtl
Licensed content date	Apr 2, 2013
Start page	201
End page	234
Type of use	Dissertation/Thesis
Requestor type	Author of this Wiley chapter
Format	Print and electronic
Portion	Full chapter
Will you be translating?	No
Title of your thesis / dissertation	Syntheses, Characterisation and Application of Nanoscale Catalysts
Expected completion date	Oct 2014
Expected size (number of pages)	250
Total	0.00 EUR
Terms and Conditions	

This is a License Agreement between Michael Keßler ("You") and John Wiley and Sons ("John Wiley and Sons") provided by Copyright Clearance Center ("CCC"). The license consists of your order details, the terms and conditions provided by John Wiley and Sons, and the payment terms and conditions.

All payments must be made in full to CCC. For payment instructions, please see information listed at the bottom of this form.

License Number	3441840553527
License date	Aug 04, 2014
Licensed content publisher	John Wiley and Sons
Licensed content publication	ChemCatChem
Licensed content title	Palladium Catalysed Aerobic Dehydrogenation of C$-$H Bonds in Cyclohexanones
Licensed copyright line	Copyright © 2012 WILEY-VCH Verlag GmbH & Co. KGaA, Weinheim
Licensed content author	Michael T. Keßler,Martin H. G. Prechtl
Licensed content date	Dec 5, 2011
Start page	326
End page	327
Type of use	Dissertation/Thesis
Requestor type	Author of this Wiley article
Format	Print and electronic
Portion	Full article
Will you be translating?	No
Title of your thesis / dissertation	Syntheses, Characterisation and Application of Nanoscale Catalysts
Expected completion date	Oct 2014
Expected size (number of pages)	250
Total	0.00 EUR
Terms and Conditions	

Acknowledgements to be used by RSC authors

Authors of RSC books and journal articles can reproduce material (for example a figure) from the RSC publication in a non-RSC publication, including theses, without formally requesting permission providing that the correct acknowledgement is given to the RSC publication. This permission extends to reproduction of large portions of text or the whole article or book chapter when being reproduced in a thesis.

The acknowledgement to be used depends on the RSC publication in which the material was published and the form of the acknowledgements is as follows:

- For material being reproduced from an article in *New Journal of Chemistry* the acknowledgement should be in the form:
  - [Original citation] - Reproduced by permission of The Royal Society of Chemistry (RSC) on behalf of the Centre National de la Recherche Scientifique (CNRS) and the RSC

- For material being reproduced from an article *Photochemical & Photobiological Sciences* the acknowledgement should be in the form:
  - [Original citation] - Reproduced by permission of The Royal Society of Chemistry (RSC) on behalf of the European Society for Photobiology, the European Photochemistry Association, and RSC

- For material being reproduced from an article in *Physical Chemistry Chemical Physics* the acknowledgement should be in the form:
  - [Original citation] - Reproduced by permission of the PCCP Owner Societies

- For material reproduced from books and any other journal the acknowledgement should be in the form:
  - [Original citation] - Reproduced by permission of The Royal Society of Chemistry

The acknowledgement should also include a hyperlink to the article on the RSC website.

The form of the acknowledgement is also specified in the RSC agreement/licence signed by the corresponding author.

Except in cases of republication in a thesis, this express permission does not cover the reproduction of large portions of text from the RSC publication or reproduction of the whole article or book chapter.

A publisher of a non-RSC publication can use this document as proof that permission is granted to use the material in the non-RSC publication.

6.3 Contributions to Publications

Title	Article	Planning	Experiments	Analytics	Manuscript	Sum
F. Heinrich, M. T. Keßler, S. Dohmen, M. Singh, M. H. G. Prechtl*, S. Mathur*, *Eur. J. Inorg. Chem.* **2012**, 36, 6027-6033.	Scientific article (co-operation)	35%	35%	35%	35%	35%
M. T. Keßler, C. Gedig, S. Sahler, P. Wand, S. Robke, M. H. G. Prechtl*, **2013**, 3, 992-1001.	Scientific article	85%	95%	90%	85%	89%
M. T. Keßler, S. Robke, S. Sahler, M. H. G. Prechtl*, *Catal. Sci. Technol.* **2014**, 4, 102-108.	Scientific article	90%	95%	90%	85%	90%
M. T. Keßler, M. K. Hentschel, C. Heinrichs, S. Roitsch, M. H. G. Prechtl*, *RSC Adv.* **2014**, 4, 14149-14156.	Scientific article	85%	95%	70%	85%	84%
M. T. Keßler, M. H. G. Prechtl*, *ChemCatChem* **2012**, 4, 326-327.	highlight article	90%	-	-	90%	90%
M. T. Keßler, J. D. Scholten, F. Galbrecht, M. H. G. Prechtl*, **2013**, ch. 6, p. 201-231, Wiley-VCH, Weinheim.	book-chapter	35%	-	-	35%	35%

A │ Appendix

A.1 NMR-spectra
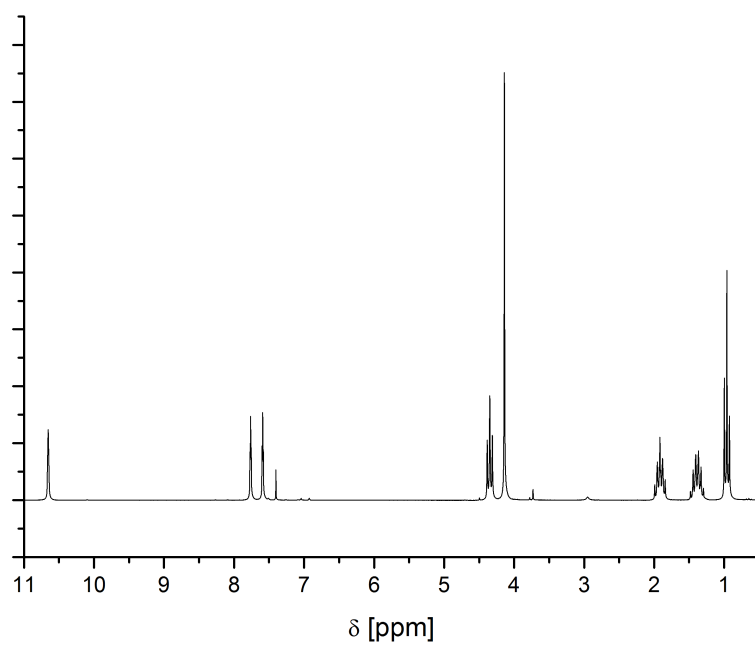
Figure A.1: ^{1}H-NMR spectrum of bmim Cl.
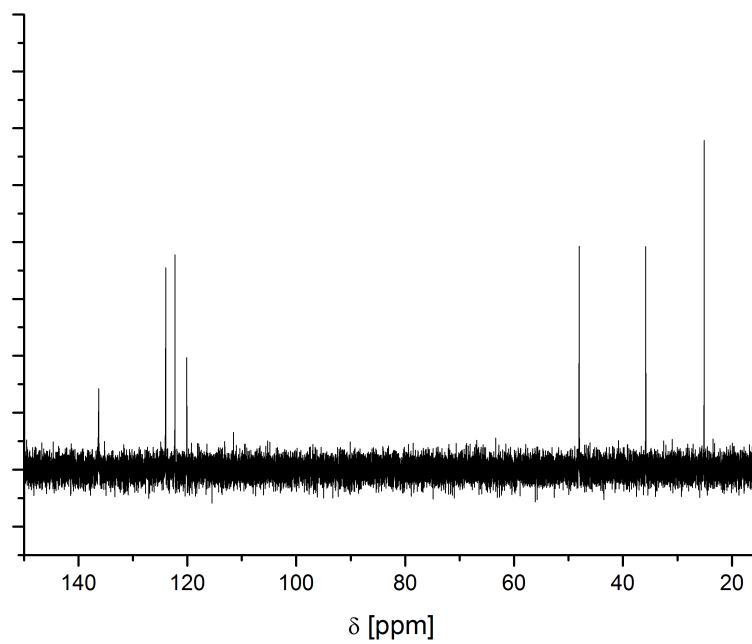
Figure A.2: ^{13}C-NMR spectrum of bmim Cl.
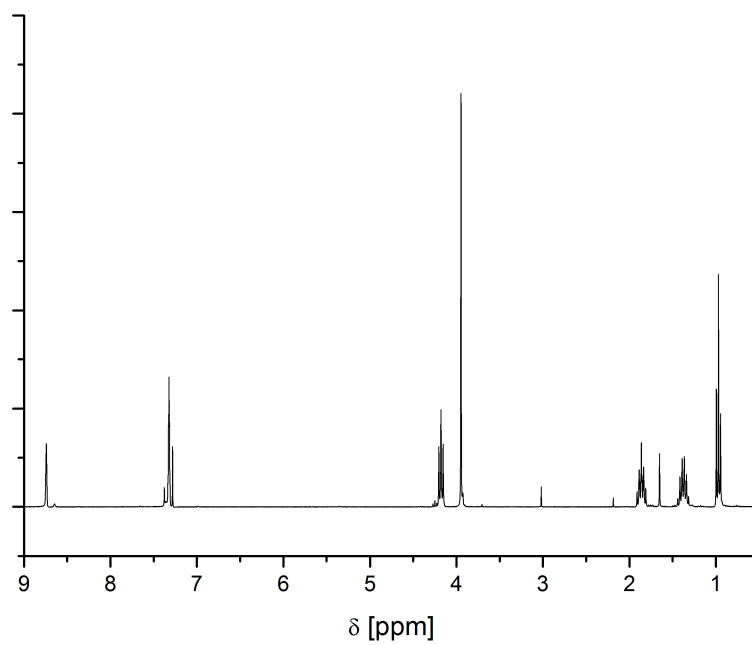
Figure A.3: ^{1}H-NMR spectrum of bmim NTf$_2$.
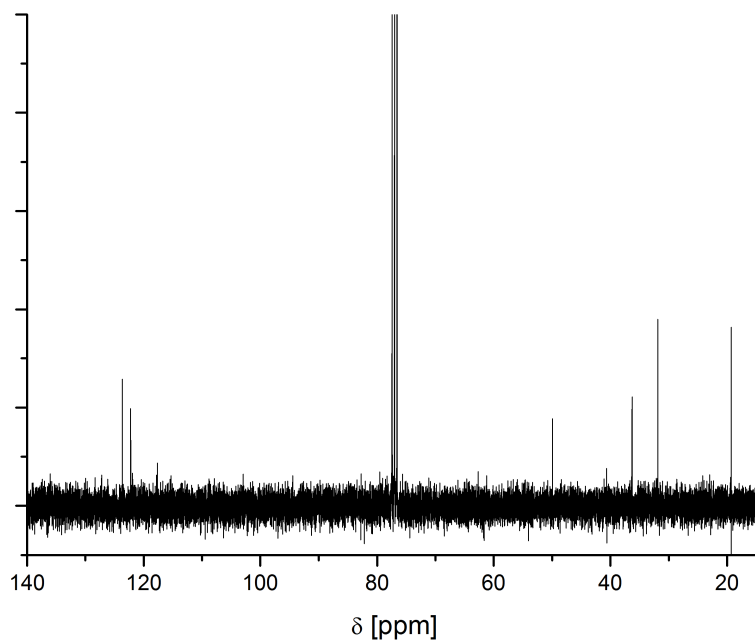
Figure A.4: ^{13}C-NMR spectrum of bmim NTf$_2$.
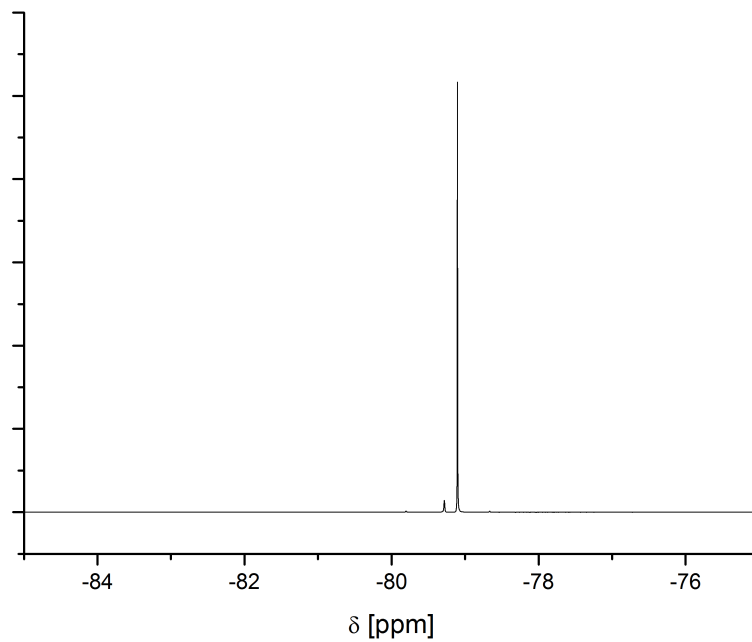
Figure A.5: ^{19}F-NMR spectrum of bmim NTf$_2$.
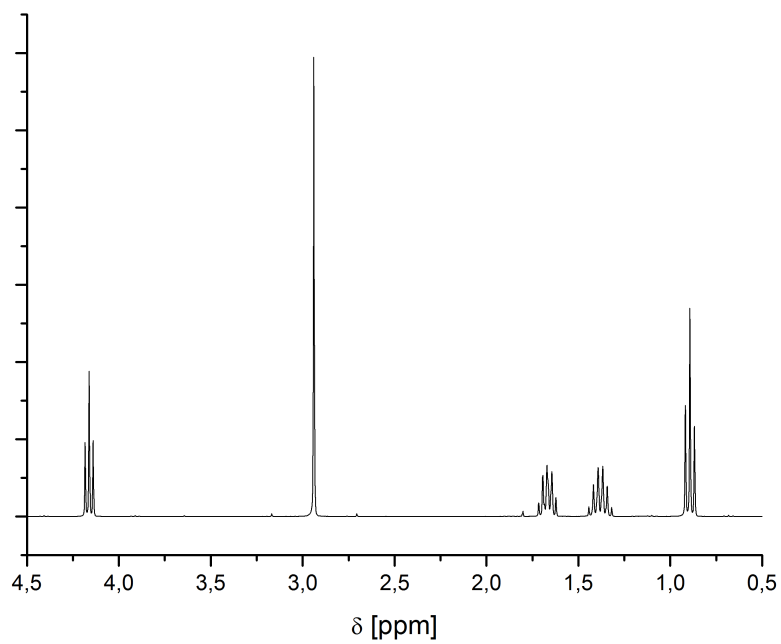
Figure A.6: ^{1}H-NMR spectrum of *n*-BuOMs.
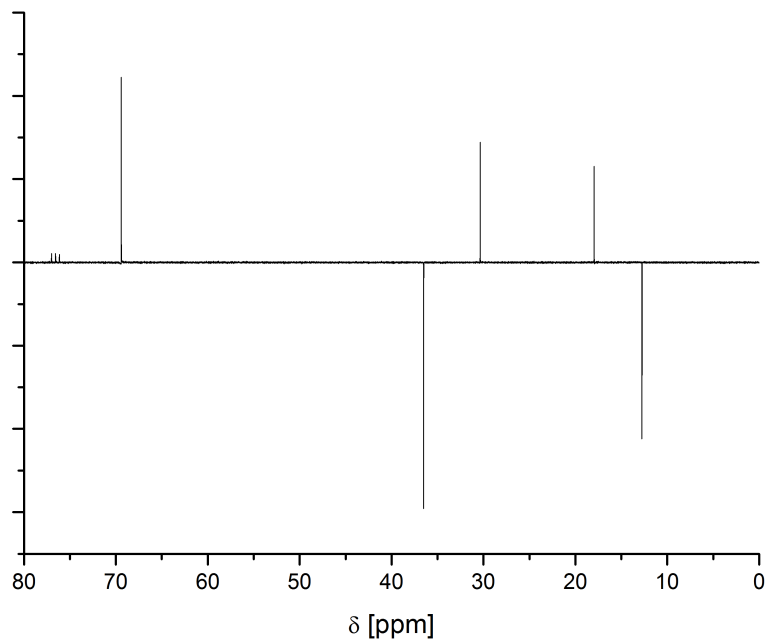
Figure A.7: ^{13}C-NMR spectrum of *n*-BuOMs.
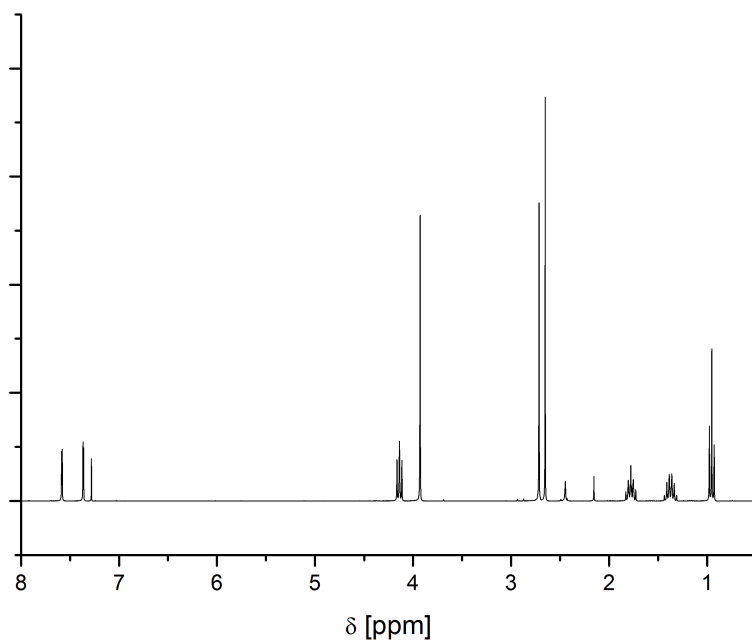
Figure A.8: ^{1}H-NMR spectrum of bmim OMs.
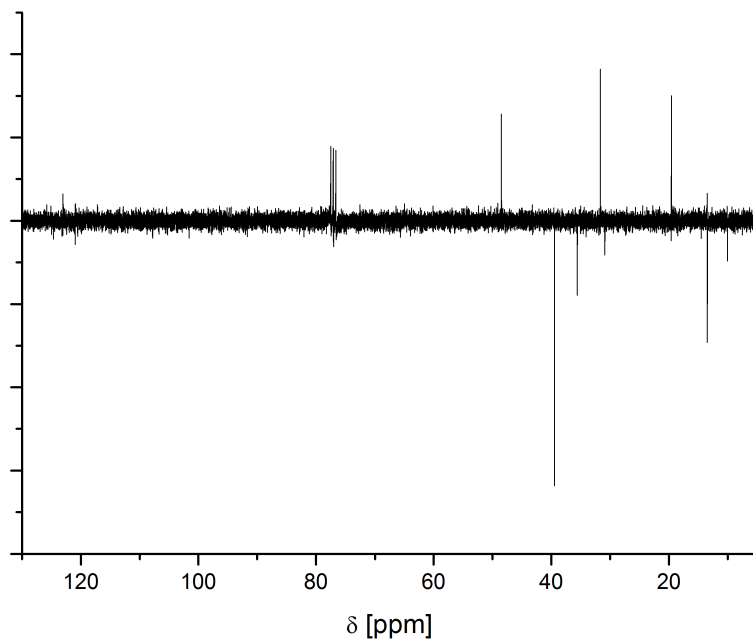
Figure A.9: ^{13}C-NMR spectrum of bmim OMs.
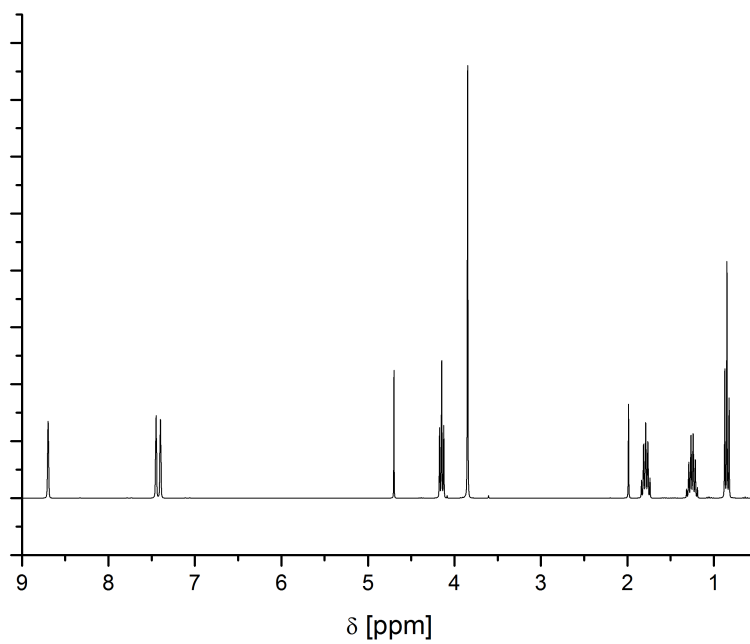
Figure A.10: ^{1}H-NMR spectrum of bmim OAc.
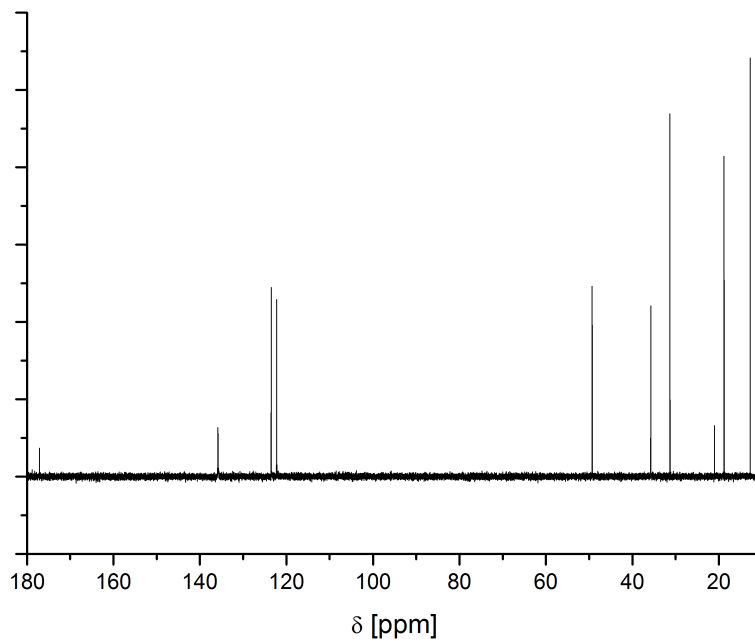
Figure A.11: ^{13}C-NMR spectrum of bmim OAc.
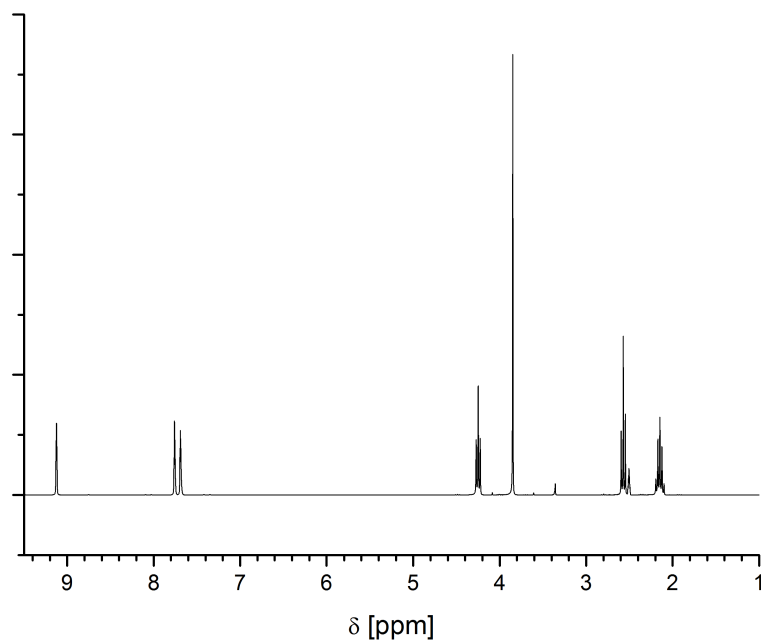
Figure A.12: ^{1}H-NMR spectrum of C$_3$CNmim Cl.
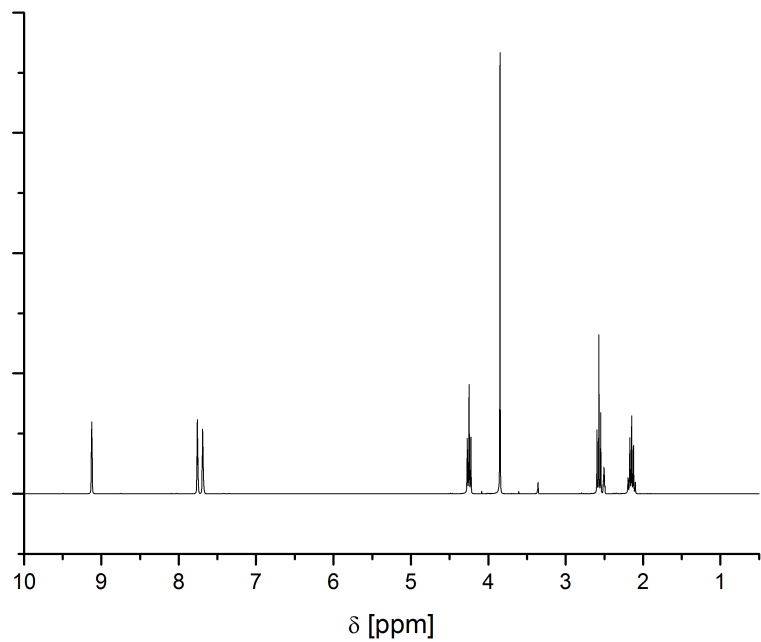
Figure A.13: ^{1}H-NMR spectrum of C$_3$CNmim NTf$_2$.
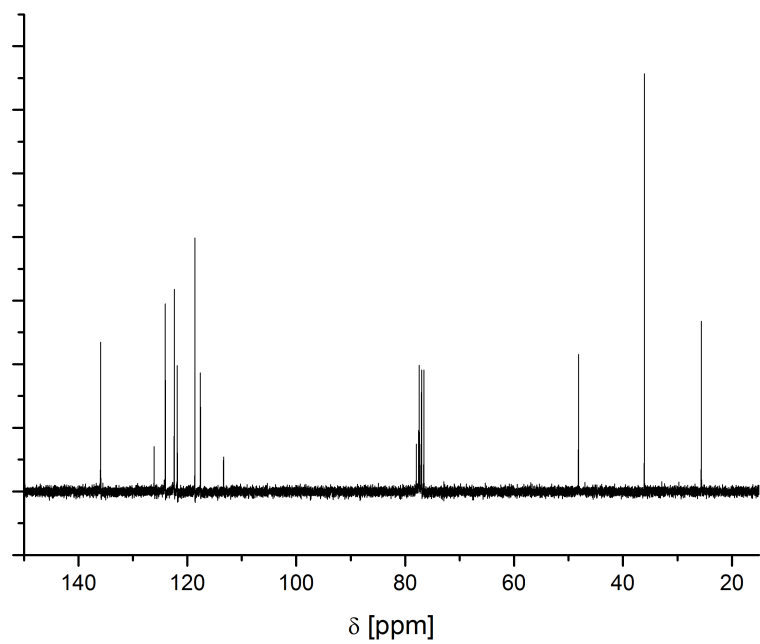
Figure A.14: ^{13}C-NMR spectrum of C$_3$CNmim NTf$_2$.
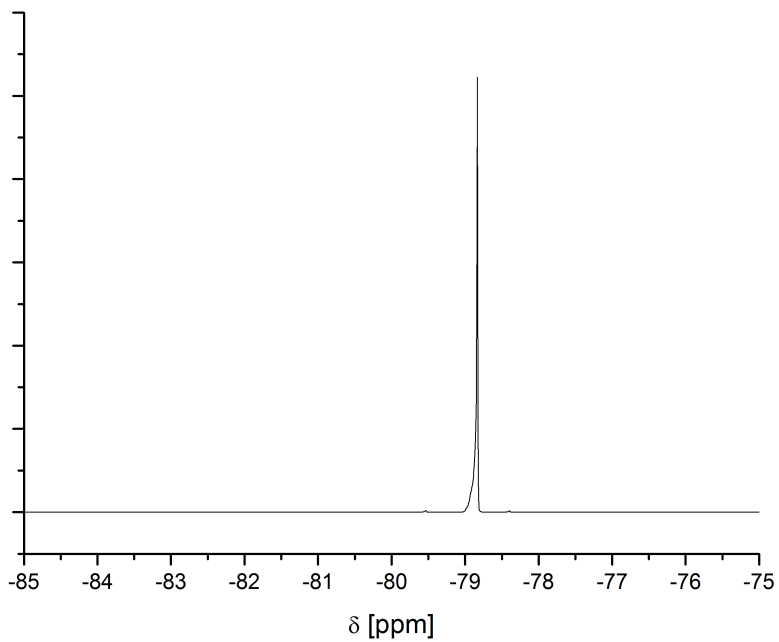
Figure A.15: ^{19}F-NMR spectrum of C$_3$CNmim NTf$_2$.
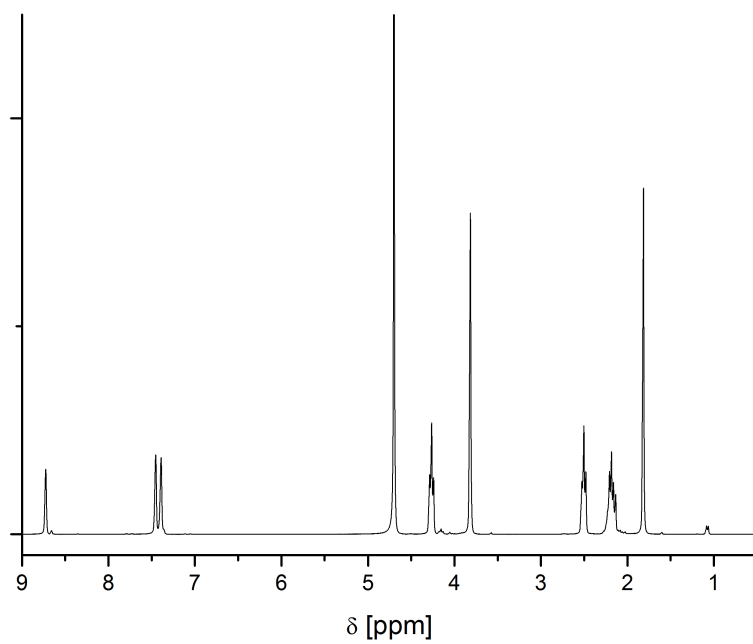
Figure A.16: ^{1}H-NMR spectrum of C$_3$CNmim OAc.
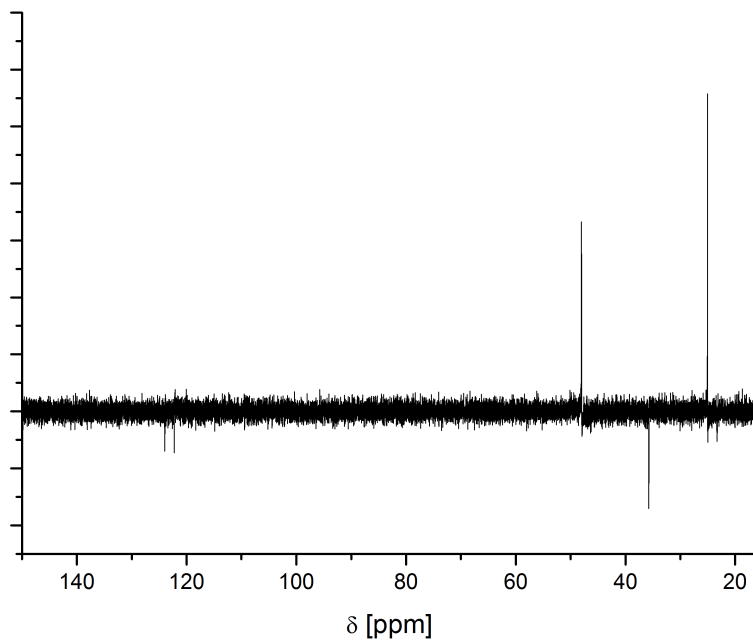
Figure A.17: ^{13}C-NMR spectrum of C$_3$CNmim OAc.
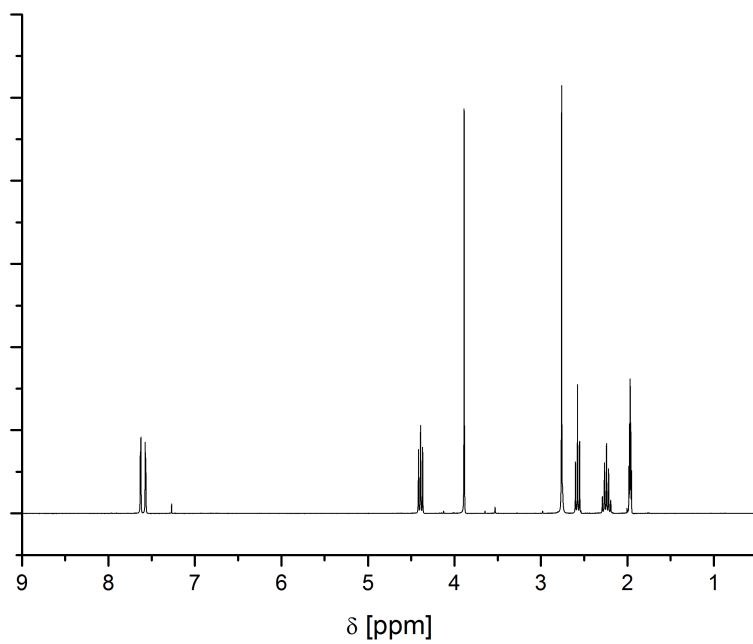
Figure A.18: [^1]H-NMR spectrum of bmmim Cl.
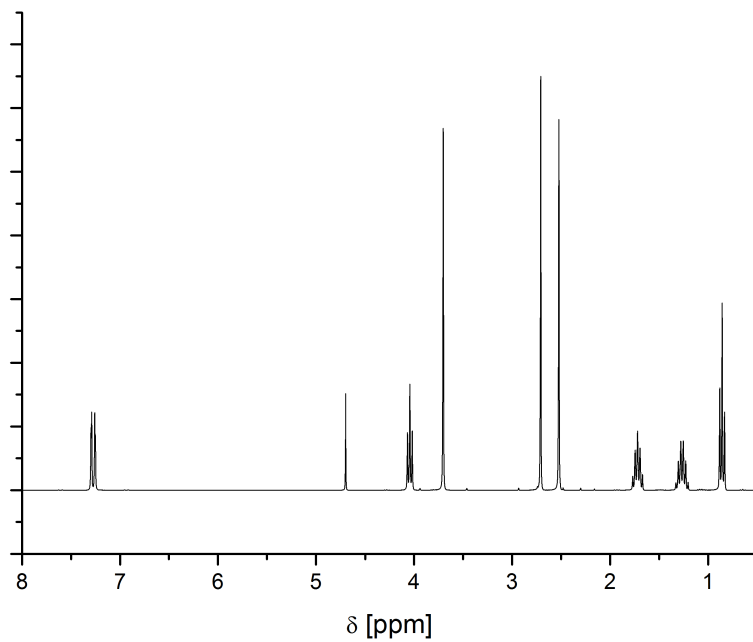
Figure A.19: [^1]H-NMR spectrum of bmmim OMs.
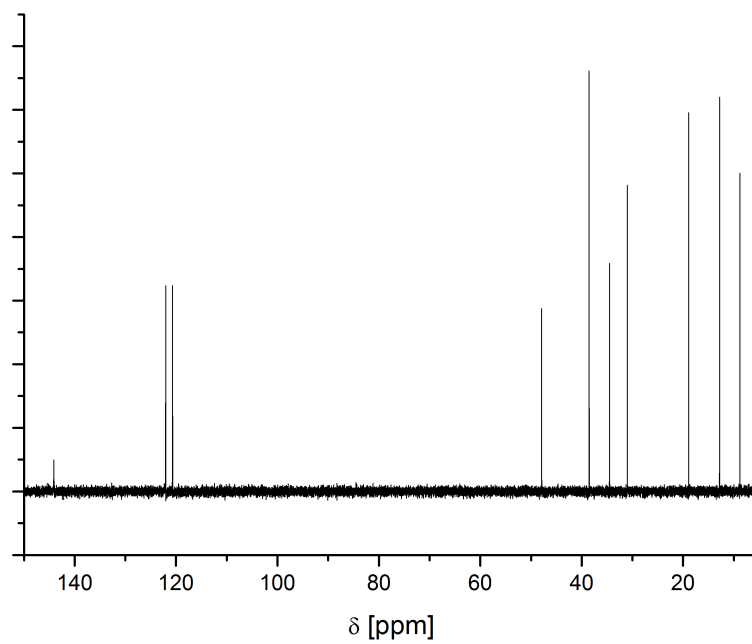
Figure A.20: ^{13}C APT-NMR spectrum of bmmim OMs.
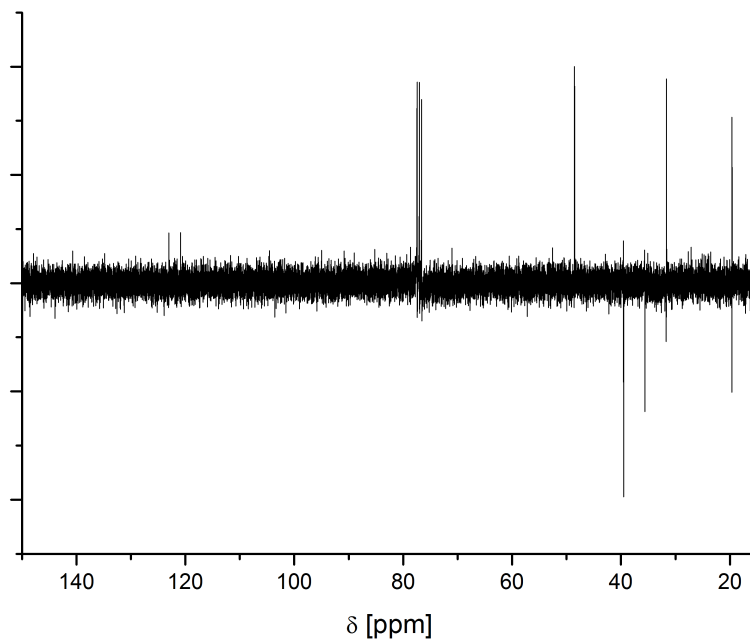
Figure A.21: ^{13}C DEPT-NMR spectrum of bmmim OMs.
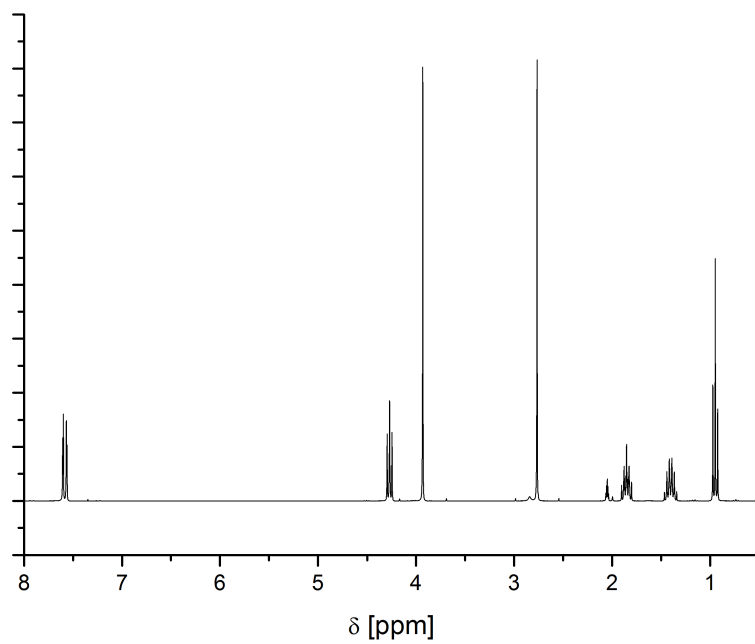
Figure A.22: ^{1}H-NMR spectrum of bmmim NTf$_2$.
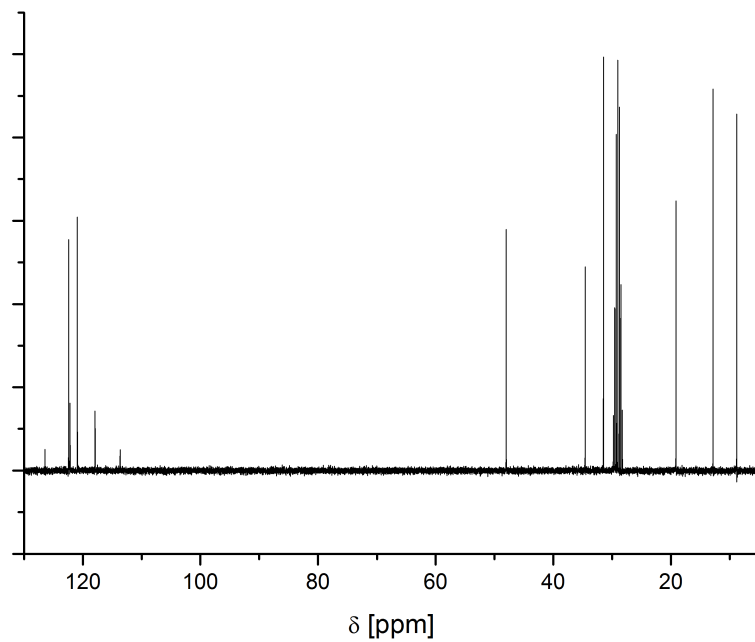
Figure A.23: ^{13}C APT-NMR spectrum of bmmim NTf$_2$.
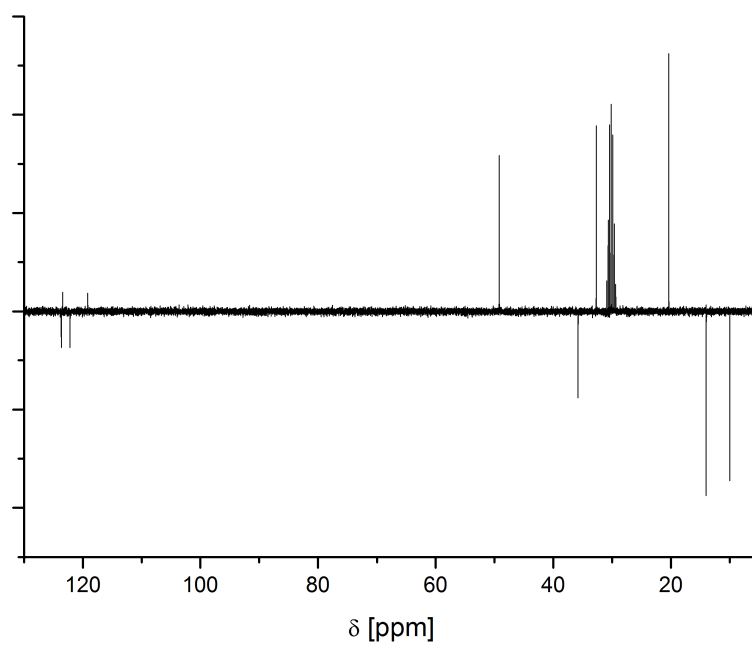
Figure A.24: ^{13}C DEPT-NMR spectrum of bmmim NTf$_2$.
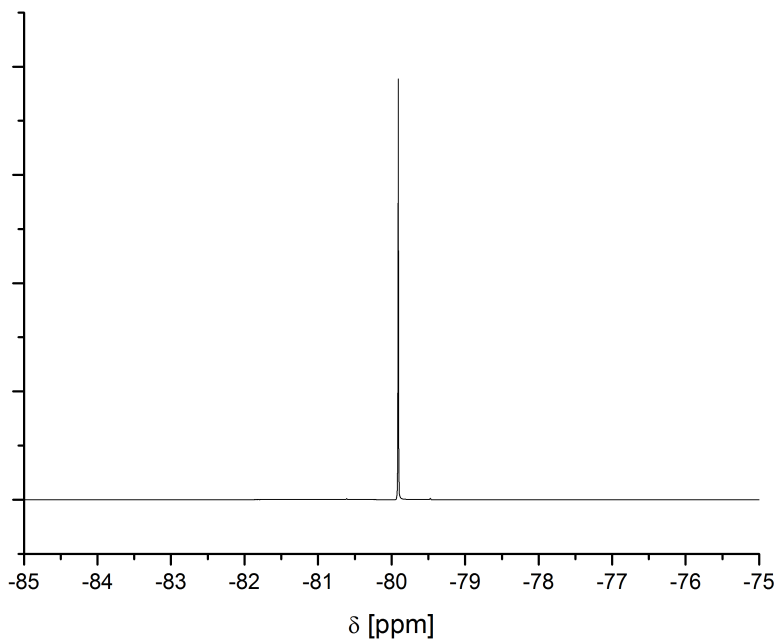
Figure A.25: ^{19}F-NMR spectrum of bmmim NTf$_2$.
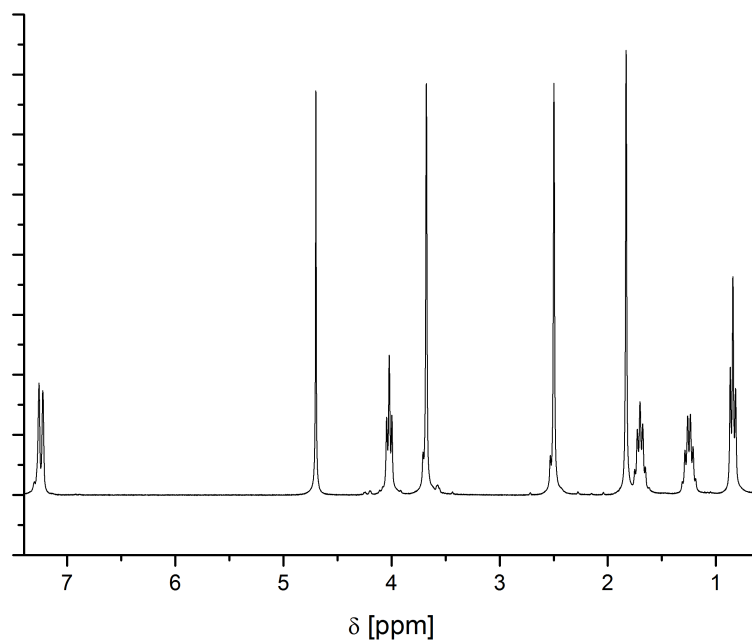
Figure A.26: ^{1}H-NMR spectrum of bmmim OAc.
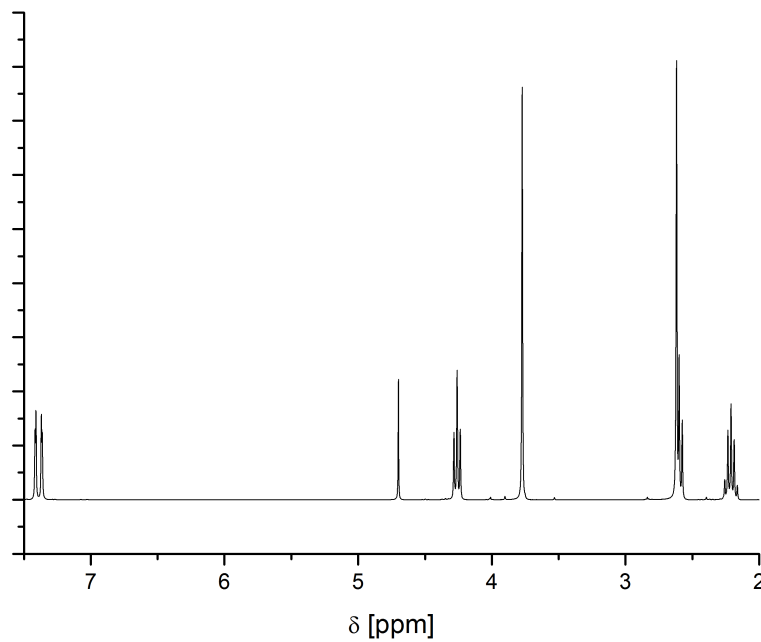
Figure A.27: ^{1}H-NMR spectrum of C$_3$CNmmim Cl.
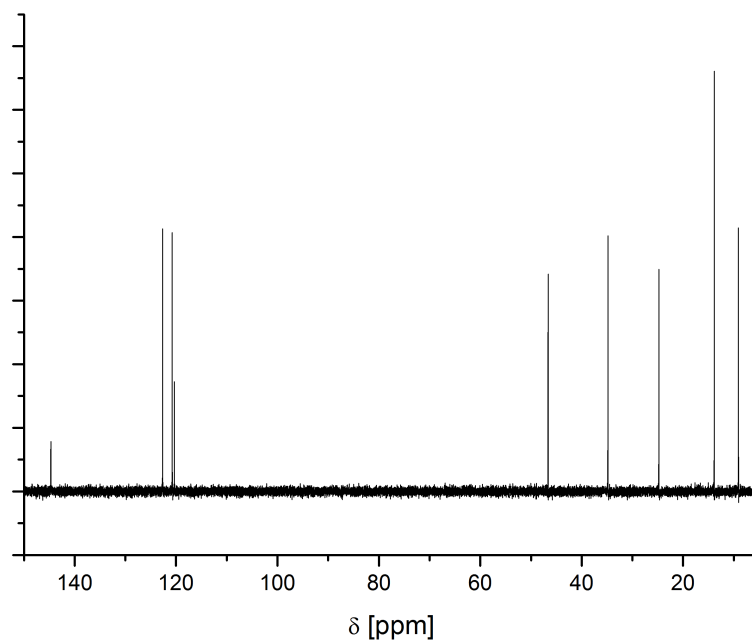
Figure A.28: ^{13}C-NMR spectrum of C_3CNmmim Cl.
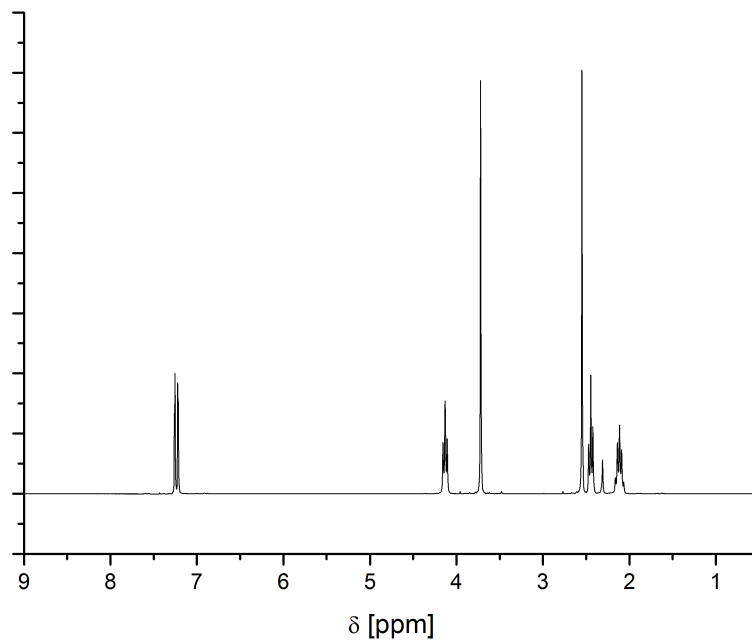
Figure A.29: ^{1}H-NMR spectrum of C_3CNmmim NTf$_2$.
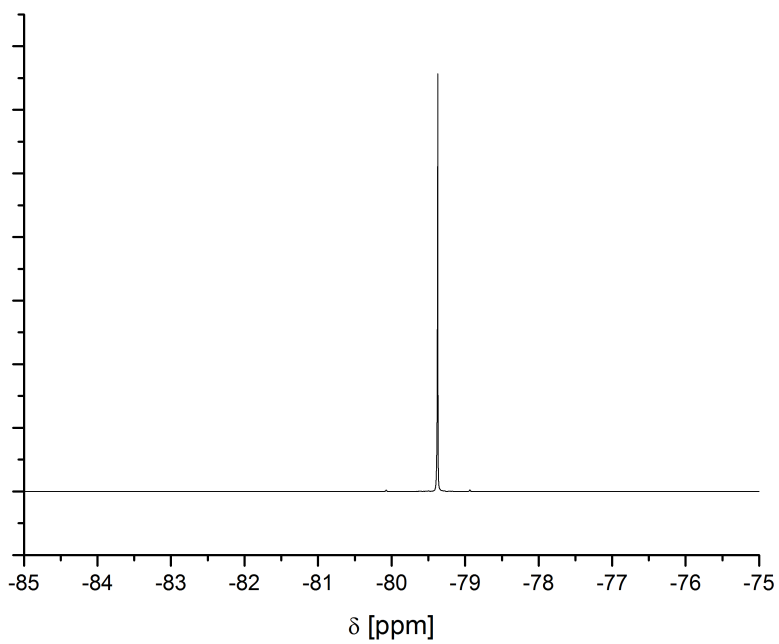
Figure A.30: ^{19}F-NMR spectrum of C$_3$CNmmim NTf$_2$.
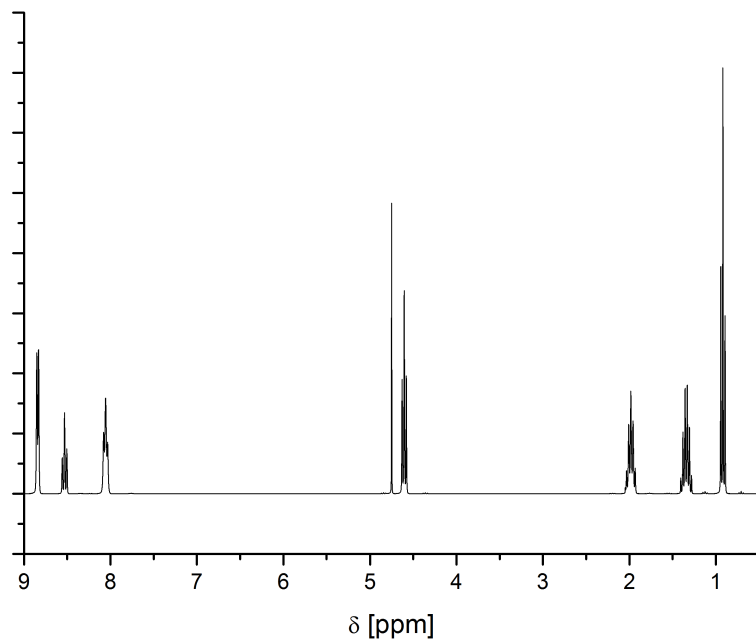
Figure A.31: ^{1}H-NMR spectrum of bpy Cl.
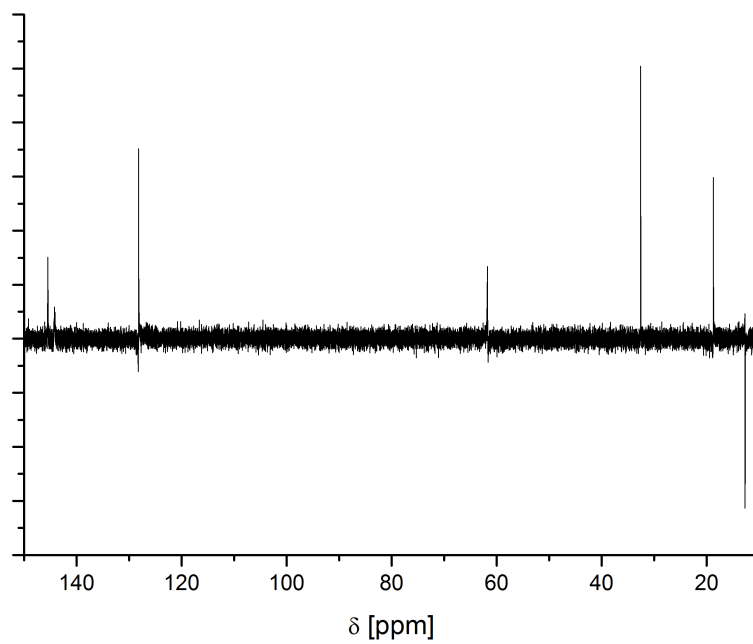
Figure A.32: ^{13}C-NMR spectrum of bpy Cl.
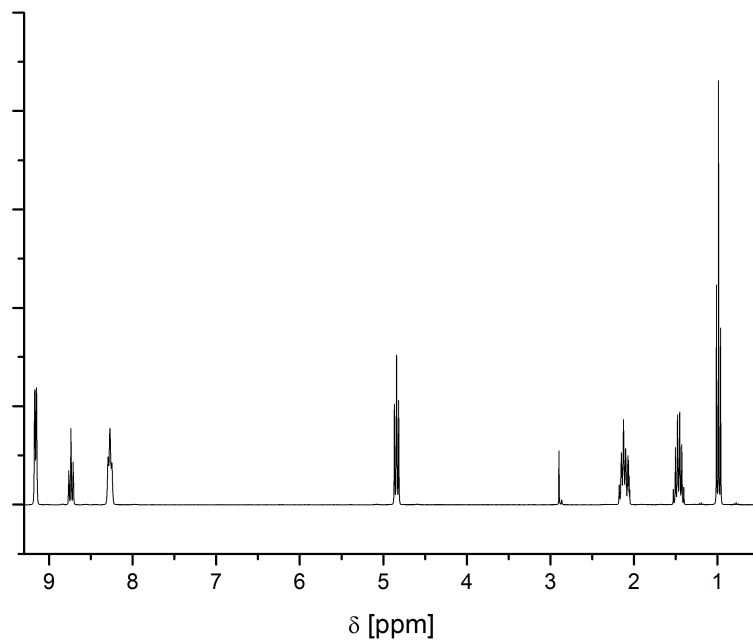
Figure A.33: ^{1}H-NMR spectrum of bpy NTf$_2$.
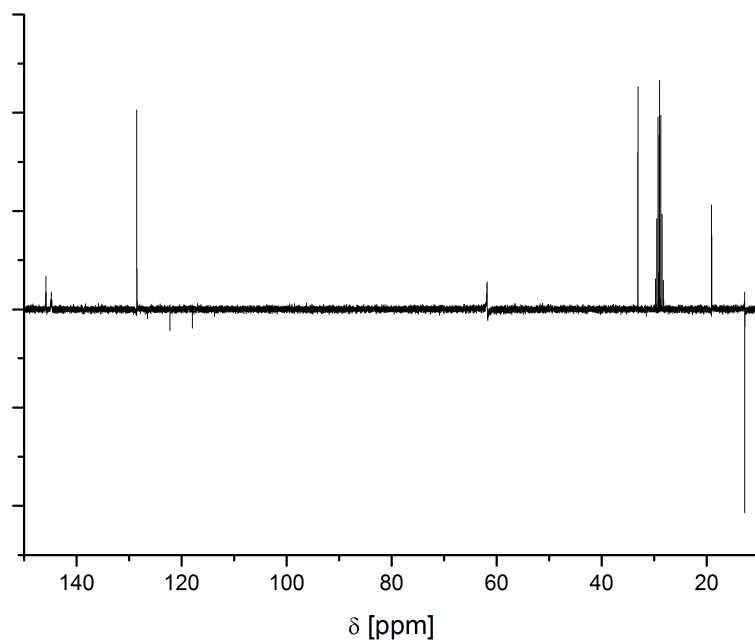
Figure A.34: ^{13}C-NMR spectrum of bpy NTf$_2$.
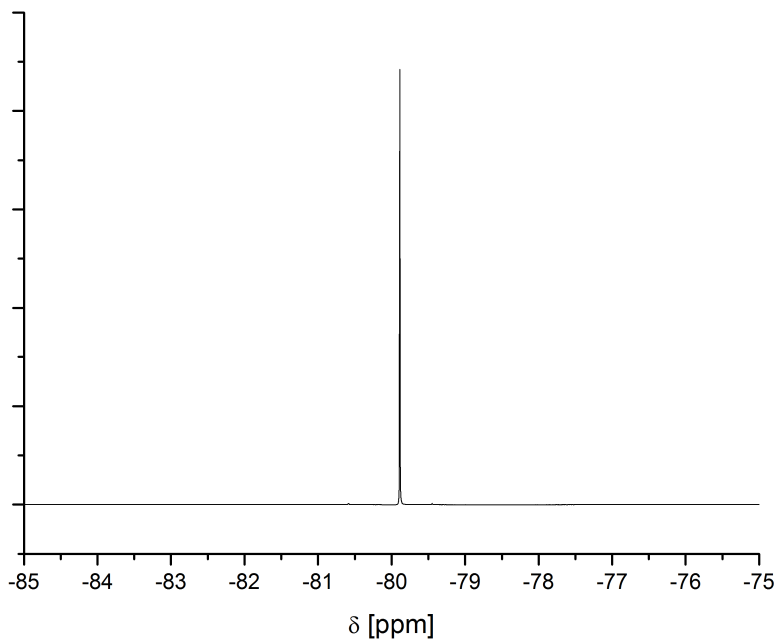
Figure A.35: ^{19}F-NMR spectrum of bpy NTf$_2$.
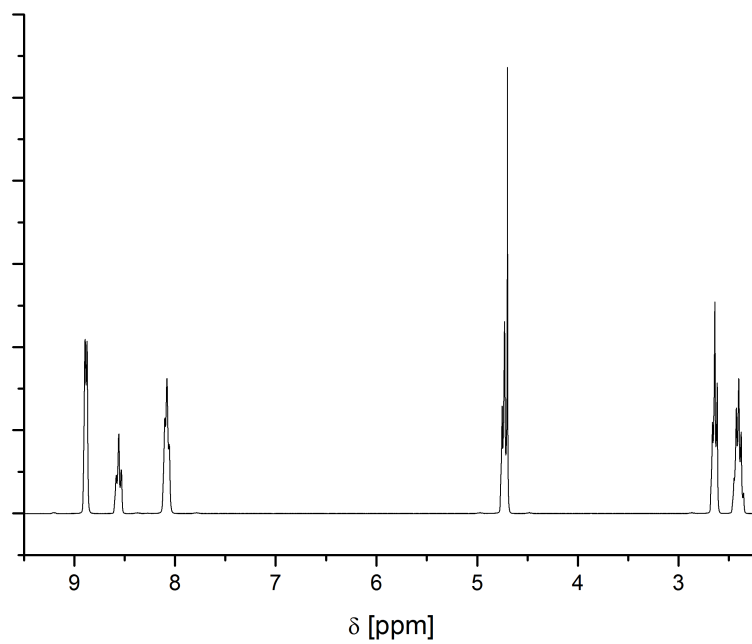
Figure A.36: ^{1}H-NMR spectrum of C$_3$CNpy Cl.
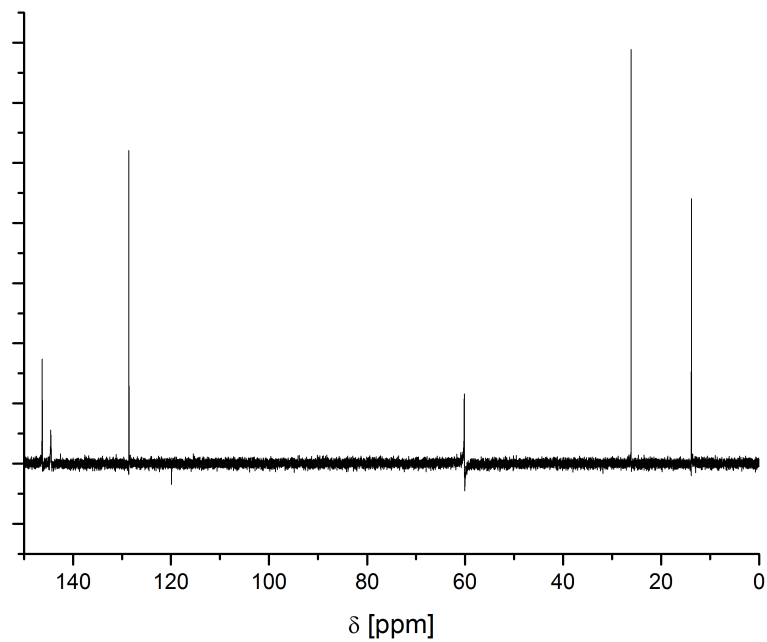
Figure A.37: ^{13}C-NMR spectrum of C$_3$CNpy Cl.
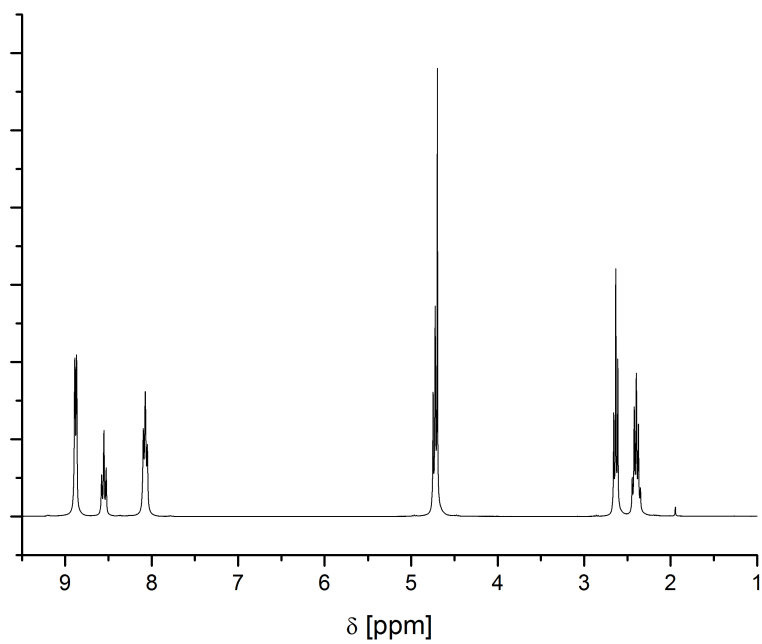
Figure A.38: ^{1}H-NMR spectrum of C$_3$CNpy OAc.
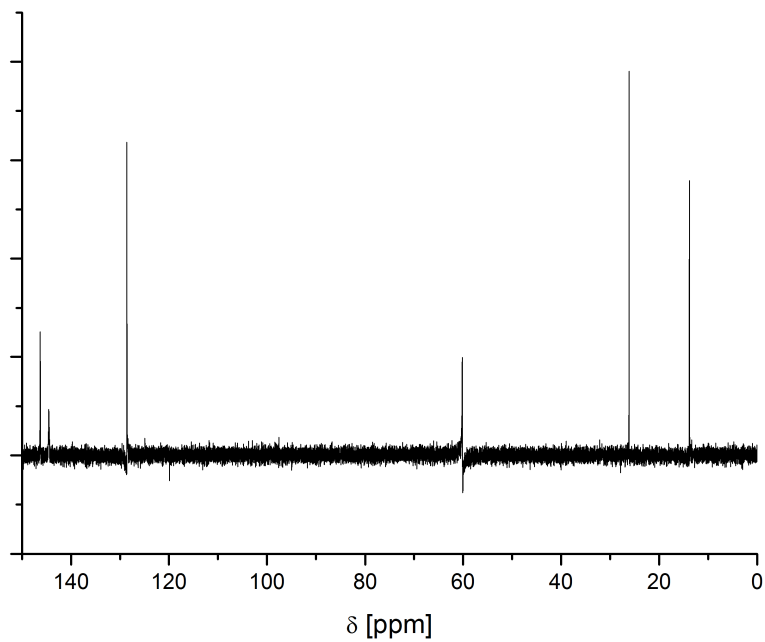
Figure A.39: ^{13}C-NMR spectrum of C$_3$CNpy OAc.
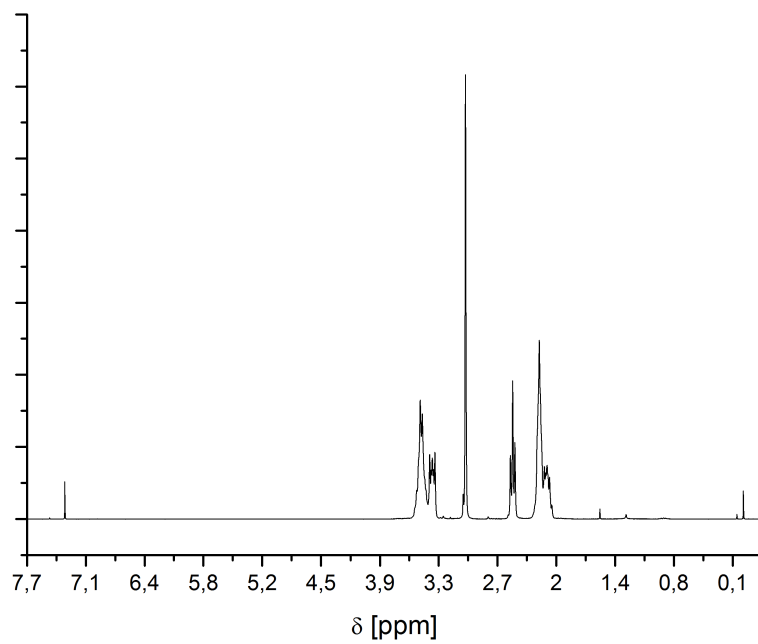
Figure A.40: ^{1}H-NMR spectrum of C$_3$CNmpyrr Cl.
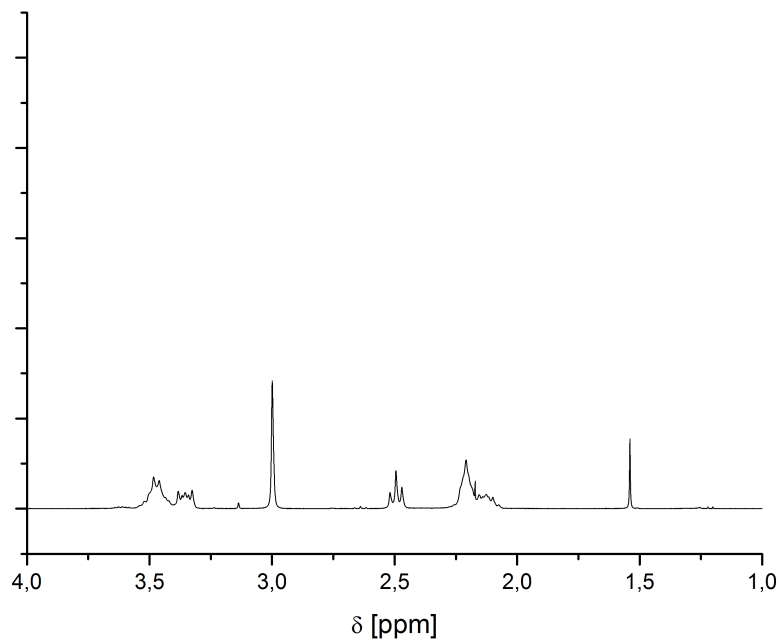
Figure A.41: ^{1}H-NMR spectrum of C$_3$CNmpyrr NTf$_2$.
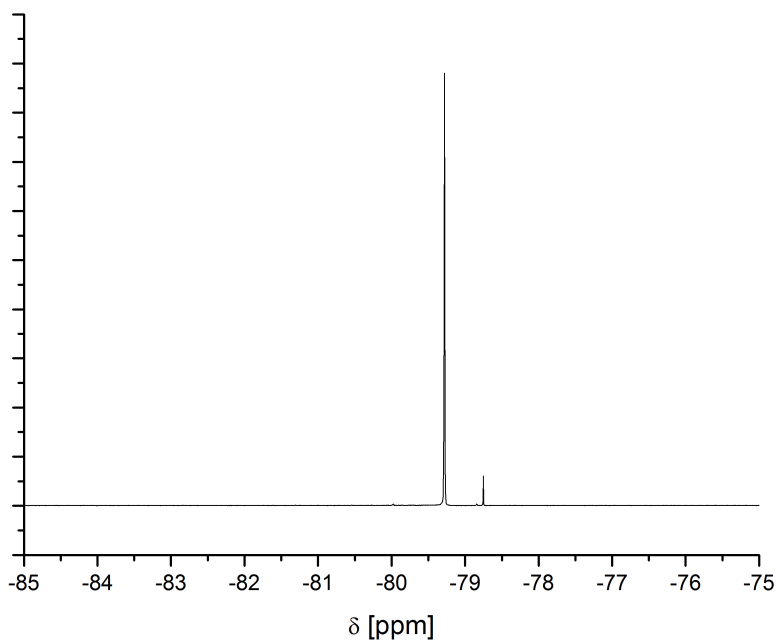
Figure A.42: ^{19}F-NMR spectrum of C$_3$CNmpyrr NTf$_2$.
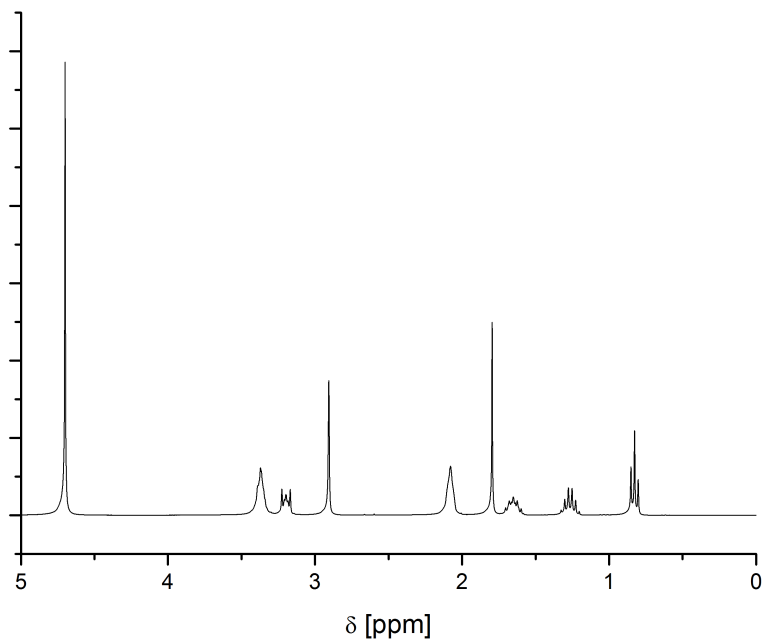
Figure A.43: ^{1}H-NMR spectrum of bmpyrr OAc.
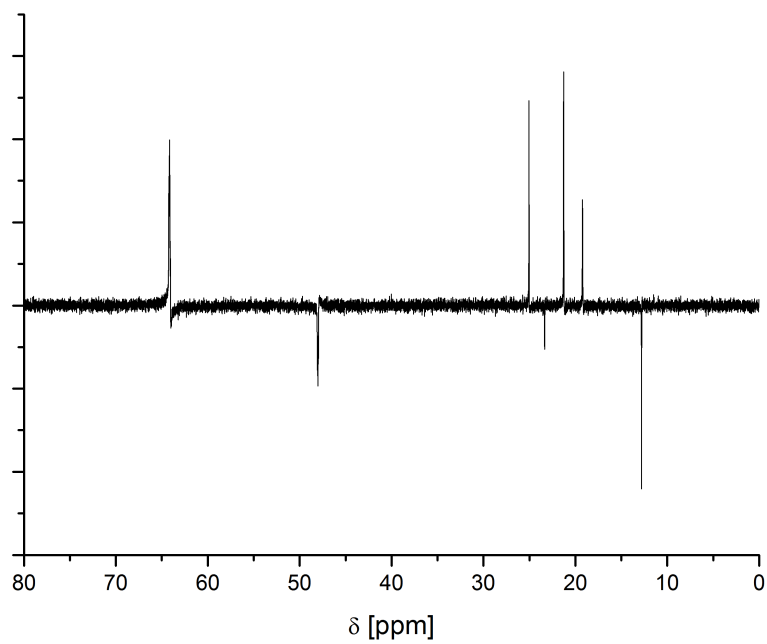
Figure A.44: ^{13}C DEPT-NMR spectrum of bmpyrr OAc.
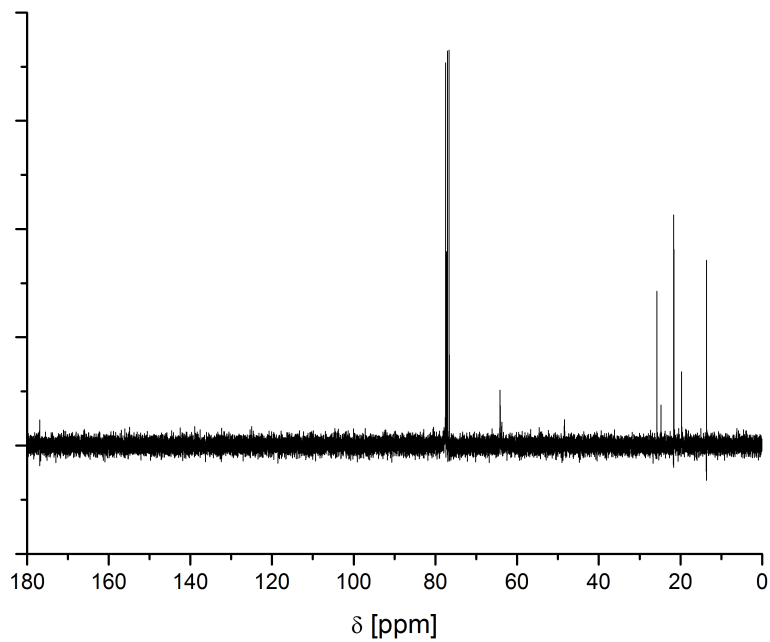
Figure A.45: ^{13}C APT-NMR spectrum of bmpyrr OAc.
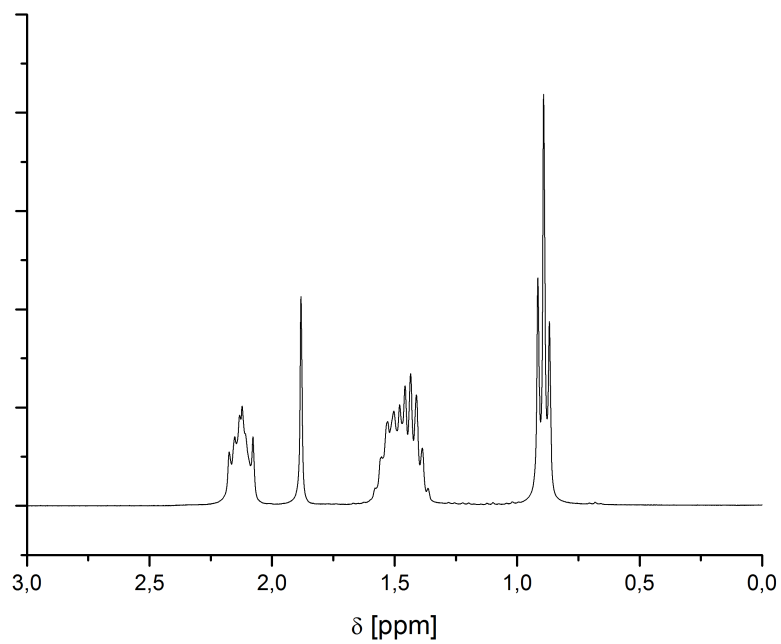
Figure A.46: ^{1}H-NMR spectrum of n-Bu$_4$POAc.
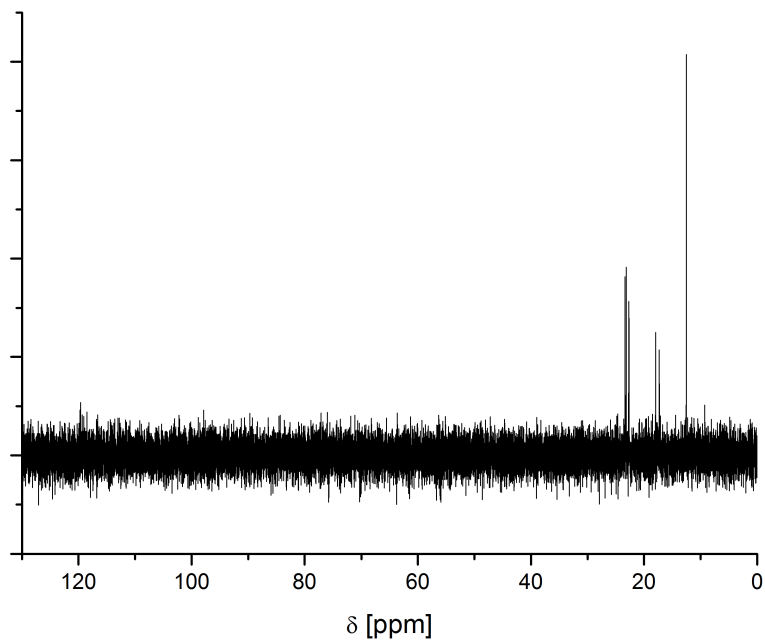
Figure A.47: ^{13}C APT-NMR spectrum of n-Bu$_4$POAc.
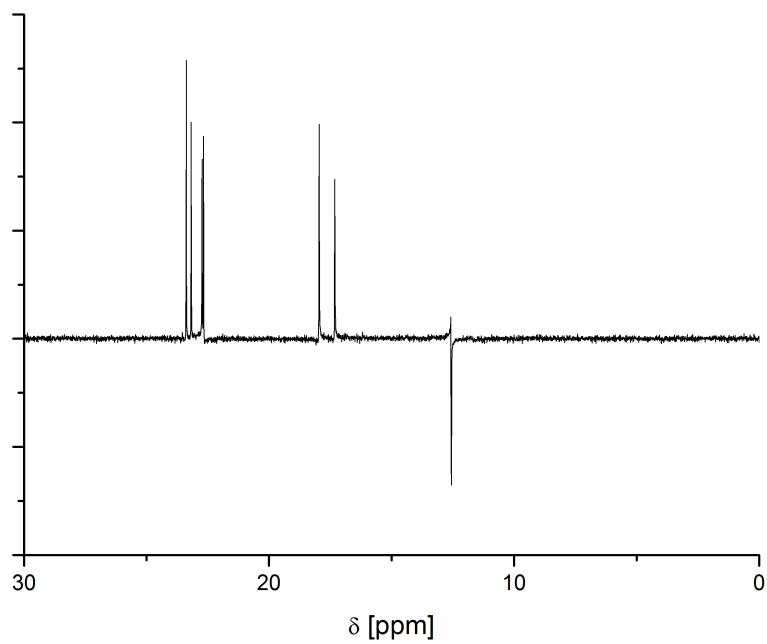
Figure A.48: ^{13}C DEPT-NMR spectrum of n-Bu$_4$POAc.
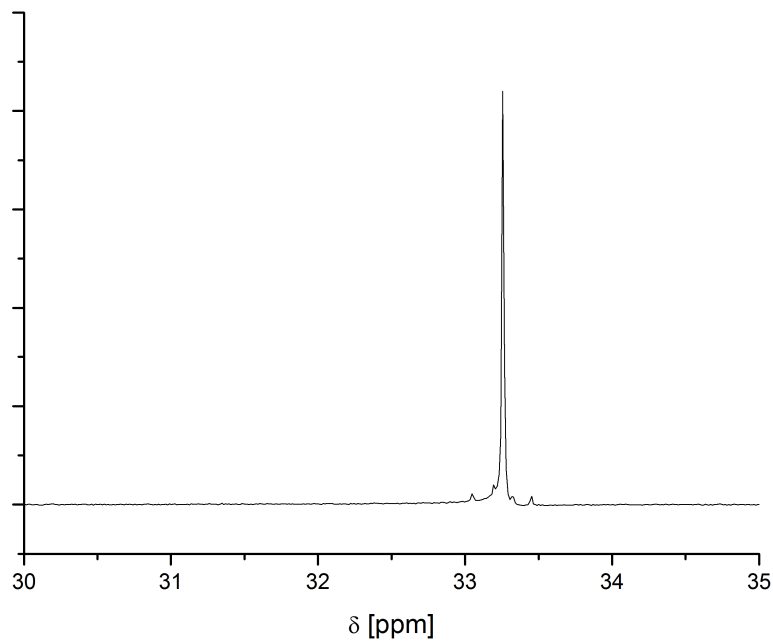
Figure A.49: ^{31}P-NMR spectrum of n-Bu$_4$POAc.
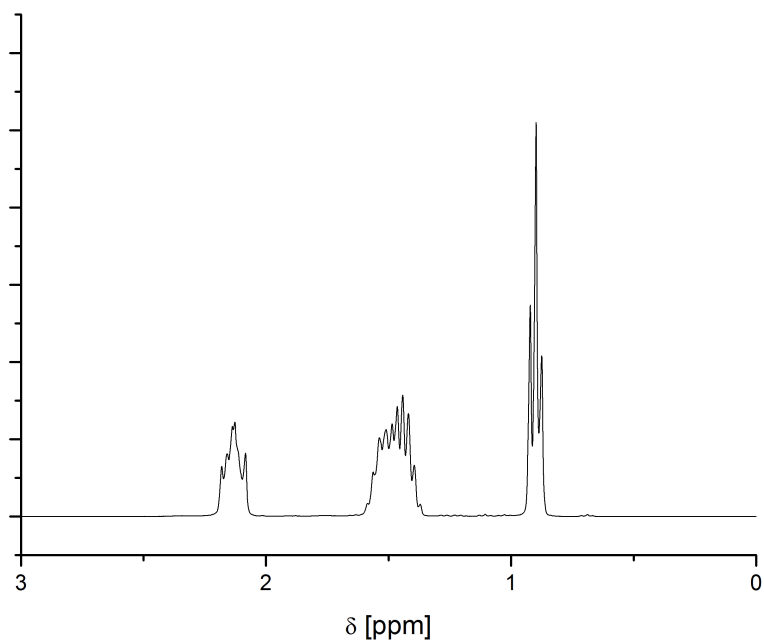
Figure A.50: ^{1}H-NMR spectrum of $(n\text{-Bu}_4\text{P})_2\text{SO}_4$.
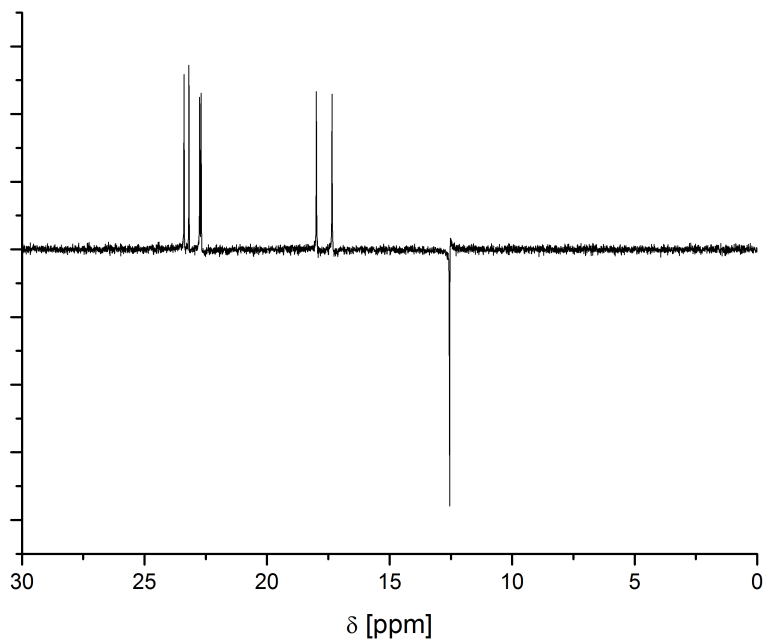
Figure A.51: ^{13}C APT-NMR spectrum of $(n\text{-Bu}_4\text{P})_2\text{SO}_4$.
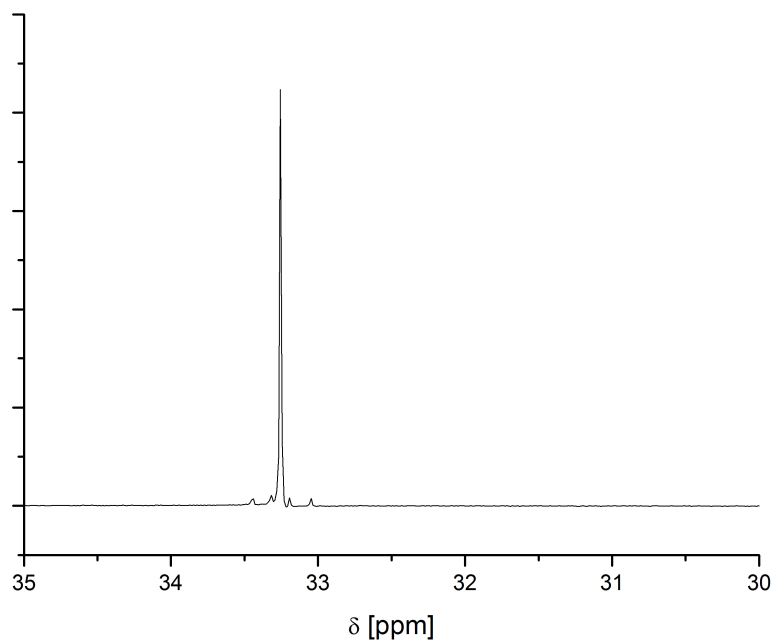
Figure A.52: ^{31}P-NMR spectrum of (n-Bu$_4$P)$_2$SO$_4$.
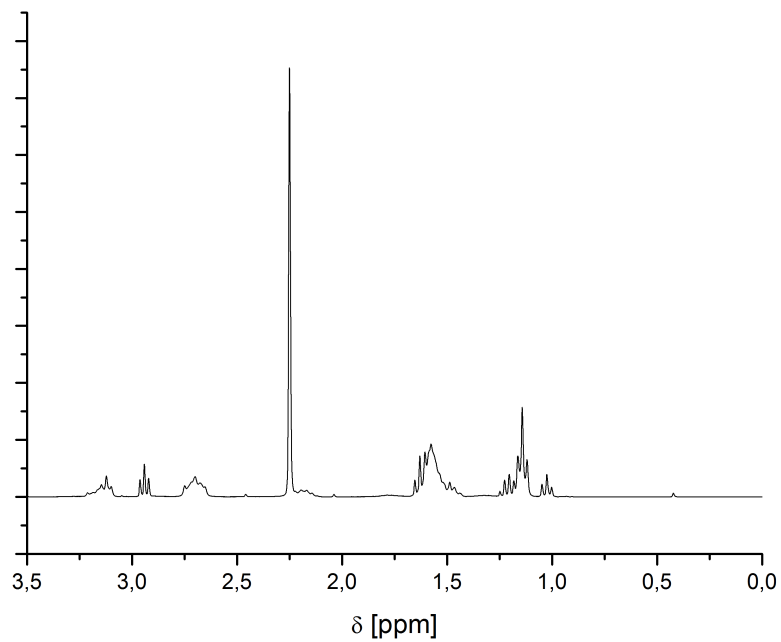
Figure A.53: ^{1}H-NMR spectrum of C$_3$CN-n-Bu$_3$PCl.
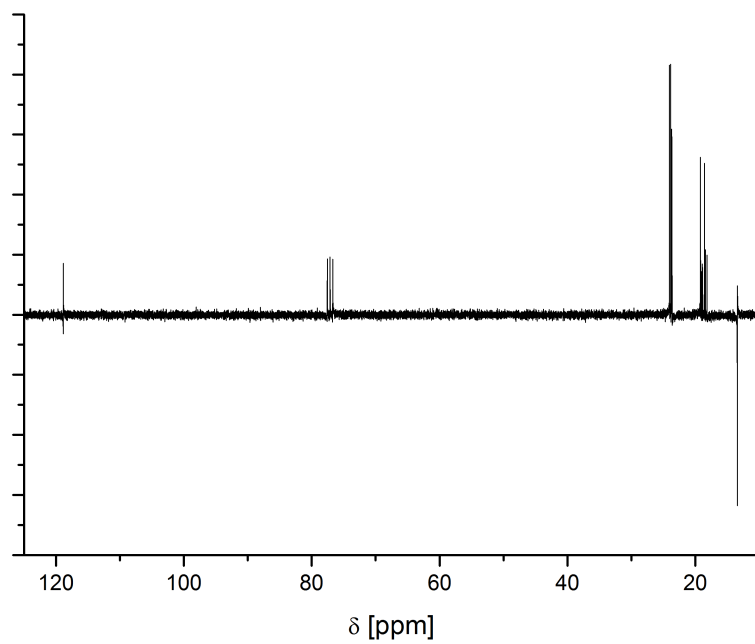
Figure A.54: ^{13}C APT-NMR spectrum of C$_3$CN-n-Bu$_3$PCl.
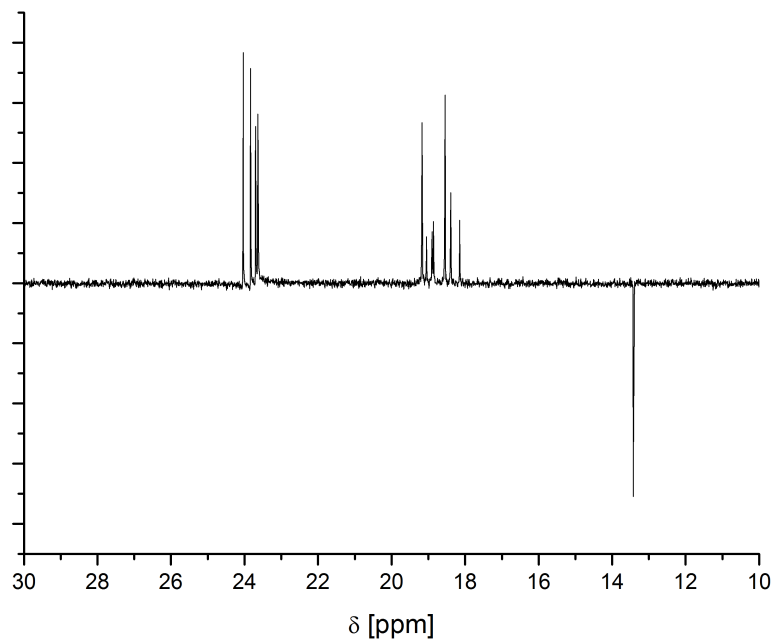
Figure A.55: ^{13}C DEPT-NMR spectrum of C$_3$CN-n-Bu$_3$PCl.
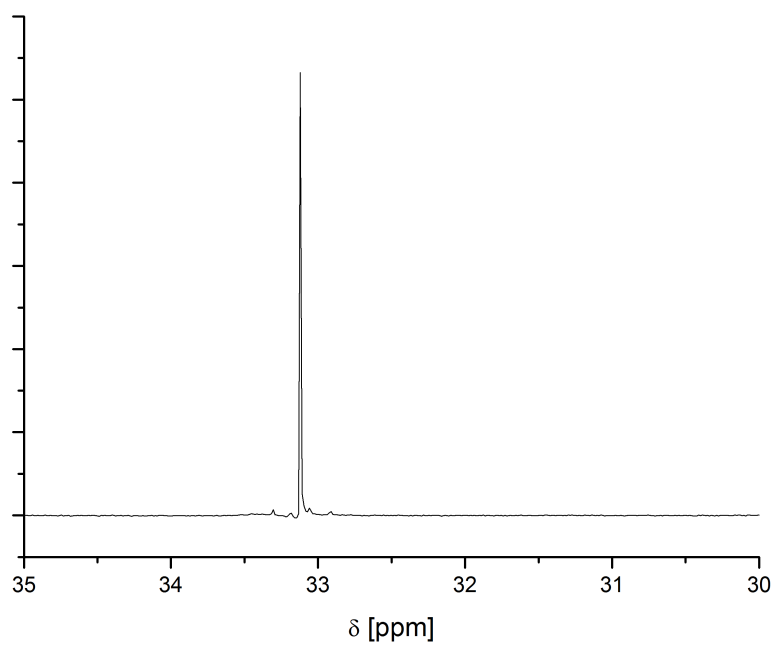
Figure A.56: ^{31}P-NMR spectrum of C$_3$CN-n-Bu$_3$PCl.
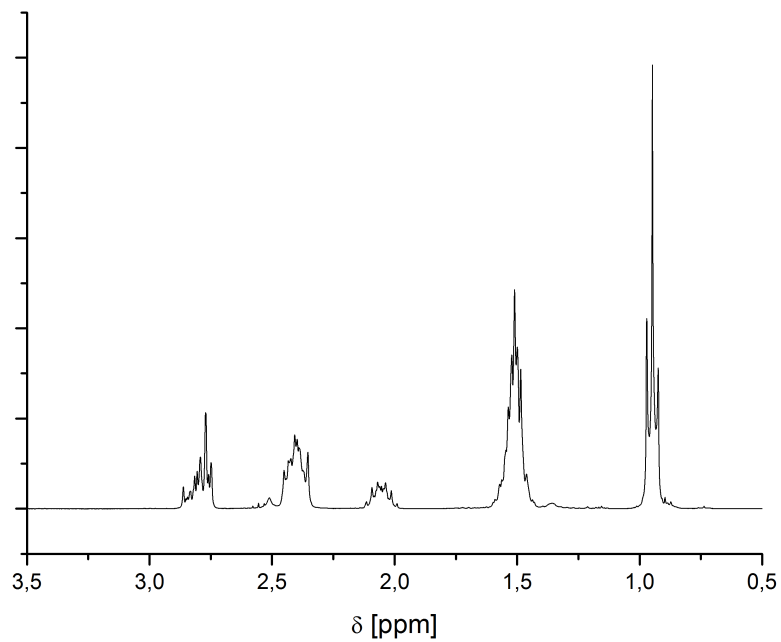
Figure A.57: ^{1}H-NMR spectrum of C$_3$CN-n-Bu$_3$POAc.
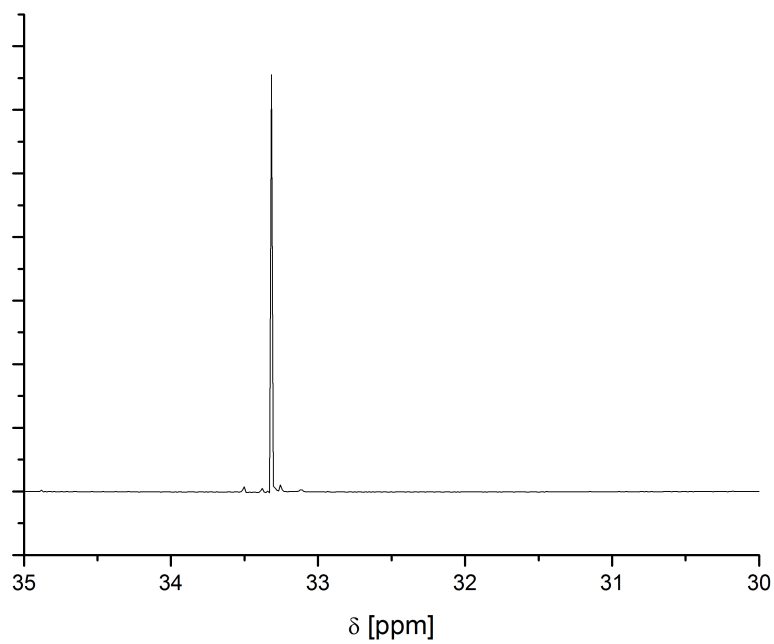
Figure A.58: ^{31}P-NMR spectrum of C$_3$CN-n-Bu$_3$POAc.
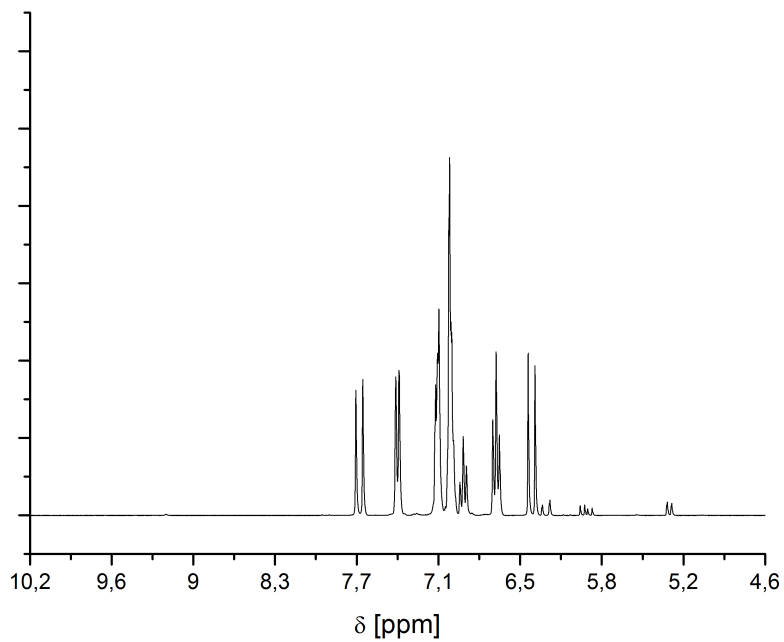
Figure A.59: ^{1}H-NMR spectrum of cinnamic acid butyl ester derived by a *Heck* coupling of iodobenzene and n-butyl acrylate.
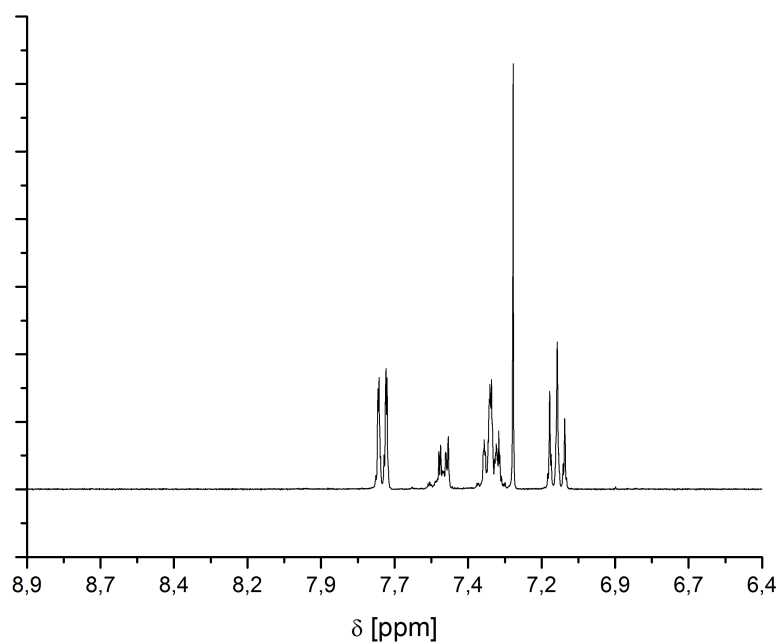
Figure A.60: ^{1}H-NMR spectrum of diphenyl acetylene derived by s *Sonogashira* coupling of iodobenzene and phenyl acetylene.
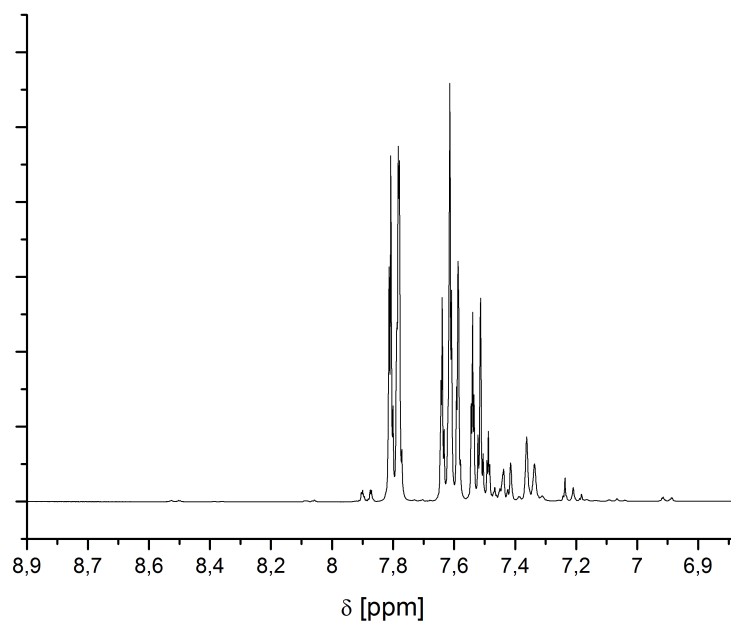
Figure A.61: ^{1}H-NMR spectrum of biphenyl derived by a *Suzuki* coupling of iodobenzene and phenyl boronic acid.
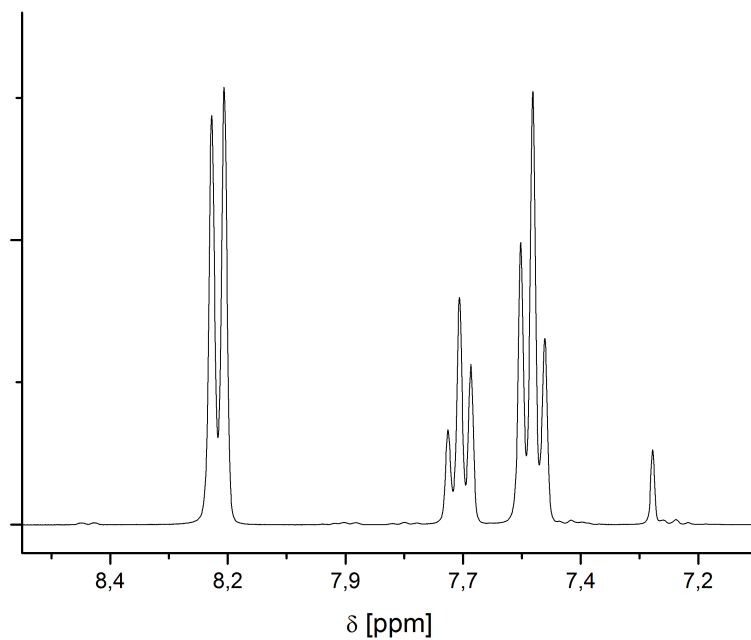
Figure A.62: ¹H-NMR spectrum of nitrobenzene derived by protodecarboxylation of 2-nitrobenzoic acid.
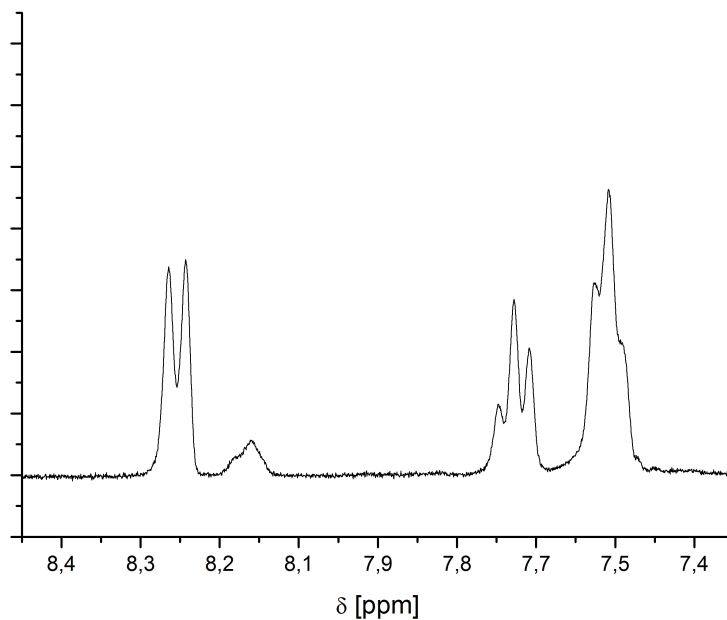
Figure A.63: ¹H-NMR spectrum of *o*-deutero-nitrobenzene derived by regioselective deuterodecarboxylation of 2-nitrobenzoic acid.
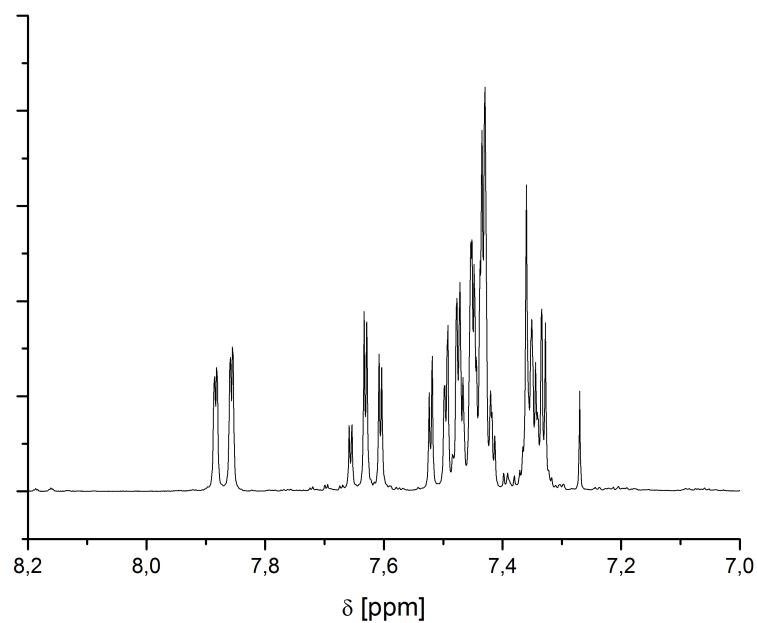
Figure A.64: ^{1}H-NMR spectrum of 2-nitrobiphenyl derived by a decarboxylative cross-coupling in C$_3$CNmpyrr NTf$_2$ and NMP.
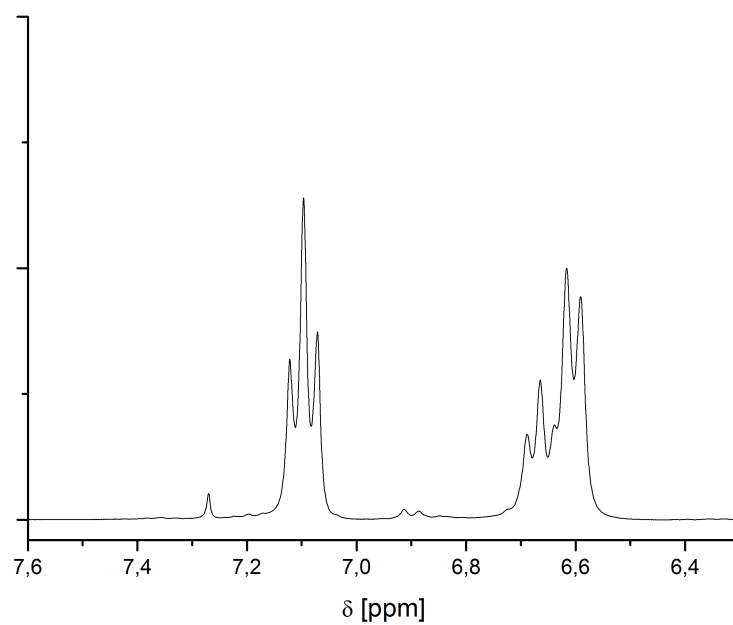
Figure A.65: ^{1}H-NMR spectrum of aniline derived by an amination reaction of iodobenzene with ammonia in n-Bu$_4$POAc.

A.2   IR-spectra
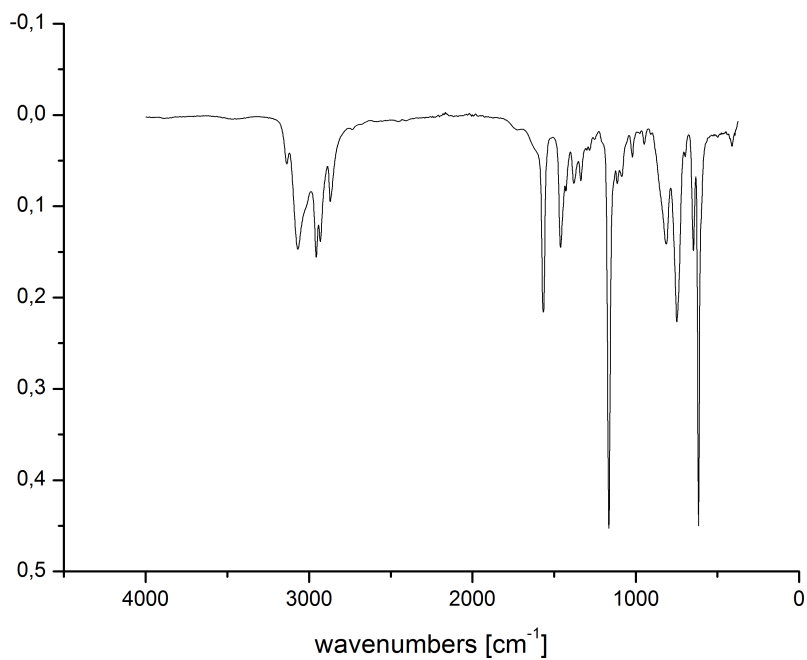
Figure A.66: Transmission IR spectrum of bmim Cl.
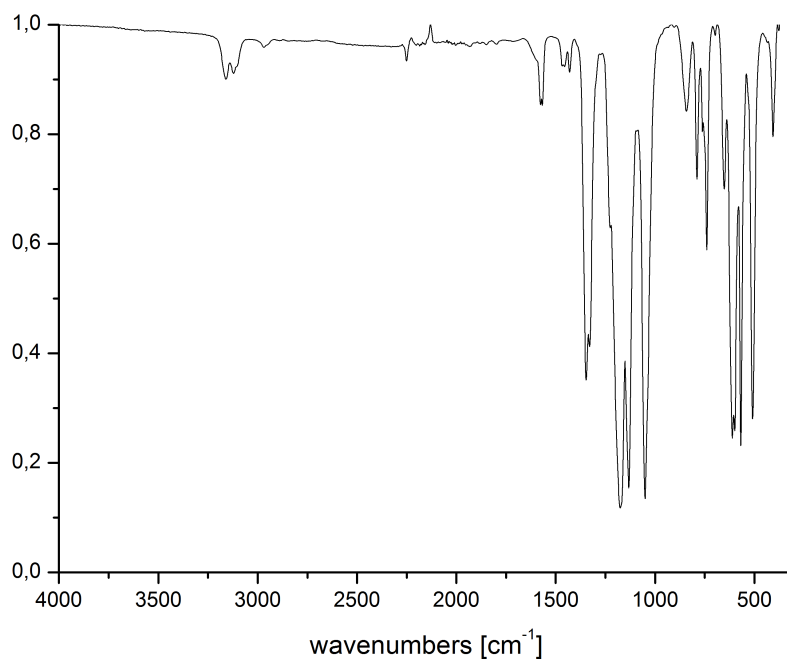
Figure A.67: Transmission IR spectrum of bmim NTf$_2$.
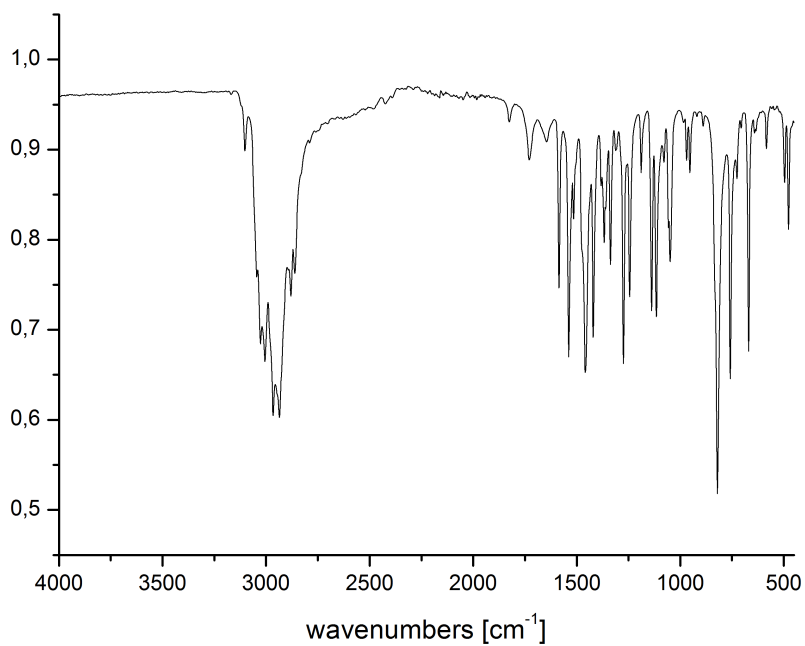
Figure A.68: Transmission IR spectrum of bmmim Cl.
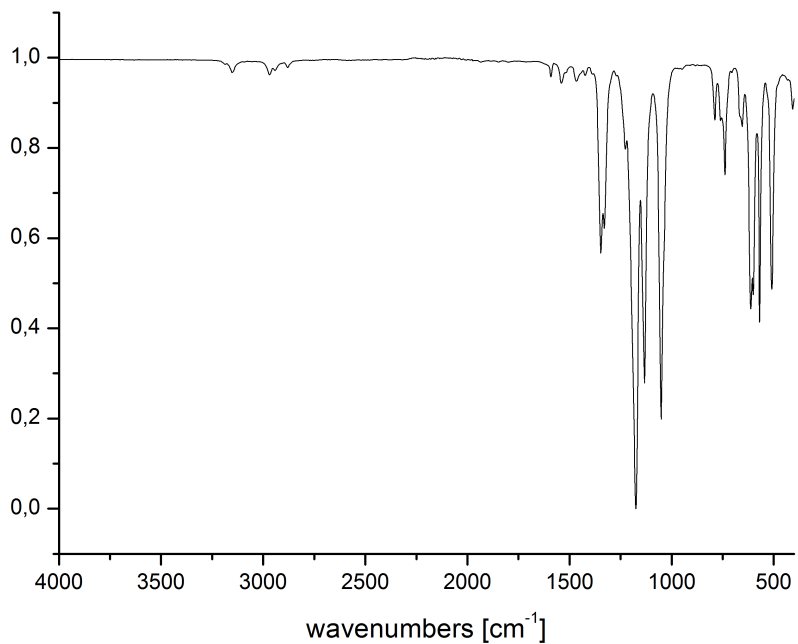
Figure A.69: Transmission IR spectrum of bmmim NTf_2.
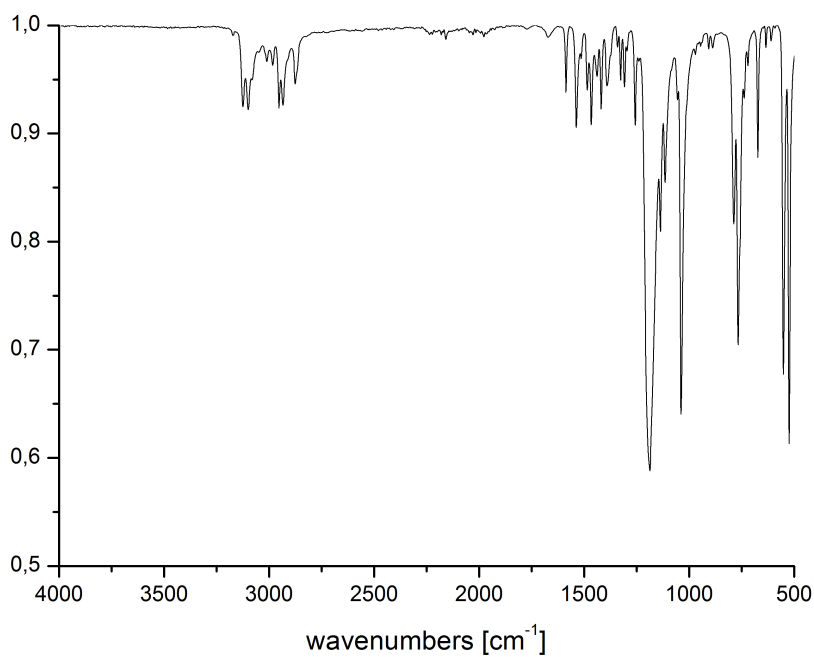
Figure A.70: Transmission IR spectrum of bmmim OMs.
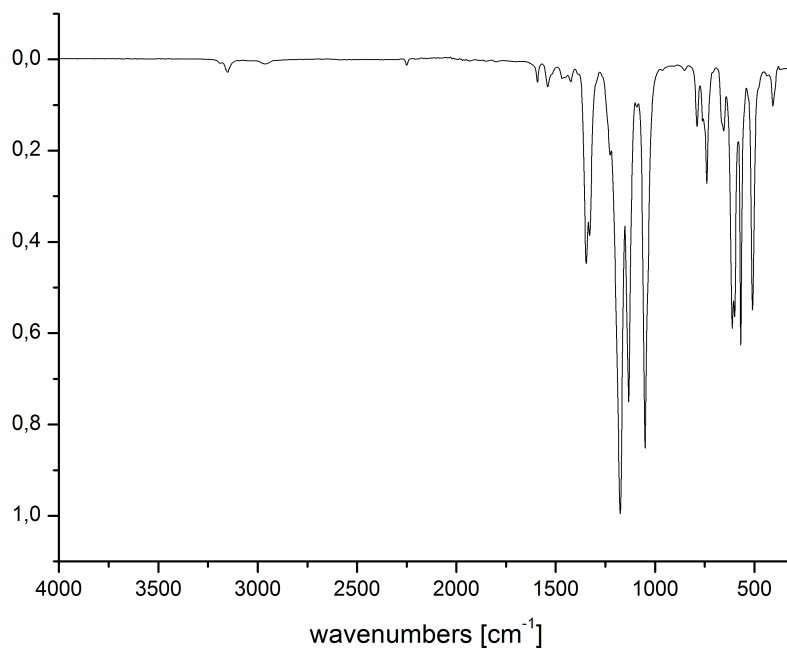
Figure A.71: Transmission IR spectrum of C_3CNmmim NTf$_2$.
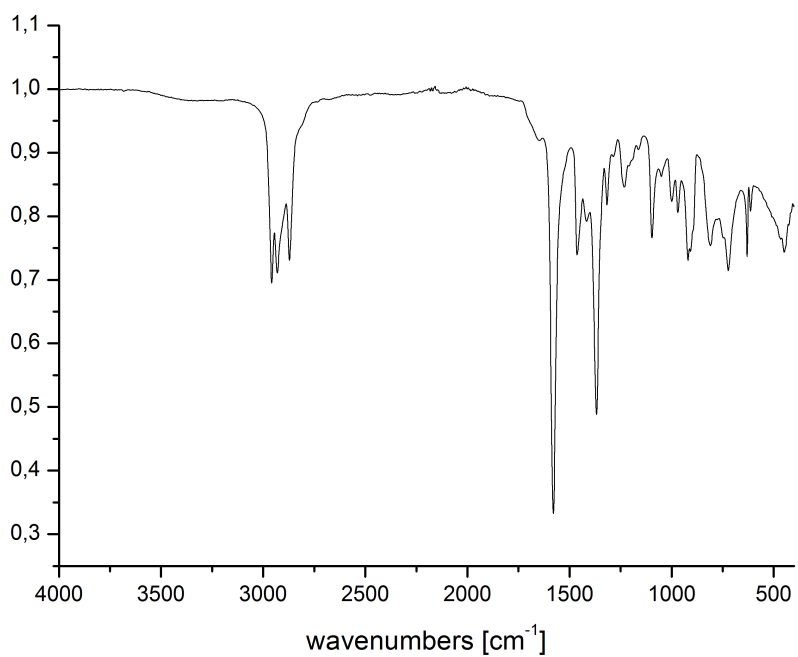
Figure A.72: Transmission IR spectrum of $(n\text{-Bu}_4\text{P})_2\text{SO}_4$.
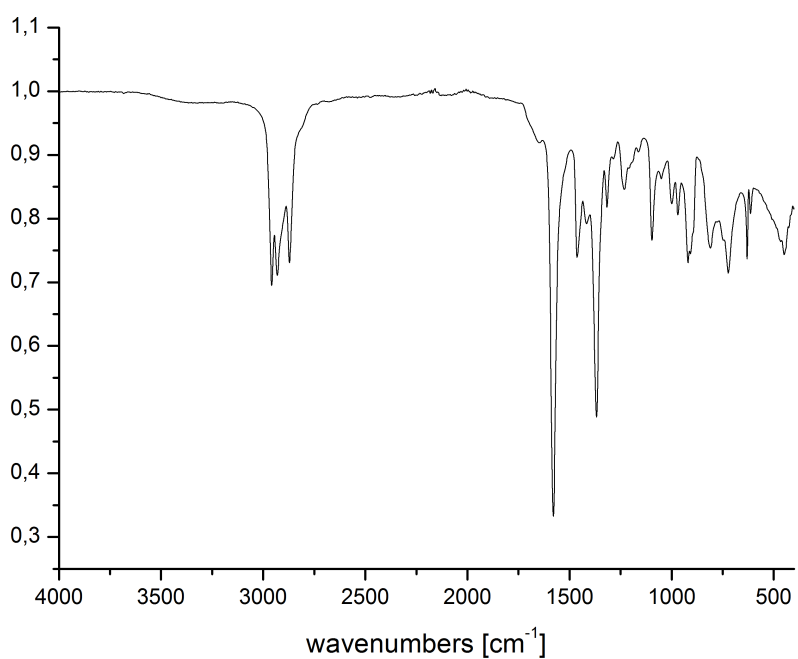
Figure A.73: Transmission IR spectrum of $n\text{-Bu}_4\text{POAc}$.
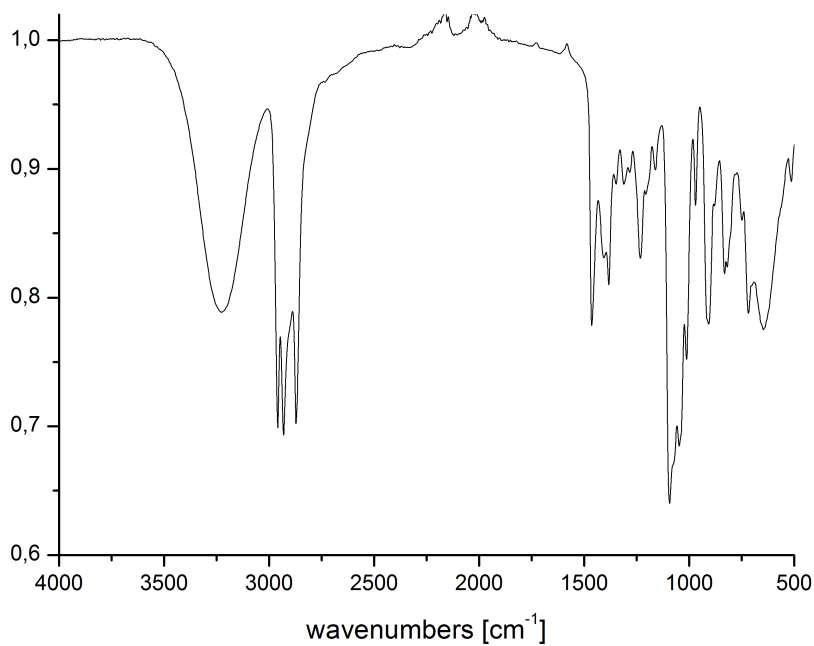
Figure A.74: Transmission IR spectrum of C_3CN-n-Bu_3PCl.
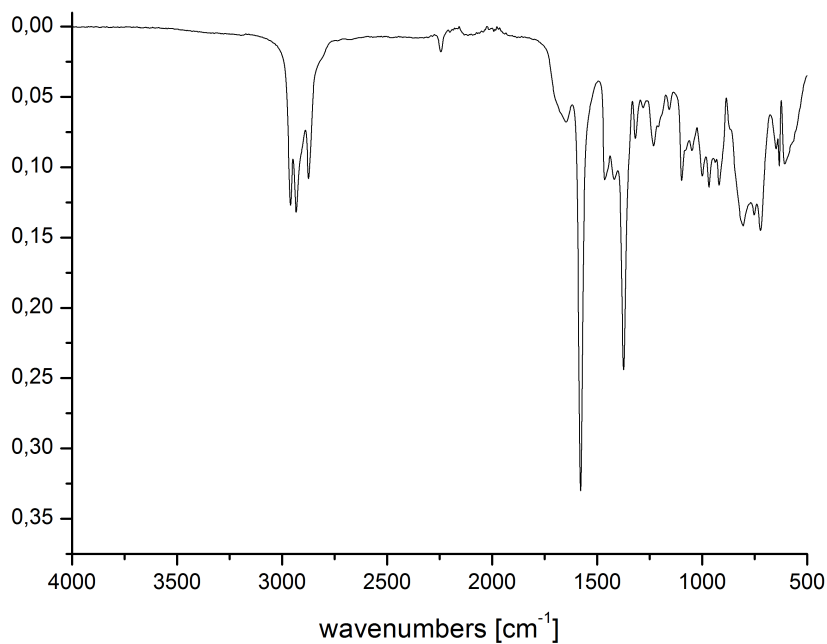
Figure A.75: Transmission IR spectrum of C_3CN-n-Bu_3POAc.

A.3 ICP-OES
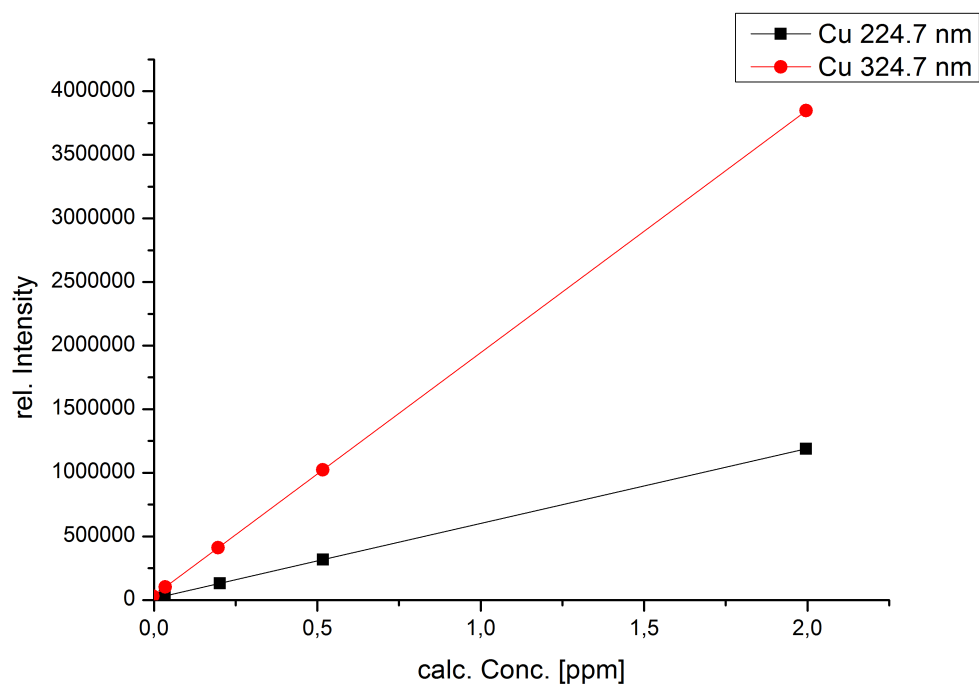
Figure A.76: ICP-OES calibration for Cu at $\lambda = 224.75$ nm and 324.70 nm.
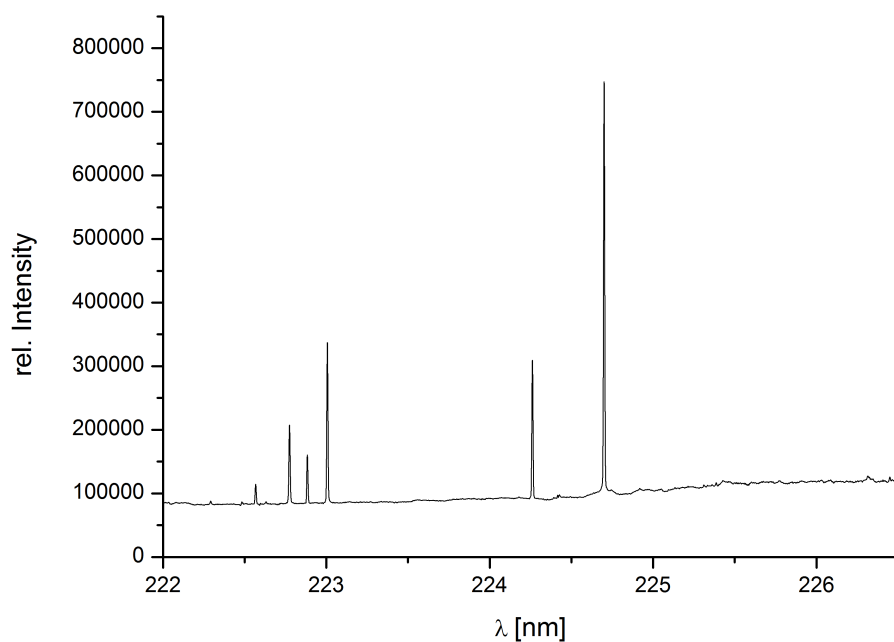
Figure A.77: ICP-OES spectrum calibrated on copper in the range of $\lambda = 222.0$ - 226.5 nm.
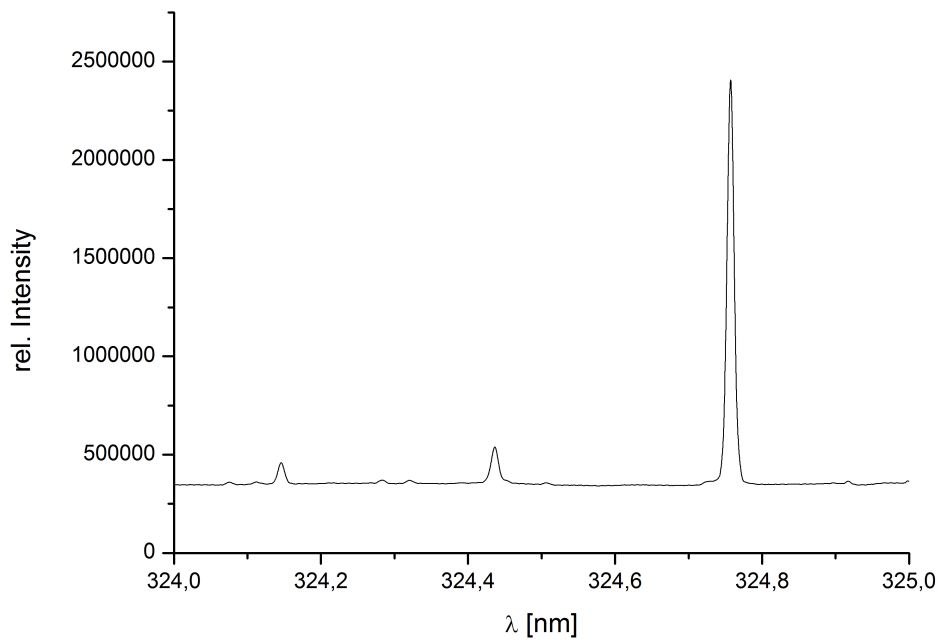
Figure A.78: ICP-OES spectrum calibrated on copper in the range of λ = 324.0 - 325.0 nm.
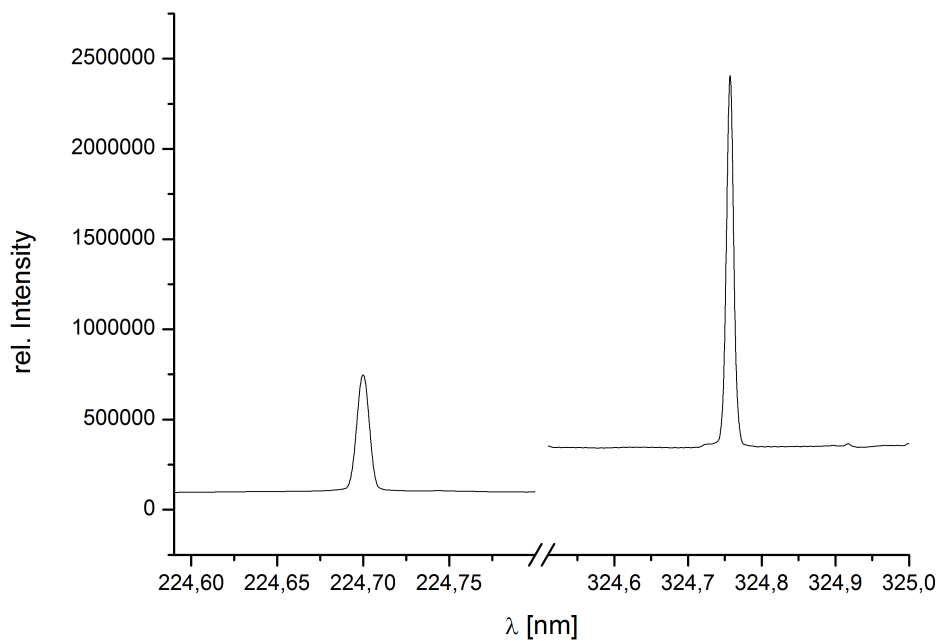
Figure A.79: Fokus on ICP-OES spectrum for two significant Cu signals at λ = 224.75 nm and 324.70 nm.

A.4 ESI Mass Spectra
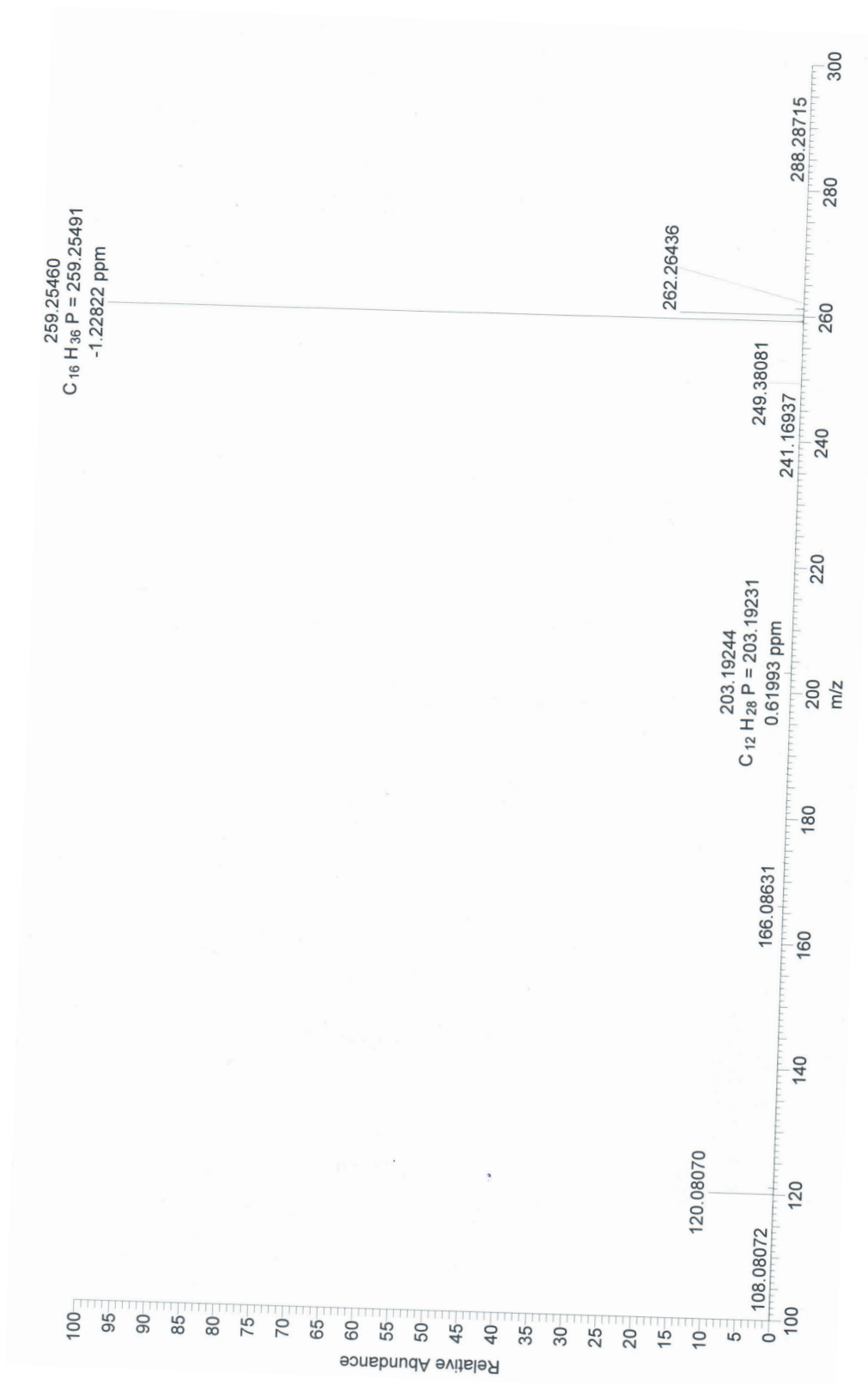
Figure A.80: ESI-MS of the n-Bu$_4$P$^+$ cation in n-Bu$_4$POAc.
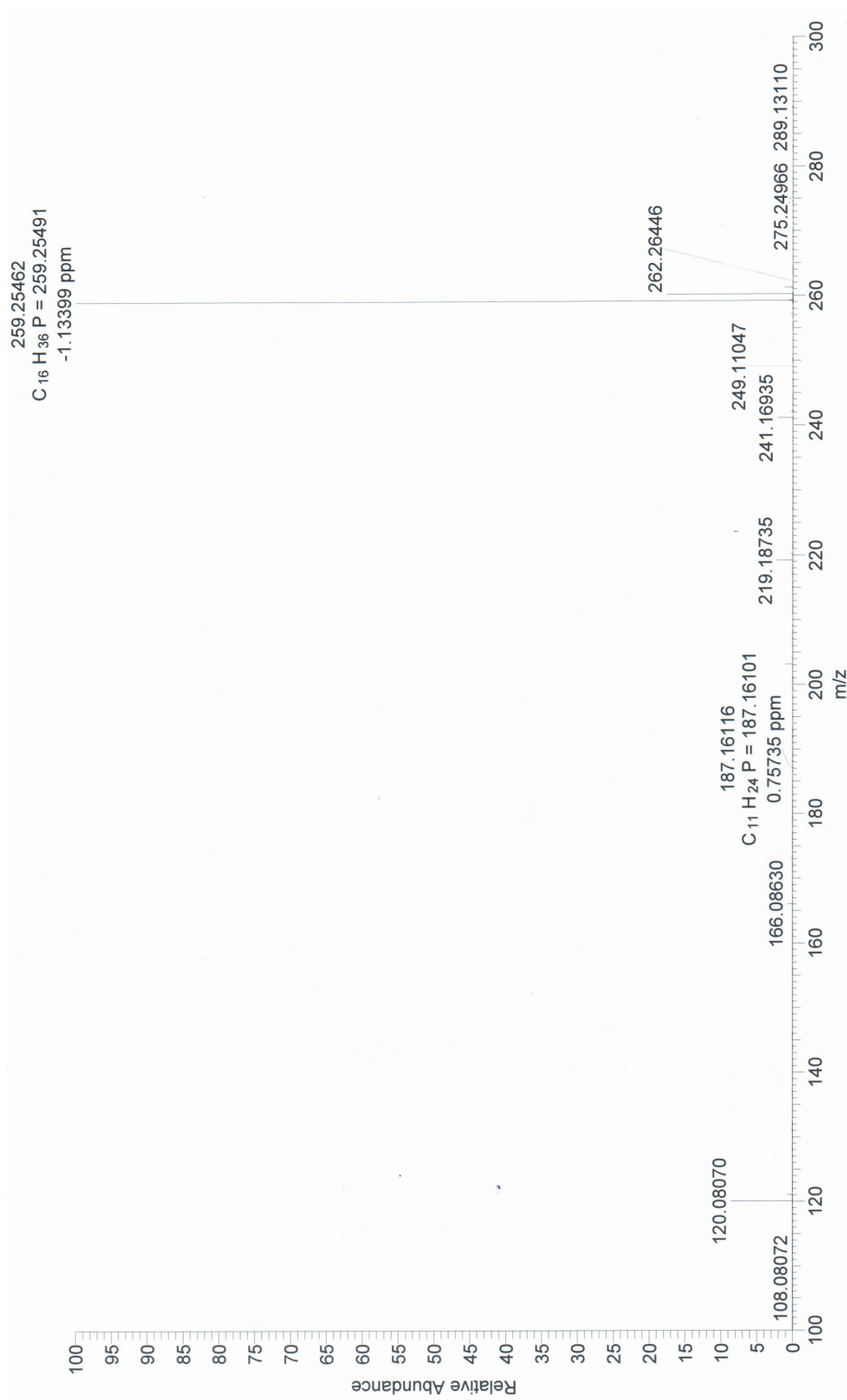
Figure A.81: ESI-MS of the n-Bu$_4$P$^+$ cation in $(n$-Bu$_4$P$)_2$SO$_4$.
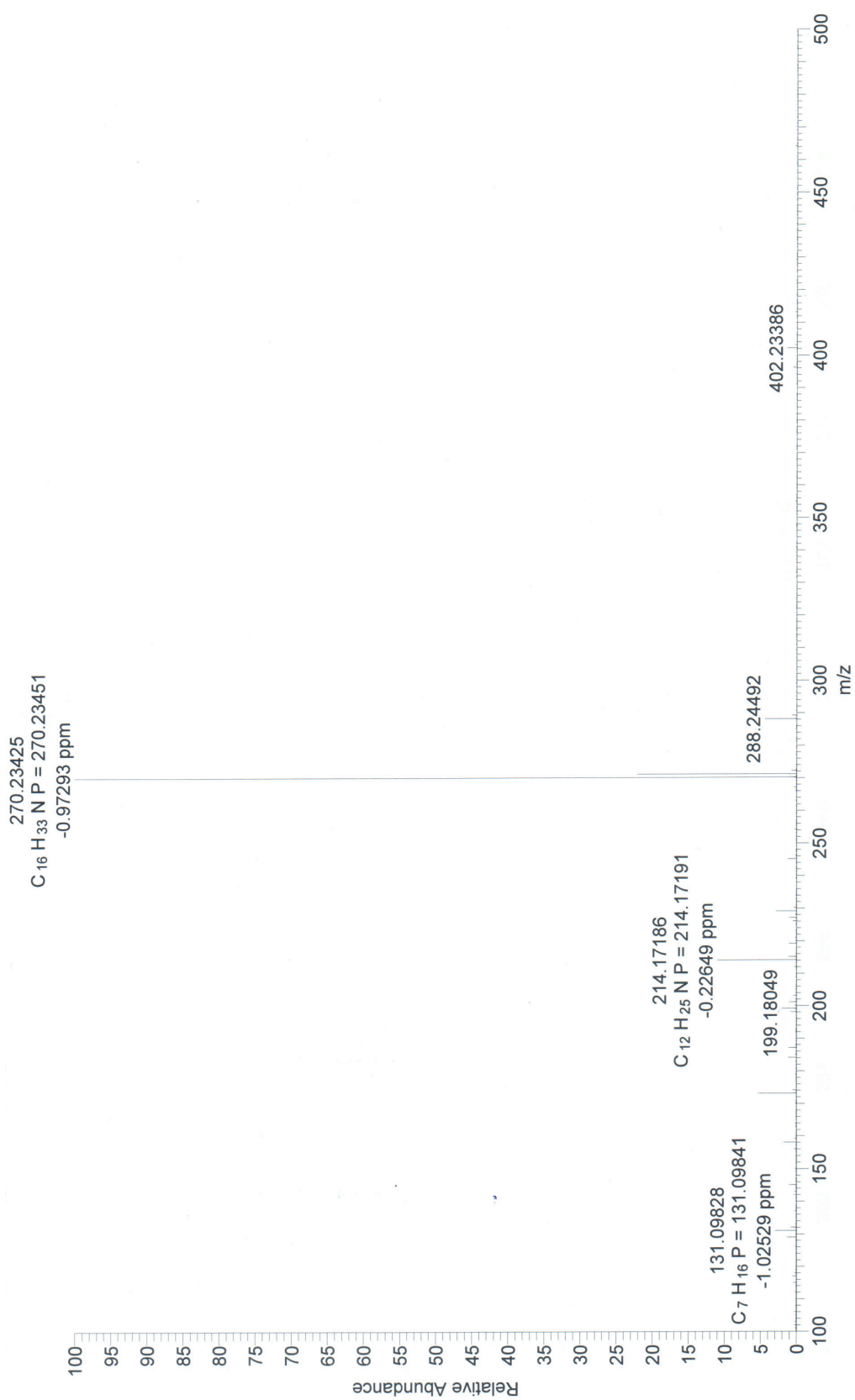
Figure A.82: ESI-MS of the C_3CNn-Bu_3P^+ cation in C_3CNn-Bu_3POAc.

A.5   Electron Microscopy
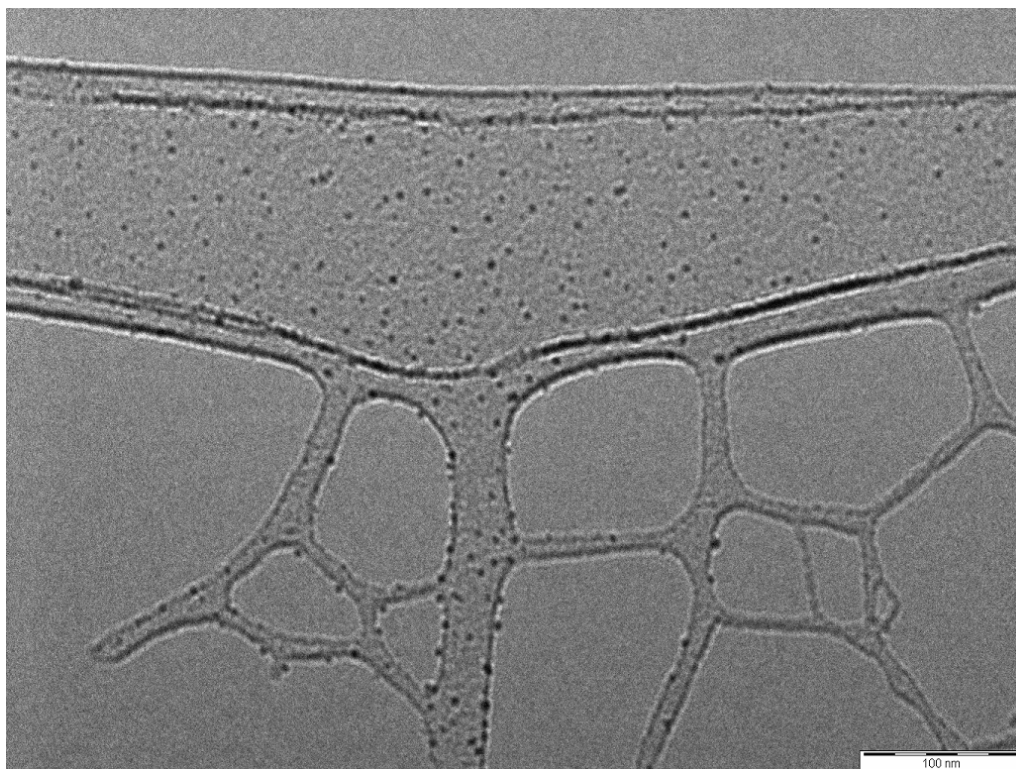
Figure A.83: Additional TEM (120 kV) picture of Cu_2O-NP in n-Bu_4POAc.
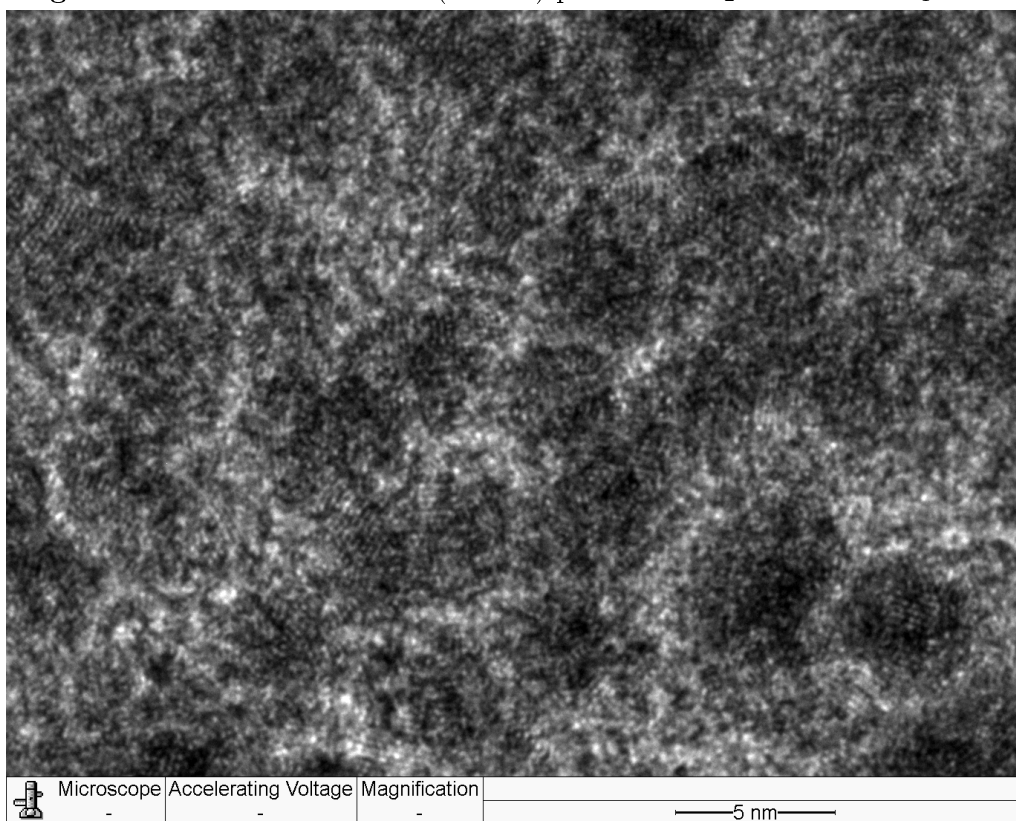
Figure A.84: Additional HR-TEM (200 kV) picture of Pd/Cu-NP in n-Bu_4POAc.
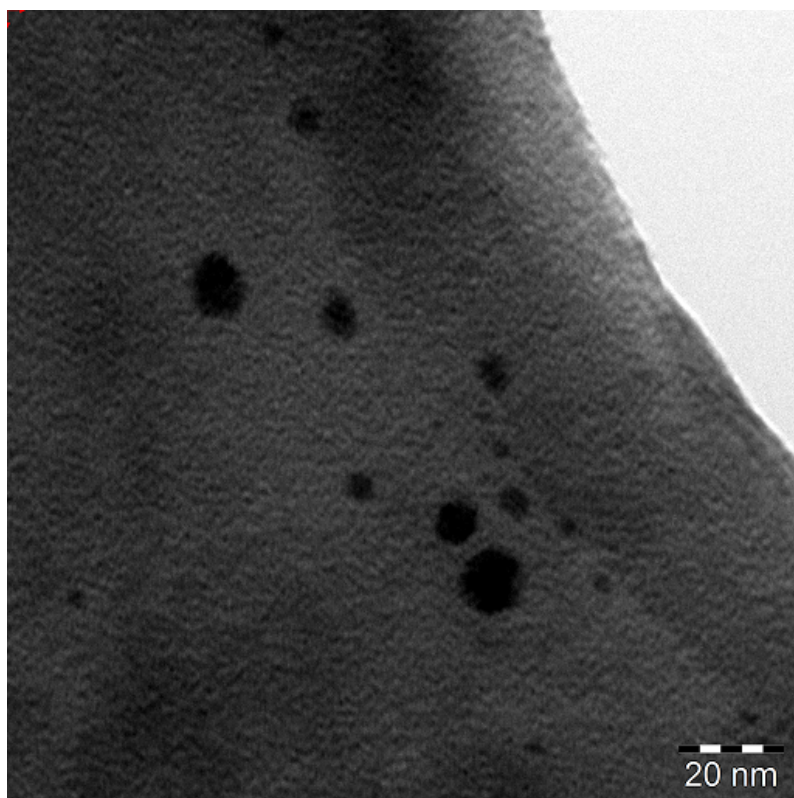
Figure A.85: Additional TEM (120 kV) picture of Ag-NP in n-Bu$_4$POAc.
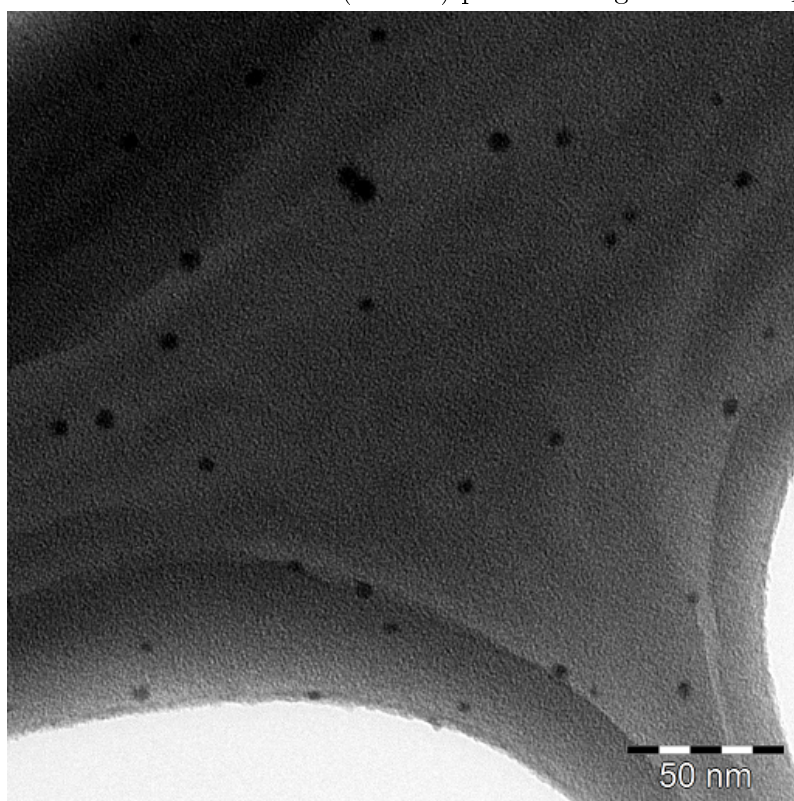
Figure A.86: Additional TEM (120 kV) picture of Ag-NP in bmmim NTf$_2$.
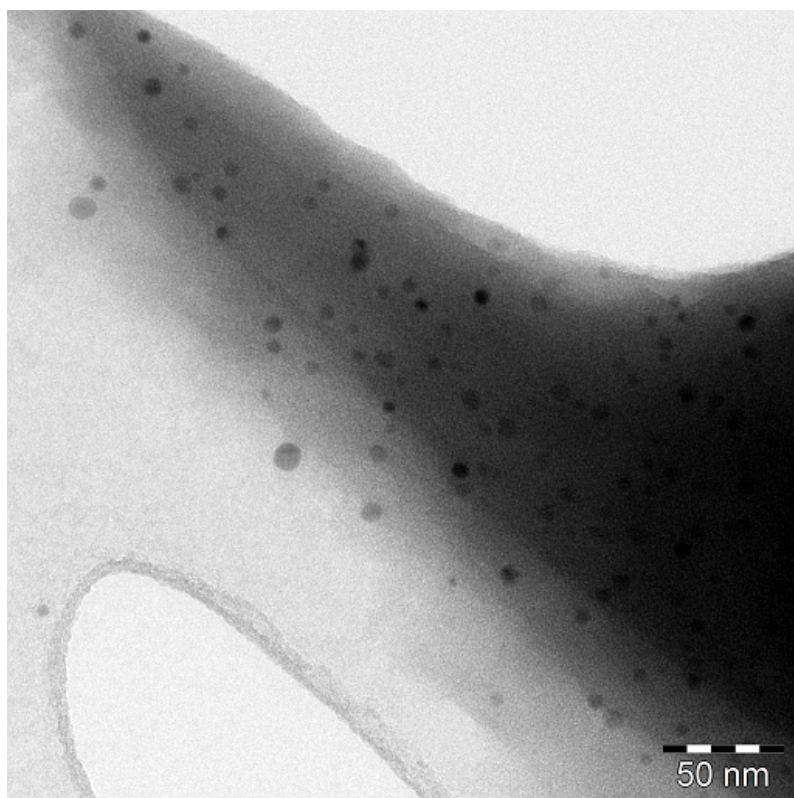
Figure A.87: Additional TEM (120 kV) picture of Cu-NP in n-Bu$_4$POAc.
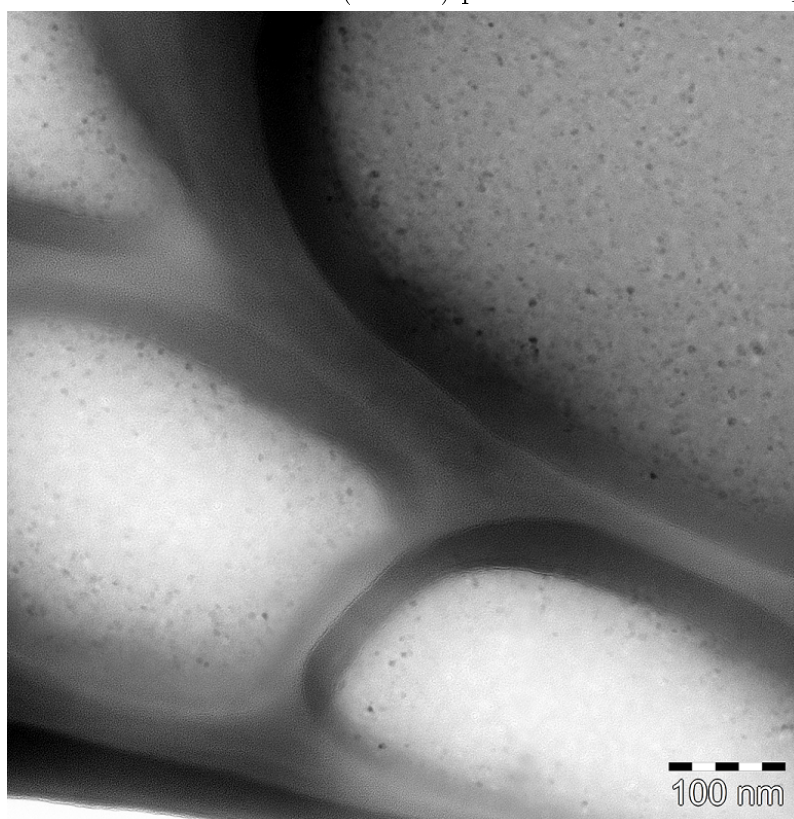
Figure A.88: Additional TEM (120 kV) picture of Cu-NP in bmmim NTf$_2$.
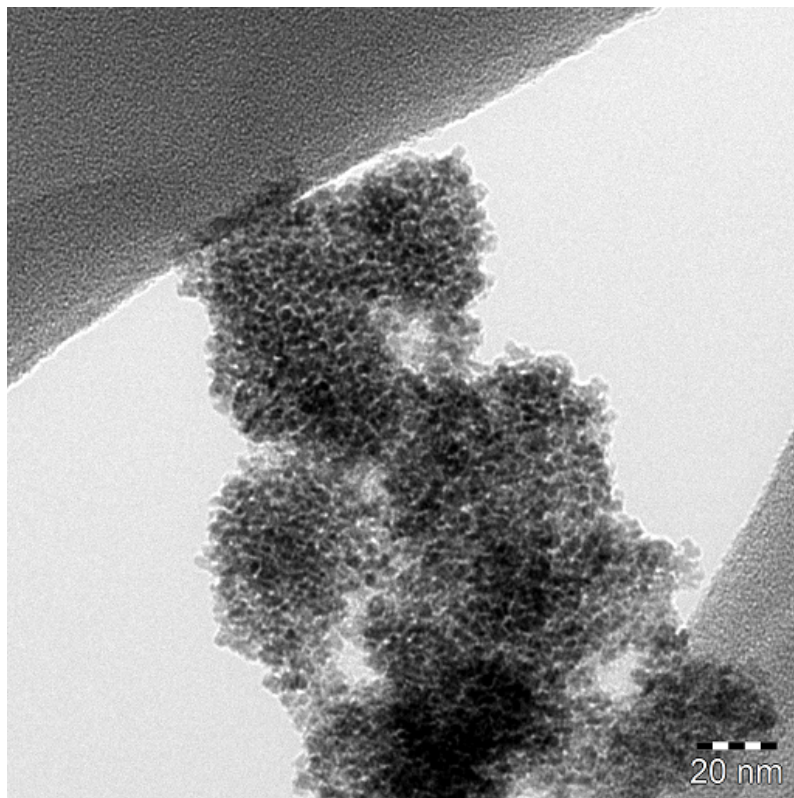
Figure A.89: Additional TEM (120 kV) picture of NiO-NP in n-Bu$_4$POAc.
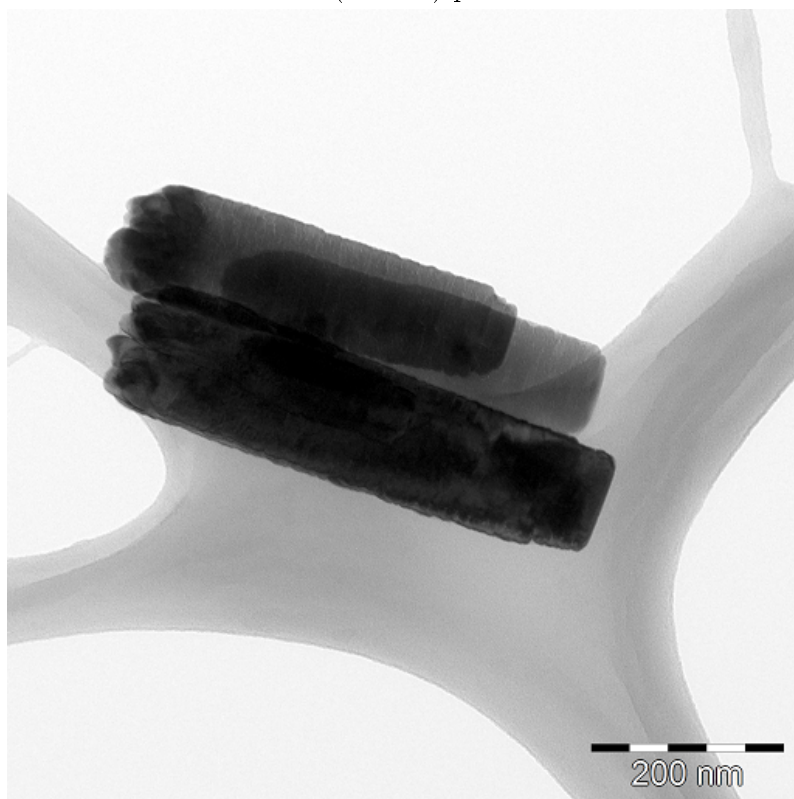
Figure A.90: Additional TEM (120 kV) picture of ZnO-NP in n-Bu$_4$POAc.
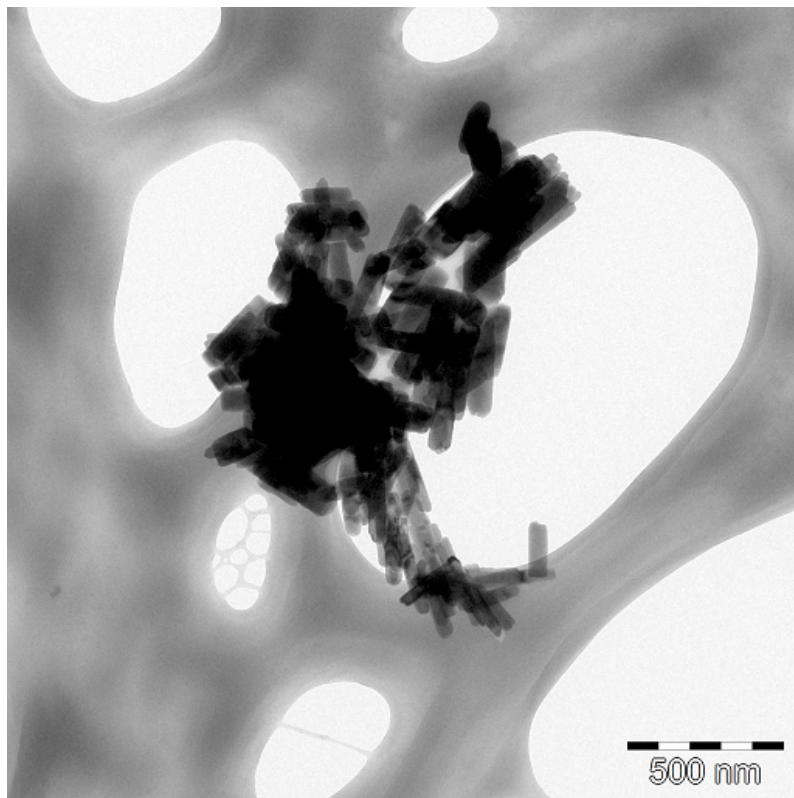
Figure A.91: Additional TEM (120 kV) picture of ZnO-NP in n-Bu$_4$POAc.

B | Abbreviations

T	temperature [°C]
t	time [s], [min], [h]
d	diameter of particle, structure etc. [nm]
r	particle radius [nm]
n	amount of substance [mol]
mol%	molar percentage of catalyst
m	mass [mg]
M	Molar mass [g/mol]
λ	wavelenght [nm]
rpm	revolutions per minute [1/min]
Hz	Hertz [1/s]
W	power, Watt
NMR	nuclear magnetic resonance spectroscopy
s	singulett - NMR descriptor
d	doublett - NMR descriptor
t	triplet - NMR descriptor
quart	quartett - NMR descriptor
quint	quintett - NMR descriptor
sext	sextett - NMR descriptor
m	multiplett - NMR descriptor
J	coupling constant [Hz]
δ	rel. chemical shift [ppm]
ppm	parts per million, e.g. chemical shift or concentration
XRD	X-ray diffraction
(2Θ)	scattering angle [°]
IR	infra red, infra red spectroscopy
w	weak - IR descriptor
m	medium - IR descriptor
s	strong - IR descriptor
$\tilde{\nu}$	wavenumber [cm^{-1}]
Å	Angström; 1 Å = 10^{-10} m
EXAFS	extended X-ray absorption fine structure
XANES	X-ray absorption near-edge structure spectroscopy
XPS	X-ray photoelectron spectroscopy
eV	electronvolts [eV]
GC-MS	gas chromatography with
ICP-OES	inductively coupled plasma optical emission spectrometry
SEM	scanning electron microscopy
TEM	transmission electron microscopy

HRTEM	high resolution TEM
SAED	selected area electron diffraction
CVD	Chemical Vapour Deposition
PECVD	Plasma Enhanced Chemical Vapour Deposition
NP	nanoparticle
IL	ionic liquid
RTIL	room temperature ionic liquid with melting point below 25 °C
bmim	1-butyl-3-methylimidazolium cation
bmmim	1-butyl-2,3-dimethylimidazolium cation
C$_3$CNmim	1-cyanopropyl-3-methylimidazolium cation
C$_3$CNmmim	1-cyanopropyl-2,3-dimethylimidazolium cation
bpy	*N*-butylpyridinium cation
C$_3$CNpy	*N*-cyanopropylpyridinium cation
bmpyrr	*N*-butyl-*N*-methylpyrrolidinium cation
C$_3$CNmpyrr	*N*-cyanopropyl-*N*-methylpyrrolidinium cation
NTf$_2$	*N,N*-bis(trifluoromethylsulfonyl)imide anion
OMs	methylsulfonate anion
COD	1,5-cyclooctadien
COT	1,3,5-cyclooctatrien
NMP	*N*-Methyl-pyrrolidone

Bibliography

[1] Lem, W.; Choudhury, A.; Lakhani, A.; Kuyate, P.; Haw, R.; Lee, S.; Iqbal, Z.; Brumlik, J. *Rec. Pat. Nanotech.* **2012**, *6*, 60–72.

[2] Wong, K. V.; Perilla, N.; Paddon, A. *J. Energ. Resour. - ASME* **2013**, *136*, 014001.

[3] Rippel, R. A.; Seifalian, A. M. *J. Nanosci. Nanotechnol.* **2011**, *11*, 3740–3748.

[4] Skocaj, M.; Filipic, M.; Petkovic, J.; Novak, S. *Radiol. Oncol.* **2011**, *45*, 227–247.

[5] Bottini, M.; Rosato, N.; Gloria, F.; Adanti, S.; Corradino, N.; Bergamaschi, A.; Magrini, A. *Int. J. Nanomed.* **2011**, *6*, 3473–3485.

[6] Ariga, K.; Hu, X.; Mandal, S.; Hill, J. P. *Nanoscale* **2010**, *2*, 198–214.

[7] Batt, C. A.; Waldron, A. M.; Broadwater, N. *J. Nanoparticle Res* **2008**, *10*, 1141–1148.

[8] Tetley, T. D. *Biochem. Soc. Trans.* **2007**, *35*, 527–31.

[9] Uskokovic, V. *J Biomed Nanotechnol* **2013**, *9*, 1441–1470.

[10] Johnson-McDaniel, D.; Barrett, C. A.; Sharafi, A.; Salguero, T. T. *J. Am. Chem. Soc.* **2013**, *135*, 1677–1679.

[11] Santamaria, A. *Methods in Molecular Biology;* volume 926 Springer Link: Berlin, 2012.

[12] Cassius, A. *De Extremo Illo Et Perfectissimo Naturae Opificio Ac Principe Terraenorum Sidere Auro;* Universitätsbiblithek Leipzig: Leipzig, 1685.

[13] Edwards, P. P.; Thomas, J. M. *Angew. Chem. Int. Ed.* **2007**, *46*, 5480–5486.

[14] Freestone, I.; Meeks, N.; Sax, M.; Higgitt, C. *Gold Bulletin* **2007**, *40*, 270–277.

[15] Faraday, M. *Philos. Trans. R. Soc. London* **1857**, *147*, 145–181.

[16] Bönnemann, H.; Brijoux, W.; Joussen, T. *Angew. Chem. Int. Ed.* **1990**, *29*, 273–275.

[17] Bönnemann, H.; Brijoux, W.; Brinkmann, R.; Joussen, T.; Korall, B.; Dinjus, E. *Angew. Chem. Int. Ed.* **1991**, *30*, 1312–1314.

[18] Granqvist, C. G.; Buhrman, R. A.; Wyns, J.; Sievers, A. J. *Phys. Rev. Lett.* **1976**, *37*, 625–629.

[19] Patzke, G. R.; Zhou, Y.; Kontic, R.; Conrad, F. *Angew. Chem. Int. Ed.* **2011**, *50*, 826–859.

[20] Pitcher, M. W. *Science* **2006**, *313*, 300.

[21] Leonard, F.; Talin, A. A. *Nature Nano* **2011**, *6*, 773–783.

[22] Ozin, G. A. *Adv. Mater.* **1992**, *4*, 612–649.

[23] Whitesides, G. M.; Mathias, J. P.; Seto, C. T. *Science* **1991**, *254*, 1312–1319.

[24] Hennon, J.; Westeren, M. *European Commission - Press release* **2011**, .

[25] Bloom, H.; Heymann, E. *Proc. RSC London, Ser. A* **1947**, *188*, 329–414.

[26] Gabriel, S.; Weiner, J. *Ber. Dt. Chem. Ges* **1888**, *21*, 2669–2679.

[27] Walden, P. *Bull. Acad. Imper. Sci. St. Petersbg.* **1914,** *8,* 405–422.

[28] Chum, H. L.; Koch, V. R.; Miller, L. L.; Osteryoung, R. A. *J. Am. Chem. Soc.* **1975,** *97,* 3264–3265.

[29] Wasserscheid, P.; Keim, W. *Angew. Chem. Int. Ed.* **2000,** *39,* 3772–3789.

[30] Dupont, J. *Accounts Chem. Res.* **2011,** *44,* 1223–1231.

[31] Wilkes, J. S.; Levisky, J. A.; Wilson, R. A.; Hussey, C. L. *Inorg. Chem.* **1982,** *21,* 1263–1264.

[32] Hussey, C. L. *Pure Appl. Chem* **1988,** *60,* 1763–1772.

[33] Freemantle, M. *Chem. Eng. News* **1998,** *76,* 32–37.

[34] Darwich, W.; Gedig, C.; Srour, H.; Santini, C. C.; Prechtl, M. H. G. *RSC Adv.* **2013,** *3,* 20324–20331.

[35] Gieshoff, T. N.; Welther, A.; Kessler, M. T.; Precht, M. H. G.; von Wangelin, A. *Chem. Commun.* **2014,** *50,* 2261–2264.

[36] Zhao, B.; Greiner, L.; Leitner, W. *RSC Adv.* **2012,** *2,* 2476–2479.

[37] Caló, V.; Nacci, A.; Monopoli, A.; Cotugno, P. *Angew. Chem. Int. Ed.* **2009,** *48,* 6101–6103.

[38] Cassol, C. C.; Umpierre, A. P.; Machado, G.; Wolke, S. I.; Dupont, J. *J. Am. Chem. Soc.* **2005,** *127,* 3298–3299.

[39] Dupont, J.; Scholten, J. D. *Chem. Soc. Rev.* **2010,** *39,* 1780–1804.

[40] Kessler, M. T.; Gedig, C.; Sahler, S.; Wand, P.; Robke, S.; Prechtl, M. H. G. *Catal. Sci. Technol.* **2013,** *3,* 992–1001.

[41] Holloczki, O.; Malberg, F.; Welton, T.; Kirchner, B. *Phys. Chem. Chem. Phys.* **2014,** *16,* 16880-16890.

[42] Tödheide, K. *Angew. Chem. Int. Ed.* **1980,** *19,* 606–619.

[43] Stegemann, H.; Rohde, A.; Reiche, A.; Schnittke, A.; Füllbier, H. *Electrochim. Acta* **1992,** *37,* 379–383.

[44] Seddon, K. R. *J. Chem. Technol. Biotechnol.* **1997,** *68,* 351–356.

[45] Seddon, K. R. *Kinet. Catal. Engl. Transl* **1996,** *37,* 693–697.

[46] Bonhôte, P.; Dias, A.-P.; Papageorgiou, N.; Kalyanasundaram, K.; Grätzel, M. *Inorg. Chem.* **1996,** *35,* 1168–1178.

[47] Elaiwi, A.; Hitchcock, P. B.; Seddon, K. R.; Srinivasan, N.; Tan, Y.-M.; Welton, T.; Zora, J. A. *Dalton Trans.* **1995,** 3467–3472.

[48] Fannin, A. A.; Floreani, D. A.; King, L. A.; Landers, J. S.; Piersma, B. J.; Stech, D. J.; Vaughn, R. L.; Wilkes, J. S.; Williams, J. *J. Phys. Chem.* **1984,** *88,* 2614–2621.

[49] Earle, M. J.; Esperanca, J. M. S. S.; Gilea, M. A.; Lopes, C.; Jose, N.; Rebelo, L. P. N.; Magee, J. W.; Seddon, K. R.; Widegren, J. A. *Nature* **2006,** *439,* 831–834.

[50] Taft, R. W.; Kamlet, M. J. *J. Am. Chem. Soc.* **1976,** *98,* 2886–2894.

[51] Jessop, P. G.; Jessop, D. A.; Fu, D.; Phan, L. *Green Chem.* **2012,** *14,* 1245–1259.

[52] Kerton, F. M.; Marriott, R. *Alternative Solvents for Green Chemistry;* RSC-Publishing: London, 2nd ed.; 2013.

[53] Kerton, F. M.; Marriott, R. *Alternative Solvents for Green Chemistry;* RSC-Publishing: London, 2nd ed.; 2013.

[54] Postleb, F.; Stefanik., D.; Seifert, H.; Giernoth, R. *Zeitschrift fur Naturforsch.* **2013,** *68,* 1123–1128.

[55] Wu, B.; Reddy, R. G.; Rogers, R. D. *Int. Sol. Energy Conf.* **2001,** 445–451.

[56] Kuboki, T.; Okuyama, T.; Ohsaki, T.; Takami, N. *J. Power Sources* **2005**, *146*, 766–769.

[57] Graenacher, C. *US-patent No. 1943176* **1934**, .

[58] Yoshizawa-Fujita, M.; Johansson, K.; Newman, P.; MacFarlane, D. R.; Forsyth, M. *Tetrahedron Lett.* **2006**, *47*, 2755–2758.

[59] Vitz, J.; Erdmenger, T.; Haensch, C.; Schubert, U. S. *Green Chem.* **2009**, *11*, 417–424.

[60] Kim, B.; Jeong, J.; Lee, D.; Kim, S.; Yoon, H.-J.; Lee, Y.-S.; Cho, J. K. *Green Chem.* **2011**, *13*, 1503–1506.

[61] Kessler, M. T.; Scholten, J. D.; Prechtl, M. H. G. *Metal Catalists Immobilized in Ionic Liquids: A Couple with Opportunities Fine Chemicals Derived from Biomass;* Elsevier: Amsterdam, 2013.

[62] Cui, Y.; Biondi, I.; Chaubey, M.; Yang, X.; Fei, Z.; Scopelliti, R.; Hartinger, C. G.; Li, Y.; Chiappe, C.; Dyson, P. J. *Phys. Chem. Chem. Phys.* **2010**, *12*, 1834–1841.

[63] Fei, Z.; Zhao, D.; Pieraccini, D.; Ang, W. H.; Geldbach, T. J.; Scopelliti, R.; Chiappe, C.; Dyson, P. J. *Organometallics* **2007**, *26*, 1588–1598.

[64] Wender, H.; Migowski, P.; Feil, A. F.; de Oliveira, L. F.; Prechtl, M. H. G.; Leal, R.; Machado, G.; Teixeira, S. R.; Dupont, J. *Phys. Chem. Chem. Phys.* **2011**, *13*, 13552–13557.

[65] Zhao, D.; Fei, Z.; Scopelliti, R.; Dyson, P. J. *Inorg. Chem.* **2004**, *43*, 2197–2205.

[66] Ananikov, V. P.; Beletskaya, I. P. *Organometallics* **2012**, *31*, 1595–1604.

[67] Pacifico, J.; van Leeuwen, Y. M.; Spuch-Calvar, M.; Sanchez-Iglesias, A.; Rodriguez-Lorenzo, L.; Perez-Juste, J.; Pastoriza-Santos, I.; Liz-Marzan, L. M. *Nanotechnology* **2009**, *20*, 95708.

[68] Carlsson, A.; Puig-Molina, A.; Janssens, T. V. W. *J. Phys. Chem. B* **2006**, *110*, 5286–5293.

[69] Polanyi, M. *Angew. Chem.* **1927**, *40*, 908–909.

[70] Loeve, S. *Hyle* **2010**, *16*, 3–18.

[71] Wiesner, M. R.; Lowry, G. V.; Casman, E.; Bertsch, P. M.; Matson, C. W.; Giulio, R. T. D.; Liu, J.; Hochella, M. F. *ACS Nano* **2011**, *5*, 8466–8470.

[72] Yamamoto, H.; Ohnuma, A.; Ohtani, B.; Kozawa, T. *Microelectron. Eng.* **2013**, *110*, 369–373.

[73] Narayana, S.; Agarwal, A. K.; Bajpai, R. P. "IETE technical review: The Institution of Electronics and Telecommunication Engineers", 2007.

[74] Carpenter, M. K.; Moylan, T. E.; Kukreja, R. S.; Atwan, M. H.; Tessema, M. M. *J. Am. Chem. Soc.* **2012**, *134*, 8535–8542.

[75] Yang, Y.; Matsubara, S.; Xiong, L.; Hayakawa, T.; Nogami, M. *J. Phys. Chem. C* **2007**, *111*, 9095–9104.

[76] LaMer, V. K.; Dinegar, R. H. *J. Am. Chem. Soc.* **1950**, *72*, 4847–4854.

[77] LaMer, V. K. *Ind. Eng. Chem.* **1952**, *44*, 1270–1277.

[78] Watzky, M. A.; Finke, R. G. *J. Am. Chem. Soc.* **1997**, *119*, 10382–10400.

[79] Turkevich, J.; Garton, G.; Stevenson, P. C. *J. Colloid Sci.* **1954**, *9*, 26–35.

[80] Zhang, Y. C.; Wang, G. Y.; Hu, X. Y. *J. Alloys Compd.* **2007**, *437*, 47–52.

[81] Bera, P.; Seok, S. *Solid State Sci.* **2012**, *14*, 1126–1132.

[82] Han, S. T.; Zhou, Y.; Wang, C.; He, L.; Zhang, W.; Roy, V. A. L. *Adv. Mater.* **2013**, *25*, 872–877.

[83] Lin, J.; Liu, X.; Guo, M.; Lu, W.; Zhang, G.; Zhou, I.; Chen, X.; Huang, H. *Nanoscale* **2012**, *4*, 5148–5153.

[84] Lu, C.; Akey, A.; Wang, W.; Herman, I. P. *J. Am. Chem. Soc.* **2009**, *131*, 3446–3447.

[85] Castelvetro, V.; de Vita, C. *Adv. Colloid Interface Sci.* **2004**, *108-109*, 167–185.

[86] Schartl, W. *Nanoscale* **2010**, *2*, 829–843.

[87] Zhou, Z.; Flytzani-Stephanopoulos, M.; Saltsburg, H. *J. Catal.* **2011**, *280*, 255–263.

[88] Chu, H.; Wang, J.; Ding, L.; Yuan, D.; Zhang, Y.; Liu, J.; Li, Y. *J. Am. Chem. Soc.* **2009**, *131*, 14310–14316.

[89] Rafique, M. Y.; Pan, L. Q.; Javed, Q. U. A.; Iqbal, M. Z.; Yang, L. H. *J. Nanoparticle Res* **2012**, *14*, 1189.

[90] Li, Y.; Liu, X.; Zhang, J. M.; Dai, Z.; Li, P.; Wei, J. *J. Pure Appl. Microbiol.* **2013**, *7*, 105–110.

[91] Kim, J.; Kim, D.; Veriansyah, B.; Kang, J. W.; Kim, J.-D. *Mater. Lett.* **2009**, *63*, 1880–1882.

[92] Seo, M.; Yoon, D.; Hwang, K. S.; Kang, J. W.; Kim, J. *Carbon N. Y.* **2013**, *64*, 207–218.

[93] Sugie, A.; Song, H.; Horie, T.; Ohmura, N.; Kanie, K.; Muramatsu, A.; Mori, A. *Tetrahedron Lett.* **2012**, *53*, 4457–4459.

[94] Liu, X.; Atwater, M.; Wang, J.; Dai, Q.; Zou, J.; Brennan, J. P.; Huo, Q. *J. Nanosci. Nanotechnol.* **2007**, *7*, 3126–3133.

[95] Adhikari, B.; Banerjee, A. *Mater. Chem. Phys.* **2013**, *139*, 450–458.

[96] Prechtl, M. H. G.; Scariot, M.; Scholten, J. D.; Machado, G.; Teixeira, S. R.; Dupont, J. *Inorg. Chem.* **2008**, *47*, 8995–9001.

[97] Batchelor-McAuley, C.; Martinez-Marrades, A.; Tschulik, K.; Patel, A. N.; Combellas, C.; Kanoufi, F.; Tessier, G.; Compton, R. G. *Chem. Phys. Lett.* **2014**, *597*, 20–25.

[98] Li, Y.; Kalia, R. K.; Nakano, A.; Vashishta, P. *J. Appl. Phys.* **2013**, *114*, 134312.

[99] Penner, S.; Wang, D.; Jenewein, B.; Gabasch, H.; tzer, B. K.; Knop-Gericke, A.; Schlögl, R.; Hayek, K. *J. Chem. Phys.* **2006**, *125*, –.

[100] Cho, S. D.; Park, H. S. *J. Colloid Interface Sci.* **2011**, *357*, 46–49.

[101] Chen, S.-W.; Chiang, C.-L.; Chen, C.-L. *Mater. Lett.* **2012**, *67*, 349–351.

[102] Shon, Y.-S.; Aquino, M.; Pham, T. V.; Rave, D.; Ramirez, M.; Lin, K.; Vaccarello, P.; Lopez, G.; Gredig, T.; Kwon, C. *J. Phys. Chem. C* **2011**, *115*, 10597–10605.

[103] Fuku, K.; Takakura, S.; Kamegawa, T.; Mori, K.; Yamashita, H. *Chem. Lett.* **2012**, *41*, 614–616.

[104] Nagarajan, R. *Nanoparticles: Building Blocks for Nanotechnology: Nanoparticles: Synthesis, Stabilization, Passivation, and Functionalization;* Am. Chem. Soc.: Washington D.C., 2008.

[105] Rao, C. R. N.; Kulkarni, G. U.; Thomas, P. J.; Edwards, P. P. *Chem. Eur. J.* **2002**, *8*, 28–35.

[106] Baun, A.; Hartmann, N. B.; Grieger, K. D.; Hansen, S. F. *J. Environ. Monit.* **2009**, *11*, 1774–1781.

[107] Zhang, H.; Chen, B.; Banfield, J. F. *J. Phys. Chem. C* **2010**, *114*, 14876–14884.

[108] Zhang, H.; Penn, R. L.; Hamers, R. J.; Banfield, J. F. *J. Phys. Chem. B* **1999**, *103*, 4656–4662.

[109] Liu, J.; Aruguete, D. M.; Murayama, M.; Hochella., M. F. *Environ. Sci. Technol.* **2009**, *43*, 8178–8183.

[110] Phenrat, T.; Saleh, N.; Sirk, K.; Kim, H.-J.; Tilton, R.; Lowry, G. *J. Nanopart. Res.* **2008**, *10*, 795–814.

[111] Mudunkotuwa, I. A.; Grassian, V. H. *J. Am. Chem. Soc.* **2010**, *132*, 14986–14994.

[112] Mudunkotuwa, I. A.; Grassian, V. H. *J. Environ. Monit.* **2011**, *13*, 1135–1144.

[113] Stebounova, L. V.; Guio, E.; Grassian, V. *J. Nanoparticle Res.* **2010**, *13*, 233–244.

[114] Taylor, R.; Coulombe, S.; Otanicar, T.; Phelan, P.; Gunawan, A.; Lv, W.; Rosengarten, G.; Prasher, R.; Tyagi, H. *J. Appl. Phys.* **2013**, *113*, 011301.

[115] Faraday, M. *Philos. Trans. R. Soc. London* **1857**, *151*, 183.

[116] Buffat, P.; Borel, J.-P. *Phys. Rev. A* **1976**, *13*, 2287–2299.

[117] Reiss, G.; Hutten, A. *Handb. Nanophysics;* CRC Press: Boca Raton, 2010.

[118] Taylor, R. A.; Phelan, P. E.; Otanicar, T. P.; Adrian, R.; Prasher, R. *Nanoscale* **2011**, *6*, 255.

[119] Anselmann, R.; Winkler, H. *J. Am. Chem. Soc.* **2002**, *224*, 433.

[120] Barron, A. R. *Dalton Trans.* **2014**, *43*, 8127–8143.

[121] Ni, W.; Wu, S.; Ren, Q. *Chem. Eng. J.* **2013**, *214*, 272–277.

[122] Ni, W.; Wu, S.; Ren, Q. *Ind. Eng. Chem. Res.* **2012**, *51*, 13157–13163.

[123] Nikje, M. M. A.; Garmarudi, A. B. *Adv. Compos. Mater.* **2011**, *20*, 79–89.

[124] Xing, Y.; Liu, Z.; Suib, S. L. *Chem. Mater.* **2007**, *19*, 4820–4826.

[125] Call, R. L.; Jaber, N. K.; Seshan, K.; Jr., J. R. W. *Sol. Energy Mater.* **1980**, *2*, 373–380.

[126] Satoh, I.; Kobayashi, T. *Appl. Surf. Sci.* **2003**, *216*, 603–606.

[127] Mornet, S.; Vasseur, S.; Grasset, F.; Veverka, P.; Goglio, G.; Demourgues, A.; Portier, J.; Pollert, E.; Duguet, E. *Prog. Solid State Chem.* **2006**, *34*, 237–247.

[128] Paladini, F.; Simone, S. D.; Sannino, A.; Pollini, M. *J. Appl. Polym. Sci.* **2014**, *131*,.

[129] Li, Z.; Hassan, A. A.; Sahle-Demessie, E.; Sorial, G. A. *Water Res.* **2013**, *47*, 6457–6466.

[130] Li, H.; Gui, X.; Zhang, L.; Wang, S.; Ji, C.; Wei, J.; Wang, K.; Zhu, H.; Wu, D.; Cao, A. *Chem. Commun.* **2010**, *46*, 7966–7968.

[131] Yamada, S. *Aerosol Air Qual. Res.* **2011**, 155–160.

[132] Hong, R. Y.; Fu, H. P.; Zhang, Y. J.; Liu, L.; Wang, J.; Li, H. Z.; Zheng, Y. *J. Appl. Polym. Sci.* **2007**, *105*, 2176–2184.

[133] Yu, J.; Huang, X.; Wang, L.; Peng, P.; Wu, C.; Wu, X.; Jiang, P. *Polym. Chem.* **2011**, *2*, 1380–1388.

[134] Chen, L.; Lin, D. F. *Constr. Build. Mater.* **2009**, *23*, 3312–3320.

[135] Guskos, N.; Zolnierkiewicz, G.; Typek, J.; Guskos, A.; Czech, Z. *Rev. Adv. Mater. Sci* **2007**, *14*, 57–60.

[136] Nazari, A.; Riahi, S. *Mater. Sci. Eng. A* **2010**, *527*, 7663–7672.

[137] Flores-Velez, L. M.; Dominguez, O. *J. Mater. Sci.* **2002**, *37*, 983–988.

[138] Kommireddy, D. S.; Patel, A. A.; Shutava, T. G.; Mills, D. K.; Lvov, Y. M. *J Nanosci Nanotechnol.* **2005**, *5*, 1081–1087.

[139] Xu, L.; Karunakaran, R. G.; Guo, J.; Yang, S. *ACS Appl. Mater. Interfaces* **2012**, *4*, 1118–1125.

[140] Paal, C.; Amberger, C. *Ber. Dt. Chem. Ges* **1904**, *37*, 124–139.

[141] Paal, C.; Amberger, C. *J. Prakt. Chem* **1904,** *2,* 258–365.

[142] Paal, C.; Amberger, C. *Ber. Dt. Chem. Ges* **1905,** *38,* 1398–1405.

[143] Paal, C.; Amberger, C. *Ber. Dt. Chem. Ges* **1907,** *40,* 1392–1404.

[144] Skita, A.; Meyer, W. A. *Ber. Dt. Chem. Ges* **1912,** *45,* 3579–3589.

[145] Bönnemann, H.; Braun, G.; Brijoux, W.; Brinkmann, R.; Schulze-Tilling, A.; Seevogel, K.; Siepen, K. *J. Organomet. Chem.* **1996,** *520,* 143–162.

[146] Reetz, M. T.; Lohmer, G. *Chem. Commun.* **1996,** 1921–1922.

[147] Reetz, M. T.; Breinbauer, R.; Wanninger, K. *Tetrahedron Lett.* **1996,** *37,* 4499–4502.

[148] Reetz, M. T.; de Vries, J. G. *Chem. Commun.* **2004,** 1559–1563.

[149] Ding, J.; Gin, D. L. *Chem. Mater.* **2000,** *12,* 22–24.

[150] Li, Y.; El-Sayed, M. A. *J. Phys. Chem. B* **2001,** *105,* 8938–8943.

[151] Miao, S.; Liu, Z.; Han, B.; Huang, J.; Sun, Z.; Zhang, J.; Jiang, T. *Angew. Chem. Int. Ed.* **2006,** *45,* 266–269.

[152] Fonseca, G. S.; Umpierre, A. P.; Fichtner, P. F. P.; Teixeira, S. R.; Dupont, J. *Chem. Eur. J.* **2003,** *9,* 3263–3269.

[153] Huang, J.; Jiang, T.; Gao, H.; Han, B.; Liu, Z.; Wu, W.; Chang, Y.; Zhao, G. *Angew. Chem. Int. Ed.* **2004,** *43,* 1397–1399.

[154] Low, J. E.; Foelske-Schmitz, A.; Krumeich, F.; Worle, M.; Baudouin, D.; Rascon, F.; Coperet, C. *Dalton Trans.* **2013,** *42,* 12620–12625.

[155] Fonseca, G. S.; Scholten, J. D.; Dupont, J. *Synlett* **2004,** *9,* 1525–1528.

[156] Zhao, M.; Crooks, R. M. *Angew. Chem. Int. Ed.* **1999,** *38,* 364–366.

[157] Rangheard, C.; de Julian Fernandez, C.; Phua, P.-H.; Hoorn, J.; Lefort, L.; de Vries, J. G. *Dalton. Trans.* **2010,** *39,* 8464–8471.

[158] Mazumder, V.; Chi, M.; Mankin, M. N.; Liu, Y.; Metin, O.; Sun, D.; More, K. L.; Sun, S. *Nano Lett.* **2012,** *12,* 1102–1106.

[159] Shimizu, K.; Kon, K.; Shimura, K.; Hakim, S. S. M. A. *J. Catal.* **2013,** *300,* 242–250.

[160] Sarkar, A.; Mukherjee, T.; Kapoor, S. *J. Phys. Chem. C* **2008,** *112,* 3334–3340.

[161] Pfeifer, P.; Schubert, K.; Emig, G. *Appl. Catal. A Gen.* **2005,** *286,* 175–185.

[162] Chimentao, R. J.; Kirm, I.; Medina, F.; Rodriguez, X.; Cesteros, Y.; Salagre, P.; Sueiras, J. E. *Chem. Commun.* **2004,** 846–847.

[163] Corma, A.; Gonzalez-Arellano, C.; Iglesias, M.; Sanchez, F. *Angew. Chem. Int. Ed.* **2007,** *46,* 7820–7822.

[164] Kapteijn, F.; Stegenga, S.; Dekker, N. J. J.; Bijsterbosch, J. W.; Moulijn, J. A. *Catal. Today* **1993,** *16,* 273–287.

[165] El-Remaily, M.; Aleem, A. A. A. E. *Tetrahedron* **2014,** *70,* 2971–2975.

[166] Sreedhar, B.; Kumar, A. S.; Reddy, P. S. *Tetrahedron Lett.* **2010,** *51,* 1891–1895.

[167] Kessler, M. T.; Robke, S.; Sahler, S.; Prechtl, M. H. G. *Catal. Sci. Technol.* **2014,** *4,* 102–108.

[168] Inamdar, S. M.; More, V. K.; Mandal, S. K. *Tetrahedron Lett.* **2013,** *54,* 579–583.

[169] Barnali, B.; Pradhan, N. C.; Neogi, S. *Catal. Today* **2013,** *207,* 28–35.

[170] Miyaura, N.; Yamada, K.; Suzuki, A. *Tetrahedron Letters* **1979,** *20,* 3437–3440.

[171] Sonogashira, K.; Tohda, Y.; Hagihara, N. *Tetrahedron Letters* **1975,** *16,* 4467–4470.

[172] Clayden, J.; Greeves, N.; Warren, S. *Organic Chemistry;* Oxford University press: Oxford, Second Edition ed.; 2012.

[173] Riedel, E.; Meyer, H.-J. *Allgemeine und Anorganische Chemie;* De Gruyter: Weinheim, 2013.

[174] Ping, E. W.; Wallace, R.; Pierson, J.; Fuller, T. F.; Jones, C. W. *Micropor. Mesopor. Mat.* **2010,** *132,* 174–180.

[175] M′aki-Arvela, P.; Snare, M.; Er′anen, K.; Myllyoja, J.; Murzin, D. *Fuel* **2008,** *87,* 3543–3549.

[176] Myers, A. G.; Tanaka, D.; Mannion, M. R. *J. Am. Chem. Soc.* **2002,** *124,* 11250–11251.

[177] Goossen, L. J.; Deng, G.; Levy, L. M. *Science* **2006,** *313,* 662–664.

[178] Boon, J. A.; Levisky, J. A.; Pflug, J. L.; Wilkes, J. S. *J. Org. Chem.* **1986,** *51,* 480–483.

[179] Fry, S. E.; Pienta, N. J. *J. Am. Chem. Soc.* **1985,** *107,* 6399–6400.

[180] Chauvin, Y.; Gilbert, B.; Guibarda, I. *Chem. Commun.* **1990,** 1715–1716.

[181] Carlin, R. T.; Wilkes, J. S. *J. Mol. Catal* **1990,** *63,* 125–129.

[182] Chauvin, Y.; Mussmann, L.; Olivier, H. *Angew. Chem. Int. Ed* **1995,** *107,* 2941–2943.

[183] Chauvin, Y.; Mussmann, L.; Olivier, H. *Angew. Chem. Int. Ed.* **1996,** *34,* 2698–2700.

[184] Kaufmann, D. E.; Nouroozian, M.; Henze, H. *Synlett* **1996,** *11,* 1091–1092.

[185] Beller, M.; Fischer, H.; Kühlein, K.; Reisinger, C.-P.; Herrmann, W. A. *J. Organomet. Chem.* **1996,** *520,* 257–259.

[186] T. Jeffery, *Tetrahedron* **1996,** *52,* 10113–10130.

[187] Jeffery, T.; David, M. *Tetrahedron Lett.* **1998,** *39,* 5751–5754.

[188] Reetz, M. T.; Westermann, E. *Angew. Chem. Int. Ed.* **2000,** *39,* 165–168.

[189] Caló, V.; Nacci, A.; Monopoli, A.; Detomaso, A.; Iliade, P. *Organometallics* **2003,** *22,* 4193–4197.

[190] Deshmukh, R. R.; Rajagopal, R.; Srinivasan, K. V. *Chem. Commun.* **2001,** 1544–1545.

[191] Durand, J.; Teuma, E.; Malbosc, F.; Kihn, Y.; Gomez, M. *Catal. Commun.* **2008,** *9,* 273–275.

[192] Gao, S.; Zhang, H.; Wang, X.; Mai, W.; Peng, C.; Ge, L. *Nanotechnology* **2005,** *16,* 1234–1237.

[193] Prechtl, M. H. G.; Scholten, J. D.; Dupont, J. *Molecules* **2010,** *15,* 3441–3461.

[194] Dupont, J.; Fonseca, G. S.; Umpierre, A. P.; Fichtner, P. F. P.; Teixeira, S. R. *J. Am. Chem. Soc.* **2002,** *124,* 4228–4229.

[195] Gelesky, M. A.; Chiaro, S. S. X.; andJ. H. Z. dos Santos, F. A. P.; Dupont, J. *Dalton Trans.* **2007,** 5549–5553.

[196] Venkatesan, R.; Prechtl, M. H. G.; Scholten, J. D.; Pezzi, R. P.; Machado, G.; Dupont, J. *J. Mater. Chem.* **2011,** *21,* 3030–3036.

[197] Redel, E.; Krämer, J.; Thomann, R.; Janiak, C. *J. Organomet. Chem.* **2009,** *694,* 1069–1075.

[198] Cimpeanu, V.; Kocevar, M.; Parvulescu, V. I.; Leitner, W. *Angew. Chem. Int. Ed.* **2009,** *48,* 1085–1088.

[199] Scheeren, C. W.; Machado, G.; Dupont, J.; Fichtner, P. F. P.; Texeira, S. R. *Inorg. Chem.* **2003,** *42,* 4738–4742.

[200] Vollmer, C.; Redel, E.; Abu-Shandi, K.; Thomann, R.; Manyar, H.; Hardacre, C.; Janiak, C. *Chem. Eur. J.* **2010,** *16*, 3849–3858.

[201] Yinghuai, Z.; Chenyan, K.; Peng, A. T.; Emi, A.; Monalisa, W.; Kui-Jin, L. L.; Hosmane, N. S.; Maguire, J. A. *Inorg. Chem.* **2008,** *47*, 5756–5761.

[202] Geldbach, T. J.; Zhao, D.; Castillo, N. C.; Laurenczy, G.; Weyershausen, B.; Dyson, P. J. *J. Am. Chem. Soc.* **2006,** *128*, 9773–9780.

[203] Xiao, C.; Cai, Z.; Wang, T.; Kou, Y.; Yan, N. *Angew. Chem. Int. Ed.* **2008,** *47*, 746–749.

[204] Caló, V.; Nacci, A.; Monopoli, A.; Damascelli, A.; Ieva, E.; Cioffi, N. *J. Organomet. Chem.* **2007,** *692*, 4397–4401.

[205] Yin, M.; Wu, C.-K.; Lou, Y.; Burda, C.; Koberstein, J. T.; Zhu, Y.; O'Brien, S. *J. Am. Chem. Soc.* **2005,** *127*, 9506–9511.

[206] Rudzki, M.; Alcalde-Aragones, A.; Dzik, W. I.; Rodriguez, N.; Goossen, L. J. *Synthesis* **2012,** *2012*, 184–193.

[207] Grainger, R.; Nikmal, A.; Cornella, J.; Larrosa, I. *Org. Biomol. Chem.* **2012,** *10*, 3172-3174.

[208] Scanlon, J. T.; Willis, D. E. *J. Chromatogr. Sci.* **1985,** *23*, 333–340.

[209] Steines, S.; Wasserscheid, P.; Driessen-Hollscher, B. *J. prak. Chem.* **2000,** *342*, 348–354.

[210] Bini, R.; Chiappe, C.; Mestre, V. L.; Pomelli, C. S.; Welton, T. *Org. Biomol. Chem.* **2008,** *6*, 2522–2529.

[211] Cassol, C.; Ebeling, G.; Ferrera, B.; Dupont, J. *Adv. Synth. Catal.* **2006,** *348*, 243–248.

[212] Zhuo, K.; Chen, Y.; Chen, J.; Bai, G.; Wang, J. *Phys. Chem. Chem. Phys.* **2011,** *13*, 14542–14549.

[213] Csihony, S.; Fischmeister, C.; Bruneau, C.; Horvath, I. T.; Dixneuf, P. H. *New J. Chem.* **2002,** *26*, 1667–1670.

[214] Zhao, D.; Fei, Z.; Geldbach, T.; Scopelliti, R.; Dyson, P. J. *J. Am. Chem. Soc.* **2004,** *126*, 15876–15882.

List of Figures

List of Schemes

List of Tables

Erklärung

Ich versichere, dass ich die von mir vorgelegte Dissertation selbständig angefertigt, die benutzten Quellen und Hilfsmittel vollständig angegeben und die Stellen der Arbeit - einschließlich Tabellen, Karten und Abbildungen -, die anderen Werken im Wortlaut oder dem Sinn nach entnommen sind, in jedem Einzelfall als Entlehnung kenntlich gemacht habe; dass diese Dissertation noch keiner anderen Fakultät oder Universität zur Prüfung vorgelegen hat; dass sie - abgesehen von unten angegebenen Teilpublikationen - noch nicht veröffentlicht worden ist sowie, dass ich eine solche Veröffentlichung vor Abschluss des Promotionsverfahrens nicht vornehmen werde. Die Bestimmungen der Promotionsordnung sind mir bekannt. Die von mir vorgelegte Dissertation ist von Dr. Martin Prechtl betreut worden.

Köln, den 18.08.2014